GEO.ALP

Veröffentlichung des Instituts für Geologie und Paläontologie der Universität Innsbruck
und des Naturmuseums Südtirol/Museo Scienze Naturali Alto Adige, Bozen/Bolzano

ISSN 1824-7741

VOLUME 8 / 2011

Blick auf die SW-Seite der Sella-Gruppe (Dolomiten) mit Sas de Pordoi (Bildmitte) und Piz Boè (links). Die untere Dolomitwandstufe wird aus dem post-vulkanischen, ladinisch-karnischen Schlerndolomit aufgebaut und zeigt typische, nach S geneigte, steile Klinoformen der progradierenden Sella-Karbonatplattform. Das schneebedeckte Band in der Mitte zeichnet die karnische Pordoi-Formation („Raibler Schichten") eindrucksvoll nach. Die obere Wandstufe wird aus Hauptdolomit/Dolomia Principale gebildet. Am Piz Boè folgen rhätischer Dachsteinkalk (helle Wandstufe), jurassischer Rosso Ammonitico und unterkretazische Puezmergel. *Foto: Lorenz Keim*

NATURMUSEUM SÜDTIROL
MUSEO SCIENZE NATURALI ALTO ADIGE
MUSEUM NATÖRA SÜDTIROL

GEO.ALP

A yearly journal devoted to Alpine geology

Jahreszeitschrift zur Alpengeologie

La rivista per la Geologia delle Alpi

GEO.ALP

Herausgeber, Eigentümer und Verleger:
Institut für Geologie und Paläontologie, Universität Innsbruck; Naturmuseum Bozen

Chefredakteur: Karl Krainer

Erscheinungsweise und Bezug:
Geo.Alp erscheint einmal jährlich und kann bei beiden herausgebenden Institutionen im Abonnement oder einzeln bezogen werden:
Institut für Geologie und Paläontologie, Innrain 52, A-6020 Innsbruck, Austria
Naturmuseum Südtirol/Museo Scienze Naturali Alto Adige, Bindergasse/via Bottai 1, I-39100 Bozen/Bolzano, Italy

Genehmigung des Landesgerichtes Bozen Nr. 12/2004 vom 5/11/2004
Verantwortlicher Direktor: Dr. Vito Zingerle

ISSN 1824-7741

Druck: PRINTER TRENTO SRL

INSTRUCTIONS TO AUTHORS

Articles may be submitted in English, German or Italian. In case of a German or Italian text, the captions and figures, plates and tables must be also in English, and an English abridged version (1000 – 1500 words) and abstract is to be delivered.

Articles shall be submitted in three copies to:

Karl Krainer, Institute of Geology and Palaeontology, University of Innsbruck, Innrain 52, A-6020 Innsbruck, Austria. E-mail: Karl.Krainer@uibk.ac.at
or to:
Benno Baumgarten, Naturmuseum Südtirol/Museo Scienze Naturali Alto Adige, Bindergasse 1/Via Bottai 1, I-39100 Bozen/Bolzano, Italy: E-mail: benno.baumgarten@naturmuseum.it

Articles must be typed double-space. The quality of line-drawings must be ready for print. In line-drawings and figures of any sort, all labellings, numbers and letters should be readable upon 50% reduction in size.

Publication titles and authors name (citations) not in capital letters and not in small capitals!

Photographs and line drawings can be submitted in original hardcopy, or in an electronic format. All photographs must be clearly labelled on the backside.

For photographic tables (plate header – e.g. "Plate 1" – included) and for text-figures: please note that the page setup of Geo.Alp is 23,47 x 16,70 cm (8 cm column width)

The final text (Word file) must be submitted on CD. The name of the author, the name and version of the word processing program(s) and type of computer on which the text was prepared must be indicated. To avoid obsolete passages in the manuscript please note that Word files should be saved after using the option "Accepted Changes" in the Tools Menu.

Word tables must be on single pages for transformation into pdf format or already in pdf format.

The text should be submitted in single column format, and should be formatted as simple as possible (e.g. no bullets and no automatic numbering). Electronic versions of figures and/or photographs must be submitted as separate files; file format: tif without LZW compression (high-resolution jpg files are also possible), photographs with a resolution of 300 dpi (due to print size), line drawings at least 600 dpi; colour images all in CMYK mode.

Referencing (Authors names not in capital letters and not in small capitals):

Articles:
Author 1, X.Y., Author 2, Z.A. (2002): Title of article. – International journal abbreviation (e.g. Sediment. Geol.), vol.: pp-pp.

Articles in books:
Author 1, X.Y., Author 2, Z.A. (2002): Title of article. – In: Person A., Person B. (eds): Title of book, pp-pp, publisher, place of publication.

Books:
Author 1, X.Y., Author 2, Z.A. (2002): Title of book. – no. of pages, publisher, place of publication.

Inhalt

Geo.Alp, Vol. 8, S. 4–19, 2011

PINAKIDE MIKROSKLEREN DEMOSPONGIIDER PORIFEREN, WEIT VERBREITET IN MESOZOISCHEN BECKENSEDIMENTEN DER NÖRDLICHEN KALKALPEN

von Helfried Mostler

Mit 7 Abbildungen und 3 Tafeln

Institut für Geologie und Paläontologie, Universität Innsbruck, Innrain 52, A-6020 Innsbruck, Austria

Zusammenfassung

Pinakide Skleren konnten nun auch in den Beckensedimenten des Hettang nachgewiesen werden. Somit ergibt sich für diesen Spicula-Typ eine neue stratigraphische Reichweite vom Unterjura bis Ende Oligozän. Untersucht wurden Kieselschwämme aus dem stratigraphischen Abschnitt vom Hettang bis in die Unterkreide mit Schwerpunkt im Lias, Malm und Unterkreide.

In allen Fällen handelt es sich um pelagische Beckensedimente, auf welche Kieselschwämme mit Pinakiden beschränkt sein dürften, zumal in zeitgleichen Ablagerungen des flachen Subditals , wie z.B. in den Schwammkalken der Schwäbischen und Fränkischen Alb trotz reicher Kieselschwammfaunen keine Pinakide nachgewiesen werden konnten.

Die Architektur der Pinakide ist z.T. recht unterschiedlich, weshalb man sie stratigraphisch gut verwerten kann. Um dies auch umsetzen zu können, wurden bestimmte Pinakid-Typen parataxonomisch erfasst. Carter (1871) hat Pinakide aus dem Cenoman Englands unter der Gattung *Dactylocalicytes* beschrieben, die von Reid (2004: 192) in die neue Gattung *Prodactylocalcites* Reid transformiert wurden. In dieser Studie werden drei neue Arten dieser Gattung zugeordnet.

Die Genese der Pinakide lässt trotz unserer Untersuchungen noch eine Reihe von Fragen offen. Die Pinakide sind die einzigen Demospongien-Skleren, die Poren entwickelten, wodurch sie sich stark von den übrigen Spicula abheben. Während Mostler (1986) eine Abkunft der Pinakide von den Phyllotriaenen vermutete, sieht Wiedenmayer eine Verbindung zu den Aspidastern. Letztere Ansicht ist schon durch das stratigraphisch viel spätere Auftreten von Aspidastern in der hohen Unterkreide in Frage zu stellen. Aber auch eine Erklärung, wie aus Aspidastern vielporige Scheibchen entstehen sollten wird von Wiedenmayer nicht gegeben.

Die Ableitung der Pinakide von symphyllotriaenen Skleren ist auch nicht nachvollziehbar. Die Pinakid-führenden Demospongien bilden somit eine eigenständige Poriferengruppe, deren systematische Stellung bisher nicht abgeklärt werden konnten. Als Ausgangsformen der Pinakide werden dünne imperforate Disken mit vielen radialen Kanälen in der Obertrias vermutet.

Abstract

Pinakid scleres were recently discovered in Hettangian (lowermost Liassic) basinal deposits. By this finding, the known stratigraphic range of this spicule type is now extended to comprise the period from the lower Jurassic to the end of Oligocene. In the present paper, siliceous sponges from the Hettangian to Lower Cretaceous were investigated with focus on the Hettangian, Upper Jurassic and Lower Cretaceous. Pinakid-bearing Demospongiae in the investigated material are restricted to basinal deposits (deep-water facies). In contemporary shallow subtidal deposits with rich siliceous sponge faunas, e.g. sponge lime-

stone of the Suevian and Frankonian Alb, so far no pinakid scleres have been recorded.

The architecture of the pinakids is rather diverse, and this allows a good stratigraphic evaluation. For stratigraphic purposes, the pinakid spicule types have been parataxonomically subdivided. Carter (1871) described pinakid scleres as *Dactylocalicytes*, and Reid (2004) transformed this genus to *Prodactylocalcites*. In the present paper three new species of this genus are described.

Concerning the genesis of the pinakid scleres several questions remain open, despite the investigation of this rich Mesozoic material. Pinakids are the only pore-bearing scleres of Demospongiae, and therefore very different from all other demospongid spicules.

Whereas Mostler (1986) assumed a derivation of the pinakid sceleres from phyllotriaens, Wiedenmayer (1994) and Reid (2004:192) assumed connection to aspidaster spicules. The latter option, can probably be excluded because aspidasters stratigraphically occur considerably later (during the Late Cretaceous) than the first pinakids (in the Liassic).

Due to the lack of a radial channel the derivation of the Pinakids from phyllotriaen spicules has also to be ruled out.

Furthermore the origin of pinakid is uncertain. Predecessors of pinakids may be imperforated discs with multiple radial canals in the upper Triassic, similar to the thin juvenile discs of aspidaster.

1. Einleitung und Problemstellung

Pinakide Mikroskleren sind die einzigen Spicula, deren Kieselscheibchen Poren aufweisen. Die mit Pinakiden bestückten Kieselschwämme sind im Oligozän erloschen. Die ältesten Vertreter dieses Spiculatyps waren bisher aus der Unterkreide (Rüst 1885) bekannt. 1986 hat H. Mostler viele Pinakide aus dem Oberjura nachweisen können. Zur Zeit der Entstehung dieser Arbeit ging man davon aus, dass Poriferen mit Pinakiden nicht vor dem Oberjura aufgetreten sind (siehe hiezu Rigby et al. 2004: 192).

Rauff (1893) hat für die zierlichen perforierten Kieselscheiben, die sich seiner Meinung nach aus dem Symphyllotriaenen entwickelten, den Begriff „Pinakid" eingeführt. Er beschreibt sie als „dünne Kieselscheibchen, die in der Mitte etwas verdickt sind und gegen den Rand hin schmäler bzw. dünner und somit transparenter werden. In Randnähe befinden sich bisquitförmige Löcher, während vom Zentrum 12-16 Kanäle zum Rand hin ausstrahlen."

Weiters führt Rauff aus, dass „die dichotom gegabelten Lappen beim Weiterwachsen verschmelzen und somit einen glatten Rand bilden. Gleichzeitig werden auch die tiefen Einschnitte ringsum in geschlossene langovale Löcher transformiert."

Unter dichtotom gegabelten Lappen versteht Rauff die lappige Struktur phyllotriaener Spicula, von welcher er die Pinakide ableitet.

Besonders reizvoll war es für eine Reihe von Bearbeitern der Entstehung dieser zarten perforierten Kieselscheibchen nachzugehen. Beginnend mit Carter (1871) hinauf bis Gasse et al. (1988) wurde eine Abkunft der Pinakide von den Phyllotriaenen angenommen. Mostler (1986) hat eine Entwicklungsreihe von Dichotriaenen ausgehend zur Diskussion gestellt, vor allem deshalb, weil in den reichen oberjurassischen Kieselschwammfaunen ähnlich gebaute und auch von der Größe her entsprechende Phyllotriaene vorlagen. An den mit Phyllotriaenen vergesellschafteten Pinakiden konnten durchlichtmikroskopisch keine Kanäle festgestellt werden.

Wiedenmayer (1994: 84) hingegen hat darauf hingewiesen, dass die radial angelegten Kanäle in den Pinakiden gegen eine Homologie mit Phyllotriaenen sprechen. Auch Reid (2004: 192) spricht sich gegen eine Entstehung der Pinakide aus Phyllotriaenen aus.

Mittlerweile hat der Verfasser der vorliegenden Studie aus dem basalen Lias viele relativ groß gebaute Pinakide gefunden, die -wie noch detailliert anzuführen ist- sehr deutlich radial angelegte Kanäle zeigen, während die Phyllotriaene deutlich triaene Kanäle mit einem Ansatz zu dichotrianen Kanälen zeigen Somit ist eine Verbindung zu den Phyllotriaenen eher abzulehnen.

Wiedenmayer(1994: 84) schrieb, dass eine Homologie mit Aspidastern wesentlich plausibler sei; auch Reid (2004: 192) vertritt diese Ansicht, insbesondere wegen der radialen Kanäle (über das weitere informiert Kapitel 5).

Ein Ziel dieser Studie ist es, die stratigraphische Verbreitung der Pinakide, insbesondere deren stratigraphischen Leitwert aufzuzeigen. Um die verschiedenen Bauformen stratigraphisch verwerten zu können, mussten diese taxonomisch erfasst werden. Abschließend wird in dieser Studie die Problematik der Pinakidentstehung diskutiert.

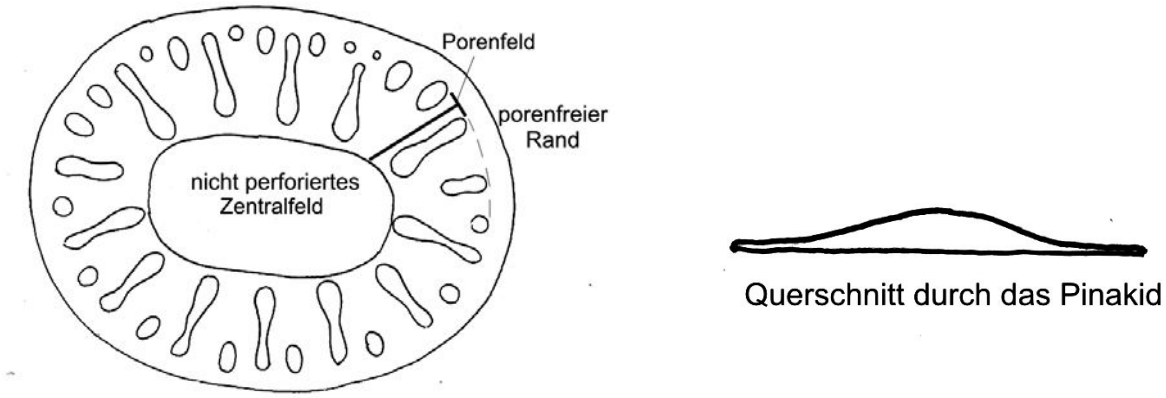

Abbildung 1

2. Bauplan der Pinakide

Den Grundbau hat bereits Rauff (1893: 154) mit zwei Abbildungen dargelegt. Nur wenige Bearbeiter haben sich mit Pinakiden befasst. Die wichtigsten Abbildungen hat Wiedenmayer (1994: 83) zusammengetragen und zeichnerisch wiedergegeben.

Zum einen gibt es Formen, die im Zentrum der oval begrenzten Scheibchen eine Andeutung einer Erhebung aufweisen, die einem reduziertem Rhabd ähneln. (z.B. bei Wiedenmayer 1994 Fig. 35-2 abgebildet). Solche Pinakid-Typen haben verschiedene Autoren veranlasst, eine Entstehung aus einem Phyllotriaen zu vermuten. In Abbildung 1 sind die wichtigsten Elemente des Bauplanes von Pinakiden zusammengetragen; in dieser ist auch ein Querschnitt durch einen Pinakid dargestellt, um die allmähliche Dickenzunahme gegen das Zentrum hin darzustellen. Bei der Beschreibung der Pinakide spielen Scheibchenform, imperforates Zentralfeld, Perforation, Kanäle und die Oberflächenbeschaffenheit eine besondere Rolle.

Wie in Abbildung 1 dargelegt, unterscheidet man ein unperforiertes Mittelfeld oder Zentralfeld, meistens erhaben, und ein daran anschließendes Porenfeld sowie einen Rand, der durch Verschmelzung der verzweigten Äste zur Porenbildung führt.

2.1. Morphologie

Es handelt sich um sehr zarte meist durchscheinende Scheibchen die im Zentrum etwas dicker sind (vgl. Abbildung 1). Die Scheibchen sind in den meisten Fällen oval bis langoval, seltener subrund. Komplett erhalten (hier sind die völlig ausgewachsenen Scheibchen gemeint) weisen sie einen schmalen glatten Rand auf. Dieser ist durch die Verschmelzung der dichotom verzweigten Äste, die sich zwischen den Kanälen entwickelten, entstanden. Die Pinakide mit „offenen Poren" sind in den meisten Fällen (häufig in den Oberalmer Schichten), in ihrem Wachstum nicht ausgereift. Sehr wahrscheinlich handelt es sich um juvenile Stadien. Eine diagenetisch hervorgerufene Auflösung des Randes scheidet aus, weil elektronenmikroskopische Aufnahmen sehr scharfe Begrenzungen zeigen; bei diagenetischer Korrosion sind die Ränder unregelmäßig buchtig und zackig entwickelt.

Das imperforate Zentralfeld richtet sich im Wesentlichen nach dem Verlauf des Außenrandes und des angrenzenden Porenfeldes. Sehr oft treten tief in das Zentralfeld, senkrecht zur Längsachse des Pinakids, eingreifende Poren auf, die zur Einschnürung des Zentralfeldes führen (vgl. hiezu Abbildung 2).

Die Poren sind radial angeordnet und gliedern sich durch Aufspaltung in große, mittlere und kleine Poren. Die großen Poren fallen durch eine Einschnürung auf, die in der Mitte ihrer Länge auftritt. Diese Konfiguration mit den langen, tief in das Mittelfeld eingreifenden Poren haben die meisten Pinakide. Völlig anders gestaltet sind die lang gezogenen, dreieckig geformten Poren, die kaum in der Größe schwanken. Diese zeigen auch keine kleineren Randporen, die gewöhnlich rund entwickelt sind. Abbildung 3 zeigt die Poren erster, zweiter und dritter Ordnung. Die Gestalt der Poren schwankt zwischen sehr lang gezogenen ovalen Poren mit Einschnürungen und rundovalen Poren; zum Teil

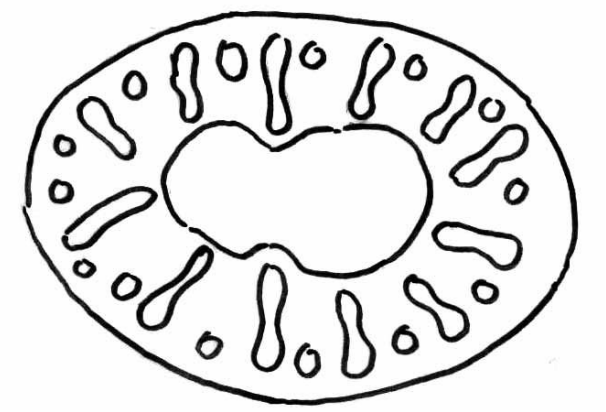

Abbildung 2
Einschnürung des Zentralfeldes durch überlange Poren

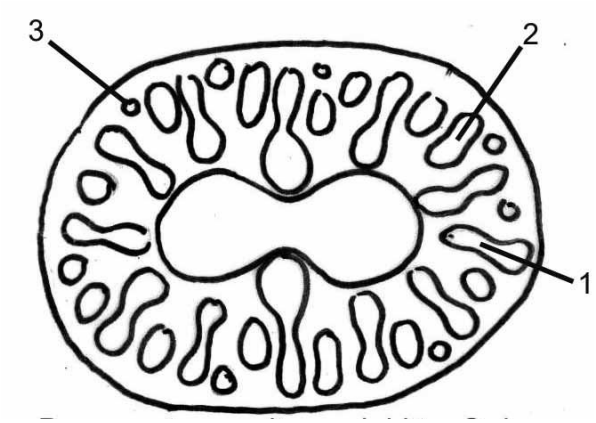

Abbildung 3
Poren erster, zweiter und dritter Ordnung

sind auch runde Poren, sowie langgezogene dreieckig gerundete entwickelt.

Die Porenzahl schwankt zwischen 20 und 44 Poren.

Was die Kanäle betrifft so ist die Sichtbarkeit der Kanäle stark vom Erhaltungszustand der Scheibchen abhängig. Es handelt sich bei gut erhaltenen Pinakiden um radial angelegte Kanäle, die stets zwischen den längeren Poren entwickelt sind, weshalb sie um die jeweilig längste Pore herumgeführt werden müssen und dadurch häufig einen bogenförmigen Verlauf nehmen (siehe Abbildung 4). In der stärksten Biegung der Scheibchen sind die Kanäle stark konzentriert bzw. eng aneinander gerückt, was mit der geometrischen Position dieser zusammenhängt. Senkrecht zur Längsachse stehen die Kanäle weit auseinander, wodurch in der Mitte eine gebogene X-förmige Struktur entsteht. In selteneren Fällen ist eine Verschweißung der Kanäle im Zentrum beobachtbar. Meist handelt es sich hierbei um ein nicht strukturiertes Feld, in dem die Verschweißung der Kanäle stattgefunden haben könnte. Es wäre durchaus denkbar, dass dieses unstrukturierte runde Feld in den zeichnerischen Darstellungen mancher Autoren mit eingeflossen ist, eine Eindellung oder Aufragung vortäuschte. Die Anzahl der Kanäle schwankt zwischen 12 und 26.

Hinsichtlich der Oberflächenbeschaffenheit ist folgendes festzuhalten. Die aus dem alpinen Lias sowie Malm, Unter- und Oberkreide stammenden Pinakide zeigen alle eine glatte Oberfläche. Die von Wiedenmayer (1994) zeichnerisch wiedergegebenen Scanaufnahmen, die aus der Arbeit Mostler (1986) stammen, zeigen eine warzige (verrucose) Oberfläche, die jedoch, wie gut im Original belegbar ist, auf diagenetische Erscheinungen zurückgeht.

In den Abbildungen der Taf. 1, Fig. 5 und 10 sowie Taf. 2, Fig. 1 und 3 kann man sehr schön die völlig glatte Struktur des Mittelfeldes erkennen. Dies wird deshalb erwähnt, weil Wiedenmayer (1994) in dieser vermeintlich warzigen Oberflächenstruktur eine Ähnlichkeit mit den Aspidastern von *Erylus monticularis* sieht. Das von Wiedenmayer (1994: Fig. 35-16) nach einer elektronenmikroskopischen Aufnahme von Mostler (1986) gezeichnete Bild ist kein Pinakid, sondern ein Phyllotriaen, weil es auf der Unterseite ein reduziertes Rhabd aufweist.

Nachfolgend sind die 5 gut unterscheidbaren Bautypen von Pinakiden dargestellt.

Bautypus 1

Stumpfovale Scheibchen mit sehr stark elongierten Poren (siehe hierzu Tafel 1, Fig. 1-5, 7-8).

Charakteristisch ist ein relativ breites glattes porenfreies Feld.

Die besonders langgezogenen Poren zeigen bei starker Vergrößerung auch noch den eingeengten Grundbauplan. Der Einschnürungsbereich der Poren ist aufgrund der starken Elongation sehr lang. Es können insgesamt drei Porengenerationen auseinandergehalten werden; nämlich sehr lange, mittellange und sehr kurze; letztere sind meist rund. Es sind nachweisbar stets 28 Poren und 26 Kanäle vorhanden. Aufgrund der senkrecht zur Achse des Spiculums in das Zentralfeld hineinreichenden überlangen Poren wird das imperforate Mittelfeld eingeschnürt.

Bautypus 2

Stark langoval ausgebildete Scheibchen mit dreieckig abgerundeten Poren. Der spitzwinkelige Dreiecksumriss der Poren ist so angeordnet, dass der spitze Winkel in Richtung Zentralfeld zeigt. Die Porenzahl schwankt zwischen 20 und 22.

Bautypus 3

Rundovale Scheibchen mit langgezogenen, im ersten Drittel ihrer Länge eingeschnürten Poren, denen runde Poren zwischengeschaltet sind.

Zum Teil ist noch eine Zwischengeneration von mittellangen Poren eingeschaltet. Dieser Typus tritt wohl am häufigsten auf und ist vom Oberjura bis in den Eozän-Oligozän Grenzbereich verfolgbar (siehe hiezu Taf. 1, Fig. 10-12; Tafel 2. Fig. 3-4, 8, 10-13). Diesem Bautypus entsprechen Formen von *P. callodiscus* (Carter).

Bautypus 4

Gerundete ovale Scheibchen mit verschieden gestalteten Poren. Parallel zur Längsachse der ovalen Scheibchen sind im stärksten Krümmungsradius dreieckig geformte Poren, während senkrecht zur Längsachse breite unregelmäßige Poren auftreten (vgl. hiezu Tafel 2, Fig.7).

Bautypus 5

Subrunde, sehr viele Poren aufweisende Scheibchen; es sind stark langgezogene eng aneinander gereihte Poren. Es handelt sich um Skleren, die meist ohne Außenrand (juveniles Stadium) auftreten (vgl. hiezu Tafel 2, Fig. 6 und 10).

3. Systematische Beschreibung

Einführende Bemerkungen: Immer dann, wenn man für stratigraphische Einstufungen Skelettelemente von Tiergruppen heranzieht, ist man auf Gattungs- und Artnamen angewiesen. Die Benennung einzelner Skelettelemente mit Gattungs- und Artnamen hat sich schon lange in der Mikropaläontologie eingebürgert, so z.B. bei Conodonten; Holothurien etc. Die hiefür verwendete künstliche Systematik wird als Parataxonomie bezeichnet.

Im Falle der Pinakide, die sich recht gut stratigraphisch verwerten lassen, hat Carter schon 1871 solche aus der tiefen Oberkreide (Cenoman) als *Dactylocalycites* beschrieben. Es ist sehr wahrscheinlich, dass es sich hier um den Bautypus 3 handelt; es muss jedoch erst abgeklärt werden, welchen Stellenwert der Struktur im Zentrum der von Carter abgebildeten Pinakide zukommt. Es könnte sich nach der Darstellung um eine zentrale Pore, jedoch auch um ein reduziertes Rhabd, oder wie bereits erwähnt in der Mitte um ein freies rundes, ein nicht strukturiertes Feld handeln.

Die pinakiden Skleren sind so typisch, dass man davon ausgehen kann, dass sie nur von einer einzigen Gruppe von Kieselschwämmen für ihren Skelettaufbau benötigt wurden. So wird davon ausgegangen, dass die kennzeichnende Autapomorphie des Taxons *Prodactylocalycites* pinakide Skleren sind.

In der systematischen Erfassung von Rigby (2004) im Poriferen Treatise werden die pinakidführenden Kieselschwämme der Ordnung Ancorinida Reid 1968 bzw. der Familie Geodiidae Gray 1867 mit der Unterfamilie Erylina Sollas 1888 zugeordnet.

Wie in Kapitel 5 dargelegt sind die Pinakide weder von den Pyhllotriaenen noch von den Aspidastern ableitbar, sondern werden als eigenständige Gruppe aufgefasst.

Klasse:
Demospongea Sollas 1875
Ordnung und Familie unbekannt
Gattung:
Prodactylocalycites Reid 2004 nom. nov. pro
Dactylocalycites (Carter 1871)
Typus Art:
Prodactylocalycites callodiscus (Carter)
Neue stratigraphische Reichweite dieser Gattung:
Hettang (basaler Lias) bis Ende Tertiär

Weitere dieser Gattung zuordenbare Arten
Prodactylocalycites liassicus n.sp.
Prodactylocalycites trigonalis n.sp.
Prodactylocalycites angustus n.sp.
Prodactylocalycites ellipticus (Carter)

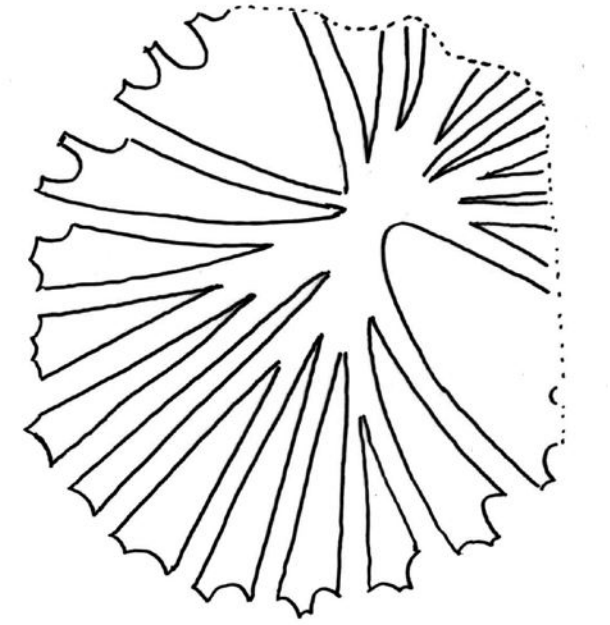

Abbildung 4
gezeichnet nach einer Durchlichtaufnahme von Kennett, Houtz et. al (1975) Pl.3, 10

Prodactylocalycites liassicus **n.sp.**
(Tafel 1, Fig. 1-5; 7-8 und Tafel 3, Fig. 1-8)
Derivatio nominis:
nach dem ausschließlichen Auftreten dieser Art im Lias
Holotypus:
Taf. 1, Fig.5
Locus typicus:
Kirchstein bei Lenggries in Bayern
Stratium typicum:
Basaler Kirchsteinkalk, *angulata* - Zone; oberes Hettang
Material:
56 Exemplare
Diagnose:
Rechteckig gerundete, stumpfovale Scheibchen mit äußerst schmalen, nahezu schlitzförmigen Poren und einem breiten porenfreien Mittelfeld. Konstant 28 Poren und 26 Kanäle aufweisend.
Beschreibung:
siehe Beschreibung des Pinakid Bautypus 1
Bemerkungen:
Gegenüber allen anderen Arten der Gattung *Prodactylocalycites* ist diese Art durch sehr schmale, nahezu schlitzförmige Poren gut abtrennbar.
Stratigraphische Reichweite:
bisher nur im unteren Lias nachgewiesen.

Prodactylocalycites trigonalis **n.sp.**
(Tafel 1, Fig. 6 und 9; Tafel 2, Fig. 1)
Derivatio nominis:
Nach den dreieckig abgerundeten Form der Poren benannt.
Holotypus:
Tafel 2, Fig. 1
Locus typicus:
Kirchstein bei Lenggries in Bayern
Stratium typicum:
Basaler Kirchsteinkalk, *angulata* Zone; oberes Hettang
Material:
36 Exemplare
Diagnose:
Stark langovale begrenzte Scheibchen mit langgezogenen dreieckig gerundeten (20-22) Poren
Beschreibung:
siehe Beschreibung des Pinakid-Bautypus 2.
Bemerkungen:
durch die langovale Außenbegrenzung und durch die spitzdreieckig gestalteten Poren von allen anderen Arten der Gattung *Prodactylocalycites* zu unterscheiden.
Stratigraphische Reichweite:
bisher auf den basalen Lias beschränkt.

Prodactylocalycites angustus **n.sp.**
(Tafel 2, Fig. 6 und 10)
Derivatio nominis:
angustus (lat.) eingeengt
Locus typicus:
Oberalm, Salzburg
Stratium typicum:
Oberalmer Kieselkalke im alten „Leitner Steinbruch"
Material:
11 Exemplare
Diagnose:
Subrunde Scheibchen mit sehr vielen eng aneinander gereihten, sehr langen Poren.
Beschreibung:
siehe Beschreibung vom Pinakid Bautypus 5
Bemerkungen
Die sehr eng aneinander geschalteten sehr langen Poren sowie die subrunde Außenbegrenzung der Scheibchen lassen eine klare Abgrenzung gegenüber anderen Arten zu.
Stratigraphische Reichweite:
Bisher nur aus dem Oberjura, Tithon nachgewiesen.

Abbildung 5: Stratigraphische Verbreitung der *Prodactylocalicytes* Arten

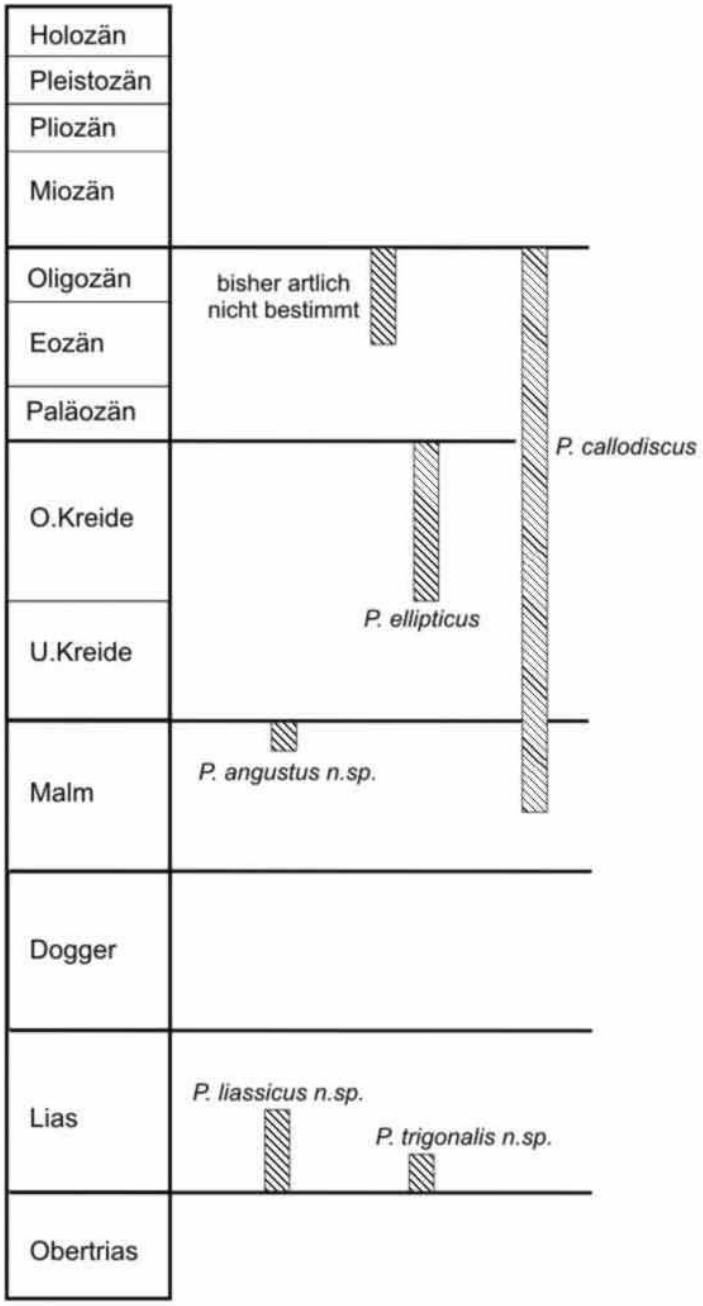

4. Stratigraphischer Aspekt (vgl. Abbildung 5)

Überraschenderweise treten schon im basalen Lias typische Pinakide auf. In der hohen Obertrias wurde trotz intensiven Suchens danach bisher kein einziges Pinakid nachgewiesen. Die aus dem oberen Hettang stammenden Skleren sind - wie zuvor beschrieben - einem eigenen Bautypus zuordenbar und haben somit auch einen stratigraphischen Leitwert, zumal keine ähnlichen Formen im Dogger und Malm auftreten.

Dies war auch der Grund, die Skleren parataxonomisch zu erfassen. So sind *Prodactylocalycites li-*

Abbildung 6
Prodactylocalycites ellipticus
gezeichnet nach dem Poniferen-Treatise

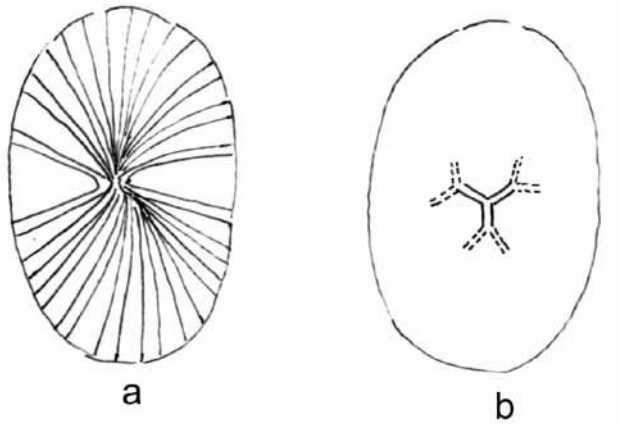

Abbildung 7
a: Radiale Kanäle eines Pinakides
b: Dichiotriaener Kanal eines Discotriaens

assicus n.sp. und *Prodactylocalycites trigonalis* n.sp. ausschließlich auf den unteren Lias beschränkt. Die Pinakide des Bautypus 3, wozu *Prodactylocalycites callodiscus* (Carter) zu stellen ist, ist wohl jene Form, die über eine große stratigraphische Reichweite verfügt. Sie tritt bereits in Kimmeridge auf und reicht bis an die Oligozän/Miozän-Grenze. Eine genaue Erfassung dieser Art konnte bisher nicht durchgeführt werden.

Die unter Bautypus 4 angeführten Pinakide sind noch zu vereinzelt, um sie taxonomisch erfassen zu können. Die von Carter 1871 beschriebene Art *Prodactylocalycites ellipticus* ist erst ab der Oberkreide bekannt. Ihre spitzovale z.T. begrenzte Form unterscheidet sich stark von allen Arten und dürfte daher eine sehr gute Leitform für die Oberkreide sein (siehe Abbildung 6).

P. angustus n.sp. ist bisher nur aus dem Tithon bekannt. Sie tritt ganz sicher im Berrias (basale Unterkreide) nicht mehr auf und ist auch in jüngeren Schichtfolgen nicht nachgewiesen.

Bemerkungen: Alle vorgestellten Pinakide stammen aus Beckensedimenten in Tiefwasserposition. Es ist bisher nicht gelungen in den zeitgleichen Sedimenten der Schwammkalke Schwabens und Frankens Pinakide nachzuweisen. Dies dürfte ein Beleg dafür sein, dass jene Schwämme, die Pinakide zum Skelettaufbau verwendet haben, eher im tieferen Wasser siedelten

5. Welche Demospongien haben Skelettelemente vom Typus Pinakid hervor gebracht ?

Das Pinakid ist das einzige aus einer Porenplatte bestehende Spiculum. Schon aus diesem Grund hebt es sich von den anderen Skleren der Demospongien ab.

Die Porenplatte in Form eines Scheibchens wurde von den meisten Autoren als ein Dermalspiculum der „Lithistida" gedeutet. Die Ableitung des Pinakids vom Phyllotriaenen wurde von einer Reihe von Autoren zuletzt von Gasse et.al (1988) angenommen.

Der Autor dieser Studie hat in einer autochthonen Kieselschwammfauna, die der oberjurassischen Beckenfazies (Oberalmer-Schichten) angehört, fast ausschließlich phyllotriaene Skleren unterschiedlichster Bauart mit unfertigen juvenilen und voll entwickelten Pinakiden vergesellschaftet festgestellt. Viele Phyllotriaene sowie Pinakide mit tiefen Einschnitten, die stark den langgezogenen in der Mitte eingeschnürten Poren ähneln, waren mit ein Grund, einen Konnex zwischen Pinakiden und Phyllotriaenen zu sehen.

Wiedenmayer (1994: 84) vertritt die Ansicht, dass eine Homologie der Pinakide und Phyllotriaenen aufgrund der Radialmuster, welches 9 bis 22 Kanäle, die nach der längeren Achse unregelmäßig gebündelt und nach der kürzeren Achse auseinandergezogen sind (Abbildung 7a), nicht aufrecht zu erhalten ist. Viel plausibler sei eine Homologie des Pinakids mit

dem Aspidaster zumal bei den spätkretazischen Pinakiden eine warzenförmige Oberfläche bekannt ist, die eine Ähnlichkeit mit den Aspidastern des rezenten Schwammes *Erylus monticularis* aufweist. Auf die Bildung der vielen Poren geht Wiedenmayer 1994 nicht ein. Zur selben Auffassung kommt Reid (2004: 192) und stellt *Prodactylocalycites* zu den Aspidaster führenden Demospongien der Subfamilie Erylinae Sollas 1888.

Aspidaster sind jedoch erst ab der hohen Oberkreide fossil überliefert und daher ist es nicht möglich, Pinakide, die bereits ab dem basalen Lias vorkommen, von den Aspidastern abzuleiten. Viel mehr müsste es in der Obertrias Formen geben, die Scheibchen ähneln, aber zunächst keine Poren aufweisen, sondern nur Kanäle. Dies wird deshalb angenommen, weil die aus dem basalen Lias nachgewiesenen Pinakide eine eher schlitzförmige Perforation zeigen, die dahin gedeutet wird, dass diese das erste Stadium der Porenbildung darstellen. Es wurden in der Obertrias rundovale und ovale Plättchen gefunden, mit stark reduzierten Rhabd, die zum Teil durch Fehlen eines Rhabds auffielen, doch haben die Durchlichtuntersuchungen ergeben, dass diese triaene bis dichotriaene Kanäle aufweisen (Abbildung 7 b).

Weil sich die Pinakide weder aus den phyllotriaenen Spicula der „Lithistida" noch aus den Aspidastern der ancoriniden Poriferen entwickelt haben, werden sie einer eigenständigen Demospongiengruppe zugeordnet.

Dank

Für die kritische Durchsicht des Manuskriptes und wichtige Hinweise danke ich sehr herzlich Dorte Janussen vom Forschungsinstitut und Naturmuseum Senckenberg, Frankfurt am Main

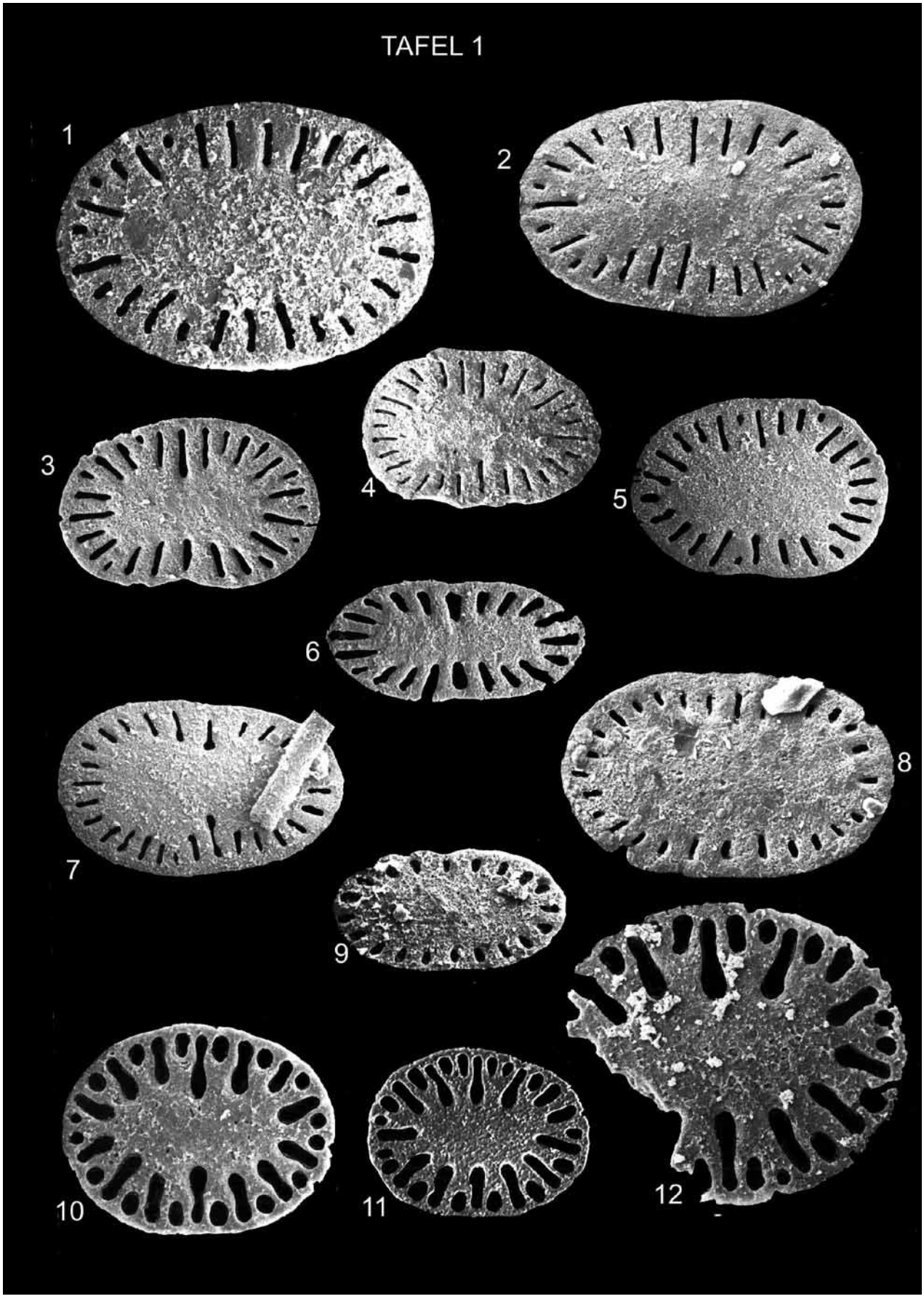
TAFEL 1
1
2
3
4
5
6
7
8
9
10
11
12

Tafel 1

Fig. 1-5; 7-8: *Prodactylocalycites liassicus* n.sp. (Vgr.: Fig.1 =4 00x, Fig. 2 = 300x; Fig. 3 = 280x; Fig. 4 = 200x; Fig. 5 = 280x, Fig. 7 = 280x, Fig. 8 = 400x) Holotypus Fig. 5

Fig. 6 und 9: *Prodactylocalycites trigonalis* n.sp. (Vgr.: Fig. 6 = 350x, Fig. 9 = 300x)

Fig. 10-11: *Prodactylocalycites callodiscus* (Carter) (Vgr. 300x; 250 x)

Fig. 12: Angebrochenes Spiculum welches in der Mitte eine deutliche Verdickung zeigt. Ebenfalls *Prodactylocalycites callodiscus* (Carter), Vergrößerung 400 x

Anmerkungen: Die Exemplare 10-12 stammen aus dem Tithon (höchster Oberjura) der Oberalmer Beckensedimente

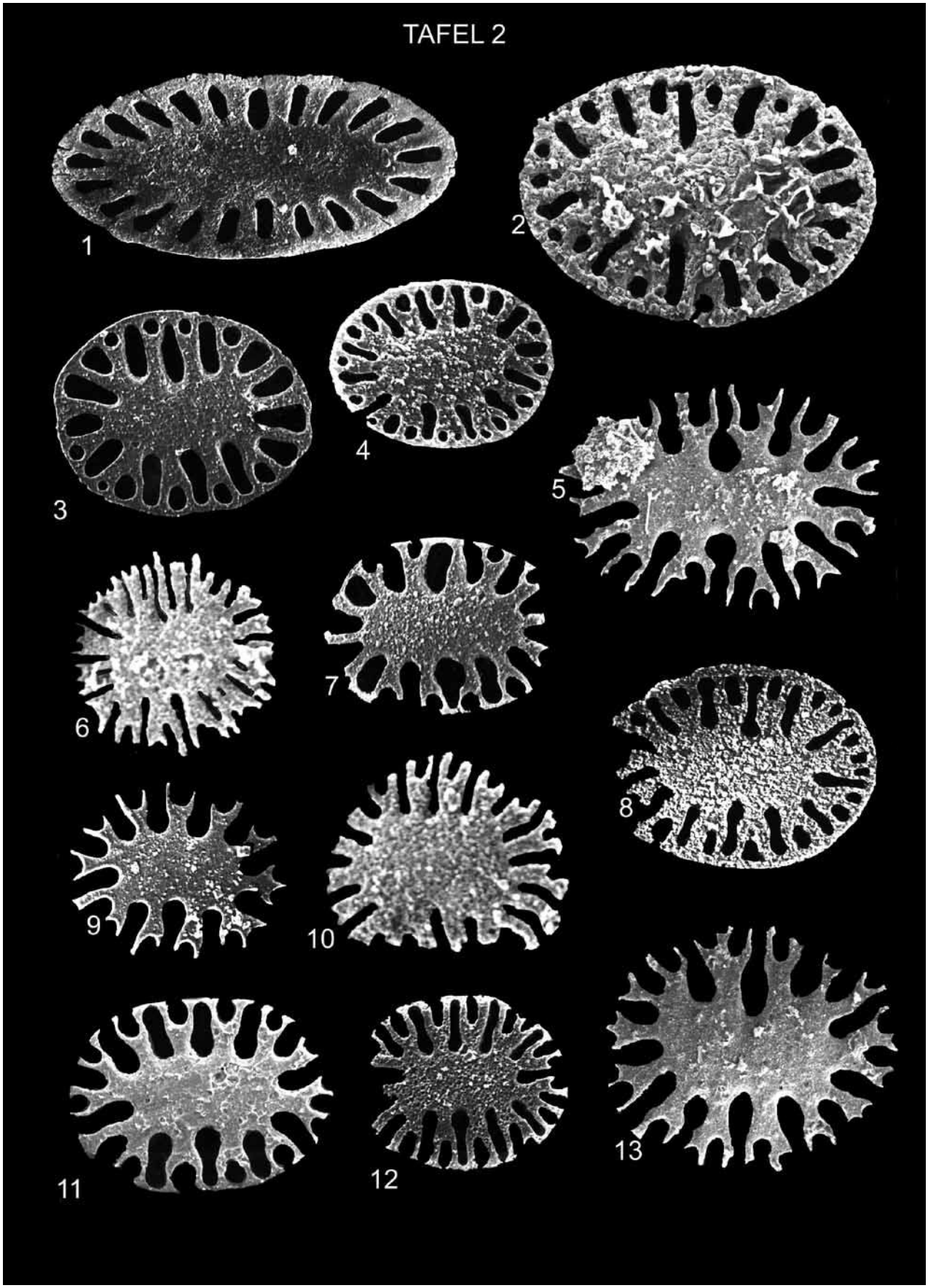
TAFEL 2
1
2
3
4
5
6
7
8
9
10
11
12
13

Tafel 2

Fig. 1: *Prodactylocalycites trigonalis* n.sp; Holotypus (400x) unterer Lias (Hettang)
Fig. 2: Hier handelt es sich möglicherweise um eine neue Art, aber nach dem nur ein Exemplar vorliegt wurde von einer näheren Bestimmung abgesehen.
Fig. 3: *Prodactylocalycites* sp. (300x) aus den unterkretazischen Rossfeld-Schichten; eine sehr außergewöhnliche Form durch die vielen runden Poren
Fig. 4: *Prodactylocalycites* sp. (300x) aus dem Malm
Fig. 5: *Prodactylocalycites* sp. (300x) aus der Unterkreide
Fig. 6: *Prodactylocalycites angustus* n.sp.: Holotypus aus dem Obertithon (300x)
Fig. 7: *Prodactylocalycites* sp. (300x) aus der Unterkreide
Fig. 8: *Prodactylocalycites* cf. *callodiscus* (aus den Rossfeld –Schichten Oberkreide
Fig. 9: juveniles Exemplar von *Prodactylocalycite*s sp. (300x) aus dem Malm
Fig. 10: *Prodactylocalycites* cf. *angustus* (300x)
Fig. 11: P*rodactylocalycites callodiscus* (300x) aus dem oberen Malm
Fig.12: *Prodactylocalycites* cf. *callodiscus* (250x) aus dem Tithon
Fig.13: juvenile Form von *P. callodiscus* (350x) aus dem Malm

TAFEL 3

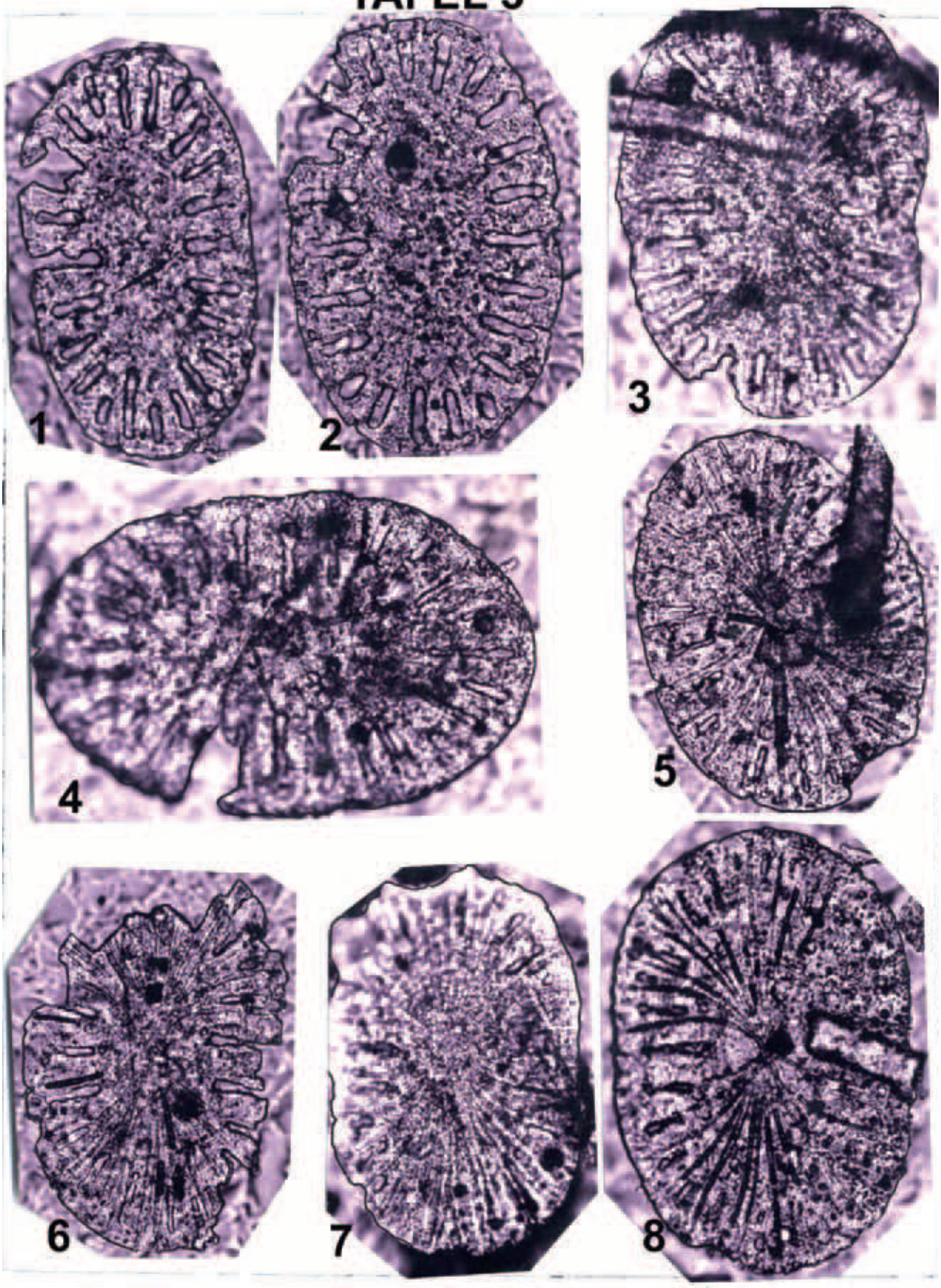

Tafel 3:
Vergrößerung aller Abbildungen = 400x
Es handelt sich um durchlichtmikroskopische Aufnahmen, die v.a. gemacht wurden, um den radialen Kanälen in den tiefliassischen Pinakiden nachzugehen.

In Fig. 1-6 sind die Kanäle sehr gut sichtbar.
Das Innere der Kanäle ist dunkel, der Kanalrand hell, wodurch die Breite der Kanäle sichtbar und wird.

In Fig. 1 und 4 entspricht die Breite der Poren der Breite der Kanäle. Die Poren verbreitern sich von Zentrum zum Außenrand. Besonders gut zu sehen ist, dass die Kanäle senkrecht zur Längsachse der Scheibchen den größten Abstand aufweisen.

Fig. 7 und 8 zeigt sehr gut die verschiedenen Längen der Poren mit sehr langen, mittellangen und kurzen Poren.
In Fig. 1 erkennt man sehr gut eine Bündelung der Kanäle; ob sie dort verwachsen sind lässt sich nicht nachweisen.

Literatur

Carter, H.J. (1871): On fossil sponge-spicules of the Greens and compared with those of the exciting species. - Ann. Mag. Nat. Hist. (4) 7; 112-141, pls.7-10.

Dendy, A. (1921). The tetraxonid sponge spicule, a study in evolution. – Acta Zool. Stockholm, 2: 95-152.

Gasse, W, Göcke, R. & Hilper, K.H. (1988): Oberkretazische Spongien des NW-Münsterlandes. - Beitr. Elektronenmikrosk. Direktabt. Oberfl. 21: 388-395, Kassel.

Kennett, J.B., Houtz R.E. & et al (1975): Site 282 - Kennett, J.B.; Houtz R.E. & et al: initial reports of deep sea drilling project, vol. 29, b. 317-363. US Government, Printing Office Washington.

Mostler, H. (1986): Ein Beitrag zur Entwicklung phyllotriaener Megaskleren (Demospongea) aus oberjurassischen Beckensedimenten (Oberalmer Schichten, Nördliche Kalkalpen). - Geol. Paläont. Mitt. Innsbruck, 13: 331-361, Innsbruck.

Rauff, H. (1893-94): Palaeospongiologie. Erster und allgemeiner Teil und zweiter Teil erste Hälfte. - Palaeontographica, 40, Stuttgart.

Reid, R.E.H. (2004): Mesozoic and Cenozoic Choristid Demosponges. – In: Rigby, J.K., Finks, R.M. & Reid, R.E.H. (eds): Treatise on Invertebrate Paleontology, Part E, Vol. 3 Porifera, Geol. Soc. of America, Kansas, 175-198.

Rigby, J.K., Finks, R.M. & Reid, R.E.H. (2004): Treatise on Invertebrate Paleontology, Part E, Vol. 3 Porifera. - Geol. Soc. of America, Kansas, 872p.

Rüst, D. (1885): Beiträge zur Kenntnis der fossilen Radiolarien aus Gesteinen des Jura. – Palaeontographica, 31: 269-322.

Sollas, W.J. (1888): Report of the Tetractinellida collected by H.M.S Challenger. - Rep. Sci. Results Voyage Challenger, Zool. 25, 63, clxvi + 458 p., 44 pls., 1 Map.

Wiedenmayer, F (1994): contributions to the knowledge of post-Paleozoic neritic and archibenthal sponges (Porifera). - Schweizerische Palaeont. Abh., 147 Seiten, Basel.

Manuskript eingereicht: 21.2.2011
Manuskript angenommen: 16.8.2011

Geo.Alp, Vol. 8, S. 20–44, 2011

MONTANGESCHICHTE, MINERALOGIE, GEOCHEMIE UND PETROLOGIE DER KUPFERLAGERSTÄTTE BARTHOLOMÄBERG/SILBERTAL (MONTAFON, VORARLBERG)

Peter Tropper[1], Daniel Bechter[1], Johannes Zambanini[1], Reinhard Kaindl[2], Franz Vavtar[1], Joachim Lutz[3]

Mit 16 Abbildungen und 3 Tabellen

[1] Institut für Mineralogie und Petrographie, Fakultät für Geo- und Atmosphärenwissenschaften, Universität Innsbruck, Innrain 52f, A-6020 Innsbruck, Österreich
[2] MATERIALS – Institut für Oberflächentechnologien und Photonik, JOANNEUM RESEARCH Forschungsges.mbH, Leobner Straße 94, A-8712 Niklasdorf, Österreich
[3] Curt-Engelhorn-Zentrum Archäometrie GmbH, D6, 3, D-68159 Mannheim, Deutschland

Zusammenfassung

Das Ziel dieser Arbeit im Rahmen des Sonderforschungsbereiches HiMAT war die mineralogische-petrologisch-geochemische Charakterisierung der historischen Kupferlagerstätte Bartholomäberg/ Silbertal um einerseits lagerstättengenetische und andererseits archäometrisch relevante Aussagen zu treffen. Die Erzmineralisation tritt in der Phyllitgneiszone auf und die Mineralparagenese in den untersuchten Proben besteht im Wesentlichen aus Chalkopyrit $CuFeS_2$, Pyrit FeS_2 und Fahlerz $Cu_{12}Sb_4S_{13}$(Tetraedrit)-$Cu_{12}As_4S_{13}$(Tennantit), das auf Grund seiner wenn auch geringen Ag Gehalte von max. 0.69 Gew.% u.a. primäres Ziel der Abbautätigkeit war. Die Fahlerze lassen auf Grund ihrer unterschiedlichen Sb:As- und Zn:Fe-Verhältnisse eine intensive, fleckige Zonierung erkennen. Dem Mineralchemismus nach können sie als Ferro-Tetraedrit bis Ferro-Tennantit und untergeordnet als Zink-Tetraedrit bis Zink-Tennantit beschrieben werden. Nur als akzessorische Gemengteile konnten Galenit PbS, Sphalerit ZnS, Arsenopyrit FeAsS, Alloklas (Co,Fe)AsS oder Glaukodot (Co,Fe)AsS, Gersdorffit NiAsS, Korynit Ni(As,Sb)S, ged. Wismut, Aikinit $PbBiCuS_3$, ged. Gold sowie die Ag-Minerale Luanheit Ag_3Hg und Akanthit Ag_2S nachgewiesen werden. Die Gangart besteht aus Quarz, Siderit-Magnesit Mischkristallen sowie untergeordnet aus Kalzit. Am Kristbergsattel tritt als weiteres Gangartmineral auch Baryt auf. Der Pauschalchemismus der Erze aus dem Montafon unterscheidet sich hinsichtlich der Neben- und Spurenelemente vor allem durch höhere Bi-Gehalte von bis zu 1 Gew.% von den anderen im Rahmen des SFB HiMAT untersuchten Kupferkieslagerstätten (Mitterberg am Hochkönig und Kelchalm bei Jochberg) sowie den Fahlerzvorkommen im Unterinntal (Schwaz/Brixlegg).
Für die genetische Interpretation der Kupferlagerstätte von Bartholomäberg/Silbertal sind die im Chalkopyrit gelegentlich erkennbaren, oleanderblattförmigen α-β-Umwandlungslamellen von hochtemperiertem, kubischem zu tieftemperiertem, tetragonalem Chalkopyrit von großer Aussagekraft. Diese Transformationslamellen weisen nach Yund und Kullerud (1966) auf eine minimale Bildungs- bzw. Umbildungstemperatur von 547 ±5° C hin. Hingegen soll nach Ramdohr (1975) tetragonaler Chalkoyprit im natürlichen System <400°C entstanden sein. Diese Mindesttemperatur müssen daher die Chalkopyrite der untersuchten Lagerstätten erfahren haben. Allerdings konnten Thöni (1981) und auch Maggetti und Flisch (1993) in den Gesteinen der Silvrettadecke lediglich alpidische Metamorphosetemperaturen von <300°C nachweisen. Somit kann es sich bei den α-β Umwandlungslamellen im Chalkopyrit der Lagerstätten nur um prä-alpidische, möglicherweise permische Relikte vermutlich in mittelbarem Zusammenhang mit der Ablagerung hochtemperierter Vulkanoklastika handeln. Unter der Annahme eines homogen eingefangenen Fluids geben die Homogenisierungstemperaturen von ca. 200°C der Flüssigkeitseinschlüsse im Quarz und in den Karbonaten der Gangart ihre Mindestbildungstemperatur an und weisen auf alpidische Temperaturen hin. Mittels der Isochoren kann der dabei vorherrschende Druck auf max. 4 kbar eingegrenzt werden, was einer Bildungstiefe von ca. 12 km entspricht.
Demnach dürfte es sich bei den Vererzungen von Bartholomäberg/Silbertal sehr wahrscheinlich um prä-alpidische, möglicherweise permische Mineralisationen handeln, die während eines tieftemperierten jungalpidischen Stadiums überprägt und mobilisiert worden sind.

Summary

In the course of the SFB (Sonderforschungsbereich) HiMAT was the ore deposit Bartholomäberg/Silbertal investigated from a mineralogical-petrological and geochemical perspective. The geological frame of the area of investigation is the Phyllitgneiszone, which is located in Vorarlberg between the Northern Calcareous Alps and the Silvretta Crystalline Complex. The ores occur in discordant veins and the main ore mineral assemblage consists of common copper sulfides such as chalcopyrite ($CuFeS_2$), pyrite (FeS_2) and fahlore-group (tetraedrite $Cu_{12}Sb_4S_{13}$ - tennantite $Cu_{12}As_4S_{13}$) minerals. Latter was mined in this area due to its Ag contents of up to 0.69 wt.%. In addition the minerals galena PbS, sphalerite ZnS, arsenopyrite FeAsS, alloklase (Co,Fe)AsS or glaukodot (Co,Fe)AsS, gersdorffite NiAsS, korynite Ni(As,Sb)S, native Bi, aikinite $PbBiCuS_3$, native Ag as well as the Ag-bearing minerals luanheite Ag_3Hg und akanthite Ag_2S were found. The gangue is mainly composed of quartz, magnesite-siderite and occasionally calcite. The whole rock composition of ore samples yielded high Bi contents up to 1 wt.%, which distinguishes it from the other East-Alpine deposits (Mitterberg, Kelchalm, Schwaz-Brixlegg) investigated in the course of this SFB.

Rare high-T α–β exsolution textures in chalcopyrites indicate a relict pre-Alpine (possibly Permian) high-T formation, namely 550°C according to Yund and Kullerud (1966) and <400°C according to Ramdohr (1975), most likely associated with volcanoclastic deposition. This result is supported by geothermometrical data, which yielded only T <300°C for the Eo-Alpine event in this region (Thöni, 1981; Maggetti and Flisch, 1993). Fluid inclusion studies support the low-T origin of the deposit Bartholomäberg/Silbertal at T of <200°C and <4 kbar most likely during the latest stages of the Alpine orogeny.

Einleitung

Die vorliegenden Untersuchungen wurden im Rahmen des Sonderforschungsbereiches SFB HiMAT (The History of Mining Activities in the Tyrol and Adjacent Areas) durchgeführt (Oeggl et al., 2008). Der SFB HiMAT hat es sich zum erklärten Ziel gesetzt, die bedeutenden Kupferlagerstätten im Westbereich des ostalpinen Raums interdisziplinär zu erforschen und zu untersuchen. Die Untersuchungen konzentrierten sich auf vier wichtige Regionen, die key areas: Bartholomäberg/Silbertal (Vlbg.), Kitzbühel-Kelchalm (T), Schwaz-Brixlegg (T) und Mitterberg (Szbg.). Die vorliegende Arbeit wurde im Rahmen des PP 10 (Projektteil 10: Mineralogisch-geochemische Erfassung historischer Bergbaue) am Institut für Mineralogie und Petrographie an der Universität Innsbruck durchgeführt. Ziel war die Charakterisierung der Erzparagenese der historischen Kupferlagerstätten Bartholomäberg und Silbertal im Hinblick auf die Lagerstättengenese und ihre archäometallurgische Relevanz.

Arbeitsmethoden

2.1 Elektronenstrahlmikrosonde (EMPA)

Die Analysen wurden am Institut für Mineralogie und Petrographie der Universität Innsbruck mit einer Elektronenstrahlmikrosonde (EMPA) vom Typ JEOL 8100 SUPERPROBE durchgeführt. Zu diesem Zweck wurde im Rahmen dieser Arbeit ein 21 Elemente umfassendes wellenlängendisperives Analysenprogramm erstellt. Mit den Elementen Fe, Zn, Cu, Ni, Sn, Te, Bi, Sb, In, Cd, Ag, Pb, S, Mo, Hg, Au, Se, As, Ge, Co, Mn und S ist es möglich, das gesamte Elementspektrum von Sulfidmineralen zu untersuchen. Die Proben wurden mit 15 kV Anregungsspannung und 10 nA Probenstrom gemessen. Die Zählzeiten betrugen zwischen 40 und 50 Sekunden für den Peak bzw. den Untergrund. Als Standardmaterialien wurden für Fe, Zn, Cu, Ni, Sn, Te, Bi, Sb, In, Cd, Ag, Mo, Au, Se, As, Ge, Co und Mn Reinstoffe, für Pb wurde PbS und für S wurde FeS verwendet. Es wurden Interferenzkorrekturen für S-Mo, Mo-Bi, Se-As, Hg-Au, Te-Ni, Te-Ag, Bi-Pb, Hg-Mo, Te-Sn, In-Cd und Bi-S gemacht. Die Elemente Fe, Zn, Cu, Ni, Co und Mn wurden mit der Kα Linie gemessen, Sn, Sb, In, Cd, Ag, Se sowie Ge mit der Lα Linie und Mo mit der Lβ Linie. Die Elemente Bi, Pb, Hg und Au wurden mit der Mα Linie gemessen.

2.2 Ramanspektrometer und Heiz-Kühltisch

Für die Untersuchungen der Flüssigkeitseinschlüsse wurden in einem ersten Schritt die Totalhomogenisationstemperaturen mittels eines Heiz-Kühltisches der Firma LINKAM™ Scientific Instruments bestimmt, der über einen Temperaturregler und eine Flüssig–stickstoffsteuerung mit Kühlbehälter verfügt. Für

die Kalibrierung der Heiz-Kühltischanalage kamen synthetische H_2O, H_2O-NaCl und H_2O-CO_2 Flüssigkeitseinschlüsse von der Montanuniversität Leoben zum Einsatz. Für die Untersuchung der Flüssigkeitseinschlüsse wurden zwei doppelseitig polierte Dünnschliffe mit einer Dicke von ca. 100 µm angefertigt. Zur Phasenidentifikation und Abschätzung der Salzgehalte der Einschlüsse wurden die Proben mittels dem LabRAM-HR800 (HORIBA™) Mikro-Ramanspektrometer am Institut für Mineralogie und Petrographie unter Mithilfe von Dr. Reinhard Kaindl untersucht. Dabei wurden die Proben mit der 633 nm Emissionslinie eines 17 mW He-Ne-Laser und der 532 nm Emissionslinie eines 30 mW Nd:YAG Lasers durch ein OLYMPUS 100X Objektive angeregt. Der Laser hatte einen Durchmesser von ca. 1 µm auf der Probenoberfläche und wies eine Energie von ca. 5 mW auf. Die spektrale Zerlegung erfolgte durch ein Gitter mit 1800 Linien/mm, das gestreute Licht wurde mit einer 1024 x 256 open-electrode CCD detektiert. Die spektrale Auflösung und Genauigkeit des Spektrometers betrug ca. 2 bzw. $\pm$ 0.5 cm^{-1}, Justage und Kontrolle erfolgte durch regelmäßige Anpassung der 0.-ten Ordnung des Gitters und Messung der Rayleigh-Linie.

2.3 Neutronenaktivierungsanalyse (NAA) und Massenspektrometrie (ICP-MS)

In den Erzen wurde eine Reihe archäometallurgisch relevanter Elemente mittels Neutronenaktivierungsanalyse (Cu, Fe, As, Sb, Co, Ni, Ag, Au, Sn, Zn, Se, Te und Hg) und Massenspektrometrie mit induktiv gekoppelter Plasmaanregung (ICP-MS; Pb und Bi) bestimmt. Diese Analysen wurden vom Projektteil PP 09 (Archäometallurgische und geochemische Erfassung des historischen Bergbaues) durchgeführt.

Geographischer Überblick

Die Ortschaft Bartholomäberg liegt auf einer nach SW hin orientierten Terrasse auf 1087 m ü. A (Abb. 1). Die Ortschaft Silbertal liegt im Silbertal und befindet sich ca. 6 km entfernt von Schruns, der größten Ortschaft des Montafons (Abb. 1). Die Straße ins Silbertal führt entlang der Litz, die bei Schruns in die Ill mündet. Das Silbertal erstreckt sich von Schruns in östlicher Richtung bis hin zur Landesgrenze von Tirol. Die Proben stammen aus den Haldenzonen Knappagruaba (Bartholomäberg) und Kristberg (Silbertal).

Geologischer Überblick

4.1 Silvrettakristallin

Den geologischen Rahmen bilden das Silvrettakristallin und die Phyllitgneiszone, wobei die Lagerstätten Bartholomäberg und Silbertal an der NW Grenze der Phyllitgneiszone zur Lechtaldecke der Nördlichen Kalkalpen liegen. Die geologische Stellung der hier beschriebenen Einheiten wurde sehr kontrovers diskutiert, wobei mehrere unterschiedliche Thesen und Modelle existieren (Tollmann, 1977, Schmid et al., 2004). Die Silvrettadecke weist eine Größe von ca. 1600 km^2 auf und wird aus gut je einem Drittel Metabasiten, Metagranitoiden und Paragneisen aufgebaut (Maggetti und Flisch, 1993). Übereinstimmende Meinungen gibt es hinsichtlich des Metamorphosegrades im nördlichen Bereich der Silvrettadecke. Die kristallinen, austroalpinen Basementareale weisen eine polymetamorphe Entwicklungsgeschichte auf (Schmid et al., 2004, Schweinehage, 2000, Mayerl, 2005). Auf Grund der tektonostratigraphischen Position blieb die Silvrettadecke von einer stärkeren eo-alpidischen Metamorphose weitgehend verschont, womit das prägende Metamorphoseereignis hinsichtlich des Gefüges und der Mineralparagenese die variszische amphibolitfazielle Metamorphose ist (Amann, 1985; Schweinehage, 2000).

Nach Frank (1987), Schuster und Frank (1999), Schuster et al. (2001) und Schmid et al. (2004) ist der Begriff des „Mittelostalpins" auf Grund strukturgeologischer und tektonstratigraphischer Aspekten als überholt anzusehen. Schmid et al. (2004) rechnen das von Tollmann (1977) postulierte Mittelostalpin zum Oberostalpin und unterteilen die oberostalpinen Einheiten in vier Deckensysteme. Sie folgen damit in groben Zügen dem tektonischen Muster von Schuster et al. (2001). Die einstige mittelostalpine Silvrettadecke wird daher nach Schmid et al. (2004) dem Silvretta-Seckau Deckensystem zugeordnet. Bei dem Silvretta-Seckau Deckensystem handelt es sich laut Schmid et al. (2004) um sämtliche austroalpinen Basementdecken, die im westlichen Randbereich der austroalpinen Decken in der Ost-Schweiz auftreten (Languard und Campo- Sesvanna Silvretta Decke). Demnach wurden diese Deckeneinheiten in der Ostschweiz über die unterostalpinen Einheiten während der eo-alpinen Orogenese in WNW-Richtung aufgeschoben. Diese WNW gerichtete eo-Alpine Deformationsphase entspricht nach Froitzheim et al. (1994) der „Trupchun" Phase.

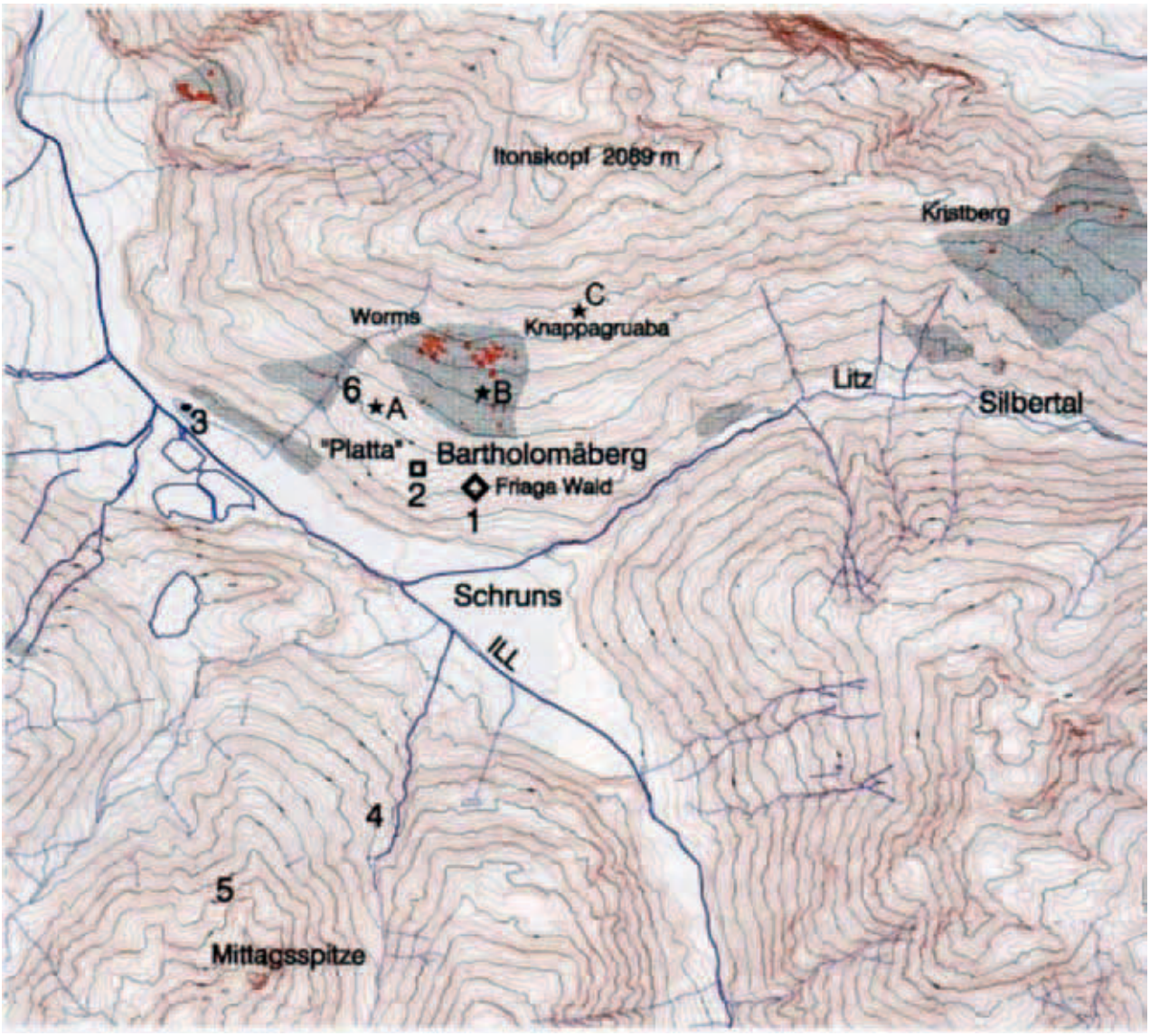

Abb. 1: Orohydrographische Karte des Schrunser Beckens mit Bartholomäberg und der Lage der prähistorischen Höhensiedlung im Friaga Wald (1), dem neu entdeckten bronzezeitlichen Siedlungsplatz auf der Platte (2), sowie den mittelalterlichen Haldenzonen im Gewann Knappagruaba, Worms und am Kristberg im Silbertal. Kartengrundlage Kataster des Montafons, Grafik Forschungsprojekt Montafon, aus Krause et al. (2004).

Aus petrologischer Sicht baut sich die Silvrettadecke aus Metasedimenten, Orthogneisen, Amphiboliten sowie untergeordnet permischen Diabasgängen und variszischen Eklogiten auf. Weiters weist die Silvrettadecke im Bereich der Ducan Mulde und des Landwassergebietes eine anchimetamorphe, permomesozoische Sedimentbedeckung auf, wobei die Schichtabfolge des Lias und die stratigraphisch höheren Ablagerungen erosiv fehlen (Leupold, 1934). In der geologischen Karte von Oberhauser und Rataj (1988) wird die Silvrettadecke von den Einheiten des Unterostalpins und den penninischen Einheiten unterlagert. Die penninischen Einheiten grenzen in Form des Engadiner Fensters am E Rand der Silvrettadecke an, wobei ein weiteres penninisches Fenster innerhalb der Silvrettadecke auftritt, nämlich das Fenster von Gargellen. Der Kontakt an den Deckengrenzen zwischen der Silvrettadecke und den penninischen Fenstern wird durch das Auftreten von Pseudotachyliten begleitet. Die östliche Begrenzung der Silvrettadecke zum Engardiner Fenster wird durch die sinistrale Engadiner Störung markiert.

Der Landecker Quarzphyllit und die Phyllitgneiszone stellen den nördlichen Rand der Silvrettadecke dar. Hammer (1918) grenzt die Phyllitgneiszone und den Landecker Quarzphyllit von der Silvrettadecke ab.

Laut Nowotny et al. (1993) dominieren zwei größere Gruppen von Metasedimenten den Bereich um Landeck. Dies sind zum einen helle quarzreiche Metapelite und zum anderen Paragneise und Zweiglimmerschiefer. Bei den von Hammer (1918) bezeichneten Phylliten, den sog. Landecker Quarzphylliten, handelt es sich laut Nowotny et al. (1993) um helle phyllitische Glimmerschiefer, die zum Teil Granat, Biotit sowie Staurolith bzw. deren Fragmentrelikte enthalten.

Nach Froitzheim et al. (1994) ist der ostalpine Deckenstapel als ein Resultat der tektonischen Verschuppung während des Jura und der Unterkreide am passiven Kontinentalrand der adriatischen Mikroplatte anzusehen. Froitzheim und Eberli (1990) korrelieren die heutige tektonische Position mit der ungefähren, damaligen paläogeographischen Lage am Kontinentalrand der adriatischen Platte. Daher nimmt die Silvrettadecke, die in der obersten Position des austroalpinen Deckenstapels liegt, eine proximale Position am Kontinentalrand ein. Die alpidische Metamorphose in den ostalpinen Einheiten westlich des Tauernfensters weist ein Temperaturmaximum bei 100 – 85 Ma auf (Thöni, 1982). Nach Dunoyer et al. (1976) und Giger (1985) wurde das Temperaturmaximum der kretazischen Metamorphose vor 110 – 90 Ma erreicht. Die eo-alpidische Metamorphose ist in der Silvrettadecke sehr gering. Während im Westen der Silvrettadecke anchizonale Bedingungen auftreten, kommt es nach Osten hin zu einer Erhöhung der Metamorphose, dokumentiert durch die grünschieferfaziellen Bildung von Stilpnomelan in den Metagraniten (Grauert, 1969, Amann, 1985).

4.2 Die sedimentären Bedeckung

Weil das Auftreten der Erzkörper auf den Kontaktbereich zur Phyllitgneiszone beschränkt ist, wird die sedimentäre Bedeckung, die sog. Lechtaldecke, des kristallinen Basements ebenfalls beschrieben. Die Sedimentation in den ostalpinen Faziesräumen umfasst den Zeitraum vom unteren Perm bis in die Kreide wobei im Zuge dieser Arbeit nur die Sedimente vom unteren Perm bis in die untere Trias (Skyth) beschrieben werden. Die Sedimentation beginnt im unteren Perm mit den Kristbergschichten (Reithofer, 1955; Mostler, 1972; Angerer, 1978, Van Ameron et al., 1982; Spiess, 1985, Mayerl, 2005). Es handelt sich um klastische Sedimente, deren Vorkommen nur auf das Montafon beschränkt ist. Sie werden in untere-, mittlere- und obere Kristbergschichten unterteilt. Die unteren Kristbergschichten bestehen aus Basisbrekzien und Konglomeraten. Die mittleren Kristbergschichten weisen Karbonate auf und bauen sich aus sandig- bis tonigen Serien auf. Die oberen Kristbergschichten bestehen aus einer mittel- bis grobklastischen Hangendserie. Der Kontakt Silvrettadecke/Kristbergschichten ist tektonischer Natur.

Darüber folgen die Unterrotliegend Serie und Grödener Formation (Angerer 1976; Angerer et al., 1978; Leichtfried, 1978). Nach Tollmann (1985) wird die Basis des Südrandes der Nördlichen Kalkalpen vom Alpinen Verrucano, der eine grob- bis feinklastische, überwiegend terrestrische Abfolge von mehreren 100 m spätvariszischer Molasse darstellt, gebildet. Die für die Unterrotliegend Serie charakteristischen sauren Vulkanite wurden erstmals durch Reithofer (1954) beschrieben. Eine sinnvolle Unterscheidung von der Unterrotliegend Serie und dem Grödener Sandstein wird erst zulässig und sinnvoll durch das Auftreten von Vulkaniteinschaltungen. Innerhalb der Unterrotliegend Serie lassen sich nach Angerer (1976) drei, zeitlich voneinander abtrennbare, vulkanische Ereignisse abgrenzen. Im mittleren und oberen Quarzporphyrhorizont sind nach Angerer et al. (1978) teilweise Ignimbrite ausgebildet, die mit disseminierten Kufpervererzungen in Zusammenhang stehen.

Bei den Sedimenten der unteren Trias (Skyth) handelt es sich um den Alpinen Buntsandstein und die Punt la Drossa-Schichten. Leichtfried (1978) weist die als „Hangendquarzite" bezeichnete Serie zur Gänze dem Alpinen Buntsandstein zu (Krainer, 1982). Nach Stingl (1987) wurde der Alpine Buntsandstein in einem Wechselspiel aus randmarinen, ästurinen und fluviatilen Sedimentationsprozessen abgelagert. Hinsichtlich der Fazies bzw. des Ablagerungsraumes lässt sich erst im Oberen Alpinen Buntsandstein eine randmarine Fazies nachweisen (Mayerl, 2005). Die Punt la Drossa Schichten, die nach Heissel et al. (1965) als Reichenhaller Rauwacke bezeichnet wurden, stellen nach Tollmann (1977) eine Sonderfazies innerhalb der Reichenhaller Formation im westlichen Abschnitt der Nördlichen Kalkalpen dar. Die Punt la Drossa Schichten sind charakterisiert durch eine ockerfarbene Rauwacke, bei denen es sich um Ablagerungen in einer seichten, hypersalinaren Lagune mit aridem Klima handeln soll (Bertle, 1979).

Abb. 2: Panoramaaufnahme westlich der Knappagruaba. Links von der Hütte sind die Halden zu erkennen. Rechts knapp oberhalb der Hütte ist ein verstürzter Stollenzug zu erkennen.

Historische Betrachtung der Siedlungsgeschichte und des historischen Bergbaues

Im Rahmen des SFB HiMAT wurden neben den geologischen und mineralogischen Aspekten der historischen Kupferlagerstätte Bartholomäberg/Silbertal auch archäologische Untersuchungen und Ausgrabungen seitens des Projektteiles PP 08 (Siedlungsarchäologie und vorgeschichtlicher Bergbau im Montafon, Vorarlberg) durchgeführt. Die Arbeiten zur (Be)-Siedlungsgeschichte wurden bereits vor Beginn des SFB HiMAT im Jahr 2000 begonnen und umfassen mehrere Ausgrabungen sowie zahlreiche wichtige archäologische Funde (Krause, 2001; Krause et al., 2004, Krause, 2005, 2006, 2007). Gegenstand und Forschungsziel ist die frühe Besiedlung des Montafon sowie die Entwicklung der Gesellschaft und die Auswirkungen des Bergbaues auf die Umwelt und auf die Sozialstruktur. Zusätzlich zu archäologischen Unteruchungen wurden von Seiten des Projektteiles PP 11 (Paläoökologie und Subsistenzwirtschaft in Bergbaurevieren) Moore in unmittelbarar Siedlungsnähe untersucht, um aus den Pollenanalysen Hinweise auf Besiedlungsspuren wie z.B. Rodungen und Nutzungen von landwirtschaftlichen Flächen zu erhalten.

Nach Krause et al. (2004) ist eine dauerhafte Nutzung und Besiedlung des Schrunser Beckens gegen Ende der Jungsteinzeit als gesichert anzusehen, was durch das Vorhandensein von festen Siedlungen in diesem Raum dokumentiert ist. Pollenanalysen weisen auf erhebliche Siedlungsaktivitäten insbesondere ab der späten Frühbronzezeit sowie in der mittleren Bronzezeit um 1700/1600 v. Chr. und im 6. Jhd. v. Chr. in der Eisenzeit hin (Oeggl, 2003). Durch Ausgrabungen konnte eine befestigte Burganlage im Friaga Wald auf 940 m.ü.A. dokumentiert werden (Krause, 2001). Diese Anlage liegt am Südrand einer Geländeterrasse mit dem Flurnamen „Platta". Die Siedlungsfläche beträgt 90 x 50 m und ist in zwei Siedllungsterrassen unterteilt. Rund 80 m lange und 2-3 m breite Trockenmauern schützten die als Burg zu bezeichnende Anlage zur Bergseite hin. Die „Platta" dürfte für feldwirtschaftliche Aspekte genutzt worden sein (Krause et al., 2004). Die Datierungen einer Lochhalsnadel und anderer Metallartefakte weisen auf die mittlere Bronzezeit hin. Innerhalb der Burganlage war ein Siedlungsplatz für etwa 30-40 Personen vorhanden, die sich auf ca. 6-8 Häuser aufgeteilt haben. Die innerhalb der Burgbefestigung lebende Bevölkerung repräsentierte wahrscheinlich den privilegierten Teil der Gesellschaft, wobei weitere Teile der Gesellschaft außerhalb der Fortifikation (militärische Befestigung) gelebt haben dürften (Krause et al., 2004).

Die Burganlage lässt sich mit den zeitlich und baulich ähnlichen Befestigungsanlagen wie Mutta bei Fellers oder mit dem Gschleirsbühel bei Matrei am Brenner (Zemmer-Planck, 1978) im Alpenraum vergleichen. In der stratigraphischen Abfolge der Siedlung im Friaga Wald lassen sich über den Schichten der Früh- und Mittelbronzezeit eisenzeitliche Schichten ausmachen die durch Keramikfunde in die späte Hallstattzeit und die frühe Latènezeit datiert werden können (Krause et al., 2004). Die geographisch günstig gelegene Talschaft mit ihren Passübergängen in die Schweiz und in den Tiroler Raum führte während der jüngeren Eisenzeit auch zu einer Vermischung zweier inneralpiner Kulturen. Dies manifestiert sich in den Funden von „Schneller Waren" aus dem Rheintal sowie von „Fritzener Schalen", welche aus dem Tiroler Inntal stammen (Krause et al., 2004).

Auf Grund von Pollenanalysen von den Mooren Garsella, Tschuga, Brannertsried, Wildes Ried und Matschwitz von Oeggl (2003) lassen sich auch detaillierte Aussagen über die Besiedlungsgeschichte dieser Region treffen. Die Pollenprofile weisen darauf hin, dass in den montanen Lagen durchwegs ein dichter Fichten- und Tannenwald mit Beteiligung von Buche vorherrschte. Erste Siedlungsanzeiger treten gegenläufig mit der Entwicklung von Tanne und Fichte auf. Die Abnahme von Tanne und Fichte und das Auftreten von Getreidepollen zeugen von lokalen Rodungen um 2500 v. Chr. Pilze, die auf Dung wachsen, weisen auf Weidenutzung hin. Lokaler Ackerbau auf den Hangterrassen ist durch Getreidepollen dokumentiert. Eine erste Siedlungsphase setzte vor ca. 2100 v. Chr. ein, wobei diese nur von kurzer Dauer war. Die zweite, weitaus intensivere Nutzung, wird durch einen massiven Einbruch von Fichte und Tanne im Pollenprofil dokumentiert und setzte gegen 1700 v. Chr. ein. Gräser und Weidezeiger weisen nun einen stark erhöhten Wert auf. Von 1600-1300 v. Chr. verstärkten sich die Siedlungsaktivitäten, wobei gegen 1300 v. Chr. nur noch geringe Indikatoren nachweisbar sind. Die vorangegangenen lokalen Rodungen erlangten im 5. Jhd. einen großmaßstäblichen Charakter welcher mit einer intensiven landwirtschaftlichen Nutzung einherging. Während der Römerzeit bis hin zur Völkerwanderung sind die anthropogenen Spuren stark rückläufig. Erst um 800 n. Chr. lassen sich wieder intensivere Nutzungen ausmachen. Dies ist durch hohe Werte von Gräsern und Weidezeigern in den Pollenprofilen dokumentiert (Oeggl, 2003).

Ein gesicherter Nachweis von prähistorischen Bergbauaktivitäten konnte bis jetzt allerdings noch nicht erbracht werden. Es ist jedoch anzunehmen, dass die Gesellschaftsentwicklung auch in Zusammenhang mit dem Abbau und der Gewinnung der in dieser Region vorkommenden Erze zu setzen ist. Aus Urkunden, die aus der Zeit Ludwigs des Frommen stammen, geht nämlich der Einkauf von Eisengütern in Rankweil (814 n. Chr.) und Bürs (820 n. Chr.) hervor (Scheibenstock, 1996). Die erste eindeutig gesicherte historische Quelle, die auf bergbauliche Aktivitäten im Montafon hinweist, stammt aus dem rhätischen Reichsurbar des Bistums Chur aus dem Jahre 842. In diesem wird ein Eisenbezirk „ministerium ferraires" ausgewiesen, der zwischen Bürs und dem Arlberg zu liegen scheint (Scheibenstock, 1996). In diesem Urbar ist auch die Rede von acht Schmelzöfen („ocoto fornaces"). Diese Schmelzöfen hatten Abgaben an den König zu leisten, wobei nur der „Schultheiß", der Bergrichter, von dieser Abgabe befreit war (Scheibenstock, 1996). Aus einer Urkunde des deutschen Königs Friedrichs des Schönen von 1319 findet sich der Hinweis auf „argetni-fodina seu mons dictus muntafune". Die Bedeutung dieser „Silbergruben oder der Berg genannt Muntafune" spiegelt sich darin, dass es sich bei dieser Grube um ein Reichslehen handelt.

Die Knappen am Kristberg erbauten als Dank für die Rettung von verschütteten Knappen die „Agathakilkli", die Kapelle zu Ehren der Bergbaupatronin St. Agatha. Der Bau der Kirche ist durch eine Urkunde aus dem Jahre 1450 verbucht (Scheibenstock, 1996). In der Kirche ist ein senkrecht nach unten verlaufender Stollen bzw. Schacht angeschlagen, der damals als Rettungsstollen für die verschütteten Knappen gedient haben soll.

Der Niedergang des Bergbaues in Bartholomäberg und Silbertal hat verschiedene Ursachen. In einer Urkunde des Jahres 1598 berichtet der Bergrichter nur noch von einem Bau. 1610 wurde der ergiebige Abbau am Lobinger wegen „Mangel des Lusts" aufgegeben (Scheibenstock, 1996). Des Weiteren wird von Religionsstreitigkeiten unter den Knappen berichtet. Die Entdeckung Amerikas und die billigeren Importe von Kupfer und Silber aus der Neuen Welt setzten dem Bergbau weiter zu (Scheibenstock, 1996).

Im 18. Jhd. kam es zu einer Wiederbelebung des Bergbaues. Da jedoch die Erzausbringung wenig ergiebig war, wurde ein Ansuchen für den Bau einer Schmelzhütte seitens der Bergbaubehörde in Schwaz abgelehnt, womit nur noch der Transport der Erze nach Brixlegg als einzige Alternative übrig blieb. Den endgültigen Niedergang des Bergbaues datiert Scheibenstock (1996) in das Jahr 1760. Im 20. Jahrhundert wurden nochmals Schürfverusuche unternommen, die jedoch nicht den gewünschten Bergsegen erbrachten. Im Zuge eines Straßenbaues ist ein Erzgang angeschnitten worden, der von einer irischen Bohrfirma untersucht wurde, wobei auch hier keine abbauwürdigen Erzkörper nachgewiesen werden konnten (Mostler, mündl. Mitteilung). Heute sind lediglich im Bereich des Fritzentobels und der Knappagrauba Halden (Abb. 2) und noch zwei offene Stollen mit Schremmspuren erhalten, die wahrscheinlich auf die Schürfversuche des 20. Jhd. hinweisen.

Lagerstättenkundliche Untersuchungen der Lagerstätte Bartholomäberg/Silbertal

6.1 Bisheriger Forschungsstand

Nach der Arbeit von Angerer et al. (1976) können die einzelnen Erzmineralisationen folgendermaßen unterteilt werden:

Disseminierte Kupfererze, die an Quarzporphyrhorizonte permischen Alters gebunden sind (intrapermische Vererzungen).

Sedimentäre Bayrtvererzung in sandigen Tonschiefer mit syngenetischen Karbonatfällungen, die in engem Kontext mit den obigen Quarzporphyrhorizonten stehen.

Sedimentäre Kupfervererzungen in Sandsteinen triassischen Alters (intraskythische Vererzungen).

Silberhaltige Chalkopyrit-Fahlerz – Gangvererzungen an jungalpidischen Bewegungsbahnen (jungalpidische Verzungen).

6.2 Disseminierte permische Kupfererze

Die disseminierten Kupfererze wurden bereits von Schmidt (1879) erwähnt. Nach Angerer et al. (1976) sind drei Quarzporphyrhorizonte im Gelände auszuweisen, deren Mächtigkeit zwischen 0.4-20 m schwankt, wobei aber nur die Ignimbrite eine Vererzung aufweisen. Die untere Quarzporphyrlage ist ca. 5-20 m mächtig, wobei die maximale Mächtigkeit im Fuchswald erreicht wird und nach E hin geringer wird. Der Quarzporphyr ist grünlich gefärbt, untergeordnet können auch rötliche Anteile vorkommen.

Der Mittlere Quarzporphyr erreicht nach Angerer et al. (1976) im Westen eine Mächtigkeit von 2-12 m und im Bereich von Bartholomäberg eine von 2 m bevor er im weiteren Verlauf gegen E hin auskeilt. Der Obere Quarzporphyr schwankt hinsichtlich seiner Mächtigkeit zwischen 0.4 im W und 2 m im Pfaffentobel im E. Die Farbe kann nach Angerer et al. (1976) mit graugrün bis grünlich angeben werden.

Saure vulkanische Ablagerungen aus dem Perm lassen sich sowohl in den Süd- als auch in den Ostalpen nachweisen. Während sie im Südalpin bis zu 1500 m mächtig werden können, erreichen sie im ostalpinen Bereich oft nur wenige Meter an Mächtigkeit. Nach Angerer et al. (1976) weisen die Ignimbrite des Montafons eine Zusammensetzung ähnlich jener eines Rhyodacites auf, wobei leichte chemische Trends zu Rhyolithen bzw. Latiten gegeben sind (Angerer et al., 1976).

Angerer et al. (1976) unterscheiden zwei Vererzungsphasen. Zunächst kam es zur Ablagerung des Mittleren Quarzporphyrhorizontes und mit einsetzender Vergrünung des Protoerzes zu einer ersten Pyritbildung. Darauf folgte eine Kupfervererzung mit anhaltender Pyritausscheidung. Daran soll eine Bornitbildung mit abschliessender Karbonatfällung anschließen. In einer 2. Phase kam es zur Kataklase und Remobilisation unter gleichzeitiger Karbonat- und Quarzausfällung. Auf Grund des hohen Cu/Mo-Verhältnisses entspricht diese Vererzung einem Cu-Mo Typ (Angerer et al., 1976).

6.3 Sedimentäre Barytvererzung

Die ca. 80 cm mächtigen, schichtkonkordanten Barytlagen am Verspeller im Golmerjochgebiet hängen mit dem sauren permischen Vulkanismus zusammen (Haditsch et al., 1979). Durch eine post-stefanische, intensive Bruchtektonik entstanden zunächst schmale intramontane Becken, in denen Grobklastika abgelagert wurden. Nach Mostler (1972) weist das Basiskonglomerat eine unmetamorphe Matrix auf. Die Gerölle lassen jedoch eine starke alpidische Diaphtorese erkennen. Haditsch et al. (1979) postulieren innerhalb der Rotschichten eine Faziesdifferenzierung zwischen dem westlichen (Golmerjoch) und östlichen Abschnitt (Bartholomäberg-Dalaas). Der westliche Bereich wird aus pelitischen bis siltigen Sedimenten aufgebaut, während der östliche Bereich im Liegenden aus Sandsteinen besteht, die sich gegen die Basis des Quarzporphyr hin zunehmend zu einer grobklastischen Serie entwickeln. Darüber finden sich im Osten stark sandige Tonschiefer mit ersten marinen Karbonatlagen und im Westen reine Tonschiefer.

Nach Angerer et al. (1976) und Haditsch et al. (1979) lassen sich auf Grund der ähnlichen Chemismen enge Beziehungen zu den liegenden Anteilen des Bozner Quarzporphyrs ableiten, der nach neueren Arbeiten als „Athesina Volcanic Group (AG)" bzw. Etschtaler Vulkanitkomplex bezeichnet wird (Marocchi et al., 2008). Nach Arbeiten von Morelli et al. (2007) entsprechen die liegendsten Anteile des Etschtaler Vulkanitkomplexes der Auer-Formation, die ebenfalls wie die Montafoner Vulkanite einen rhyolithischen Chemismus aufweisen. Am Verspeller können nach Haditsch et al. (1979) die Rotschichten in eine Liegendserie mit brekziösen Kieslagen und Fein- bis Grobsandsteinen mit einer Mächtigkeit von 130-150 m und einer Hangendserie mit einer Wechsellagerung von Sandsteinen und Tonschiefern unterteilt werden.

Nach Haditsch et al. (1979) folgt darüber eine karbonatführende Tonschieferserie, mit drei zwischengeschalteten Eruptivgesteinsfolgen. Die mittlere Abfolge wird als „Subvulkan" mit einer Mächtigkeit von ca. 30 m und einer lateralen Erstreckung von 600 m ausgewiesen. Im Hangenden des Subvulkans ist an der SW-Flanke des Verspellers ein Barytvorkommen aufgeschlossen, das eine Mächtigkeit von ca. 80 cm und eine weiße- bis hellbräunliche Farbe aufweist und in Wechsellagerung mit Karbonaten (Dolomit) auftritt. Der Baryt weist keinerlei Spuren von Sulfiden auf. Die Bildung des Baryts wird als die erste hydrothermale Mineralisation, die in engem Konnex mit dem permischen Vulkanismus zu setzten ist, bezeichnet. Die zeitliche Einordnung ist auf Grund der späteren Förderung der dritten und letzten Rhyodazitlage möglich, womit dem Baryt am Verspeller ein Rotliegendes Alter zuzuordnen ist.

Mayerl (2005) konnte im Profil des Verspeller jedoch weder im Schliff noch im Gelände eine Evidenz für einen Subvulkan ausmachen. Vielmehr beschreibt er die Gesteine des sog. Subvulkans als einen gewöhnlichen Quarzporphyr neben dem auch Tuffe, Tuffite mit wechselnden Gehalten von Karbonat und Nebengesteinslithoklasten auftreten.

6.4 Intraskythische, exogen-sedimentäre Kupfervererzungen

Die Bearbeitung der exogenen, sedimentären Kupfervererzungen im Montafon und Arlberggebiet wurde erstmalig durch Haditsch et al. (1978) und Krainer (1982) durchgeführt. Die vererzten Arkosen treten innerhalb der Serie der Hangendquarzite auf, die ihrerseits von der höheren, skythischen bis tiefanisischen Rauwacken (Reichenhaller Rauwacke, Punt la Drossa) überlagert und von der Serien der „Mürben Sanstein-serie" unterlagert werden.

Die Hangendquarzite lassen sich eindeutig als eine marine Bildung ausweisen (Haditsch et al. 1978; Krainer, 1982). Dabei handelt es sich um Protoquarzite, die Aufarbeitungsprodukte im strand- und küstennahen Milieu darstellen. Die vererzten Arkosen repräsentieren Rinnensedimente (channel fill sandstones). Die weißen Quarzite weisen generell eine gute Rundung auf. Die Reife bewegt sich nach Haditsch et al. (1978) zwischen überwiegend subreif und reif. Die Zementation der Sublitharenite erfolgt durch sekundäre Kieselsäure, welche die Porenräume ausfüllte. Die vererzten Arkosen weisen keine Schichtung und einen sehr geringen bis kaum vorhandenen Porenraum auf (Haditsch et al., 1978).

Als Mineralbestand führen Haditsch et al. (1978) monokristallinen und untergeordnet polykristallinen Quarz, Feldspäte und lithische Fragmente an. Bei den Feldspäten treten sowohl Orthoklas als auch Schachbrettalbite auf. Des Weiteren tritt Malachit als sekundäres Alterationsprodukt in verschiedenen Formen auf. Als Erparagenese beschreibt Krainer (1982) Fahlerz + Kupferkies + Pyrit. Nach Haditsch et al. (1978) sind die vererzten Arkosen eindeutig als intraskythische, lokale, stratiforme Mineralisationen exogen-sedimentärer Natur zu bezeichnen. Die metallische Anreicherung der Arkosen kann in direkten Zusammenhang mit den Aufarbeitungsprodukten der disseminierten Kupfererze permischen Alters gesetzt werden und ist folglich eine mechanisch-sedimentäre Bildung. Chalkopyritkörner und z.T. idiomorphe Pyrite sowie deren Alterationsprodukte treten bei diesem Typ von Arkose als Lithoklasten auf (Haditsch et al., 1978). Nach Krainer (1982) handelt es sich bei diesen Vererzungen um syndiagenetische- bis epigenetische Ausfällung aus zirkulierenden, relativ tieftemperierten hydrothermalen Sulfosalzlösungen.

6.5 Jungalpidische Kupfervererzungen

Die jungalpidischen Gangvererzungen stellen die jüngsten Vererzungen im Montafon dar (Haditsch und Mostler, 1986; Haditsch und Krainer, 1992). Der Fokus des mittelalterlichen Bergbaues lag ebenfalls auf diesem Vererzungstypus. Nach Haditsch und Mostler (1986) lassen sich die Mineralisationen in drei geographische Bereiche unterteilen:

Fillifau, Ganeu und Golmerbach (Rellstal)
Bartholomäberg
Kristbergsattel

In der vorliegenden Arbeit wird insbesondere auf die letzten zwei Lokalitäten näher eingegangen. Nach Haditsch und Mostler (1986) werden in Ganeu die Schiefer des Altkristallins von quergreifenden Klüften, die mit Quarz und nur wenig Chalkopyrit verfüllt sind, und von Sideritgängen durchschlagen. In unweiter Nachbarschaft dazu lassen sich zwei chalkopyritreiche Gänge bis über den Golmerbach hinaus verfolgen. Im Zuge des Straßenbaues von Bartholomäberg nach Schruns wurde im Jahre 1966 ein Chalkopyritgang von ca. 1 m Mächtigkeit angefahren (Haditsch

und Mostler, 1986). Dieser konnte jedoch im Rahmen dieser Arbeit nicht mehr angetroffen und untersucht werden. Der Gang bestand vorwiegend aus Chalkopyrit mit kleineren Pyrrhotinmineralen, die jedoch häufig in Limonit umgewandelt waren. Die Genese der jungalpidischen Gänge wird von Haditsch und Mostler (1986) auf Grund von Zinkblendeentmischungen im Chalkopyrit als eine heiß-hydrothermale Lagerstättenbildung interpretiert. Kontrollierende Faktoren waren hier Störungen sowie Decken- und Schuppengrenzen, entlang derer die Erzlösungen transportiert wurden, wobei mindestens zwei Bruchsysteme erforderlich waren. Diese Vererzungen weisen auch wahrscheinlich einen genetischen Zusammenhang mit den Zinkblende-Gangvererzungen bei St. Christoph, etwa 20 km entfernt, auf (Haditsch und Krainer, 1992).

Da nach Thöni (1981) während der alpidischen Metamorphose Temperaturen von 250-300°C nicht überschritten wurden, ist nach Haditsch und Mostler (1986) eine externe Wärmequelle notwendig. Für diese Autoren stellen tieferliegende, nicht näher bekannte Krustenbereiche den Ursprung der Vererzung dar, wobei keine Unterscheidung zwischen magmatischen und sekundär-hydrothermalen Lösungen erfolgt.

7. Petrographie der Erze und Gangart

Die petrographischen Untersuchungen konzentrierten sich auf die jungalpidischen, diskordanten Vererzungen von Bartholomäberg und Silbertal. Beide Vererzungen befinden sich in der Phyllitgneiszone. In Bartholomäberg durchschlagen die Vererzungen Glimmerschiefer und am Kristbergsattel (Silbertal) durchschlagen sie Glimmerschiefer und Orthogneise.

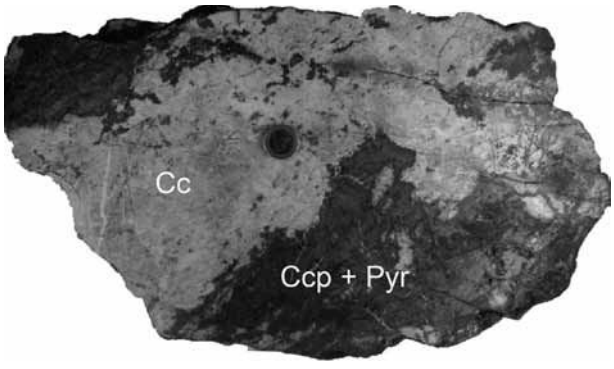

Abb. 3: Aufnahme eines Probenanschnittes aus dem Fritzentobel. Hellbrau bis leicht orange erscheint die karbonatische Gangart (Cc). In dunkelgelb-gelbgräulich erscheinen die feinkörnigen Pyrit-Chalkopyrit-Aggregate.

Die Proben weisen eine starke karbonatische Gangart auf. Die Eisenkarbonate färben die Erzbruchstücke daher intensiv rot- bis hellbraun. In beiden Lokalitäten findet sich hauptsächlich Chalkopyrit und Pyrit (Abb. 3).

7.1 Erzparagenese

Fahlerz

Unter Fahlerz wird die Mischreihe zwischen dem As-Fahlerz Tennantit $Cu_{12}As_4S_{13}$ und dem Sb-Fahlerz Tetraedrit $Cu_{12}Sb_4S_{13}$ zusammengefaßt, wobei mikroskopisch keine Unterscheidung getroffen werden kann. Für eine genauere Differenzierung der einzelnen Zusammensetzungen der Fahlerz Mischreihe wurden Backscattered Electron (BSE) Bilder angefertigt, die auf Grund der chemischen Unterschiede die Mischkristalle besser darstellen. Abbildung 4 stellt einen zonierten Fahlerzmischkristall mit drei Wachstumsgenerationen dar. Fahlerz ist auch stets vergesellschaftet mit Pyrit und Chalkopyrit (Abb. 5), sowie untergeordnet mit Arsenopyrit und Hg-Ag-Amalgam.

Chalkopyrit

Chalkopyrit $CuFeS_2$ ist neben Pyrit und Fahlerz das am häufigsten anzutreffende Mineral in den Erzparagenesen beider Lokalitäten. Er tritt häufig in Form xenomorphkörniger Aggregate auf und ist eng mit Pyrit und Fahlerz vergesellschaftet (Abb. 4). Entlang von Rissen zeigt er Verwitterungserscheinungen zu Covellin und Limonit. Mitunter sind im Chalkopyrit „oleanderblattförmige" α-β Umwandlungslamellen, die auf eine hochtemperierte Bildung bzw. Umbildung hindeuten, zu erkennen (Abb. 6).

Pyrit

Pyrit FeS_2 ist wie Chalkopyrit und auch Fahlerz häufig in den Erzproben anzutreffen. Die Pyrite zeigen idiomorphe Kristallformen. In manchen Fällen sind die Pyritaggregate kataklastisch zerlegt, wobei die ursprüngliche, idiomorphe Kornform noch teilweise erkennbar ist. Risse sind mit Limonit, untergeordnet auch mit Chalkopyrit und Covellin verheilt. Auf Grund der starken Tendenz zur Idiomorphie wird Pyrit oft als „älteste" Mineralisation angesehen (Ramdohr, 1975). Dies ist jedoch nicht in allen Fällen zutreffend.

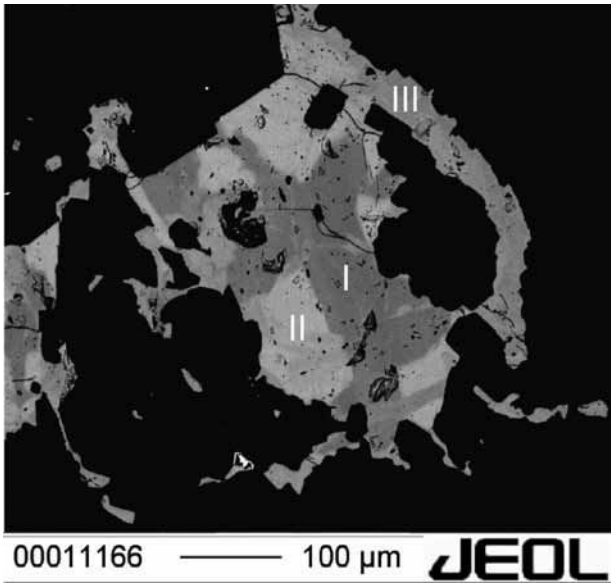

Abb. 4: BSE-Aufnahme eines chemisch zonierten Fahlerzmischkristalls. Deutlich sind aufgrund der Graustufen drei Wachstumsgenerationen (I-III) zu erkennen. Probe PK1.

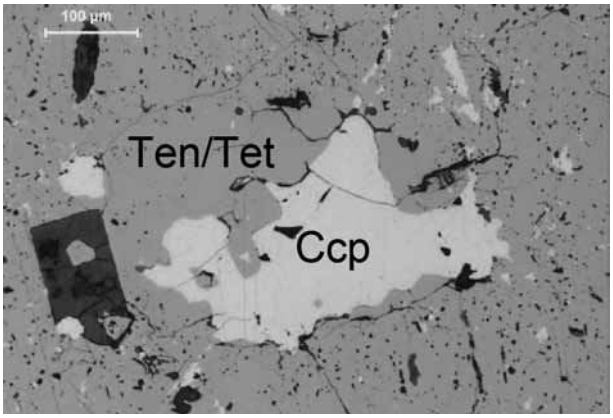

Abb. 5: Auflichtaufnahme bei // Nicols. Chalkopyrit (Ccp) wird verdrängt von Fahlerz (Ten/Tet). Im Fahlerz finden sich noch Chalkopyrit Verdrängungsreste. Probe PK1

Abb. 6: Auflichtaufnahme bei leicht gekreuzten Nicols. Deutlich zu erkennen sind hier die „oleanderblattförmigen" a-b Umwandlungslamellen (a-b) im Chalkopyrit (Ccp). Probe HP2.

Galenit

Galenit PbS kommt nur in sehr geringen Mengen vor und ist häufig mit ged. Wismut vergesellschaftet (Abb. 7). Wie auch aus den NAA Analysen ersichtlich, ist der Absolutgehalt von Pb in den Erzproben sehr gering. Auf Grund der sehr geringen Korngrößen (selten >30 µm) konnte Galenit nur mittels der EMPA nachgewiesen werden.

Sphalerit

Sphalerit ZnS tritt in der Erzparagenese ebenfalls nur als akzessorischer Gemengteil auf, und zwar in Form kleinerer Einschlüsse im Pyrit.

Arsenopyrit

Arsenopyrit FeAsS konnte nur in fahlerzreichen Proben gemeinsam mit Chalkopyrit nachgewiesen werden. Er ist meist xenomorphkörnig ausgebildet und wird entlang von Rissen durch Limonit und Covellin verdrängt.

Co-reicher Arsenopyrit: Alloklas oder Glaukodot

Es wurde in einigen Proben ein Co-reicher Arsenopyrit gefunden. Laut chemischer Zusammensetzung könnte es sich um Alloklas (Co, Fe)AsS oder Glaukodot handeln. Glaukodot, (Co,Fe)AsS ist ein Mischkristall aus der unvollkommenen Mischreihe Arsenopyrit FeAsS – Danait (Fe,Co)AsS – Glaukodot (Co,Fe)AsS – Cobaltit CoAsS. Die Phase tritt untergeordnet in den untersuchten Erzproben auf und die gefundenen Körner weisen eine Größe von unter 10 µm auf. Größere, idiomorphe Kristalle fehlen vollständig. Eine Unterscheidung wäre nur mittels röntgenographischer Methoden möglich (Alloklas: monoklin, Glaukodot: orthorhombisch).

Gersdorffit

Gersdorffit NiAsS ist in Form kleinerer z.T. leicht kataklastischer Aggregate akzessorisch in der Erzmineralparagenese vertreten (Abb. 8). Er besitzt eine weiße Reflexionsfarbe und zeigt im Vergleich zu Pyrit ein leicht geringeres Reflexionsvermögen. Gersdorffit kommt in den Proben stets als Einschluss im Chalkopyrit vor.

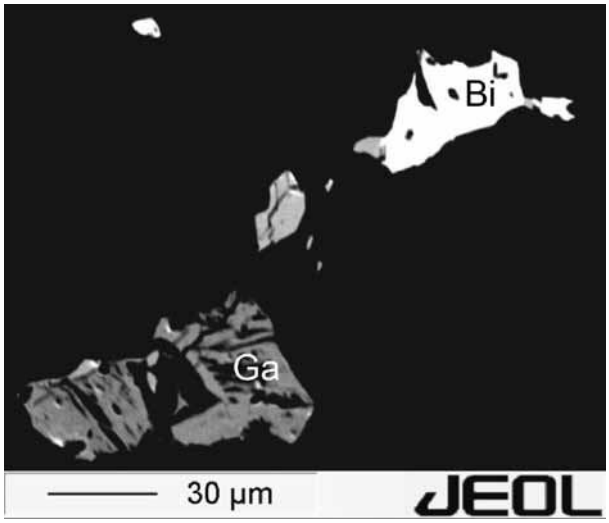

Abb. 7: BSE-Bild von Galenit (Ga) und gediegen Bi. Probe K2d.

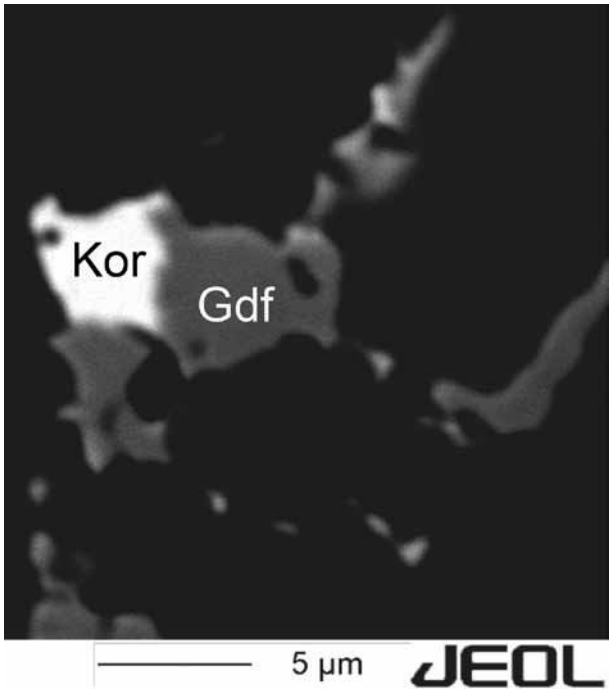

Abb. 8: BSE-Aufnahme von Gersdorffit (Gdf) und Korynit (Sb-reicher Gersdorffit, Kor). Probe Db2.

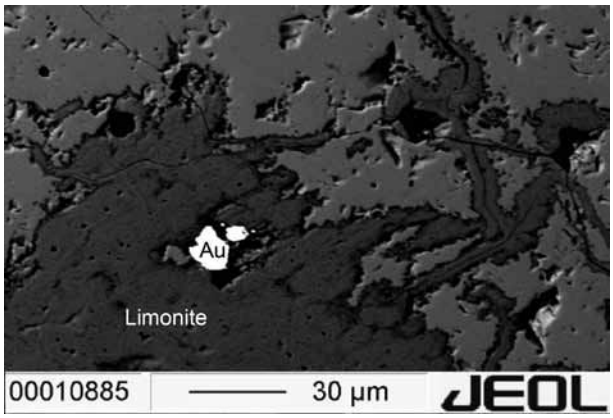

Abb. 9: BSE Bild von gediegen Gold (Au) in einer Matrix aus Limonit. Probe K2d.

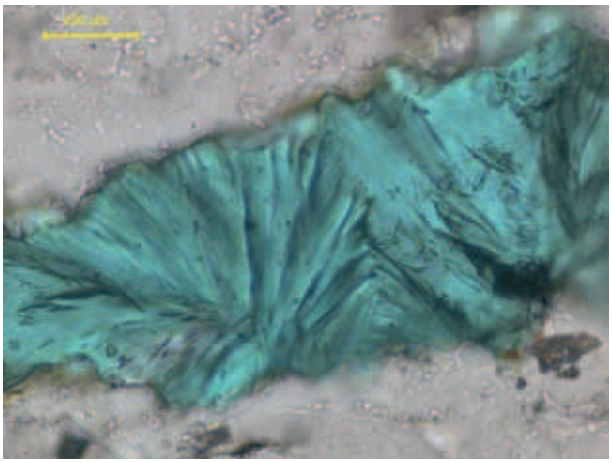

Abb. 10: Durchlichtaufnahme von Tirolit bei // Nicols. Deutlich ist hier die büschelige und radialstrahlige Ausbildung zu erkennen. Probe Re2.

Korynit – antimonreicher Gersdorffit

Korynit Ni(As,Sb)S konnte auf Grund des seltenen Auftretens und wegen der sehr geringen Körngrößen nur mittels der EMPA bestimmt werden (Abb. 8).

Gediegen Wismut

Die sehr feinen Bi-Tröpfchen sind meist eng mit Galenit und Fahlerz vergesellschaftet (Abb. 7).

Aikinit

Aikinit $PbBiCuS_3$ ist in den Erzparagenesen von Bartholomäberg und Silbertal sehr selten und nur auf verwitterte und limonitisierte Bereiche beschränkt. Er wird daher wohl als eine sekundäre Bildung zu interpretieren sein.

Gediegen Gold

Gold kommt in gediegenem Zustand in Form mikroskopisch kleiner, bis max. 5 µm großer Aggregate, im Limonit vor und konnte nur mittels EMPA nachgewiesen werden (Abb. 9). Auf Grund der Vergesellschaftung mit Limonit ist davon auszugehen, dass es sich hier um ein sekundäres Alterationsprodukt handelt. Die Menge an mikroskopisch sichtbarem Gold, und der Absolutgehalt von Au in den Erzparagenesen von Bartholomäberg und Silbertal sind jedoch sehr gering.

Ag-Hg Amalgam

Ag-Hg Amalgam ist eng mit Fahlerzen vergesellschaftet. Unter dem Mikroskop zeichnet sich Amalgam, das in der Zusammensetzung jener des Luanheit (Ag_3Hg) entspricht, durch ein hohes Reflexionsvermögen und eine weißliche Reflexionsfarbe aus.

Akanthit

Akanthit Ag_2S, ein weiteres Silbermineral, tritt in den untersuchten Erzproben meist sehr fein verteilt im Nahbereich von Fahlerzen auf, jedoch in weit geringerem Maße als die Hg-Ag-Amalgame. Die von Ramdohr (1975) beschriebenen Umwandlungslamellen von der kubischen Hochtemperaturphase β-Ag_2S (>179°) zur monoklinen Tieftemperaturphase Akanthit konnte auf Grund der geringen Korngrößen nicht nachgewiesen werden.

7.2 Sekundäre Bildungen

Unter sekundären Bildungen werden in dieser Arbeit sämtliche durch Verwitterungsprozesse entstandenen Minerale zusammengefasst.

Limonit

Limonit tritt entlang von Korngrenzen und Rissen in den primären Sulfidmineralen auf. In der karbonatischen Gangart zeichnet Limonit z.T. sehr deutlich die Spaltbarkeiten nach, entlang derer Limonit eingedrungen ist bzw. sich gebildet hat. Nach optischen Befunden wie Innenreflexen und Anisotropieeffekten handelt es beim Limonit um das Eisenhydroxid Goethit α-FeO(OH).

Covellin

Covellin CuS zeigt unter dem Auflichtmikroskop die typische marineblaue Reflexionsfarbe, einen kräftigen Reflexionspleochroismus und extrem hohe, farbige Anisotropieeffekte. Bei Beobachtung unter Ölimmersion ist ein Farbumschlag von Blau zu Violett zu sehen. Covellin tritt bevorzugt entlang von Rissen im und als randliche Verdrängung um Chalkopyrit auf.

Malachit

Malachit $Cu_2(CO_3)(OH)_2$ bildet Verwitterungskrusten in feinen Rissen der Erzproben.

Tirolit

Das Kupferarsenat Tirolit mit der Formel $Ca_2Cu_9(AsO_4)OH_8(CO_3)(H_2O)_{11}H_2Ox$ wobei x = 0-1 (Krivovichev et al., 2006) zeichnet sich durch ein strahliges und büscheliges Gefüge aus und ist in den meisten Fällen von Limonit umkrustet (Abb. 10).

7.3 Gangartminerale

Quarz

Quarz ist das häufigste Gangartmineral der Erzparagenese. Im erznahen Bereichen tritt Quarz meist in Form von feinkörnigen Aggregaten auf. In kleineren Klüften bzw. Gängen kommt es zur Ausbildung von z.T. hypidiomorphen Kristallen, wobei hier eine Kristallisationsabfolge von fein- zu grobkörnigen Quarzkristallen zu erkennen ist. In erznahen Klüften sind oft „pallisadenartige" Kristallformen entwickelt. Die Gangartquarze sind reich an feinen Flüssigkeitseinschlüssen. Vor allem an Quarzen, die in Sulfiden eingeschlossen sind, wurden die chemische Zusammensetzung und die Homogenisierungstemperaturen der Flüssigkeitseinschlüsse untersucht und gemessen.

Karbonat

Die karbonatische Gangart wird von chemisch stark zoniertem Siderit und untergeordnet Kalzit gebildet (Abb. 11). Sie sind oft idiomorph bis hypidiomorph in Hohlräumen und Klüften gewachsen und können in Form von kleineren Adern auch das Nebengestein durchziehen. In solchen Adern sind dann meist wandständig Karbonate und im inneren Bereich quarzhältige Partien zu erkennen. Auch die Karbonate weisen einen hohen Anteil an feinsten Flüssigkeitseinschlüssen auf.

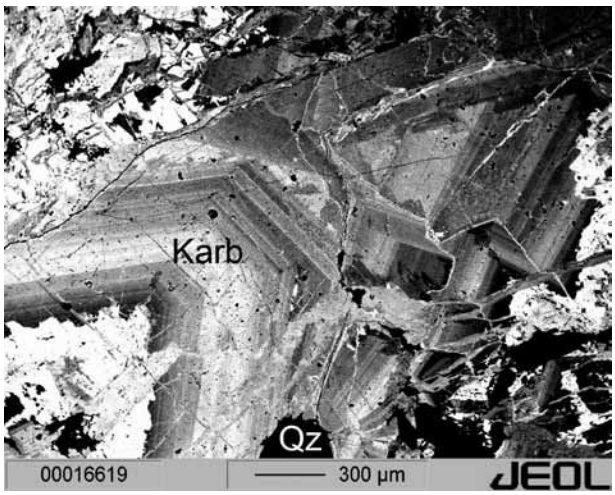

Abb. 11: BSE-Bild der chemisch stark zonierten karbonatischen Gangart (Karb) verwachsen mit Quarz (Qz).

Baryt

Baryt kommt nur in der Gangart am Kristbergsattel vor. Die hypidiomorphen Kristalle sind generell längsprismatisch und zeigen einen tafeligen Habitus.

Erz- und Mineralchemie

Seitens des Projektteiles PP 09 (Archäometallurgische und geochemische Erfassung historischen Bergbaus) wurde eine Serie ausgewählter Erzproben analysiert. Die Erze wurden in einer Kugelmühle pulverisiert (Bulk-Analyse) und anschließend wurden die Elementgehalte von Cu, Fe, Ni, Co, As, Sb, Au, Ag, Se, Te, Zn, Sn, Hg, Bi, Pb mittels NAA bzw. ICP-MS bestimmt. Bei den untersuchten Proben handelt es sich um Erzproben, die auf den Abraumhalden gesammelt worden sind. Makroskopisch bestehen die Proben aus den Erzen Chalkopyrit, Pyrit und Fahlerz.

Die ermittelten Gehalte an Cu, Fe und Zn in der Erzparagenese stammen von den Sulfidmineralen Chalkopyrit, Pyrit und Sphalerit. Aber auch die Fahlerze enthalten Zn in Spuren. Die z.T. hohen Gehalte von As und Sb ergeben sich aus dem Gehalt an Fahlerz in den Proben. Untergeordnet können dafür auch Arsenopyrit, Alloklas bzw. Glaukodot und Korynit in Frage kommen. Erhöhte Ni- und Co-Werte zeigen Gersdorffit, Korynit sowie Alloklas bzw. Glaukodot im Gestein an. Die Konzentrationen sind jedoch relativ gering. In Proben mit hohen As- und Sb-Werten sinken die Co-Werte auf ca. 3-5 µg/g. In chalkopyritreichen Proben liegen die durchschnittlichen Co-Werte bei 81 µg/g. Für Ni lassen sich keine Aussagen bezüglich einer Korrelation mit hohen As und Sb Werte treffen. Die durchschnittlichen Ni-Gehalte liegen bei ca. 132 µg/g.

Ag kann sowohl als Spurenelement im Fahlerz als auch in Form selbständiger Ag-Minerale wie z.B. Akanthit und Hg-Ag Amalgam auftreten. Die Ag-Gehalte korrelieren mit hohen As- und Sb-Gehalten. Eine Ausnahme hierbei bildet eine Probe mit geringen As- und Sb-Werten, aber einem Ag-Gehalt von 263 µg/g. Hier dürfte der erhöhte Silbergehalt auf größere Anteile an Akanthit und/oder Hg-Ag Amalgam zurückzuführen sein. Die Bi-Gehalte im Erz vom Bartholomäberg und Silbertal sind sehr hoch und stellen ein signifikantes Unterscheidungsmerkmal zu den anderen Cu-Lagerstätten wie Kitzbühel, Mitterberg oder Schwaz/Brixlegg dar. Proben aus Hochgallmigg, im Oberinntal zwischen Prutz und Landeck gelegen,

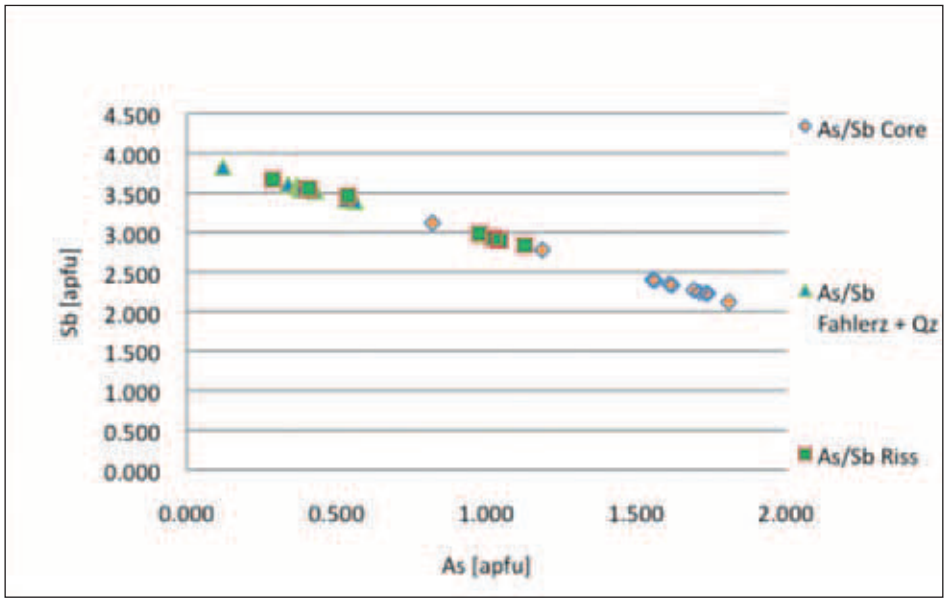

Abb. 12: Verhältnis von As/Sb, wobei hier die unterschiedlichen Zusammensetzungen (Core = 1. Generation; Riss = 2. Generation, Fahlerz + Quarz = 3. Generation) der verschiedenen Fahlerzgenerationen dargestellt sind.

die ebenfalls im Rahmen des SFB HiMAT untersucht wurden und in ähnlicher geologischer Position auftreten, zeigen ebenfalls sehr hohe Bi Werte. Die ermittelten Werte für Bi in den Erze aus dem Montafon variieren zwischen 9.4 µg/g und 11900 µg/g (1.19 Gew.%!), der Mittelwert beträgt 0.26 Gew.% Bi. Die hohen Bi-Gehalte sind auf das Auftreten von Gediegen Wismut zurückzuführen.

Die Gehalte an Pb sind relativ gering und variieren zwischen 3 und 1600 µg/g. Die Zn-Gehalte korrelieren eindeutig mit hohen As und Sb Werten und sind wiederum repräsentativ für die Gehalte an Fahlerz.

8.1 Mineralchemie der Erzparagenese

Chalkopyrit

Die gemessenen Durchschnittsgehalte für Cu, Fe und S in Chalkopyrit vom Bartholomäberg/Silbertal ergeben 24.62 El.% (Element Gew.%) Cu, 24.77 El.% Fe und 50.31 El.% S. Dies entspricht einem Metall/Schwefel-Verhältnis von 0.982. An Spurenelementen konnten noch Zn bis 0.05 El.%, Ni bis 0.61 El.% und Co bis 0.1 El.% nachgewiesen werden (Tab. 1).

Pyrit

Pyrit weist eine von der Stöchiometrie leicht abweichende Zusammensetzung auf. Die durchschnittlichen Element-Gehalte pro Formeleinheit betragen 34.58 El.% Fe und 65.05 El.% S, was einem Metall/Schwefel-Verhältnis von 0.532 entspricht. Aus den EMPA Analysen geht hervor, dass Pyrit noch geringe, jedoch stets detektierbare Mengen an As (0.23 El.% im Durchschnitt), In (0.02 El.% im Durchschnitt) und Pb (0.02 El.% im Durchschnitt) enthält. Die Konzentrationen von Ni und Co sind sehr gering und liegen unterhalb der Nachweisgrenze. Eine Ausnahme bildet die Probe DB7, bei der randlich sehr geringe, jedoch noch detektierbare Mengen an Ni mittels einer Linienmessung sowie eines Elementverteilungsbildes analysiert werden konnten.

Fahlerz

Unter dem mineralogischen Begriff „Fahlerz" versteht man nach Johnson et al. (1986, 1987, 1988) Sulfosalze mit der Mineralformel $^{IV}M(1)_6\ ^{III}M(2)_6\ [^{III}X^{IV}Y_3]_4\ ^{VI}Z$, wobei die M(1)-Position mit Cu, Fe, Zn, Mn, Hg und Cd besetzt ist und die M(2) mit Cu, Ag. Auf die X-Position wird Sb, As, Bi, Te verteilt. Auf der Y- und Z-Position sind S und Se. Das As-hältige Endglied mit der vereinfachten Formel $(Cu,Fe)_{12}As_4S_{13}$ wird als Tennantit bezeichnet, das Sb-hältige mit der vereinfachten Formel $(Cu, Fe)_{12}Sb_4S_{13}$ Pendant dazu als Tetraedrit.

Bei den mineralchemischen Untersuchungen der Fahlerze, zeigt sich vorallem in den BSE- und Elementverteilungs-Bildern eine starke Zonierung. Verantwortlich dafür sind unterschiedliche As- und Sb-Gehalte, wobei beim Einbau von As und Sb auf

Tabelle 1: Repräsentative Mikrosondenanalysen von Gersdorffit, Fahlerz und Chalkopyrit

	Chalkopyrit	Chalkopyrit	Fahlerz	Fahlerz	Gersdorffit	Gersdorffit
As	n.d.	n.d.	10.53	1.38	41.34	40.00
S	35.27	34.59	26.69	25.64	19.27	20.12
Ag	n.d.	0.82	6.86	0.185	0.02	n.d.
Cu	34.73	34.57	35.17	36.58	0.66	1.32
Ni	n.d.	n.d.	n.d.	n.d.	31.95	30.15
Ge	n.d.	n.d.	n.d.	0.03	n.d.	n.d.
Pb	n.d.	0.13	n.d.	0.12	0.21	n.d.
Sn	n.d.	n.d.	n.d.	0.16	0.03	0.04
Fe	30.77	30.02	5.55	3.85	1.89	2.05
Zn	0.15	0.06	3.59	5.56	n.d.	0.03
Se	n.d.	0.04	0.04	0.03	0.15	0.07
Sb	n.d.	n.d.	12.53	27.73	1.12	1.75
In	0.13	0.04	0.09	0.11	0.14	0.05
Co	0.06	0.01	n.d.	n.d.	0.79	3.14
Te	0.01	n.d.	n.d.	n.d.	0.37	0.30
Au	0.08	0.08	n.d.	n.d.	0.02	0.03
Cd	n.d.	0.15	n.d.	0.04	n.d.	0.02
Bi	0.04	n.d.	0.03	0.17	1.13	0.31
Hg	n.d.	0.11	n.d.	0.09	n.d.	n.d.
Mo	n.d.	0.08	n.d.	0.04	n.d.	n.d.
Total	99.70	100.04	101.09	101.72	99.09	99.37
As	n.d.	n.d.	2.308	0.298	0.909	0.845
S	2.000	2.000	13.692	12.949	0.992	0.995
Ag	n.d.	0.014	1.044	0.028	<0.001	n.d.
Cu	0.992	1.007	9.087	9.305	0.017	0.033
Ni	n.d.	n.d.	n.d.	n.d.	0.897	0.813
Ge	n.d.	n.d.	n.d.	0.007	n.d.	n.d.
Pb	n.d.	0.001	n.d.	0.010	0.002	n.d.
Sn	n.d.	n.d.	n.d.	0.022	<0.001	0.001
Fe	1.000	0.995	1.632	1.114	0.056	0.058
Zn	0.004	0.002	0.901	1.374	n.d.	0.001
Se	n.d.	0.001	0.009	0.006	0.003	0.001
Sb	n.d.	n.d.	1.690	3.682	0.015	0.023
In	0.002	0.001	0.013	0.015	0.002	0.001
Co	0.002	<0.001	n.d.	<0.001	0.022	0.084
Te	<0.001	n.d.	n.d.	n.d.	0.005	0.004
Au	0.001	0.001	n.d.	n.d.	<0.001	<0.001
Cd	n.d.	0.003	n.d.	0.006	n.d.	<0.001
Bi	<0.001	n.d.	0.003	0.013	0.009	0.002
Hg	n.d.	0.001	n.d.	0.007	n.d.	n.d.
Mo	n.d.	0.001	<0.001	0.006	n.d.	n.d.
Total	2.005	2.022	11.888	0.298	2.930	2.861

Chalkopyrit normiert auf 2 S, Gersdorffit auf 1 S + Te + Se und Fahlerz auf 4 Semimetalle. n.d.: not detected.

der ^{III}X-Position eine lineare Korrelation zu erkennen ist. Die As- bzw. Sb-Gehalte schwanken in den Sb-reichen Mischgliedern zwischen 0.029 apfu (atoms per formula unit) As und 3.967 apfu Sb und in den As-reichen zwischen 2.602 apfu As und 1.279 apfu Sb (Abb. 12). Die Fahlerze aus dem Montafon zeigen eine größere Tendenz zu Tetraedrit.

Für die Fahlerze von Bartholomäberg konnten aus den Analysen folgende durchschnittliche Hauptelementgehalte berechnet werden:

2.771 apfu Sb (min. 2.076 apfu – max. 3.623 apfu),
1.174 apfu As (min. 0.333 apfu – max. 1.882 apfu),
1.532 apfu Fe (min. 1.288 apfu – max. 1.911 apfu)
und
0.508 apfu Zn (min. 0.340 apfu – max. 0.746 apfu).

Ferner weisen die Fahlerze von Bartholomäberg im Durchschnitt folgende Spurenelementgehalte auf:

0.070 apfu Ag (min. 0.049 apfu – max. 0.111 apfu),
0.048 apfu Bi (min. 0.019 apfu – max. 0.072 apfu),
0.024 apfu Hg (min. 0.007 apfu – max. 0.046 apfu),
0.012 apfu In
und bis max. 0.009 apfu Au gemessen werden.

Für die Fahlerze vom Kristbergsattel ergeben sich folgende durchschnittliche Hauptelementgehalte:

2.108 apfu Sb (min. 1.252 apfu – max. 3.967 apfu),
1.783 apfu As (min. 0.029 apfu – max. 2.610 apfu),
1.480 apfu Fe (min. 0.418 apfu – max. 2.404 apfu)
und
0.561 apfu Zn (min. 0.323 apfu – max. 1.551 apfu).

Auch in den Fahlerzen vom Kristberg konnten folgende durchschnittliche Spurenelementgehalte nachgewiesen werden:

0.039 apfu Ag,
0.087 apfu Bi (max. 0.195 apfu),
0.006 Hg (max. 0.054 apfu),
0.017 apfu In
und bis max. 0.015 apfu Au.

In einer Probe (PK1) lassen sich texturell drei Fahlerzgenerationen mit unterschiedlichen Zusammensetzungen erkennen (Abb. 4, 12). Die erste Generation ist As-reich (Tennantit) und bildet die Grundmasse. Entlang von kleineren Rissen wird die erste Generation durch eine zweite Generation mit As-reicherer Zusammensetzung verdrängt. Als dritte und letzte Generation kristallisierte, koexistierend mit Quarz, der die Hohlräume ausfüllt, Sb-reiches Fahlerz (Tetraedrit). Repräsentative Analysen sind in Tabelle 1 aufgeführt.

Alloklas oder Glaukodot

Alloklas besitzt fast Endgliedzusammensetzung und weist als Substitutionen nur Fe Gehalte von <5 El.% und Ni Gehalte von <1 El.% auf.

Galenit

Im Galenit sind geringe Spuren von Fe (1.24 El.%) und Bi (1.23 El.%) sowie erhöhte Se-Gehalte von bis zu 4.65 El.% nachweisbar.

Sphalerit

Die untersuchten Sphalerite zeichnen sich durch einen durchschnittlichen Fe-Gehalt von 2.28 El.% aus. In Sphalerit waren mit Ausnahme von Fe sowie geringen Mo Konzentrationen keine weiteren Elemente feststellbar.

Gersdorffit

Das Metall/S Verhältnis im Gersdorffit sollte stöchiometrisch bei 2:1 liegen in den untersuchten Proben liegt es bei ca. 1.8:1 (Tab. 1). Die durchschnittliche As Konzentration beträgt 30.01 El.% und jene von Ni 29.91 El.%. Da Gersdorffit in der Erzparagenese meist mit Korynit vergesellschaftet ist, sind die Co-Gehalte in den gemessenen Gersdorffiten z.T. erheblich. Die durchschnittlichen Gehalte betragen 2.1 El.%, wobei maximale Gehalte bis zu 3.55 El.% gemessen wurden. Außerdem konnten Spuren von durchschnittlich 1.27 El.% Fe, 0.53 El.% Cu, 0.66 El.% Sb und geringe Te- und Bi-Gehalte nachgewiesen werden.

Ag-Hg Amalgam

Die Ag-Hg Amalgame lassen mitunter eine leichte, fleckige Zonierung erkennen, die durch unterschiedliche Ag- und Hg-Gehalte hervorgerufen wird. Im Röntgenverteilungsbild eines Ag-Hg Amalgamkornes zeigt sich eine leichte Abnahme der Ag-Konzentration im äußersten Randbereich. Das direkt angrenzende Fahlerzkorn weist daher eine randlich erhöhte Ag-Konzentration auf. Das generelle Verhältnis von Hg zu Ag liegt zwischen 0.83 und 0.46. Dies entspricht einem Maximalwert für Ag in Amalgam von

Tabelle 2: Repräsentative Mikrosondenanalysen von Ag-Hg Amalgam

	k1b-3	k1b-5	k1b-4	k1b-7	k1b-6
As	n.d.	n.d.	n.d.	n.d.	n.d.
S	0.04	0.13	0.04	0.03	0.09
Ag	67.15	63.06	60.45	56.29	53.91
Cu	0.16	0.67	0.19	0.07	0.43
Ni	n.d.	n.d.	n.d.	0.03	n.d.
Ge	0.04	0.04	n.d.	0.06	n.d.
Fe	0.84	1.01	0.38	0.26	0.95
Zn	0.06	0.06	n.d.	n.d.	0.06
Se	0.02	n.d.	n.d.	0.03	0.03
Sb	0.19	n.d.	n.d.	n.d.	n.d.
In	0.19	0.16	0.16	0.11	0.17
Co	n.d.	n.d.	n.d.	0.01	n.d.
Te	0.12	0.21	0.19	0.22	0.19
Au	n.d.	0.07	n.d.	0.01	0.05
Cd	0.68	0.51	0.45	0.53	0.26
Hg	30.63	34.51	38.25	41.87	44.95
Mo	n.d.	n.d.	n.d.	n.d.	n.d.
Total	100.12	100.44	100.11	99.53	101.10

Tabelle 3: Einteilung, Wirtsmineral, Anordnung, Zusammensetzung und Dichte der Flüssigkeitseinschlüsse

Typ	Ia,b	II
Wirtsmineral	Quartz, Karbonat	Quarz
Anordnung	Einzeleinschlüsse, intergranulare Kluster und Trails	Intergranulare Kluster und Trails
Chemisches System	H_2O-NaCl± CH_4	CO_2
Tm (°C)	-1.5 to -12	n.b.
Th (°C) Salzgehalt	99 - 147	n.b.
(Gew.% NaCl)	3 - 20	n.b.
D (gcm-3)	0.93 – 1.06	0.25

Tm – Letztes Schmelzen; Th – Homogenisation (in die flüssige Phase); D – Dichte; n.b. – nicht bestimmt

67.15 El.%. und einem Minimalwert von 53.91 El.% Ag (Tab. 2). Murphy und Preston (1931) beschrieben im binären Ag-Hg System drei Phasen, eine α-Phase mit 0-50 El.% Hg, eine β-Phase mit ungefähr 60 El.% Hg und eine γ-Phase, die in der Zusammensetzung der natürlichen Phase Moschellandsbergit Ag_2Hg_3 entspricht. Die α-Phase wird nach Murphy und Preston (1931) unterteilt in Eugenit Ag_9Hg_3 und Luanheit Ag_3Hg_2 wobei im binären System Ag-Hg der Anteil von Luanheit zwischen 35 und 51 El.% Hg liegt. Seeliger und Mücke (1972) rechnen zur β-Phase den Schachnerit $Ag_{1,2}Hg_{0,8}$ und den Paraschachnerit Ag_3Hg_2. Die Analysenergebnisse zeigen, dass das Ag-Hg-Amalgam der Erzparagenese von Bartholomäberg und Silbertal der α-Phase zuzuordnen ist und dem Mineral Luanheit Ag_3Hg_2 entspricht.

Karbonatische Gangart

Die Karbonate zeigen unter den BSE Bildern deutliche Zonierungs- bzw. Wachstumserscheinungen. Die Siderit-Magnesit Mischkristalle, die den Hauptbestandteil der Gangart darstellen, weisen geringe Ca Gehalte auf. Die Ca-Gehalte liegen im Mittel bei 0.14 apfu Ca. Mn wird durchschnittlich mit 1.94 apfu Mn eingebaut. Im Gesamten sind die Siderit-Magnesitkristalle sehr Fe- reich sowie untergeordnet Mg-reich.

Petrologie und Mikrothermometrie

T-fS_2 Bedingungen

Anhand der ermittelten Erzparagenese konnten limitierende Aussagen bezüglich der herrschenden fS_2 vs. T-Verhältnisse gemacht werden. Als indikative Mineralphasen dienten hierbei Chalkopyrit, Pyrit sowie Tetraedrit. Ferner wurden die durchschnittlichen Fe-Gehalte von 3.44 Gew.% im Sphalerit miteinbezogen. Auf Grund der Mineralphasen sowie der Temperatur der alpidischen Metamorphose (ca. 300-350°C), kann für log fS_2 ein Bereich zwischen -5.8 und -7.8 eingegrenzt werden. Da in den Erzproben aus dem Silbertal und Bartholomäberg keinerlei Hinweise für das primäre Auftreten von Bornit gegeben sind, muss folglich fS_2 zu geringen Werten tendieren. Als limitierende Paragenese zu höheren fS_2 Werten kann die Paragenese Bornit + Pyrit angegeben werden.

Flüssigkeitseinschlüsse

Die Untersuchungen der Flüssigkeitseinschlüsse wurden mit dem Ramanspektrometer, gekoppelt mit einem Heiz-Kühltisch, durchgeführt. Um für die Bildung der Vererzung repräsentative Messergebnisse zu erhalten, wurden Flüssigkeitseinschlüsse von Gangartmineralen sowohl im Nahbereich der Erzminerale als auch von Gangartmineralen, die in Erzmineralen eingeschlossen sind, untersucht. Auf Grund von texturellen und chemischen Unterscheidungsmerkmalen konnten zwei Haupttypen von Flüssigkeitseinschlüssen nachgewiesen werden (Tab. 3).

Typ I weist eine Zusammensetzung von H_2O+NaCl±CH_4 auf (Abb. 13). Bei Typ I wird eine weitere Unterscheidung in Abhängigkeit des Wirtsminerals eingeführt. Die Typ Ia Einschlüsse treten im Quarz auf und Typ Ib tritt in den Karbonaten auf. Typ II konnte bisher ausschließlich in Quarz nachgewiesen werden. Typ I Einschlüsse weisen eine unregelmäßig bis längliche Form auf und erreichen einen maximalen Längsdurchmesser von ca. 10 µm. Typ I Einschlüsse weisen sowohl eine gasförmige als auch eine flüssige Phase auf. Beim Abkühlen im Heiz-Kühltisch wurde ein Ausfrieren bei ca. -50°C beobachtet, beim nachfolgenden Aufheizen das Schmelzen eines Festkörpers zwischen -12 und -1.5°C. Während des weiteren Aufheizens konnte ein Verschwinden der Gasblase (Homogenisierung in die flüssige Phase) zwischen 99°C und 147°C gemessen werden. Diese Temperaturen können als minimale Bildungstemperaturen der Quarz- und Karbonatwirtskristalle angesehen werden. Bei den mikro-Raman-spektroskopischen

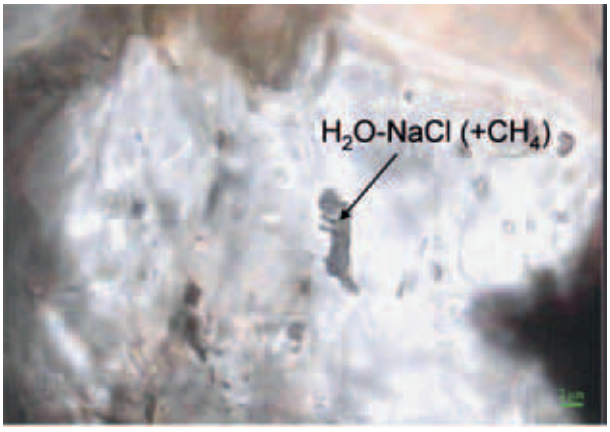

Abb. 13: Durchlichtaufnahme eines Typ-1 Einschlusses mit H_2O + NaCl ± CH_4 in Quarz bei // Nicols.

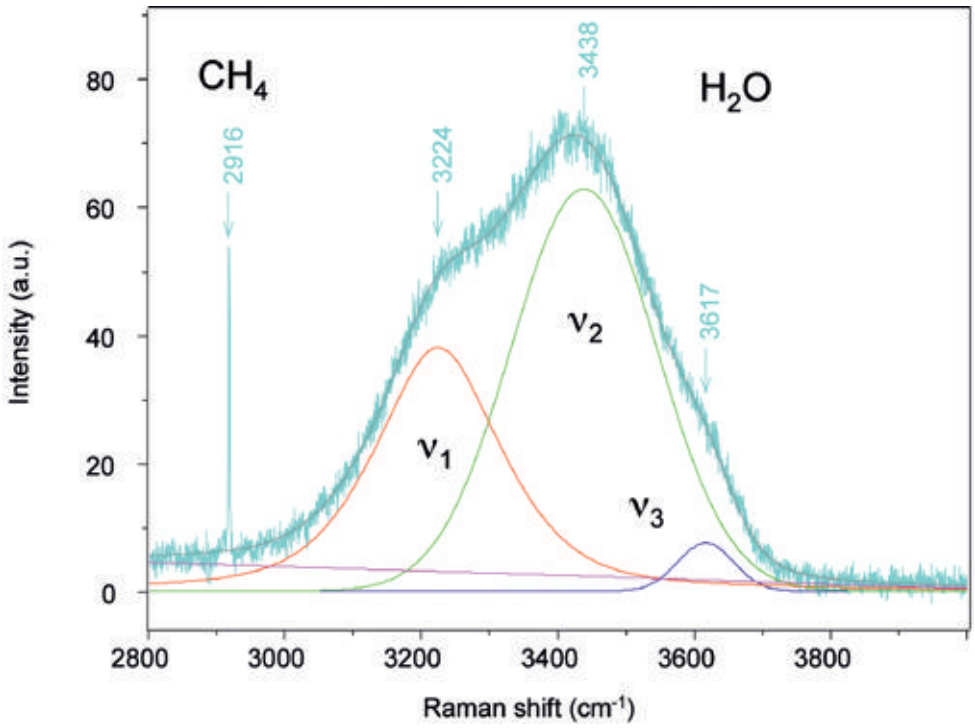

Abb. 14: Ramanspektrum des Einschlusses in Abbildung 13. Die breite Bande zwischen 2800-3800 cm^{-1} lässt sich einer H_2O-NaCl Lösung zuweisen und mit drei Gauss-Lorentz-Funktionen (ν_{1-3}) beschreiben. Der scharfe Peak bei 2916 cm^{-1} ist charakteristisch für CH_4

Untersuchungen konnte in den Flüssigkeitseinschlüssen eine H_2O-NaCl Lösung nachgewiesen werden. Ferner traten Einschlüsse mit einem H_2O-NaCl±CH_4 Fluid auf (Abb. 14). Nach dem Modell von Baumgartner und Bakker (2003) konnte auf Grund der Raman-Verschiebung der ν1 Bande im Spektrum der H_2O-NaCl Lösung ein Salzgehalt von 4-20 Gew.%. NaCl errechnet werden, was gut mit den mikrothermometrischen Ergebnissen übereinstimmt. Die Dichten der Einschlüsse wurden mit dem Programm Fluids von Bakker (2003) berechnet und liegen zwischen 0.93 bis 1.05 g/cm^3. Die Typ Ib Einschlüsse weisen eine sehr geringe Größe auf und liegen im Bereich von ca. 1 µm. Texturell treten die Einschlüsse in Form von Clustern oder intergranularen Trails in der karbonatischen Matrix auf.

Typ II konnte bisher aussschließlich in Quarz nachgewiesen werden (Abb. 15). Dieser Einschlusstyp ist dunkler gefärbt und sehr selten. Wie die Typ Ib Einschlüsse sind auch die Typ II Einschlüsse durch eine sehr geringe Größe von ca. 1-5 µm und eine länglich-rundliche Form gekennzeichnet. Texturell treten sie in Form von intergranularen Trails auf. Bei Raumtemperatur sind die Einschlüsse meist einphasig. Die dunkle Farbe wird auf eine im Vergleich zu Wasser geringere Dichte und damit größeren Unterschied der Brechungsindizes zwischen Einschluß und Wirtsmineral zurückgeführt. Mittels Mikro-Raman-Spektroskopie konnten in einem ca. 5 µm länglichen Einschluss Schwingungsbanden von CO_2 nachgewiesen werden (Abb. 16). Die ebenfalls vorhandenen Banden von H_2O und OH sind gegenüber einer wässrigen Salzlösung deutlich verschoben und werden deshalb eher als Schwingungsbanden eines wasserhältigen Minerals interpretiert (z.B. Glimmer). Aus dem Abstand der für CO_2 charakteristischen Schwingunsbanden bei 1387 cm^{-1} und 1284 cm^{-1}, also 103 cm^{-1}, lässt sich nach Kawakami et al. (2003) eine relativ geringe Dichte von 0.25 g/cm^3 abschätzen.

Zusammenfassend lässt sich feststellen, dass es sich bei den Flüssigkeitseinschlüssen vom Chemismus her um Einschlüsse im H_2O-NaCl System (Typ I) handelt, wobei untergeordnet auch CH_4 und CO_2-reiche Einschlüsse auftreten können (Tab. 3). Der Salzgehalt der Lösungen war vergleichsweise gering (maximal 20 Gew.% NaCl), ebenso wie ihre Homogenisierungstemperaturen von maximal 147° C. Nach Wilkinson (2001) ist dieser Typ von Flüssigkeitseinschlüssen typisch für epithermale Lagerstätten, die sich durch Zirkulation von meteorischen Wässern im Sprödbereich der Kruste in Zonen mit erhöhter Permeabilität und Wärmefluss bildeten. In diesem Fall entsprechen die beobachteten Homogenisierungstemperaturen in guter Näherung den Einfangtemperaturen der Einschlüsse und daher den Bildungsbedingungen der Wirtsminerale. Durch die sehr steilen Isochoren steigen die Drucke mit zunehmender Temperatur sehr stark an. Die Annahme einer Bildungstemperatur von

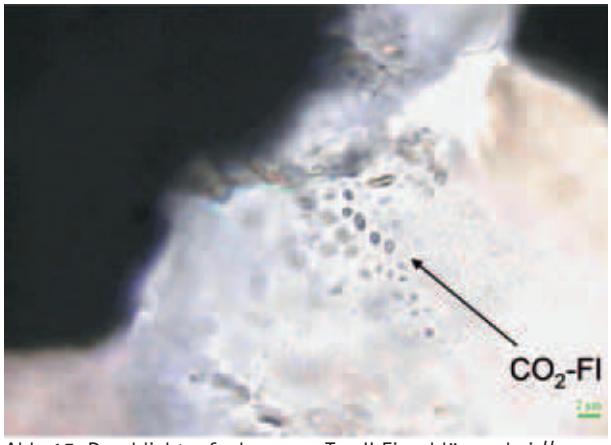

Abb. 15: Durchlichtaufnahme von Typ II Einschlüssen bei // Nicols. Diese treten texturell in Form von intergranularen Trails auf und erscheinen sehr dunkel.

200°C würde somit einen Druck von minimal 1 kbar bzw. einen Maximaldruck von 2.5 kbar, entsprechend einer Krustentiefe von minimal 3 km bzw. max. 7.5 km. Wahrscheinlich lagen die Bildungsbedingungen der Einschlüsse vom Typ I jedoch deutlich unter 200°C.

Es handelt es sich bei den Lösungen der historischen Lagerstätte Bartholomäberg/Silbertal also wahrscheinlich um epithermale, wahrscheinlich meteorische Wässer, welche in einer spröden Kruste mit hoher Permeabilität und Wärmefluss wiederholt zirkulierten.

Interpretation und Diskussion

Im Rahmen dieser Arbeit wurde versucht, ein möglichst vollständiges Bild der geologischen und petrologischen Verhältnisse zu erarbeiten und zu erhalten. Bei den Erzparagenesen von Bartholomäberg und Silbertal (Kristbergsattel) handelt es sich um eine hydrothermale Gangvererzung. Die vollständige Auflistung der Erzparagenese lautet wie folgt: Chalkopyrit + Pyrit + Fahlerz ± Galenit ± Sphalerit ± Arsenopyrit ± Alloklas/Glaukodot ± Gersdorffit ± Korynit ± ged. Wismut ± Aikinit ± ged. Gold ± Luanheit ± Akanthit. Fahlerz, das auf Grund seiner Ag Gehalte primäres Ziel der Abbautätigkeit war, zeigt eine intensive fleckige Zonierung auf Grund variierender Sb:As- und Zn:Fe Verhältnisse. Die Fahlzerze können als Ferro-Tetraedrit bzw. untergeordnet Ferro-Tennantit mit untergeordnetem Auftreten von Zink-Tetraedrit und Zink-Tennantit beschrieben werden. Die Werte für Ag schwanken relativ stark, erreichen jedoch z.T. Maximalwerte von 0.111 apfu. Da es sich hier bei den Proben um Lesefunde von Halden handelt, können die Werte im abgebauten Erz jedoch weit höher gelegen sein. Als weitere Silberminerale konnten in den Vererzungen von Bartholomäberg/Silbertal Ag-Hg Amalgame und Akanthit nachgewiesen werden. Diese treten jedoch nur als Akzessorien auf. Die Gangart besteht aus Quarz, Siderit, Akerit, Kalzit und Baryt. Baryt konnte jedoch nur in Haldenstücken vom Kristbergsattel nachgewiesen werden.

Hinsichtlich der Analysen, die seitens des Projektteiles PP09 mit der NAA durchgeführt wurden, ergeben sich im Vergleich zu anderen im Rahmen des SFB HiMAT untersuchten Kupferlagerstätten sehr hohe Bi-Gehalte von bis zu 1 Gew.%. Die erhöhten Sb + Ag + As Werte in den Schlacken lassen darauf schliessen, dass Fahlerze verhüttet wurden. Leicht erhöhte Bi-Werte lassen sich auch in den (mittelalterlichen?) Kupferschlacken aus dem Silbertal nachweisen, was darauf schliessen lässt, dass lokale Erze (Knappagruaba, Kristbergsattel) zur Verhüttung verwendet worden sein könnten (Bechter, 2009). Trotz intensiver Grabungstätigkeit (Krause, 2001, 2005) konnte der prähistorische Bergbau in diesem Gebiet aber noch nicht definitiv nachgewiesen werden.

Für die genetische Interpretation der Lagerstätten Bartholomäberg und Silbertal sind neben den Flüssigkeitseinschlüssen in Erz- und Gangartmineralen vor allem oleanderblattförmige α-β-Umwandlungslamellen von hochtemperiertem kubischem zu tieftemperiertem tetragonalem Chalkopyrit von besonderer Bedeutung. Für diese Umwandlungslamellen ermittelte Cheriton (1952) an natürlichen Chalkoypyriten mittels der differentiellen thermischen Analyse eine Inversionstemperatur von 540°C. Nach Yund und Kullerud (1966) weisen diese Inversionslamellen auf eine Mindesttemperatur von 547 ± 5°C hin. Ramdohr (1975) hingegen führt für die Bildung von tetragonalem Chalkoyprit im natürlichen System eine Temperatur von <400°C an. Da nach Thöni (1981) und Maggetti und Flisch (1993) die Silvrettadecke alpidische Metamorphosetemperaturen von <300°C aufweist, kann es sich bei den α-β Umwandlungslamellen im Chalkopyrit somit nur um präalpidische, möglicherweise permische Relikte handeln, die während der hochtemperierten Ablagerung der Vulkanoklastika entstanden sein könnten.

Die gangartige Ausbildung der Quarze in den untersuchten Proben lassen jedoch auf Temperaturen von <<300°C schliessen. Unter der Annahme eines homogen eingefangenen Fluides geben die Homogenisierungstemperaturen der Flüssigkeitseinschlusse von >100°C die Mindestbildungs-Temperaturen der

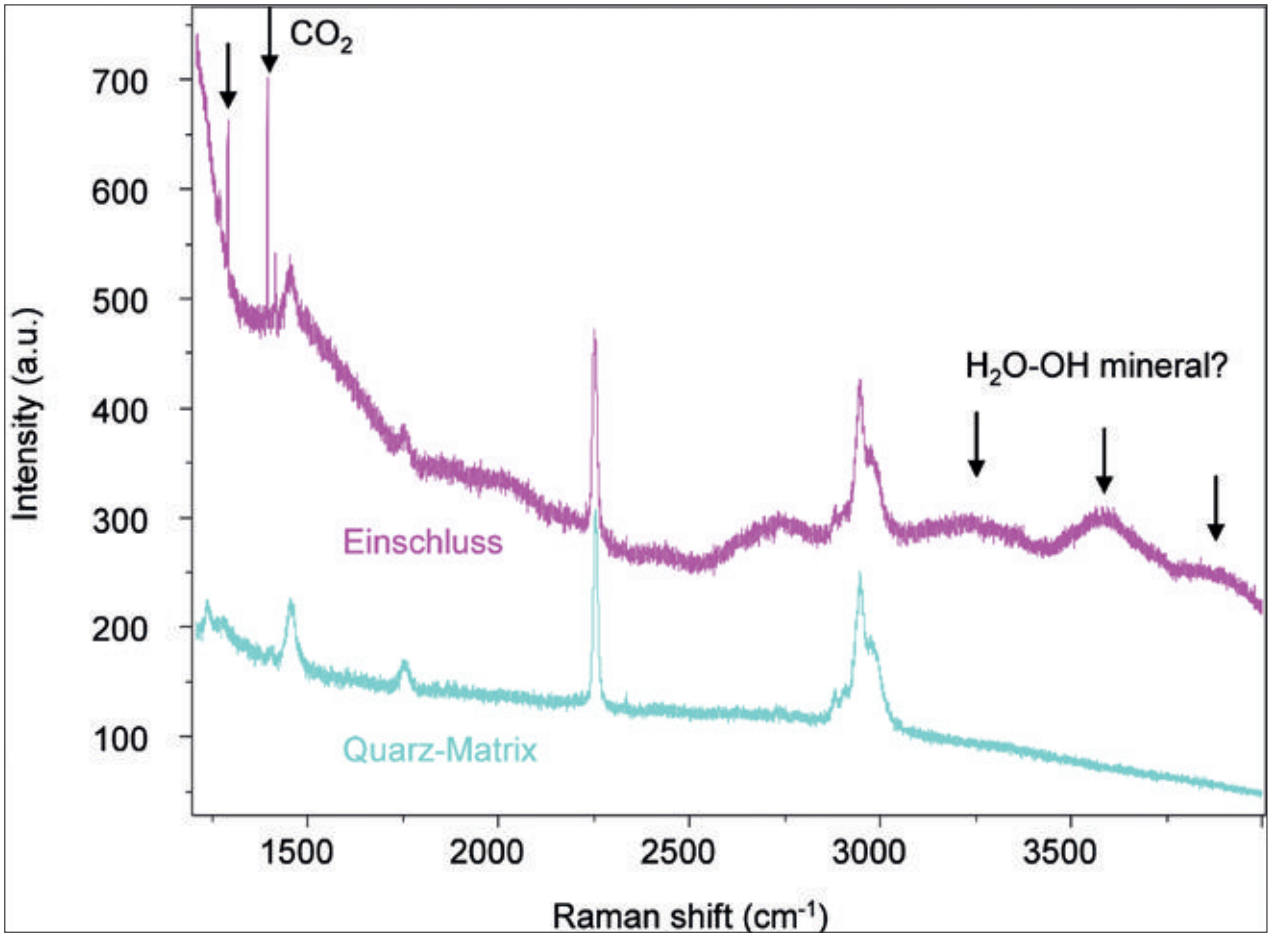

Abb. 16: Ramanspektrum des Einschlusstyps II (rosa). Charakteristisch sind die Schwingungsbanden von CO_2. Das Ramanspektrum des Wirtsminerals (Quarz) ist in türkis gehalten. die restlichen Banden stammen wahrscheinlich von einer wasserhältigen Einschlussphase bzw. Klebstoffresten aus der Probenpräparation.

Lagerstätte an. Somit ist ein Temperaturbereich von 100°C bis ca. 250°C (wahrscheinlicher sind allerdings auf Grund der Quarzgänge eher Temperaturen von 100 – 200°C) anzunehmen. Mittels der Isochoren kann der dabei vorherrschende Druck bzw. die Bildungstiefe auf annähernd 0 bar (Oberflächenbedingungen) bis maximal 4 kbar (ca. 12 km Tiefe) eingegrenzt werden. Vermutlich erfolgte die Vererzung am Bartholomäberg und im Silbertal also prä-alpidisch - permisch und wurde während einer tieftemperierten, (spät?) alpidischen Metamorphose bei Temperaturen von 100 – 250°C und Drucken im Bereich von 0 – 4 kbar teilweise überprägt und remobilisiert.

Da zwei chemische Systeme von Flüssigkeitseinschlüssen, H_2O-NaCl$\pm CH_4$ und CO_2 vorhanden sind, könnten letztere in Zusammenhang mit der älteren, hochtemperierten prä-alpidischen Mineralisation stehen. Dies müsste allerdings erst durch weitere Untersuchungen belegt werden.

Danksagung

Dem FWF wird für die finanzielle Unterstützung im Zuge des Sonderforschungsbereiches HiMAT (F3110-G02 Projekt PP10 für P.T.), Matthias Krismer und Karl Krainer wird für die kritische Durchsicht des Manuskriptes gedankt.

Literaturverzeichnis

Amann, A. (1985): Zur Metamorphose des nördlichen Silvrettakristallins. – Unveröffentlichte Dissertation Universität Innsbruck, 117 S.

Angerer, J. (1978): Postvariszische Sedimente im Montafon (Vorarlberg). – Unveröffentlichte Dissertation Universität Innsbruck, 153 S.

Angerer, H., Haditsch, J., Leichtfried, W. und Mostler, H. (1976): Dissemeninierte Kupfererze im Perm des Montafon (Vorarlberg). – Geologisch Paläontologische Mitteilungen Innsbruck, 6/7-8: 1-57.

Bakker, R. J. (2003): Package FLUIDS 1. Computer programs for analysis of lfuid inclusion data and for modelling bulk fluid properties. – Chemical Geology, 194: 3-23.

Baumgartner, M. und Bakker, R. J. (2008): Raman spectroscopy of pure H2O and NaCl-H2O containing synthetic fluid inclusions in quartz-a study of polarization effects. – Mineralogy and Petrology, 95: 1-15.

Bechter, D. (2009): Petrologische, geochemische und montanarchäologische Untersuchungen der historischen Kupferlagerstätte Bartholomäberg und Silbertal (Montafon, Vorarlberg, Österreich). – Unveröffentlichte Diplomarbeit, Universität Innsbruck, 162 S.

Bertle, H. (1979): Führer zum Geologischen Lehrwanderweg. – Veröffentlichungen des Heimatschutzvereins im Tale Montafon, Schruns, 36 S.

Cheriton, C. G. (1952): Chalcopyrite, oder-disorder. – Unpubl. Ph.D.-Thesis, Harvard University, Cambridge, Massachusetts.

Dunoyer DE Segonzac, G. und Bernoulli, D. (1976): Diagenèse et métamorphisme des argiles dans le Rhétien Sud-Alpin et Austro-Alpin Lombardi et Grison. – Bulletin Societie Géologie France 18: 1283–1293.

Frank, W. (1987): Evolution of the Austroalpine elements in the Cretaceous. – In: Flügel, H.W. und Faupl, P. (Hrsg.): Geodynamics of the Eastern Alps. Deuticke, Vienna: 379–406.

Froitzheim, N. und Eberli, G. P. (1990): Extensional detachment faulting in the evolution of a Tethys passive continental margin, Eastern Alps, Switzerland. – Geological Society of America Bulletin, 102: 1297-1308.

Froitzheim, N., Schmid, S. M. und Conti, P. (1994): Repeated change from crustal shortening to orogen-parallel extension in the Austroalpine units of Graubünden. – Eclogae Geologae Helveticae, 87: 559–612.

Giger, M. (1985): Petrographisch-Geologische Untersuchungen der Davoser Dorfberg-Decke und ihrer benachbarten tektonischen Einheiten im Gebiet Weissfluhjoch-Schaflaeger-Dorfberg. – Unveröffentlichte Lizensiatsarbeit, Bern, 403 S.

Grauert, B. (1969): Die Entwicklungsgeschichte der Silvrettadecke aufgrund radiometrischer Altersbestimmungen. – Unveröffentlichte Dissertation, Universität Bern: 166 S.

Haditsch, J.G. und Krainer, K. (1992): Jungalpidische Erzmineralisationen in der Phyllitgneiszone des Arlberggebietes (Tirol/Vorarlberg). – Mitteilungen der Österreichischen Geologischen Gesellschaft, 84: 239–264.

Haditsch, J.G. und Mostler, H. (1986): Jungalpidische Kupfervererzungen im Montafon (Vorarlberg). – Geologisch Paläontologische Mitteilungen der Universität Innsbruck, 13: 277–296.

Haditsch, J., Leichtfried, W. und Mostler, H. (1978): Intraskythische, exogene (mechanisch)- sedimentäre Cu- Vererzungen im Montafon (Vorarlberg). – Geologisch Paläontologische Mitteilungen der Universität Innsbruck, 8: 183-207.

Haditsch, J., Leichtfried, W. und Mostler, H. (1979): Über ein stratiformes Schwerspatvorkommen in unterpermischen Schichten des Montafons (Vorarlberg). – Geologisch Paläontologische Mitteilungen der Universität Innsbruck, 7/6: 1-14.

Hammer, W. (1918): Die Phyllitgneiszone von Landeck (Tirol). – Jahrbuch der Geologischen Reichsanstalt, 205-258.

Heissel, W., Oberhauser, R., Reithofer, O. und Schmiedegg, O. (1965): Geologische Karte des Rätikon 1: 25.000. – Geologische Bundesanstalt, Wien.

Johnson, N. E., Craig, J. R. und Rimstidt, J. D. (1986): Compositional trends in tetrahedrite. – Canadian Mineralogist, 24: 385-397.

Johnson, N. E., Craig, J. R. und Rimstidt, J. D. (1987): Substitutional effects on the cell dimension of tetrahedrite. – Canadian Mineralogist, 25: 237-244.

Johnson, N. E., Craig, J. R. und Rimstidt, J. D. (1988): Crystal chemistry of tetrahedrite. – American Mineralogist, 73: 389-397.

Kawakami, Y., Yamamoto, J. und Kagi, H. (2003): Micro-Raman densimeter for CO_2 inclusions in mantle-derived minerals. – Applied Spectroscopy, 57: 1333-1339.

Krainer, K. (1982): Zur Sedimentologie und Vererzung der "Hangendquarzite" im Stanzertal/Arlberggebiet (Tirol). – Geologisch Paläontologische Mitteilungen der Universität Innsbruck, 12: 81–94.

Krause, R. (2001): Siedlungsgeschichte und Bergbauforschung: Ein interdisziplinäres Projekt zur Erforschung der inneralpinen Tallandschaft im Montafon/Vorarlberg (Österreich). – Jahrbuch des Vorarlberger Landesmuseumsvereins 2001, Bregenz: 43-61.

Krause, R. (2005): Settlement archaeology and prehistoric mining: a new interdisciplinary research project in the Alpine valley Montafon in Vorarlberg (Austria). – Prehistoria Alpina, 39: 211-218.

Krause, R., (2006): Zur bronzezeitlichen Siedlungskammer im Montafon. Neue Ausgrabungen in Bartholomäberg, Bezirk Bludenz. – Jahrbuch des Vorarlberger Landesmuseumsvereins, 2005: 47-60.

Krause, R. (2007): The prehistoric settlement of the inneralpine valley of Montafon in Vorarlberg (Austria). – Prehistoria Alpina, 42: 119-136.

Krause, R., Oeggl, E. und Pernicka, E. (2004): Eine befestigte Burgsiedlung der Bronzezeit im Montafon, Vorarlberg. Interdisziplinäre Siedlungsforschungen und Montanarchäologie in Bartholomäberg und in Silbertal. – Archäologie in Österreich, 15/1: 4–21.

Krivovichev, S. V., Chernyshov, D. Y., Döbelin, N., Armbruster, T., Kahlenberg, V., Kaindl, R., Ferraris, G., Tessadri, R., Kaltenhauser, G. (2006): Crystal chemistry and polytypism of tyrolite. – American Mineralogist, 91: 1378-1384.

Leichtfried, W. (1978): Feinstratigraphische Untersuchungen im Permoskyth des Montafon (Vorarlberg). – Unveröffentlichte Dissertation, Universität Innsbruck.

Leupold, W. (1934): Arosa - Alteinfurka - Glaris (Davos) - Filisur. – Geologischer Führer der Schweiz, Exkursion 87: 997-1013.

Mayerl, S. (2005): Geologie des östlichen Rätikon (Vorarlberg): Stratigraphie, Tektonik und Kinematik. – Unveröffentlichte Diplomarbeit, Universität Innsbruck: 157 S.

Maggetti, M und Flisch, M. (1993): Evolution of the Silvretta Nappe. – In: Raumer, J. F. von und Neubauer, F. (Hrsg.): Pre- Mesozoic geology in the Alps. Springer, Berlin: 464-484.

Marocchi, M., Morelli, C., Mair, V., Klötzli, U. und Bargossi, G. M. (2008): Evolution of Large Silicic Magma System: New U-Pb Zircon Data on the NW Permian Athesian Volcanic Group (Southern Alps, Italy). – Journal of Geology, 116: 480-498.

Morelli , C., Bargossi, G. M., Mair, V., Marocchi, M., Moretti, A. (2007): The lower Permian Volcanics along the Etsch Valley from Meran to Auer (Bozen). – Mitteilungen der Österreichischen Mineralogischen Gesellschaft, 153: 195-218.

Mostler, H. (1972): Postvariszische Sedimente im Montafon (Vorarlberg). – Verhandlungen der Geologischen Bundesanstalt, 1972: 171-174.

Murphy, A. J. und Preston, G. D. (1931): The constitution of the alloys of silver and mercury–the X-ray examination of the system silver-mercury. – Journal of Instruments and Metals, 46: 507-527.

Nowotny, A., Pestal, G, und Rockenschaub, M. (1993): Der geologische Bau der nördlichen Silvrettamasse und die Problematik der geologischen Stellung der Zone von Puschlin. – In: Geologie des Oberinntaler Raumes – Schwerpunkt Blatt 144 Landeck. Arbeitstagung der Geologischen Bundesanstalt, 1993: 55-91.

Oberhauser, R. und Rataj, W. (1988): Geologisch-tektonische Übersichtskarte von Vorarlberg 1: 200.000 mit Erläuterungen. – Geologische Bundesanstalt, Wien: 42 S..

Oeggl, K. (2003): Vegetations- und Siedlungsgeschichte im Montafon. – Rheticus, 3: 49-59.

Oeggl, K., Mathis, F., Moser, J., Schneider, I., Leitner, W., Tomedi, G., Stöllner, T., Krause, R., Pernicka, E., Tropper, P., Schibler, J., Nicolussi, K., Hanke, K. (2008): The history of mining activities in the Tyrol and adjacent areas: impact on environment and human societies (HiMAT). – Antiquity, 82, 317.

Ramdohr, P. (1975): Die Erzminerale und ihre Verwachsungen. – 4. Auflage, Akademie Verlag Berlin.

Reithofer, O. (1954-1963): Aufnahmsberichte für die Jahre 1953-1962 auf den Blättern Feldkirch (141) und Schruns (142). – Verhandlungen der Geologischen Bundesanstalt, 1954-1963.

Reithofer, O. (1955): Neue Vorkommen von Grauwacke im Klostertal und im Montafon. – Verhandlungen der Geologischen Bundesanstalt 1955: 180-187.

Scheibenstock, E. (1996): Bergknappen, Stollen, Erze. Zur Geschichte des Bergbaues im Montafon. –Bludenzer Geschichtsblätter 31.

Schmid, S. M., Fügenschuh, B., Kissling, E. und Schuster, R. (2004): Tectonic map and overall architecture of the Alpine Orogen. – Eclogae Geologae Helvetiae, 97: 93-117.

Schmidt, A. R. (1879): Bergbaue, Erz- und Kohlenfunde und besonders nutzbare Gesteinsarten in Vorarlberg. – Österreichische Zeitschrift für Berg- und Hüttenwesen XXVI: 349-351, 361-362, 376-378.

Schuster, R. und Frank W. (1999): Metamorphic evolution of the Austroalpine units east of the Tauern window: indications for Jurassic strike slip tectonics. – Mitteilungen der Gesellschaft für Geologie und Bergbaustudenten in Österreich, 42: 37-58.

Schuster, R., Scharbert, S., Abart, R. und Frank W. (2001): Permo-Triassic extension and related HT/LP metamorphism in the Austroalpine–Southalpine realm. – Mitteilungen der Gesellschaft für Geologie und Bergbaustudenten in Österreich, 45: 111-141.

Schweinehage, R. (2000): Metamorphite der Silvrettadecke/Ostalpen: Thermobarometrische und geochemische Untersuchungen zur präalpidischen Entwicklung. – Uveröffentlichte Dissertation, Universität Stuttgart: 330 S.

Spiess, R. (1985): Kristallingeologisch-geochronologische Untersuchungen zur Entwicklungsgeschichte des Westrandes der Phyllitgneiszone i.w.S. im Montafon (Vorarlberg). – Unveröffentlichte Dissertation Universität Wien, 78 S.

Stingl, V. (1987): Die fazielle Entwicklung des Alpinen Buntsandsteins (Skyth) im Westabschnitt der Nördlichen Kalkalpen (Tirol, Salzburg, Österreich). – Geologische Rundschau, 76/2: 647-664.

Thöni, M. (1981): Degree and Evolution of the Alpine Metamorphism in the Austroalpine Unit W of the Hohe Tauern in the light of K/Ar and Rb/Sr Age Determination on Micas. – Jahrbuch der Geologischen Bundesanstalt, 124/1: 111-174.

Thöni, M. (1982): Einfluss der kretazischen Metamorphose im Westabschnitt der Ostalpinen Einheiten: Interpretation geochronologischer Daten. – Mitteilungen der Gesellschaft für Geologie und Bergbaustudenten in Österreich, 28: 17- 34.

Tollmann, A. (1977): Geologie von Österreich, Band 1 Die Zentralalpen. – Deuticke, Wien, 766 S.

Tollmann, A. (1985): Geologie von Österreich, Band 2. – Deuticke, Wien, 710 S.

Van Ameron, H. W. J., Angerer, H. und Mostler, H. (1982): Über die Autuno- Stephanische Flora aus den Kristbergschichten im Montafon, Vorarlberg (Österreich). – Jahrbuch der Geologischen Bundesanstalt, 124: 283-323.

Wilkinson, J. J. (2001): Fluid inclusions in hydrothermal ore deposits. – Lithos, 55: 229-273.

Yund, R. A. und Kullerud, G. (1966): Thermal Stability of Assemblages in the Cu-Fe-S System. – Journal of Petrology, 7, 454-488.

Zemmer-Planck, L. (1978): Ein bronzezeitliches Gehöft auf dem Gschleirsbühel bei Matrei am Brenner. – Veröffentlichungen des Tiroler Landesmuseums Ferdinandeum, 58: 157-209.

Manuskript eingereicht: 1.6.2011
Manuskript angenommen: 9.8.2011

Geo.Alp, Vol. 8, S. 46–55, 2011

LITHOSTRATIGRAPHY AND BIOSTRATIGRAPHY OF OLIGOCENE MIOCENE DEPOSITS (ASMARI FORMATION) IN SOUTH-WEST IRAN (ZAGROS BASIN, NORTHERN KHORRAMABAD)

Parvaneh Roozbahani

With 1 Figure, 2 Tables and 2 Plates

Islamic Azad University, Khorramabad Branch, Department of Geology, Iran
email: dr.roozbahani@gmail.com

ABSTRACT

For the lithostratigraphic and biostratigraphic analysis of the Asmari Formation in south-west of Iran (northern Khorramabad), two geological sections, one in the Kakareza region and the other one in the eastern Makhkalkuh, were selected and sampled. ≠It consists mainly of limestones, clayey limestones and sandy limestones. The Asmari Formation overlies the Shahbazan Formation with a paraconformity and underlies conformably the Gachsaran Formation. Based on micropalaeontologic research 40 genera and 19 species of benthic foraminifera, 3 genera and 2 species of pelagic foraminifera and 4 genera of calcareous algae (accompanied by a number of non-foraminifera) have been identified indicating a Burdigalian age for the sections under study. Based on the associated index foraminifera the *Borelis melo curdica - Meandropsina iranica - Schlumbergerina* assemblage zone has been selected. This biozone is comparable with the biozone NO. 1 of Adams & Bourgeois (1967) and biozone NO.61 of Wynd (1965). The *Borelis melo curdica - Meandropsina iranica - Schlumbergerina* assemblage zone is also considered to be equivalent to the biozone which was reported from the Upper Asmari Formation by Thomas (1948,1949).

Key words: Lithostratigraphy, biostratigraphy, foraminifera, Asmari Formation, Oligocene-Miocene, Iran

Introduction

The Asmari Formation is the youngest and most important reservoir rock of the Zagros Basin in the south-west of Iran which has been the focus of attention of a large number of geologists. There are, however still problems with respect to the exact litho- and chronostratigraphic position of this unit: with regards to the lithostratigraphy in the complete sections, the Asmari Formation has been divided into two members: one is the Sandstone Member of Ahwaz in the south-west of the Khuzestan area and the other one is the Evaporite Member of Kalhur in the Lorestan Province. With respect to the chronostratigraphy, according to Thomas (1948, 1949), this formation is divided into three units: the Lower Asmari with an Oligocene age, the Middle Asmari with an Aquitanian age, and the Upper Asmari with a Burdigalian age. However, these divisions do not exist everywhere, whether with regards to lithostratigraphy nor chronostratigraphy which is in itself extremely significant. Also, in some parts of Iran, the lower boundary of the Asmari Formation is in contact with the Pabdeh Shale Formation which is of Paleocene-Oligocene age, but in central Lorestan this formation is overlying the Late Eocene Shahbazan Formati-

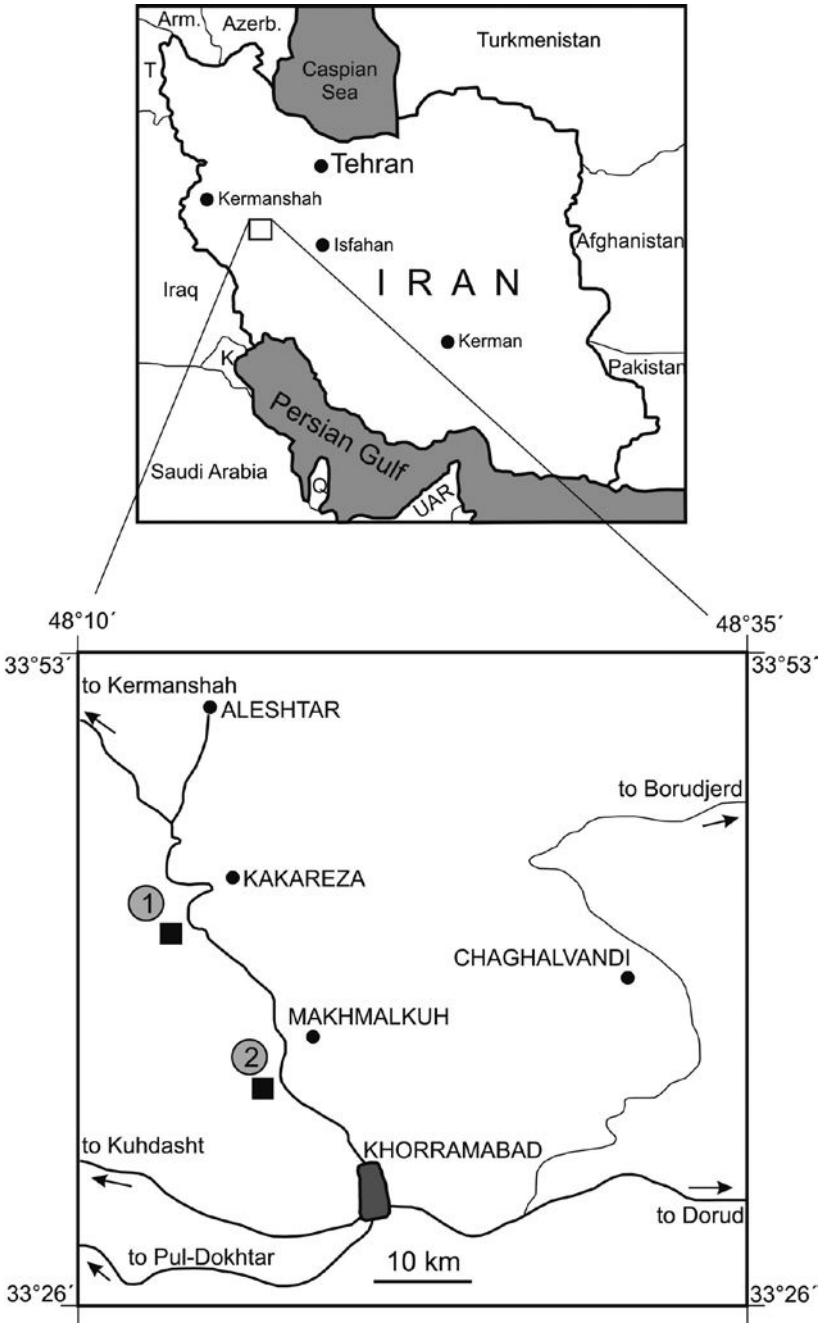

Fig.1: Locality map of the studied sections.

on and in internal Fars it shows a paraconformable contact with the Jahrum Formation (Eocene).

Considering the upper boundary, in certain areas the Asmari Formation is covered by anhydrites of the Gachsaran Formation which is of Early Miocene age, and in internal Fars the upper boundary of Asmari Formation is in contact with the Early Miocene Razak Formation. Therefore, the type of contact of the Asmari Formation with the underlying and overlying formations varies considerably. As a result, although many years have passed since the stratigraphy in the south-west of Iran was defined by James & Wynd (1965) and much information has been collected about the Asmari Formation more studies need to be done in order for a better bio- and chronostratigraphic correlation of the ambiguous parts of this formation.

Methods

The methodology in this research includes library, field and laboratory studies.

A) Library studies include all materials and scientific achievements related to the subject under study such as books, articles, magazines, unpublished reports, theses and the internet as well. Important information was also derived from personal communications with specialists.

B) In the field studies, various visits have been done for the overall geologic analysis of the area under study for a better understanding of the geological formations and the relationships between various structures and the identification of the faults in the region. Following this procedure the sampled locations were selected by means of air photographs, topographical maps 1:50.000, (Rahman Shahi (II)) and Sarab Doreh (III), geological map of 1:250000 Khorramabad and the field visits made.

The sampling of the geological sections under study has been done in variable distances (30 cm to up to one meter) with respect to the facies differences of the strata, and all sampling locations have been spray-marked.

Generally five main factors were considered in measuring the sections: 1- strike, 2- dip, 3- azimuth, 4- inclination, 5- length. The real thickness of the layers were then determined through the triangular method. The total number of samples taken from the sections under study is 211.

C) Laboratory studies include the preparation of thin sections from all collected rock samples. The microfossils were studied and determined using a binocular microscope OLYMPUS-BH-2.

Geographic Location and Stratigraphy of Sections

The sections under study in this text are located in Zagros folded zone and their geographical coordinates are as follows (Fig.1):

3.1 Kakareza section

This section is located 27.5 km north-west of Khorramabad (the road from Khorramabad to Aleshtar) in an area called Kakareza with the geographical coordinate of 48°14'10" eastern longitude and 33°44'26" northern latitude.

3.2 East Makhmalkuh section

This section is located 10 km north-west of Khorramabad (the road from Khorramabad to Aleshtar) in an area called East Makhmalkuh with the geographical coordinate of 48°17'33" eastern longitude and 33°36'22" northern latitude.

Lithostratigaphy of the sections

The sampling in both sections under study starts from the upper limit of red shale and sandstones belonging to the Kashkan Formation (Middle Eocene) and continues to marly and gypsum layers of the overlying Gachsaran Formation (Early Miocene). Due to lithological similarities in the field, the dolomitic limestone of the Shahbazan Formation (Late Eocene) is not separable macroscopically from the overlying Asmari Formation. The boundary between these two formations can only be determined by micropaleontological studies. All the samples collected from the upper boundary of the Kashkan Formation up to 36.70 meters thickness in the Kakareza section and to 45.20 meters thickness in the eastern Makhmalkuh section are belonging to the Shahbazan Formation and are devoid of any type of fossils. Above this stratigraphical niveau we are suddenly facing a high variety and abundance of fossil types which are representative for the upper Asmari Formation and indicative of Early Miocene (Burdigalian).

The lithostratigraphy of each section under study is presented separately:

4.1 Kakareza section

The thickness of this section is 82.60 m, the strike is 55-60° NE and dip is 30–40° NW. At this section, the Asmari Formation overlies the Shahbazan Formation (Late Eocene) with a paraconformity and underlies conformably the Gachsaran Formation (Early Miocene). In this section the Asmari Formation consists exclusively of carbonates comprising 5 rock units as follows:

Unit 1: dark gray, medium to thick-bedded limestone with frequent macrofossil fragments (28.10 m)

Unit 2: light gray, medium-bedded limestone with interbeds of clayey limestone (14.20 m)

Unit 3: dark gray, thick-bedded limestone with chert nodules (12.80 m)

Unit 4: dark gray, medium- to thick-bedded limestone with frequent macrofossil fragments (19.30 m)

Unit 5: light gray, medium-bedded clayey limestone (8.20 m)

4.2 Eastern Makhmalkuh section

The thickness of this section is 102.10 m, the strike is 30–40° NE and the dip is 45–50° NW.

In the eastern Makhmalkuh section, the Asmari Formation also overlies the Late Eocene Shahbazan Formation with a paraconformity and is conformably overlain by the Early Miocene Gachsaran Formation.

At this locality the Asmari Formation consists of carbonates which are divisible into 7 rock units as follows:

Unit 1: cream to light gray, medium-bedded limestone (7.60 m)

Unit 2: dark gray, medium to thick-bedded limestone with frequent macrofossil fragments (18.40 m)

Unit 3: dark gray, thick-bedded to massive limestone with chert and frequent macrofossil fragments (12.30 m)

Unit 4: light gray, medium-bedded limestone with sandy limestone interbeds (15.60 m)

Unit 5: gray, medium- to thick-bedded limestone with frequent macrofossil fragments (28.40 m)

Unit 6: gray, thick-bedded to massive limestone with chert & frequent macrofossil fragments (13.10 m)

Unit 7: light gray, medium-bedded clayey limestone (6.70 m)

Biostratigraphy of the sections

Various papers (Postuma 1971, Bolli & Saunders 1987, Sampo 1969, Mehrnoosh & Partoazar 1977, Loeblich & Tappan 1988, Kalantary 1992) were used to identify the microfossils. In total, based on the present micropaleontological study, 40 genera and 19 species of benthic foraminifera, 3 genera and 2 species of pelagic foraminifera, 4 genera of calcareous algae as well as a number of other micro- and macrofossils were identified from the sections which altogether indicate a Burdigalian age for the deposits under study.

The identified benthic foraminifera are as follows: *Meandropsina iranica*, *Borelis melo curdica*, *Miogypsina irregularis*, *Haplophragmium slingeri*, *Peneroplis evolutus*, *Austrotrillina howchini*, *Borelis* **cf.** *pygmaea*, *Miogypsinoides complanatus*, *Peneroplis thomasi*, *Cibicides* gr. *lobatus*, *Dendritina rangi*, *Triloculina trigonula*, *Austrotrillina asmariensis*, *Spiroclypeus* cf. *vermicularis*, *Operculina complanata*, *Nephrolepidina tournoueri*, *Spirolina cylindracea*, *Meandropsina anahensis*, *Miogypsina basraensis*, *Gypsina* sp., *Schlumbergerina* sp., *Elphidium* sp., *Nummulites* sp., *Heterostegina* sp., *Archaias* sp., *Assilina* sp., *Eouvigerina* sp., *Pseudochrysalidina* sp., *Bolivina* sp., *Planorbulina* sp., *Asterigerina* sp., *Nezzazata* sp., *Victoriella* sp., *Miniacina* sp., *Amphistegina* sp., *Anomalina* sp., *Gyroidina* sp., *Eponides* sp, *Discorbis* sp., *Pyrgo* sp., *Rotalia* sp., *Valvulina* sp., *Bigenerina* sp., *Quiqueloculina* sp., *Textularia* sp., miliolids, valvulinid.

The identified pelagic foraminifera are as follows: *Globigerinoides trilobus*, *Globigerina* sp., *Globorotalia* sp., *Globigerina* sp.

The identified non-foraminifera include the following ones:
Calcareous algae: *Lithothamnium* sp., *Archaeolithothamnium* sp., *Lithophyllum* sp., *Solenomeris* sp.

Kuphus arenarius, Tubucellaria sp., *Ostrea* sp., *Ditrupa* sp., corals, gastropods, ostracods, echinoderms, bryozoans, worm tubes, lamellibranchia.

Following these studies, based on the first and last occurrences and the proposed stratigraphic range of the identified microfossils, one assemblage zone was considered for both sections, namely:
Borelis melo curdica -Meandropsina iranica-Schlumbergerina Assemblage Zone

The thickness of this biozone is 82.60 m at Kakareza section and at Makhmalkuh section it has a thickness of 102.10 m. The base of this biozone which is located at the beginning of the section under study, is marked by the first appearance of Early Miocene index microfossils (*Meandropsina iranica, Dendritina rangi, Elphidium* sp.) associated with *Borelis melo curdica* and its top corresponds to the last appearance of *Schlumbergerina* sp. and *Elphidium* sp.

The most characteristic microfossils associated with this biozone are as follows:
Peneroplis evolutus, Borelis melo curdica, Borelis cf. *pygmaea, Meandropsina iranica, Miogypsinoides complanatus, Dendritina rangi, Miogypsina irregularis, Operculina complanata, Spirolina cylindracea, Meandropsina anahensis, Austrotrillina asmariensis, Miogypsina* cf. *basraensis, Schlumbergerina* sp., *Elphidium* sp., *Archaias* sp.

Considering the identified microfossil associations, particularly the presence of *Meandropsina iranica*, the age of this biozone is suggested to be Burdigalian. With regard to the age, this biozone is comparable with the *Meandropsina iranica - Borelis melo* group Assemblage Zone presented by Adams & Bourgeois 1967 and biozone No. 61 of Wynd (1965) from Iran's south-western regions (Zagros). This biozone may also be equivalent to the Upper Asmari Formation defined by Thomas (1948, 1949).

Conclusion

In contrast to stratigraphic data of the geological map 1:250000 Khorramabad, the Asmari Formation in each section under study is proved to be of Burdigalian age.

The lithology of Asmari Formation consists of limestone, clayey limestone and sandy limestone. The lower boundary of this formation has a paraconformity with the Shahbazan Formation, and its upper boundary is conformable with the Gachsaran Formation. The paraconformity at the base of the Asmari Formation can be attributed to the Pyrenean Tectonic Event in addition to abiotic and chemical changes within the Zagros Basin. The deposits of the Asmari Formation reflect a progression of the Early Miocene Sea as a result of Savin's stretched phase which is often accompanied by subsidence.

Acknowledgements

I wish to thank Dr. Resch (Innsbruck) and Dr. Mette (Innsbruck) for critically reading the manuscript and Dr. Fekri (Teheran) for research facilities and providing financial support.

References

Aghanabati, A. (2004): Iran's geology. - Geological Survey of Iran, Teheran.

Adams, T.D. & Bourgeois, F. (1967): Asmari Formation Biostratigraphy. - IOOC Report No.1074, Teheran (unpubl.).

Adams, T.D. (1969): Asmari Formation of Lurestan and Khuzestan Proviences. - IOOC Report No.1154, Teheran (unpubl.).

Bolli, H.M. & Saunders, J.B. (1985): Planktic stratigraphy. – Micropaleontology, 33 (1): 87-92.

Bozorgnia, F. (1966.): Qum Formation Stratigraphy of the central basin of Iran and its intercontinental position. – Bull. Iran. Petrol. Inst., 24: 69-75.

James, G.A. & Wynd, J.G. (1965): Stratigraphy Nomenclature of Iranian Oil Consortium Agreement Area. - AAPG Bull., 49 (12): 2182–2245.

Kalantary, A. (1992): Lithostratigraphy and Microfacies of Zagros. - Iran's National Oil Co. Press, Tehran.

Khosrotehrani, Kh. (1998): Micropaleontology (Foraminifera). - Tehran University Press.

Khosrotehrani, Kh. (2003): Iran's geology. - Tehran University Press.

Loeblich, A.R. & Tappan, H. (1988): Foraminiferal genera and their classification. - Van Nostrand Reinhold Company, New York, 970p.

Mehrnush, M. & Partoazar, H. (1977): Selected Microfauna of Iran. - Geological Survey of Iran, Report No.3, Teheran.

Motiei, H. (1993): Lithostratigraphy of Zagros. – Geological Survey of Iran, Report No.11, Teheran.

Postuma, J.A. (1971): Manual of planktonic foraminifera. - Elsevier Publishing Company, Amsterdam.

Rahimzadeh, F. (1994): Iran`s Geology (Oligocene- Miocene- Pliocene) ,. - Geological Survey of Iran, Report No.12, Teheran.

Sampo, M. (1969): Microfacies and Microfossils of the Zagros area, S.W. Iran (from Permian to Miocene). - Int. Sed. Petr. Ser., 12: 1–102.

Seyrafian, A., Vaziri, H. & Torabi, H. (1996): Biostratigraphy of the Asmari Formation, Burujen area. - Iran. J. Sci. I. R. Iran, Report No. 7/1: 31–47, Tehran.

Seyrafian, A. and Hamedani, A. (1998): Microfacies and depositional environments of the upper Asmari Formation (Burdigalian), North - Central Zagros Basin, Iran. - Jb. Geol. Paläont. Abh., 208: 164–167.

Seyrafian, A. (2000): Microfacies and depositional environments of Asmari Formation at Dehdez area (a correlation across Central Zagros Basin), carbonate and evaporates. - Geological Survey of Iran, Report No. 15, Teheran .

Seyrafian, A. & Hamedani, A. (2003): Microfacies and paleoenvironmental interpretation of the lower Asmari Formation (Oligocene), North-Central Zagros Basin, Iran. - N. Jb. Geol. Palaont. Mh., 210(2): 129–141.

Soheili, M. (1992): Geological Map 1:250000 Khorramabad. - Geological Survey of Iran, Teheran.

Thomas, A.N. (1948): The Asmari Limestone of Southwest Iran. - AIOC Report No.705, Teheran (unpubl.).

Thomas, A.N. (1949): Tentative isopachyte map of the Upper Asmari Limestone of the Oligocene and Lower Miocene in Southwest Iran. - AIOC Report No.731, Teheran (unpubl.).

Wynd, J. G. (1965): Biofacies of the Iranian Oil Consortium Agreement Area. - IOOC Report No.1082, Teheran (unpubl.).

Manuscript submitted: 11.4.2011
Revised manuscript accepted: 16.8.2011

Plate 1 (all samples: x40, age: Burdigalian)

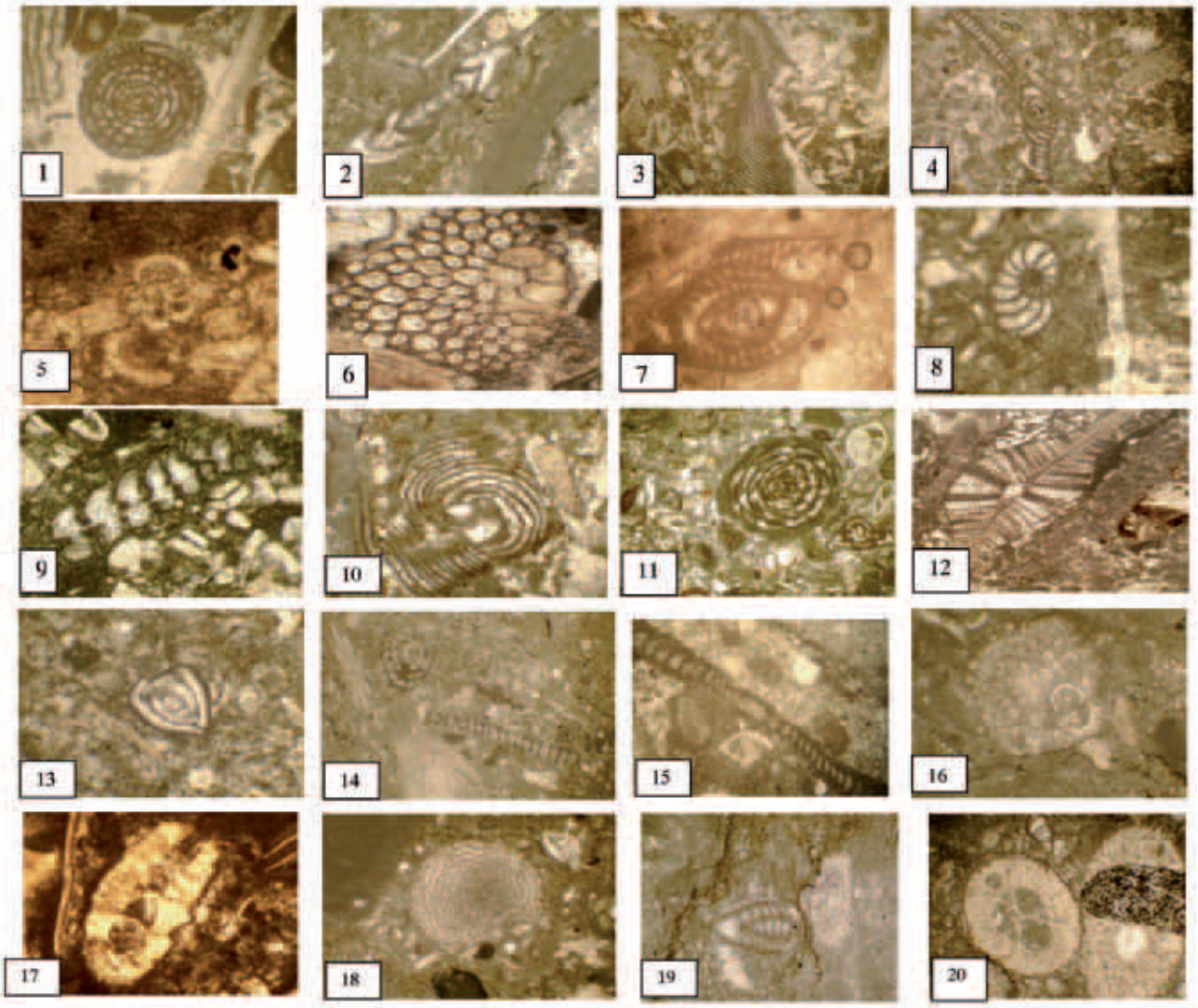

1 *Borelis melo curdica* (Reichel), Kakareza section
2 *Dendritina rangi* d'Orbigny, Makhmalkuh section
3 *Meandropsina anahensis* Henson, Kakareza section
4 *Peneroplis thomasi* Henson, Kakareza section
5 *Globigerina* sp., Makhmalkuh section
6 *Miogypsina irregularis* (Micheloti), Kakareza section
7 *Austrotrillina asmariensis Adams* , Makhmalkuh section
8 *Spirolina cylindracea* (Lamarck), Kakareza section
9 *Haplophragmium slingeri* Thomas, Kakareza section
10 *Peneroplis evolutus* Henson, Makhmalkuh section
11 *Borelis* cf. *pygmaea* (Hanzawa), Makhmalkuh section
12 *Nephrolepidina tournoueri* Lemoine and Douville, Kakareza section
13 *Triloculina trigonula* (Lamarck), Kakareza section
14 *Meandropsina iranica* Henson, Makhmalkuh section
15 *Meandropsina iranica* Henson, Kakareza section
16 *Miogypsina basraensis* Bronnimann, Kakareza section
17 *Miogypsinoides complanatus* (Schlumberger), Kakareza section
18 *Gypsina* sp., Makhmalkuh section
19 *Elphidium* sp., Kakareza section
20 *Tubucellaria* sp., Makhmalkuh section

Plate 2 (all samples: x40, age: Burdigalian)

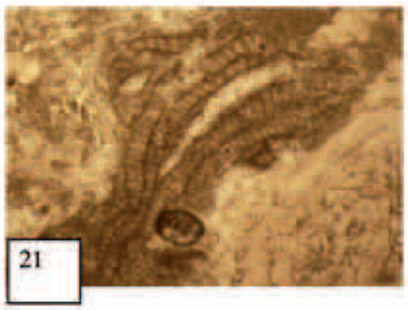

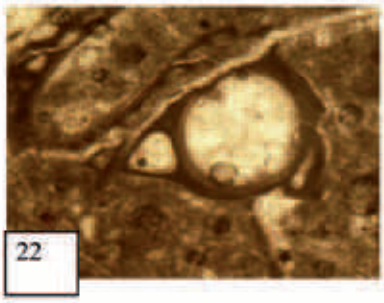

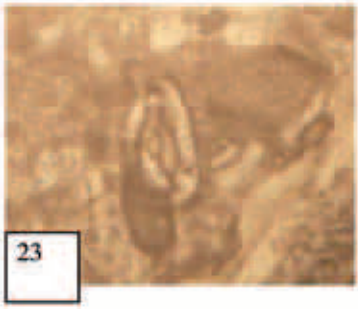

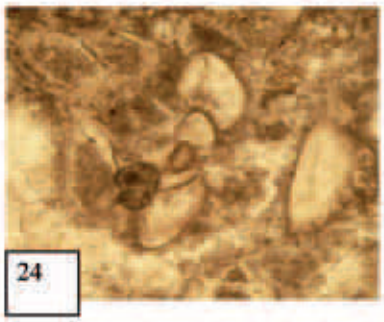

21 *Archaeolithothamnium* sp., Makhmalkuh section
22 *Kuphus arenarius* Lamarck, Kakareza section
23 *Schlumbergerina* sp. , Makhmalkuh section
24 *Anomalina* sp.., Kakareza section

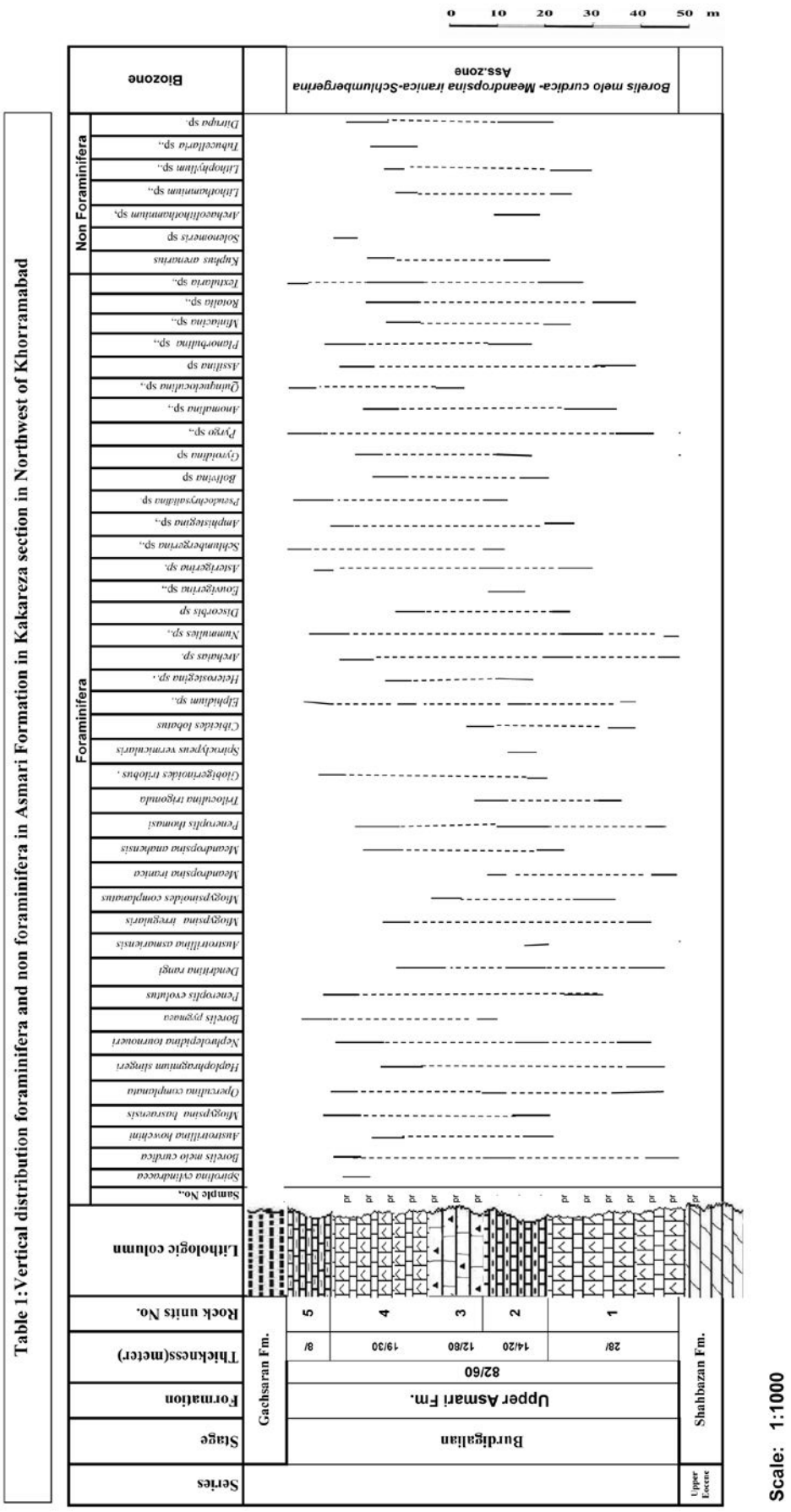

Scale: 1:1000

Table 1: Stratigraphy and microfossils of the Asmari Formation at Kakareza section.

Table 2:Vertical distribution foraminifera and non foraminifera in Asmari Formation in Makhmalkuh section in north west of Khorramabad

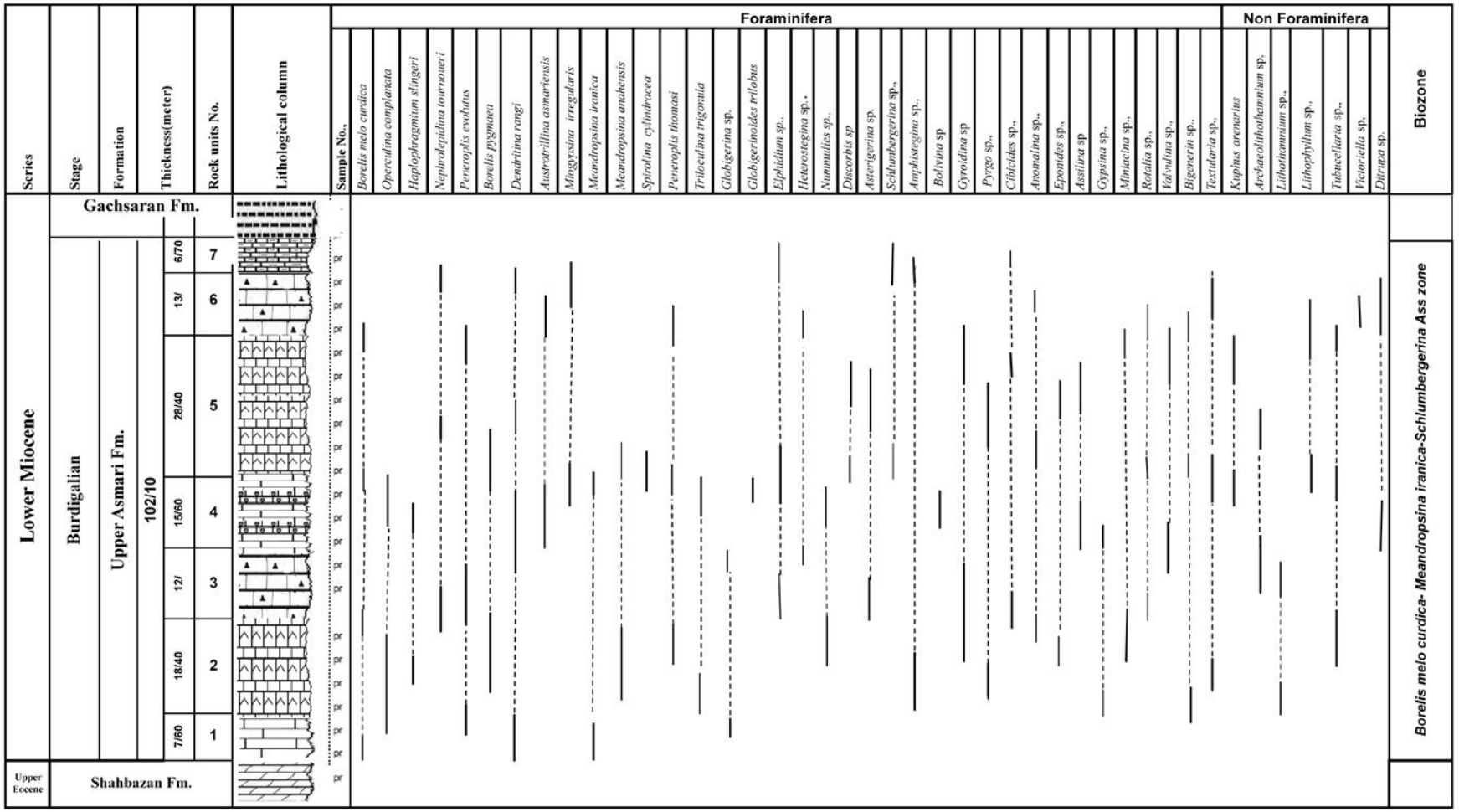

Scale: 1:1000

Table 2: Stratigraphy and microfossils of the Asmari Formation at Makhmalkuh section.

Geo.Alp, Vol. 8, S. 56–75, 2011

FACIES ANALYSIS, GEOMETRY AND ARCHITECTURE OF A CARNIAN CARBONATE PLATFORM: THE SETTSASS/RICHTHOFEN REEF SYSTEM (DOLOMITES, SOUTHERN ALPS, NORTHERN ITALY)

Gian Luigi Trombetta
with 22 Figures

P.tta S. Michele, 3/3 – 44121 Ferrara, Italy
E-mail address: gianluigi.trombetta@libero.it

ABSTRACT

The Settsass/Richthofen Reef carbonate platform system, together with the other central-western Dolomites post-volcanic carbonate complexes, forms the palaeogeographic scenario of the Lower Carnian. These Lower Carnian platforms were dwelled by coral patch-reefs and sponge mounds separated by small lagoons characterized by muddy sedimentation. The Settsass/Richthofen Reef is a small platform system (3-4 km^2 in plain view and about 150 m thick) and is characterized by two superimposed carbonate complexes (DC 1 and DC 2) showing different geometric features:
a) the lower complex, known as the Richthofen Reef (DC 1), shows a plane-convex geometry where the core is constituted by coral patch-reefs and sponge bodies, while the lateral portion is represented by the slope sediments interfingering with the basinal deposits (San Cassiano Formation);
b) the upper complex, the proper Settsass relief (DC 2), shows a tabular geometry and/or some thickening basinward. This upper complex covers a variety of depositional settings, from inner platform deposits (back-reef) at the southwestern side, to slope deposits at the southeastern side. Its slope deposits are formed by clinostratified breccias with slope angles ranging from 20° - 25° in the proximal area, to 10° - 15° more distally. The Settsass platform complex shows a basinward progradation (NE direction) which can be traced in outcrops for almost 2 km.

Keywords: Carbonate platforms, Cassian Dolomite, Sponges and Coral-reefs, clinoforms, progradation, Triassic, Dolomites Region, Southern Alps,

Introduction

The Dolomites are physiographically located in the eastern part of the Southern Alps and form a fold and thrust belt (one of the major structural units of the Alpine Chain). They are constituted by a large (several tens of km) pop-up synclinorium of Neogene age which is well confined within the Southern Alps domain (Castellarin, 1979; Doglioni & Castellarin, 1985; Doglioni & Bosellini, 1987; Schönborn, 1999). They are characterized by a slightly deformed sequence of sedimentary and volcanic rocks, offset southwards during the Alpine collision as a very coherent upper crust slab.

As a region which was only weakly deformed during the Alpine orogenic phases the Dolomites represent unique geologic outcrops and display many well preserved types of carbonate platform-slope-basin systems which have been objects of detailed geological studies in the last decades.

In particular, the Dolomites are well known for their spectacularly exposed Middle-Late Triassic progradational carbonate platforms, which have been studied in great detail in terms of geometries (Leonardi, 1968; Bosellini & Rossi, 1974; Bosellini, 1984; Kenter, 1990; Keim & Schlager, 2001; Keim et al.,

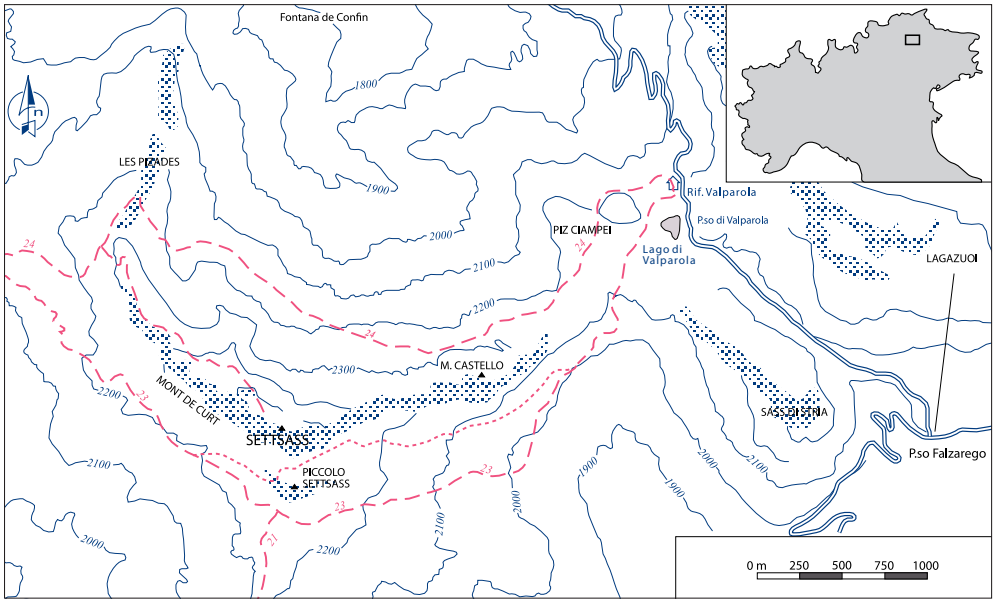

Fig. 1: Topographic map showing the study area and the main outcrop areas (stop points). The Settsass outcrops between the Valparola Pass and the Badia Valley.

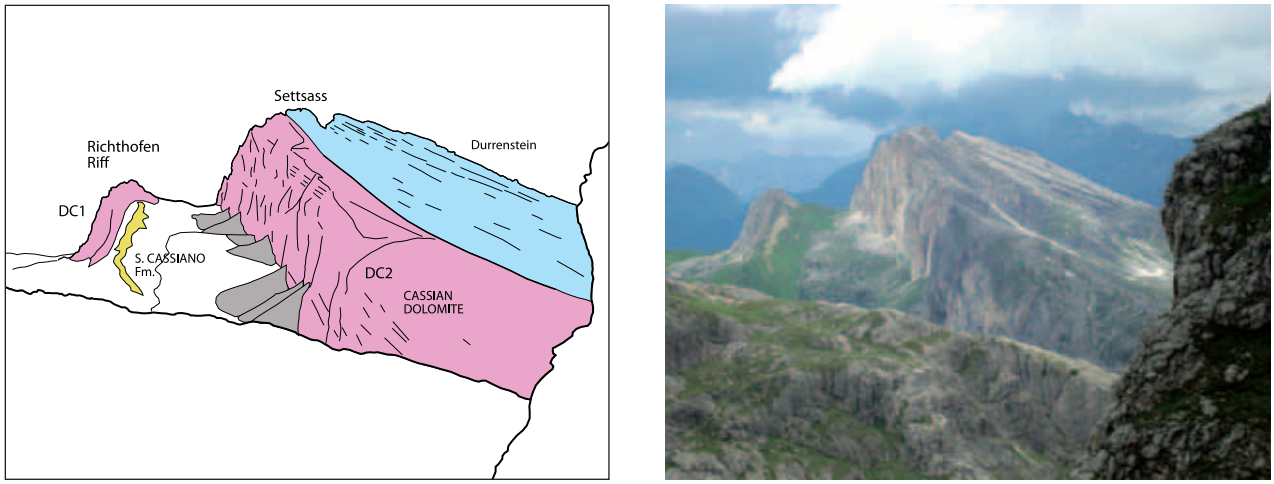

Fig. 2: Panoramic view of the Settsass from the Lagazuoi cableway. Note, from left to right, the Richthofen Reef relief, the San Cassiano Formation, the Settsass platform and the onlap relationships of the Heiligkreuz Formation. In the foreground, the slope scarp of the Cassian Dolomite of Sass di Stria is visible.

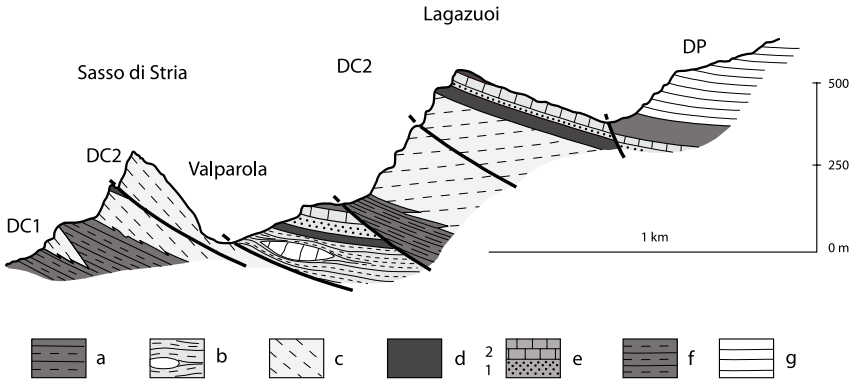

Fig. 3: Cross-section through the Sass di Stria and the Lagazuoi. Note the opposite progradation direction of the Cassian Dolomite of Lagazuoi and the Sass di Stria – Settsass carbonate platform. a) San Cassiano Formation; b) shallow-water deposits of the San Cassiano Fm; c) Cassian Dolomite; d) Heiligkreuz Formation ; e) Dibona sandstone, (1) lower member of marls, calcarenites and sandstones; (2) upper carbonate beds; f) Travenanzes Fm; g) Dolomia Principale (redrawn after Bosellini et al., 1982).

2001) and facies (Gaetani et al., 1981; Brandner et al., 1991a, b; Harris, 1993; Russo et al., 1997).

The growth and the development of the various carbonate edificies in the Dolomites region was mainly controlled by carbonate bioconstructors forming coral patch-reefs and sponge mounds, whose framework was stabilized by diverse types of binding communities, such as blue-green algae, spongiostromata, *Tubiphytes* and biogenic crusts related to different encrusting organisms (Biddle, 1980; Gaetani et al., 1981; Brandner et al., 1991). Subsequently other authors have described the occurrence of various biotic micritic crusts, microproblematica and syndepositional cements to support the stabilization of the bioconstructed framework (Harris, 1993); in other cases, the slope sediments have been regarded as in situ boundstones primarily composed of micritic crusts, early cements and various microproblematic organisms (Blendinger, 1994). Recently, the importance of automicrite (i.e. autochthonous micrite, as originally described by Wolf, 1965) has been used to explain the stabilization of the platform margin and the upper slope (Keim & Schlager, 2001).

The various carbonate edifices of the Dolomites have been divided into three groups according to their age:

a) The pre-volcanic carbonate edifices (Sciliar Dolomite of Lower Ladinian age) developed from the previous topographic highs of the sedimentary substrate (Masetti & Trombetta, 1998) during a relative rise of the sea-level. These edifices show progradational and aggradational geometrical features with limited amount of deposits transported into the basins, which were then evolving under deepening-upward conditions. The final geometry of this platform type displays an almost tabular architecture (often over 1000 meter thick) like the Catinaccio/Rosengarten platform (Bosellini, 1984; Bosellini & Stefani, 1991; Maurer, 1999, 2000).

b) The post-volcanic carbonate edifices (Cassian Dolomite of Lower Carnian age) developed during a relative sea-level still-stand. The carbonate platforms show marked progradation features; this platform-type was characterized by abundant resedimented deposits infilling the adjacent basins. In this respect, the basins display a shallowing-upward trend marked by a thinning outward geometry of the platforms (such as the climbing clinoforms of the Carnian Sella Platform, e.g. in Bosellini, 1984).

c) The pre-Cassian Dolomite carbonate platforms (= SD II, or "Rosszähne Fm." - Fm. di Denti di Terrarossa; Brandner, 1991; Brandner et al., 2007; Geologische Karte der Westlichen Dolomiten 1:25.000, 2007; Gianolla et al., 2010) whose slope deposits interfinger with volcaniclastic deposits (Wengen Fm and/or Marmolada Conglomerates); these edifices were characterized by huge volumes of megabreccia with typical blocks derived from the platform margin (like the Cipit boulders).

This paper summarizes the preliminary results of a study addressing the geometry and architecture of the carbonate platforms in the Richthofen/Settsass system, and is part of a larger and detailed research focusing on the petrography, sedimentology and stratigraphy of this peculiar post-volcanic carbonate platform system.

Geological setting of the Settsass

The Mt. Settsass is located in the surrondings of the Falzarego Pass, SW of the Valparola Pass at the head of the Badia Valley, one of the geologically most famous sectors in the Dolomites (Fig. 1). This area is crossed by an important tectonic structure known as the Passo Falzarego Line (Bosellini & Semenza, in Leonardi, 1968), a wide overthrust of E-W direction and northward dip (Fig. 2) which overimposed the northern Lagazuoi–Tofane system on top of the southern block (Cinque Torri, Nuvolau, Averau, Col Gallina, Stria Sass and the Settsass). Due to the structural setting of the footwall, the Settsass is actually a homoclinal dipping block of N-N10°E direction, with dip angles of about 35° - 40°. The subject of this study is the Settsass/"Richthofen Riff" (Fig. 1), an isolated carbonate platform of Carnian age (3 - 4 km^2 in plain view and about 150 m thick), located between the Falzarego Pass and the Badia Valley (Fig. 3). The formation is here called "Cassian Dolomite" (Bosellini, 1984; Bosellini and Neri, 1991). In the entire region of the Dolomites the Carnian paleogeography was characterized by carbonate platforms prograding across the relatively shallow basins (Bosellini & Neri, 1991). In the selected study area, the clinoform heights and the dip slope angles represent important geometric proxies which allow to estimate the maximum Cassian basin paleodepth in this area to be about 80 - 100 meters. At the Settsass/"Richthofen Reef" the clinostratification shows NE progradation and interfingering with basinal sediments of the Cassian Formation. The entire platform shows pervasive dolomitization and this has discouraged detailed facies studies up

till now. Intensive downslope transport is indicated by debris aprons at the toe of the clinoforms formed by debris-flow breccias, swarms of metre-size boulders and turbidites. In contrast to the huge breccia volumes of the clinoforms, the inner-platform and back-reef deposits, located at the southwest side of the Settsass, are poorly preserved because they were largely eroded. Therefore the history of the platform interior cannot be conclusively addressed.

Post-volcanic palaeogeography

At the Ladianian-Carnian boundary, about 236 Ma (Mundil et al., 2010), a regional sea level fall of several tens of meters triggered subaerial exposure leading to erosion and dismantling of huge amounts of volcanic and volcaniclastic deposits and of karstified flanks of the pre-volcanic platforms (Biddle, 1984; Haq et al., 1987).

From these topographic highs, which included relict volcanic reliefs, two new generations of carbonate platforms developed: the first edifices were pre-Cassian platforms (Upper Ladinian age) because their slope deposits interfingered with the Marmolada Conglomerate (see Schlern/Seiser Alm system; Brandner, 1991; Brandner et al., 1991; Punta Grohmann/Sasso Piatto; Russo et al., 1997; Col Rossi and Crepe Rosse/Mt. Padon; Bosellini et al., 1977) the so-called Cassian platforms. The subsequent generation of carbonate platforms (Cassian Dolomite of Lower Carnian age) developed under conditions of sea-level still-stand and, as a result, they are characterized by relatively thin, even-bedded platform-top facies and consist mainly of clinostratified coarse slope debris.

The palaeogeographic scenario of the Lower Carnian platforms is similar to the previous Lower Ladinian and is characterized by the following carbonate main edifices (illustrated in details in Fig. 4, redrawn after Bosellini, 1996):

- Pale di S. Martino/Civetta, a northward prograding carbonate platform;
- Sass Beccè, a small clinostratified megabreccia body prograding northward, connected with a wider Carnian platform that probably covered the whole Marmolada area (now completely dismantled);
- Sassolungo and Sassopiatto reliefs: the first one formed by the southward and westward clinostratified megabreccia slope; the second one corresponding to a spectacular submarine escarpment;
- Gardenaccia, a subrounded carbonate platform which outgrew from the Ladinian flank of the Odle Group and prograded outward;
- Sella, an almost subcircular atoll, radially prograding outward;
- Settsass/Nuvolau, examples of small northestward prograding platforms;
- Lagazuoi, a Carnian platform whose northern and eastern terminations are probably respectively overlain by the La Varella and the Tofana di Rozes mountain group;
- Picco di Vallandro/Monte Piana/Cadini di Misurina group, forming a wide southward and westward prograding platform which started from the Ladinian platform of the Dolomiti di Sesto.

Several Cassian Platforms consist of two or more superimposed carbonate edifices, showing the same direction of progradation and being nucleated on the same pre-existing topographic high. This has suggested that subsequent pulses of platform growth and demise took place during the development of the Cassian platforms. The various episodes of progradation and retreat of the overimposed platforms may be recognizable only basinward, where two or three platform progradational tongues are separated by wedges of basinal deposits (S. Cassiano Formation), thinning out until vanishing towards the central area of the carbonate buildup.

Post-volcanic stratigraphy

The post-volcanic basins of the Dolomites are characterized by an overall shallowing-upward trend, due to the combined effect of low subsidence rate, relative sea-level still-stand and high sediment supply from the adjacent carbonate platforms. Moreover, the lateral progradation of the carbonate platforms progressively reduced their extension. The result was the almost complete infilling of these intervening basins, an event that, most probably, was not synchronous over the whole area of the Dolomites (Bizzarrini et al., 1989, Mastandrea et al., 1997; Mietto & Manfrin, 1995; Neri et al., 1994; Russo et al., 1997).

The stratigraphic interval which is exposed at the Mt. Settsass and has been the subject of this study is mainly characterized by the Cassian Dolomite

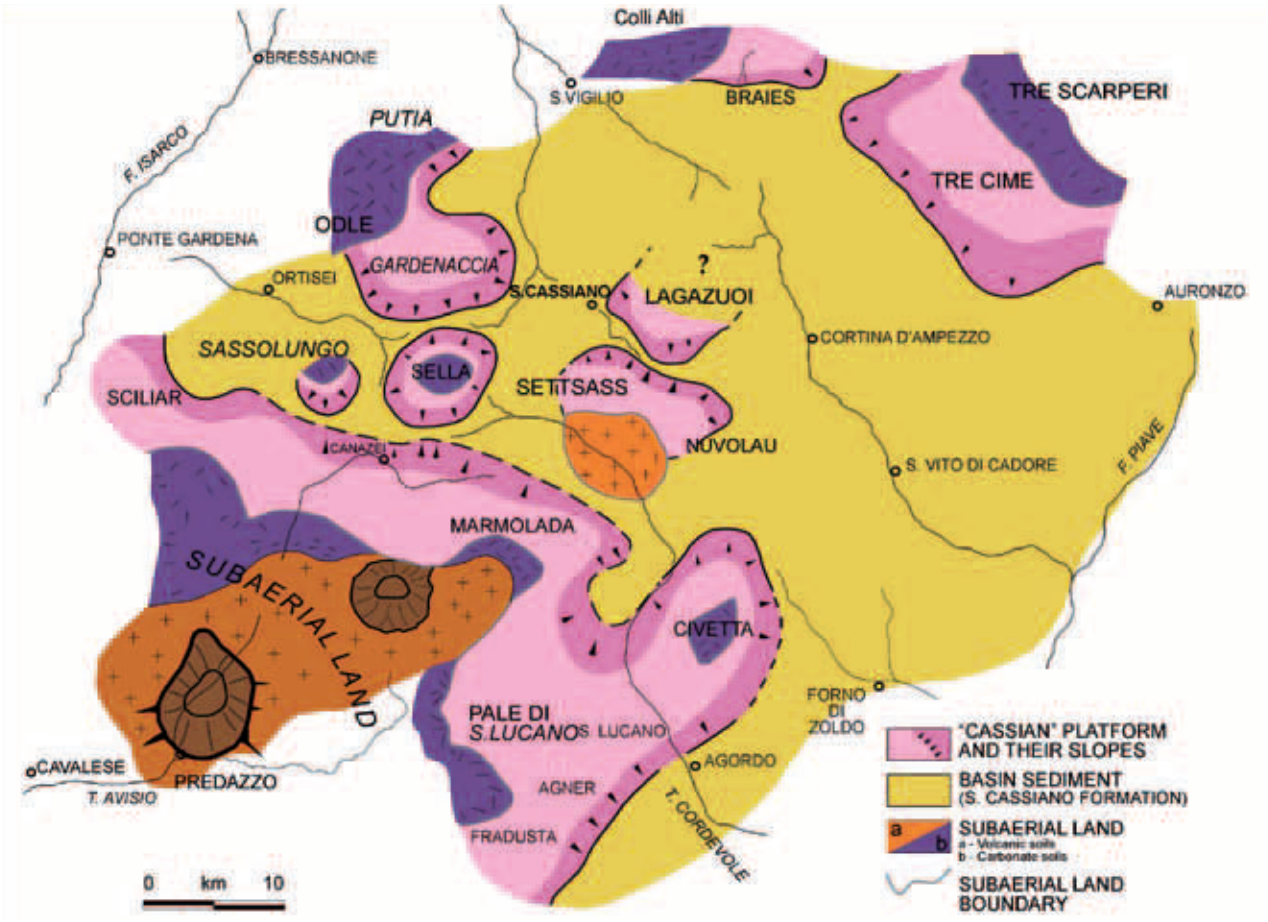

Fig. 4: Palaeogeographic map representing schematically the distribution of post-volcanic Triassic carbonate platforms of the Dolomites region and the spatial relationships with the Predazzo and the Monzoni volcanic edificies (redrawn after Bosellini, 1996).

and, marginally, by the San Cassiano Formation. At the base of Mt. Settsass the volcanoclastic deposits of the Wengen Formation and Marmolada Conglomerate are exposed, while the upper part is marked by the terrigenous-carbonate deposits of the Heiligkreuz and Travenanzes Formations (Fig. 5).

From the base to the top, the stratigraphic units which have been described at the Mt. Settsass are: a) Wengen Formation; b) San Cassian Formation; c) Cassian Dolomite; d) Heiligkreuz Formation; e) Travenanzes Formation. In the ensuing section an overview of their characteristics and interpretations is presented.

a) Wengen Formation. This unit is characterized by volcanoclastic turbidites with a composition analogous to the heterotopic underlying Marmolada Conglomerate (i.e. trachy-andesitic and andesitic) (Rossi et al., 1977; Sacerdoti & Sommavilla, 1962; Viel, 1979). The Marmolada Conglomerate is interpreted as a sedimentary sequence formed by the dismantling the volcanic edifices within the Predazzo - Monzoni district, and by the subsequent discharge of large amounts of volcanoclastic sediments through high density turbidite flows (Bottoli & Trombetta, 1998).

The Wengen Formation is formed by a sequence of thin, black, normally graded sandstone layers, ranging from cm to dm in thickness, alternating with finely laminated black pelitic beds. This formation represents the most distal parts of the Marmolada Conglomerate widely outcropping south of Mt. Settsass in the surroundings of Mt. Padon. The transition between the Wengen Formation and the Marmolada Conglomerate is markedly heterotopic, and mostly controlled by proximal-to-distal factors in relation to the sediment source areas.

b) San Cassiano Formation. This unit is a cyclic succession of shales and marls alternating with micritic limestone and oolitic-bioclastic calcarenites (Fig. 6). The San Cassiano Fm shows a coarsening and thickening-upward arrangement which results from

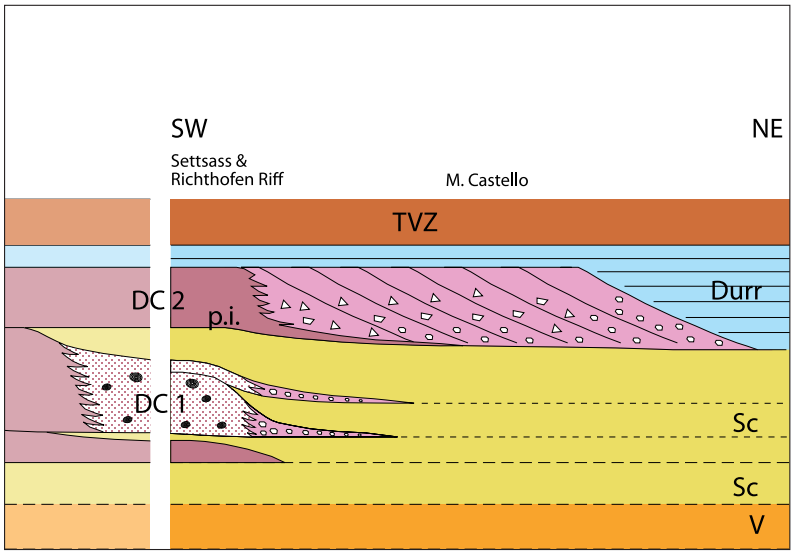

Fig. 5. Lithostratigraphic model showing various phases of carbonate platform growths and the lateral shifts of platform margin and slope facies: a) the first step is marked by a breccia platform base wedge (DC 1a), probably connected to the clinoform breccias derived from an older carbonate platform. These breccia deposits represent a first nucleus of a carbonate platform; b) the following step is characterized by the development of the second bioconstructed body (DC 1b) from the previous nucleus; c) the Richthofen Reef represents a topographic high surrounded by basinal deposits (San Cassiano Formation) and provides the development of the Settsass platform (DC 2) development. (V: Marmolada Conglomerate; Sc: San Cassiano Fm.; DC1: Cassian Dolomite 1; DC 2: Cassian Dolomite 2; HKS: Heiligkreuz Fm.; TVZ: Travenanzes Fm).

Fig. 6: Graded calcarenites derived from the platform areas from the lower portion of the San Cassiano Fm (outcrop at the base of the Richthofen Riff).

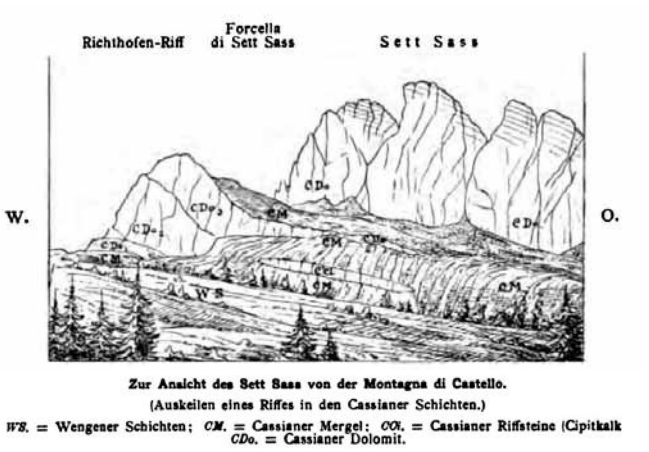

Zur Ansicht des Sett Sass von der Montagna di Castello.
(Auskeilen eines Riffes in den Cassianer Schichten.)
WS. = Wengener Schichten; *CM.* = Cassianer Mergel; *COr.* = Cassianer Riffsteine (Cipitkalk *CDo.* = Cassianer Dolomit.

Fig. 7: Original sketch of the Richthofen Riff and Settsass relief drawn by Mojsisovics (1879).

Fig. 8: a) Shallow water carbonate platform deposits: subtidal cycles of Packstones and skeletal Grainstones. Note large gastropods, oncolites, oolites and algae.

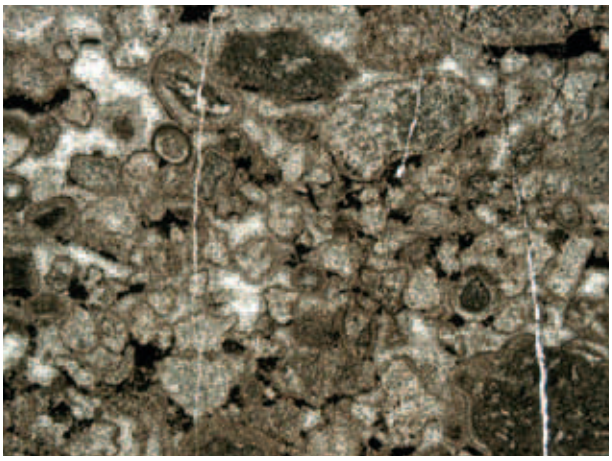

Fig. 8: b) Grainstone-Packstone with oolites and coated grains of the Dürrenstein Fm.

multi-meter thick cycles linked to the sediment supply derived from the platforms basinward, and driven by periodic sea-level change (Masetti et al., 1991).

This unit can be subdivided in two vertically stacked members. The lower member is dominated by volcanoclastic turbidites while the upper member is formed by a cyclic alternation of marls and micritic limestones, with less carbonate turbidites, and is characterized by a very rich and diverse fossil content (e.g. Fürsich & Wendt, 1977, Urlichs, 1994, Broglio Loriga et al., 1999,). The entire succession records a shallowing-upward evolution due to the basin infilling and the progradation of the Cassian platforms.

c) Cassian Dolomite. In the past decades the Falzarego Pass area has been the object of several studies which focused on the geometry and architecture of the Cassian Dolomite. This area shows evidence of two platforms convergently prograding over a basinal sequence recorded in the "Tra i Sass" stratigraphic section (Bosellini et al., 1982): the Lagazuoi platform in the north and the Nuvolau platform in the south with progradation directions respectively towards SSE and NE (Fig. 2).

In this palaeogeographic scenario the Settsass ridge is here interpreted as a platform isolated from the nearby Sasso di Stria platform (also located south of the Falzarego Line), but bearing the same progradation direction towards NE. These two platforms appear not tectonically displaced by faults and the Settsass clinoforms seem to prograde toward the inner platform deposits of the Sass di Stria platform. Based on these evidences, therefore, it seems difficult to consider the Settsass and the Sass di Stria as one single platform system. Both of these relatively small scale depositional systems are composed of two stacked platform carbonate sequences, subdivided by the San Cassiano Fm, which is here characterized by relatively shallow marine deposits, as testified by the occurrence of coral patch-reefs in growth position (Fig. 14)

At the Mt. Settsass two separate platforms can be distinguished: the Settsass strictu sensu (which constitutes the bulk of the ridge) and the Piccolo Settsass, also known in the literature as the Richthofen Riff (Fig. 7).

The Cassian Dolomite is here mainly composed of dolomitized slope breccias, often organized in clinostratified deposits, while the inner platform and platform margin deposits are outcropping only in limited parts of the studied field area. This recent geological field mapping campaign and the associated sedimentological studies have in fact allowed to describe the inner platform facies along the southwestern side of the Richtofen Reef, and distinguish them from the bioconstructional marginal facies of the already known Richthofen Reef.

d) Heiligkreuz Formation and Dürrenstein Dolomite.

This unit was introduced by Wissmann & Münster in 1841 and then described in detail by Koken (1913) and ascribed to the Upper Carnian. Later it was named "Strati di Santa Croce" (Bosellini et al., 1965a,b) and "Dürrenstein Formation ("sensu" De Zanche et al., 1993). In the last decades, the Heiligkreuz Formation was redefined (Keim et al., 2001; Stefani et al., 2004; Neri et al., 2007).

The Heiligkreuz Fm. is divided into three members (Neri et al., 2007) which testify the filling phases of the remaining Cassian basins and the crisis of the rimmed carbonate platforms.

The lower member (HKS 1) is made up of dolomitic limestone, arenaceous dolomite and well-stratified hybrid arenite with abundant pelitic intervals.

The overlying member (HKS 2) is composed of the Dibona Sandstone (Bosellini et al., 1982) formed by polymict conglomerate, cross-bedded sandstone, brown, gray or blackish pelites, with frequent oolitic-bioclastic packstone-grainstone beds.

These two members are not exposed at the Mt. Settsass; in fact only the upper member was deposited here: this is defined as HKS 3 (Lagazuoi member; Neri et al., 2007) and represents the levelling of the paleotopography in this area with the subsequent re-establishment of the carbonate platform growth conditions.

This upper member (HKS 3) consists of a cyclic succession of dolomitized shallow water platform carbonates which conformably overlie the Cassian Dolomite. This inner platform succession is arranged in meter-thick peritidal cycles (Fig. 8), formed by the repeated vertical stacking of subtidal deposits and tepee lithofacies ultimately capped by subaerial exposure surfaces (Hardie et al., 1986; Claps, 1996 in Bosellini, Neri & Stefani, 1996).

The Dürrenstein Dolomite crops out in the uppermost part of the Settsass ridge but yields only a limited thickness due to the dip of the homocline.

The subtidal lithofacies is constituted of replacive microcrystalline dolomite forming massive layers, ranging from a few tens of cm to about one meter in

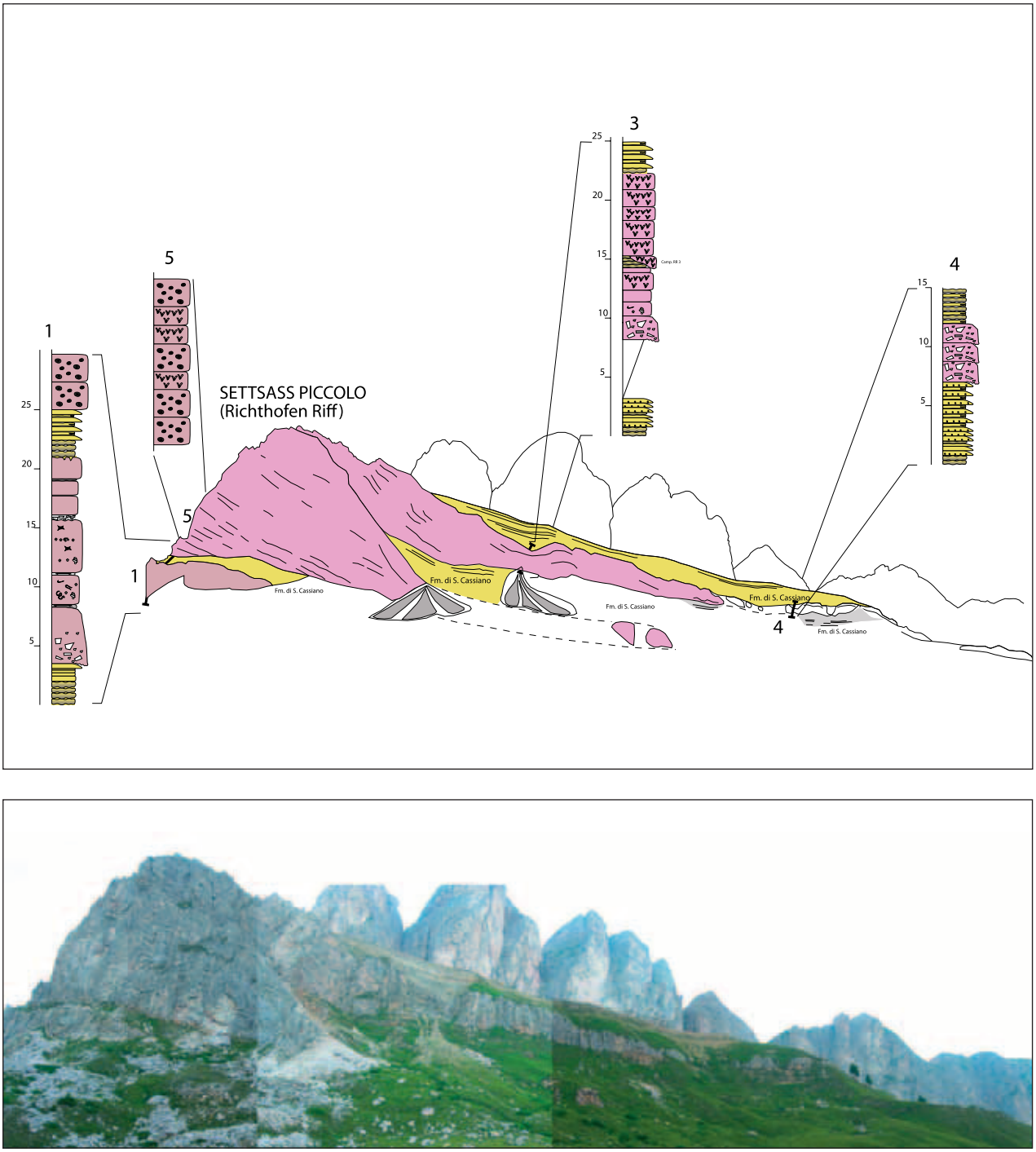

Fig. 9: The "Richthofen Reef" (Cassian Dolomite 1) is subdivided into three carbonate units. The lower unit starts with reworked breccias deposits. The second unit represents a reefal complex with sponges, corals and microbialitic mats, laterally interfingering with the basinal deposits of the San Cassiano Fm. The upper unit is a thrust wedge and represents the margin/slope deposits of the underlying unit, which is dominated by coral and sponge bioherms.

RICHTHOFEN RIFF

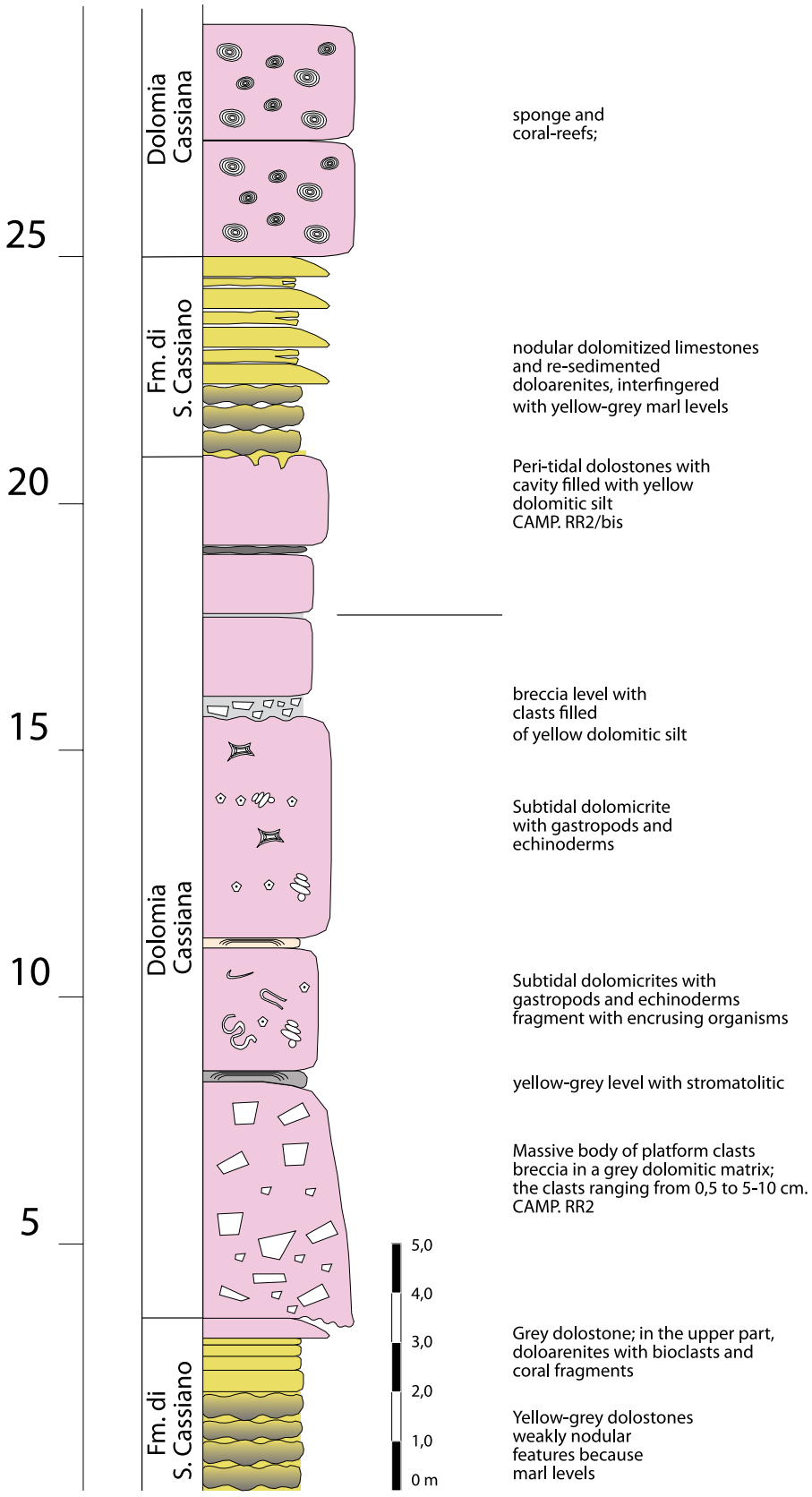

Fig. 10: The base of the Richthofen Reef (DC 1a) represents a carbonate wedge overlying the basin deposits with an erosional base (San Cassiano Fm). Note the details of the stratigraphic section.

thickness, and bearing megalodonts, gastropods and small bivalves. Isolated coral patch-reefs also occur. The tepee litofacies with subaerial exposure surfaces commonly mark the top of the depositional cycles (tepee caps, Hardie et al., 1986), showing early diagenetic alteration, and are often associated with breccia horizons. The tepees can be locally polyphase and, in association with mudcracks and sheet-cracks (Demicco and Hardie, 1994), are the most significant structures characterizing this formation. Interbedded within the deformed tepee structures are lenses of pisolitic grainstones and reworked mud intraclasts derived by the erosion of dessicated substrates. From a depositional standpoint the Heiligkreuz Formation has been interpreted as a Bahama-type carbonate platform developed within a mostly tropical climate. This environmental and climatic setting appears to dominate the shallowest part of the Cassian platform-rim-slope systems, developed during the Carnian (Hardie et al., 1986; Claps, 1996).

e) Travenanzes Formation. This stratigraphic unit has been recently formalized (Neri et al., 2007) for the Western and central Dolomites areas and it replaces the previous Raibl group (Assereto et al., 1968), which is now limited to the Eastern Dolomites area.

In the Falzarego Pass area, the Travenanzes Formation consists of terrestrial to shallow-marine, mixed siliciclastic-carbonate sediments (Bosellini at al., 1996; Neri et al., 2007). This unit is mainly composed of green, red, violet and gray pelites and marls alternating with clear aphanitic dolomites; other deposits which occur near the base of the succession are thin beds of green and gray sandstone and reddish conglomerates.

The boundary with the underlying Heiligkreuz Formation is marked by a sharp erosive surface with associated breccia levels; the boundary with the overlying Dolomia Principale is gradual, with a transition from dolomitic limestone and green-whitish dolostone to gray subtidal dolostones alternated with black dolomitic stromatolites organized in metric peritidal cycles.

The Travenanzes Formation marks the beginning of a new megasequence which also includes the overlying Dolomia Principale. The depositional environment of this carbonate unit is referred to as coastal shallow marine, and includes fluvial-deltaic settings, marsh-lagoons, tidal flats, tide-controlled shoals, beaches and wave-dominated shelves (Bosellini et al., 1982).

Settsass and Richthofen Reef

The results presented in this paper are based on an integrated approach combining detailed geological mapping, facies analysis of key outcrops and analysis of several stratigraphic sections of the Settsass ridge; as a result this integrated study has lead to reconstruct the main characteristics of the complex Settsass platform system as well as its vertical and lateral evolution.

The Richthofen Reef

The term "Richthofen Reef" was introduced by Mojsisovics (1879) in honor of Baron F. v. Richthofen (1860) for his geological pioneer work in the Dolomites.

The Richthofen Reef can be subdivided in two main carbonate bodies (as displayed in Fig. 9).

The sedimentary succession begins with a carbonate breccia at the base, unconformably overlying the basinal deposits with an erosional base (Fig. 10). The breccia is composed of clasts ranging in size from

Fig. 11: Polished slab of clast-supported carbonate breccia constituted of light clasts ranging in size froma few mm to 3-4 cm. Scale is in cm

granules to pebbles within a calcarenitic matrix (Fig. 11); this breccia represents probably a remnant of clinoforms of a previous carbonate platform (DC 1a of Fig. 5). These chaotic deposits of the lower platform body are 5 - 6 m thick; they can be laterally traced over a distance of about 60 - 80 m, and represent the first paleotopographic reliefs which were colonized by carbonate producers in a relatively shallow basinal setting. In fact the first carbonate deposits overlying these braccia layers were formed by subtidal dolomicrites rich in diverse shallow marine fossils (such as echinoderm fragments, gastropods, bivalves and a variety of encrusting organisms). These deposits are capped by thin layers characterized by reddish shales and dolomitic crystal silt filling subvertical cavities, which are interpreted as deposited during a subaerial exposure event.

The overall vertical evolution of this first phase of deposition of the Piccolo Settsass in the post-volcanic complex records a general shallowing-upward trend.

This lower platform unit is overlain by thin basinal deposits of the San Cassiano Fm, with nodular grey limestone and yellowish-grey marls. At the Piccolo Settsass the San Cassiano Fm reaches a maximum thickness of 3 - 3.5 m (Fig. 10, Fig. 12).

The overlying carbonate body has been duplicated by a southward overthrust (Doglioni, 1992 Geologische Karte der Westlichen Dolomiten 1:25.000, 2007; DC 1b of Fig. 5, 9): the thrust portion is represented by the lateral deposits of the lower carbonate body, which formed the core of the Piccolo Settsass.

The sedimentation of this second carbonate body started on these thin layers of the San Cassiano shallow deposits. The succession is composed of massive dolomitized beds (ranging in thickness from 1 m to about 3 m) intercalated with dark dolomicritic thin beds (a few cm thick).

These massive beds are characterized by the occurrence of coral and sponge patch-reefs, interpreted as bioconstructed mounds, whereas the thin dolomicritic layers represent muddier intermound deposits (Fig. 12).

The core of the coral and sponge bioconstructed bodies of the Piccolo Settsass reaches up to about 80 - 100 m of thickness and extends laterally over at least 300 m (Fig. 9).

This massive carbonate body grades laterally into a sedimentary breccia tongue that interfingers with the basinal deposits of the San Cassiano Fm. These deposits, which form the thrust body (Fig. 9), are composed of breccia units about 1 - 2 m in thickness bearing mainly platform-derived clasts. These breccias are overlain by meter-scale coral-dominated patch-reefs, which indicate a shallow marine environment with the establishment of platform margin-type depositional conditions.

The vertical evolution of the bioconstructed nucleus of the Richthofen Riff shows a northeastward progradation over the basin with a slope dip angle of about 20° - 25°, in the proximal area, flattening out over the basinal deposits in the more distal parts (downslope dip, Fig. 13).

The boundary between the two carbonate systems of the Cassian Dolomite, as mentioned before, (Fig. 9, DC 1b and DC 2 of fig. 5) is marked by a few meters thick succession of yellow/light grey bioturbated marls and calcilutites of the San Cassiano Formation. These basinal deposits testify the final drowning of the Piccolo Settsass platform. Nevertheless, in this portion of the San Cassiano Formation the occurrence of several coral patch-reefs, with typical growth position assemblages (about 0.5 m thick, as illustrated in Fig. 14), have been documented, and this proves the shallow-water conditions reached by the San Cassiano Fm at this location.

The duplicated part of the carbonate unit DC 1b (the southward overthrust) of the Piccolo Settsass shows a shallowing-upward trend too: the basinal deposits of the San Cassiano Formation are overlain by breccia units which are about 1 - 2 meter thick and contain mainly platform-derived clasts. These are overlain by meter-scale, coral-dominated patch-reefs, which represent again a shallow marine, platform-margin type depositional environment.

The intervening basin was filled by a substantial amount of volcanoclastic sediment derived from the dismantlement of the volcanic edifices located therein (Marmolada Conglomerate and Wengen Formation), and then followed by mixed carbonate-clastic basinal sediments typical of the San Cassiano Fm. (locally characterized by large platform-derived olistolites).

The Settsass

The Settsass represents the second generation of the Cassian Dolomite platforms (indicated as CD 2) and is well exposed along the southeastern and southwestern flanks of the Settsass Mt. (Fig. 15 and Fig. 16).

At the southwestern side, the inner platform deposits of the Cassian Dolomite show a monotonous cyclic succession (Fig 17) with dominantly subtidal, fine

Fig. 12: a) Platform margin of the Richthofen Riff: massive coral reefs intercalated with thin layers of a muddy intermound lithofacies

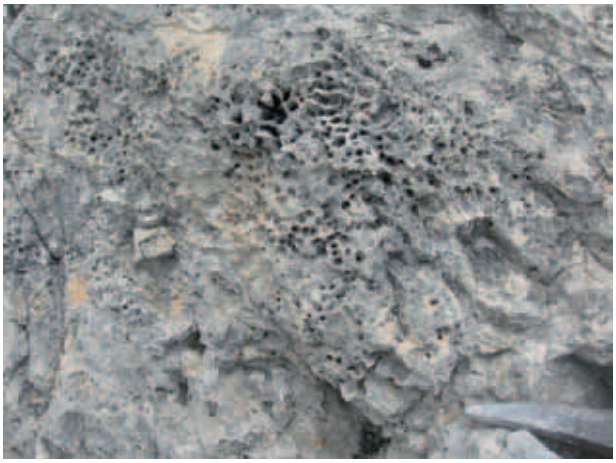

Fig. 12: b) Detail of coral patch-reef.

Fig. 13: The core of the Richthofen Riff: down-lap between the clinostratified breccia slope and overlying basin deposits. The down-lap angle is about 20°-25°. On the left, the first body of the Cassian Dolomite (DC 1/a), which dips conformably on the basin deposits below (not shown in the photograph).

Fig. 14: Coral patch-reef in growth position occurs within the San Cassiano Formation located between the Richthofen Riff and Settsass. The coral are well preserved because the interbedded marls and shales inhibited the penetration of dolomitization fluids.

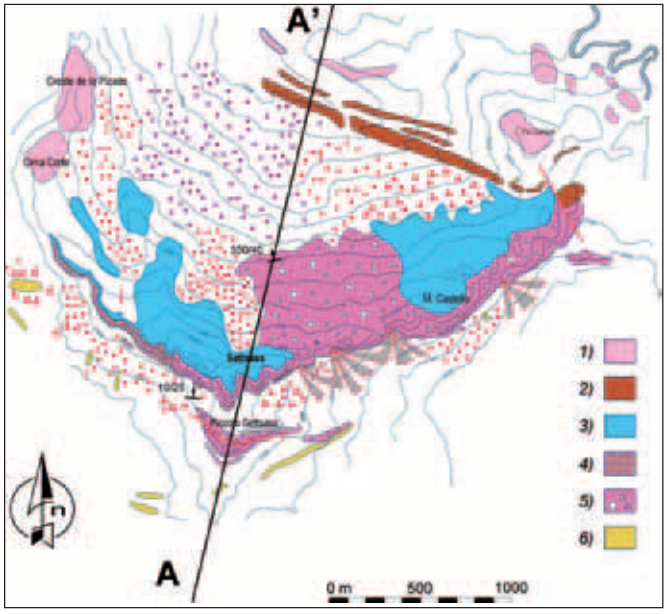

Fig. 15: Geologic map of the Settsass/Richthofen Reef interpretated as an homoclinal block dipping N-N10°, with dip angles of about 35°-40°. Note that the southwestern side is formed by the inner platform facies of the Cassian Dolomite while the southeastern side is constituted by the breccia slope of the Cassian Dolomite. 1) Dolomia Principale; 2) Travenanzes Formation; 3) Heiligkreuz Formation; 4) Cassian Dolomite (slope facies); 5) Cassian Dolomite (inner platform facies); 6) San Cassiano Formation.

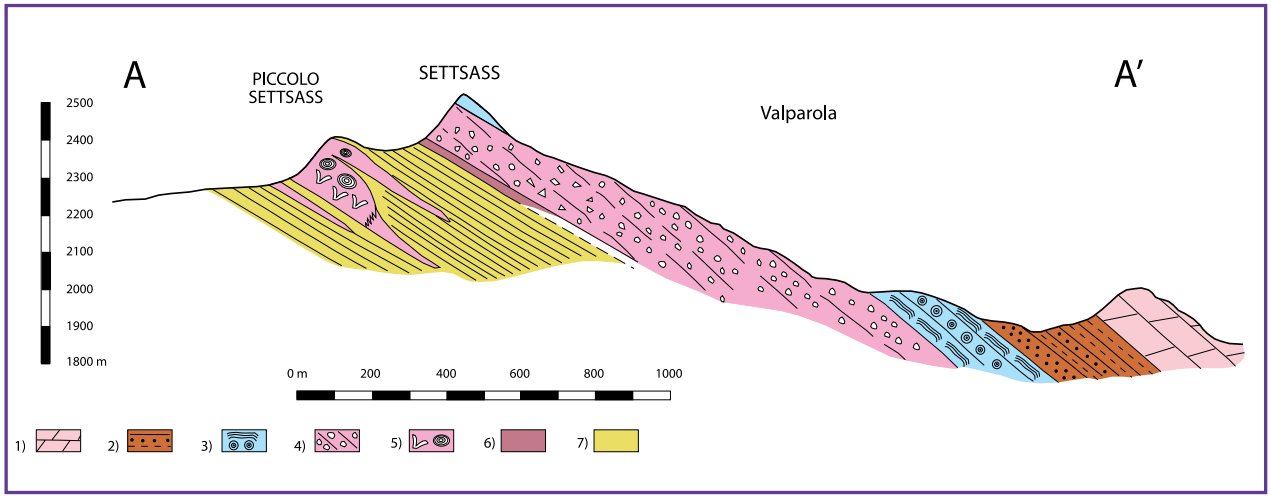

Fig. 16: Cross-section across the Piccolo Settsass (Richthofen Riff) and the Grande Settsass (approximately in N-S direction) showing two Cassian Dolomite platforms. Note the Settsass clinostratification over the basin deposits (San Cassiano Formation). 1) Dolomia Principale; 2) Heiligkreuz and Travenanzes Fms; 3) Dürrenstein Formation; 4) Cassian Dolomite (slope facies); 5) Cassian Dolomite (margin platform facies); 6) Cassian Dolomite (inner platform facies); 7) San Cassiano Formation.

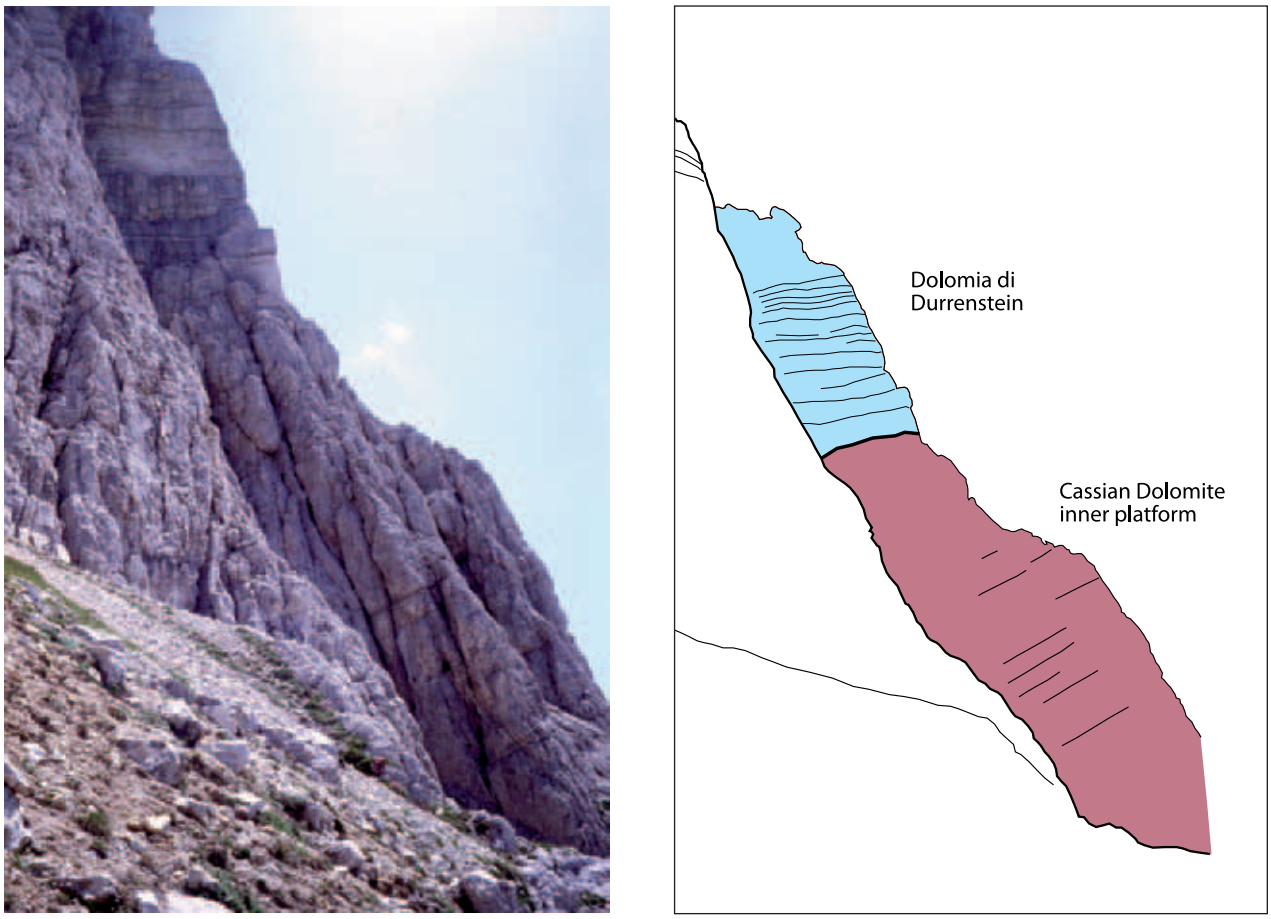

Fig. 17: Southwestern side of the Settsass showing the stratigraphic boundary between the inner platform facies of the Cassian Dolomite and the Dürrenstein Formation.

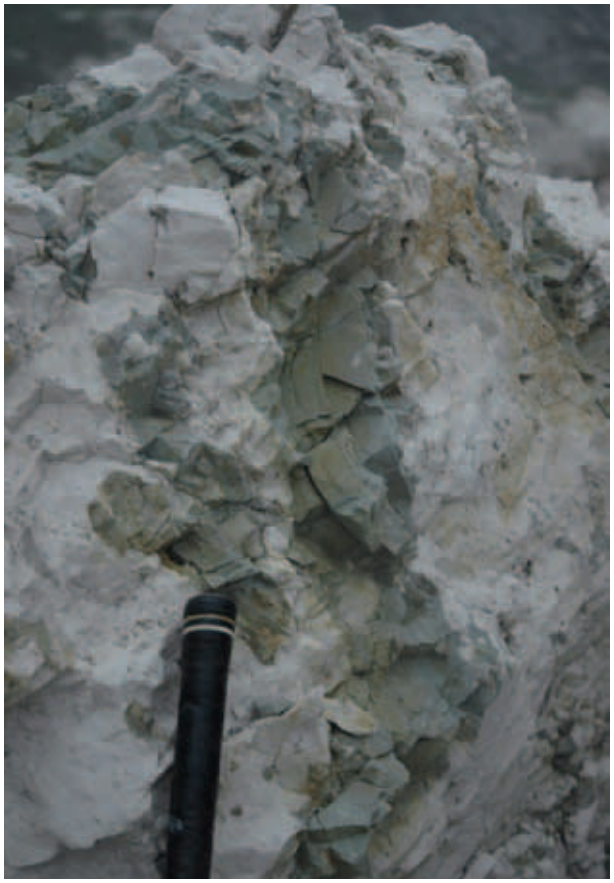

Fig. 18: Sedimentary dikes originated at exposure surfaces and are filled with light-green silt, cross-cutting well cemented microbial limestone, which are interpreted as microkarstic features.

grained facies (skeletal-peloidal packstones) capped by thin subaerial exposure surfaces with deeply incised internal pockets filled with greenish-grey shales (microkarst cavities, Fig. 18). In the vicinity of the clinostratifications microbial and algal-clotted peloidal limestone patches occur. These bodies are locally incised by subaerial exposure surfaces and are characterized by the presence of dissolution vugs filled by subsequent cement phases (Fig. 19). Some of these cavities are filled with reddish shale and dolomitic silt. This platform sequence is overlain by the Heiligkreuz Formation (Fig. 16).

The southeastern side of the Settsass shows clinostratified breccias downlapping over the basinal deposits of the San Cassiano Fm. The downlap angle between the clinoforms and the basinal deposits ranges from 20° - 25° in the proximal area, decreasing to to 10° - 15° in its distal part.

The clinostratified breccia is mostly composed of platform-derived debris with grain size from a few mm up to 5 - 10 cm, Fig. 20). At the toe of the slope the breccia tongues interfinger with the basinal deposits, associated to the carbonate turbidites and grey-yellow dolomitized nodular fine grained limestones of the San Cassiano Formation. The progradation of the Settsass platform over the basin reaches a horizontal offset of about of 2 km (Fig. 21).

The downlap surface between the clinoforms and the basinal beds is in most places covered by quaternary deposits at the toe of the rock walls, but appears to be well exposed at a few key locations (as displayed in Fig. 22).

The Settsass platform geometry is constrained by its upper and lower stratigraphic boundaries: at the top, the boundary with the overlying Heiligkreuz Formation is flat (toplap), while the lower boundary with the underlying San Cassiano Formation corresponds to an unconformity surface (Fig. 16 and 21). The resulting Settsass platform geometry is therefore tabular and/or slightly thickening outward, with an overall slightly descending progradation pattern.

Summary of the platform margin architecture and main depositional features

The Settsass-Richthofen Reef platform system consists of two superimposed carbonate edifices, nucleated on a stable topographic high, which is the remnant of a clinoform body originated from a predecessor carbonate platform (DC 1a of Fig. 5). These two systems were then aggrading vertically and prograding in the same direction towards northeast. The various progradation phases are recognized by the interfingering of the slope breccia deposits and the basinal deposits of the San Cassiano Fm above the shallow carbonate facies (Fig. 5). The carbonate platform productivity in these two systems came to a temporary stop probably due to subsequent eustatic sea-level falls which caused subaerial exposure and some degree of karstification of the platform interior and platform margin system.

The main features of the Settsass platform system can be summarized as follows:

- its overall platform geometry is tabular, with an outcropping thickness of about 150m, and is slightly thickening basinward;
- its evolution is conformable to the preexisting basin morphology (Richthofen Reef platform-basin system);
- its upper boundary displays a toplap geometric relationship;

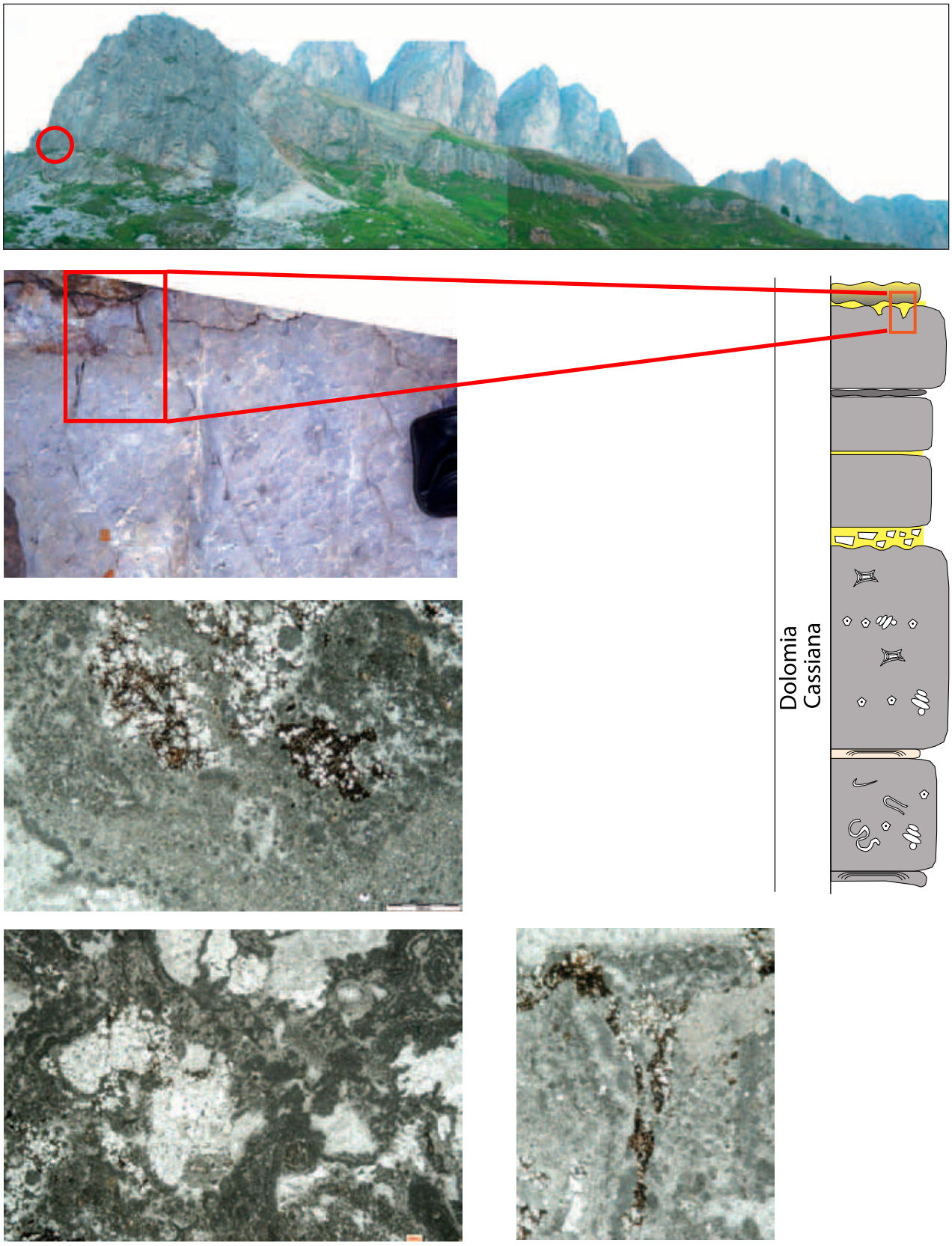

Fig. 19: Subaerial unconformity cutting through microbial and clotted peloidal limestone. The subaerial exposure is testified by the occurrence of microkarstic cavities. Dissolution vugs now appear mostly cemented and are filled with reddish shale and siltstone composed of dolomite crystals.

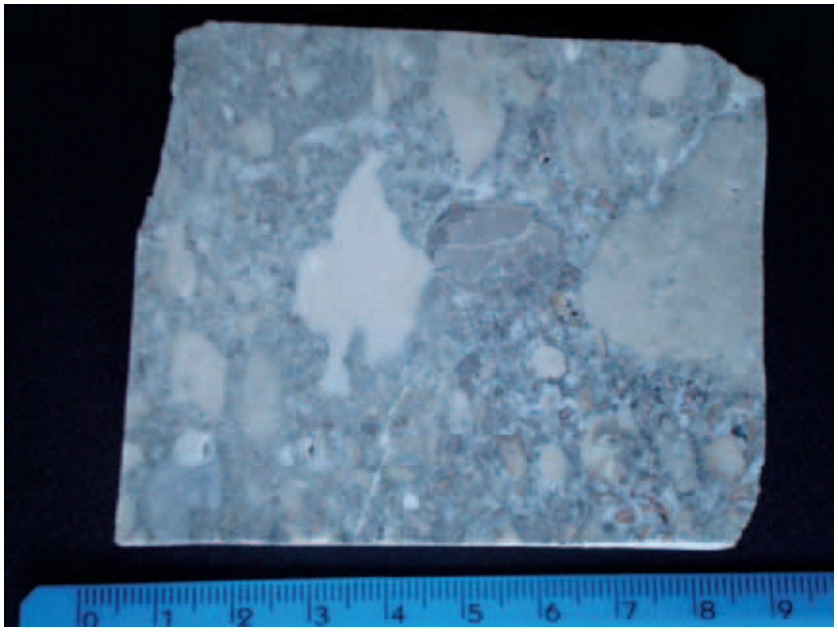

Fig. 20: Polished slab of a clinostratified breccias deposit. The light-colored clasts are derived from the platform areas. Outcrop at the lower portion of the slope, under the M. Castello rock wall.

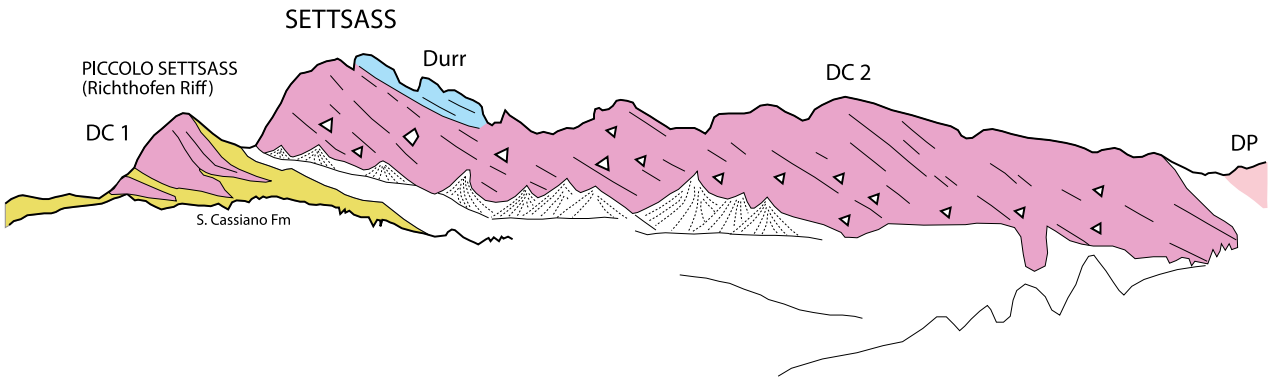

Fig. 21: Geological interpretation of the Settsass group. In the foreground the Richthofen Reef (Cassian Dolomite 1, CD 1) is constituted by a Carnian reef system and two platform progradational lenses intercalated with the adjacent basinal deposits, which then in turn onlap the platform margin body (S. Cassian Fm). The Settsass (in the background, Cassian Dolomite 2, CD 2) clearly shows the clinostratification geometry of the youngest platform, laterally prograding on the basin. The extent of the progradation measures at least about 2 km. DC 1a & DC 1b: Cassian Dolomite (Richthofen Reef); DC 2: Cassian Dolomite (Settsass); SC: S. Cassiano Formation; HKS: Heiligkreuz Formation; DP: Dolomia Principale.

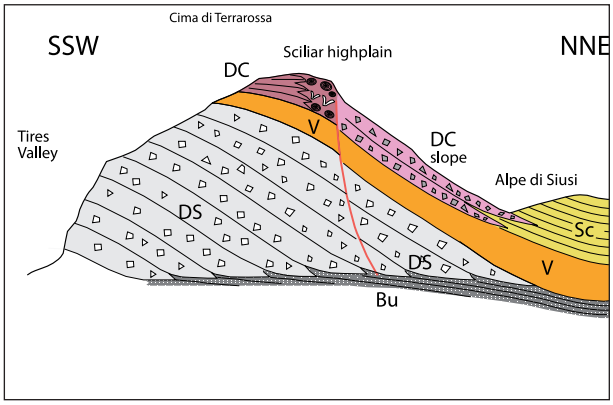

Fig. 22: The lower portion of the clinostratification in the rock cliff beneath Castello Mountain. Note the load structures linked to the large boulder deforming the underlying thin strata of calcilutites and calcarenites. Sc = San Cassiano Fm.; Dc slope = Cassian Dolomite (slope facies); DC = Cassian Dolomite

- its lower boundary is represented by an unconformity and bears a slightly descending geometry;
- the adjacent basin shows shallow water conditions, probably controlled by a relative sea-level stillstand and low subsidence rate
- the slope angle of the clinoforms range from 20° - 25° in the proximal area to 10° - 15° in the distal part;
- the extent of the platform progradation can be traced in outcrop over a distance of about 2 km.

Conclusions

The Settsass/Richthofen Reef shows common features with the other Lower Carnian edifices, like the occurrence of huge volumes of carbonate megabreccias (including the olistolithic blocks known as "Cipit" blocks) which interfinger with the basinal deposits of the San Cassiano Formation. The megabreccia slopes are often organized in clinostratified deposits with dip angle slopes ranging from 20° - 25° to 40° - 45°. These steep slope cannot be explained only with the grain-size of the reworked sediments (Kenter, 1990); in fact the carbonate platform slope flanks were also stabilized by microbialites, early cementation and activity of encrusting microorganisms (as discussed in Keim & Schlager, 2001).

The presented case study of the Settsass/Richthofen Reef provides new insights about the Lower Carnian platform evolution that can be summarized as follows:

a) At the Settsass/Richthofen Reef two carbonate platform systems are clearly identified by the occurrence of platform margin bioconstructors (i.e. coral patch-reefs in growth position) and the two platform growth phases (DC 1 and DC 2) are subdivided by the intervening relatively shallow basinal deposits.

b) The Richthofen Reef shows a plane-convex geometry reaching up to about 80 - 100 m in thickness and extending at least 300 m laterally. This reef is formed by two main bodies (DC 1a and DC 1b):

1) DC 1a is constituted by white carbonate breccias, overlying the basinal deposits (San Cassiano Formation) with an erosional base. This first body presents a tabular geometry;

2) DC 1b represents the reef core, and corresponds to a bioconstructed body formed by coral patch-reefs and sponge mounds as well as by margin/slope deposits which interfinger with basinal deposits. This second body yields an overall plane-convex geometry.

c) The Settsass platform (DC 2) displays a tabular geometry and records a complete depositional environment spectrum from its inner platform succession (back-reef) down to the slope deposits composed of clinostratified breccias. The inner platform succession, which has not been documented before, is arranged in shallowing-upward cycles overlain by the Heiligkreuz Formation. The slope deposits are formed by clinoforms with a slope dip angle ranging from 20° - 25° in the proximal area to 10° - 15° more distally.

The Settsass platform shows a basinward (NE direction) progradation over a distance of almost 2 km comparable to other examples from the Dolomites (Bosellini, 1984; Bosellini & Stefani, 1991; Maurer, 1999; Keim & Schlager, 2001).

ACKNOWLEDGMENTS

The author is indebted to M. Claps (Petroleum Development Oman, R. Longoni (ENI), A. Boz (ENI) and M. Cella (ENI) for fruitful discussions during the field work. The review by L. Keim and K. Krainer considerably improved the first version of this manuscript. The early English version was kindly revised by M. Claps.

References

Assereto, R., Desio, A., Di Codalberto, D. & Passeri, L. (1968): Note illustrative della Carta geologica d'Italia. Foglio 14a Tarvisio. pp. 1-70; Ser. Geol. d'Italia, Roma.

Biddle, K.T. (1980): The basal Cipit boulders: indicators of middle to upper Triassic buildup margins, Dolomite Alps, Italy. – Riv. It. Paleont. Strat. 86: 779-794.

Biddle, K.T. (1984): Triassic sea level changes and the Ladinian-Carnian stage boundary. – Nature 308: 631-633.

Bizzarrini, F., Laghi, G., Nicosia, U. & Russo, F. (1989): Distribuzione stratigrafica dei microcrinoidi (Echinodermata) nella Formazione di San Cassiano (Triassico superiore, Dolomiti): studio preliminare. - Atti Soc. Nat. Mat. 120: 1-14.

Blendinger, W. (1994): The carbonate factory of the Middle Triassic buildups in the Dolomites, Italy: a quantitative analysis. – Sedimentology 41: 1147-1159.

Bosellini, A. (1965a): Lineamenti strutturali delle Alpi Meridionali durante il Permo-Trias. Mem. Mus. St. Nat. Ven. Trid. 15: 1-72.

Bosellini, A. (1965b): Schema strutturale del Permo-Trias postercinico nelle Alpi Meridionali. Acc. Naz. Lincei, Rend. Sc. Fis., Mat., Nat. Serie VIII, 38: 216-222.

Bosellini, A. (1984): Progradation geometries of carbonate platforms: examples from the Triassic of the Dolomites, Northern Italy. – Sedimentology 31: 1-24.

Bosellini, A. (1996): La storia geologica delle Dolomiti. 148 pp., Edizioni Dolomiti, Pordenone.

Bosellini, A. & Neri, C. (1991): The Sella Platform (Upper Triassic, Dolomites, Italy). - In: Dolomieu Conference on Carbonate Platforms and Dolomitization, Guidebook Excursion B, 30 pp, Ortisei, Italy.

Bosellini, A. & Rossi, D. (1974): Triassic carbonate buildups of the Dolomites, northern Italy. - In Laporte L.F. (ed), Reefs in time and space: SEPM, Spec. Publ. 18: 209-233.

Bosellini, A. & Stefani, M. (1991): The Rosengarten: A platform-to-basin carbonate section (Middle Triassic, Dolomites, Italy). - In: Dolomieu Conference on Carbonate Platforms and Dolomitization, Guidebook Excursion C, 24 pp, Ortisei, Italy.

Bosellini, A., Masetti, D. & Neri, C. (1982): La geologia del Passo del Falzarego. - In: A. Castellarin & G.B. Vai (a cura di): Guida alla geologia del Sudalpino centro-orientale. Guide Geol. Reg. S.G.I., 273-278, Bologna.

Bosellini, A., Neri, C. & Stefani, M. (1996a): Geologia delle Dolomiti, introduzione geologica. - 78a riunione estiva della Soc. Geol. It., Guidebook, pp. 9-53, San Cassiano.

Bosellini, A., Neri, C. & Stefani M. (1996b): Geometrie deposizionali stratigrafia fisica a grande scala di piattaforme carbonatiche triassiche. - 78a riunione estiva della Soc. Geol. It., Guidebook, pp. 1-36, San Cassiano.

Bosellini, A., Castellarin, A., Rossi, P.L., Simboli, G. & Sommavilla, E. (1977): Schema sedimentologico e stratigrafico per il Trias medio della Val di Fassa ed aree circostanti (Dolomiti Centrali). – Gior. Geologia (2), 17: 83-108.

Bottoli, S. & Trombetta, G.L. (1998): Analisi di facies ed ambiente deposizionale del Conglomerato della Marmolada: un sistema torbiditico dominato da flussi ad alta densità (Gruppo Col Rossi-Porta Vescovo, Dolomiti Occidentali). – Mem. Soc. Geol. It., 53: 341-357.

Brandner, R. (1991): Geological setting and stratigraphy of the Schlern-Rosengarten buildup and Seiser Alm basin. In Brandner, R., Flügel, E., Koch, R. & Yose, L.A. (eds.): The Northern Margin of the Schlern/Sciliar – Rosengarten/Catinaccio Platform, 4-16, Dolomieu Conference on Carbonate Platforms and Dolomitization, Guidebook Excursion A, 61 pp, Ortisei, Italy.

Brandner, R., Flügel, E. & Senowbari-Daryan, B. (1991): Microfacies of Carbonate Slope Boulders: Indicator of the Source Area (Middle Triassic: Mahlknecht Cliff, Western Dolomites). - Facies, 25: 279-296.

Brandner, R., Gruber, A. & Keim, L. (2007): Geologie der Westlichen Dolomiten: von der Geburt der Neotethys im Perm zu Karbonatplattformen, Becken und VulKaniten der Trias. – Geo.Alp., 4: 95-121.

Broglio Loriga, C., Cirilli, S., De Zanche, V., Di Bari, D., Gianolla, P., Laghi, G., Lowrie, W., Manfrin, S., Mastandrea, A., Mietto, P., Muttoni, G., Neri, C., Posenato, R., Reichichi, M., Rettori, R. & Roghi, G. (1999): The Prati di Stuores/Stuores Wiesen Section (Dolomites, Italy): a candidate Global Stratotype Section and Point for the base of the Carnian stage. – Riv. It. Paleont. Strat. 105: 37-78.

Castellarin, A. (1979): Il problema dei raccorciamenti crostali nel Sudalpino. Rend. - Soc. Geol. It. 1: 21-23.

Demicco, R. V. and Hardie, L.. A. (1994): Sedimentary Structures and Early Diagenetic Features of Shallow Marine Carbonate Deposits. – SEPM Atlas Series No. 1, 265 pp.

De Zanche, V., Gianolla P., Mietto P., Siorpaes C. & Vail P. (1993): Triassic sequence stratigraphy in the Dolomites (Italy). Mem. Sci. Geol. 45: 1-27.

Doglioni, C. (1992): Escursione nel Sudalpino Orientale (Dolomiti e Prealpi Venete). - AGIP guide book, 118 pp.

Doglioni, C. & Bosellini, A. (1987): Eoalpine and mesoalpine tectonics in the Southern Alps. - Geol. Rundschau 76: 735-754.

Doglioni, C. & Castellarin, A. (1985): A geologic schematic cross section of eastern Southern Alps. - Rend. Soc. Geol. It. 8: 35-36.

Fürsich, F.T: & Wendt, J. (1977): Biostratinomy and palaeoecology of the Cassian Formation (Triassic) of the Southern Alps. - Palaeogeog., Palaeoclimatol., Palaeoecol. 22: 257-323.

Gaetani, M., Fois, E., Jadoul, F. & Nicora, A. (1981): Nature and evolution of Middle Triassic carbonate buildups in the Dolomites (Italy). - Marine Geology 44: 25-57.

Geologische Karte der Westlichen Dolomiten 1:25.000 (2007): Autonome Provinz Bozen – Südtirol, Amt f. Geologie u. Baustoffprüfung, Bozen/Kardaun.

Gianolla, P., Andreetta, R., Furin, S., Furlanis, S. & Riva, A. (2010): Nomination of the Dolomites for inscription on the World Natural Heritage List UNESCO. - 7th Intern Triassic Field Workshop, Field Trip to the World Heritage Site of the Tethyan Triassic, September 5-10.

Hardie, L.A., Bosellini, A. & Goldhammer, R.K. (1986): Repeated subaerial exposure of subtidal carbonate platforms, Triassic, Northern Italy: evidence for high frequency sea level oscillations on a 10000 year scale. - Paleoceanography 1: 447-457.

Haq, B.U., Hardenbol, J. & Vail, P.R. (1987): Chronology of fluctuating sea-levels since the Triassic. – Science 235: 1156-1166.

Harris, M. T. (1993): Reef fabrics, biotic crusts and syndepositional cements of the Latemar reef margin (Middle Triassic), northern Italy. - Sedimentology 40: 383-401.

Keim, L. & Schlager, W. (2001): Quantitative compositional analysis of a Triassic carbonate platform (Southern Alps, Italy). - Sedimentary Geology 139: 261-283.

Keim, L., Brandner, R., Krystyn, L. & Mette, W. (2001): Termination of carbonate slope progradation: an example from the Carnian of the Dolomites, Northern Italy. - Sedimentary Geology 143: 303-323.

Kenter, J.A.M. (1990): Carbonate platform flanks: slope angle and sediment fabric. - Sedimentology 37: 777-794.

Koken, E. (1913): Beiträge zur Kenntniss der Schichten von Heiligkreuz. – Abhandl. Geol. R. A. 16.

Leonardi, P. e collaboratori (1968): Le Dolomiti. Geologia dei monti tra Isarco e Piave.

Manfrini Editore, Rovereto (Trento), 1019 pp.

Masetti, D. & Trombetta, G.L. (1998): Eredità anisica nella nascita ed evoluzione delle piattaforme medio-triassiche delle Dolomiti Occidentali. - Mem. Sci. Geol. 50: 213-237.

Masetti, D., Neri, C. & Bosellini, A. (1991): Deep-water asymmetric cycles and progradation of carbonate platforms governed by high-frequency eustatic oscillations (Triassic of the Dolomites, Italy). - Geology 19: 336-339.

Mastandrea, A., Neri, C. & Russo, F. (1997): Conodont biostratigraphy of the San Cassiano Formation surrounding the Sella Massif (Dolomites, Italy): implications for sequence stratigraphic models of the Triassic of the Southern Alps). - Riv. It. Paleont. Strat. 100: 39-52.

Maurer, F. (1999): Wachstumsanalyse einer mitteltriadischen Karbonatplatform in den westlichen Dolomiten (Sudalpen). - Eclogae Geol. Helv. 92: 361-378.

Maurer, F. (2000): Growth mode of Middle Triassic carbonate platforms in the Western Dolomites (Southern Alps, Italy). - Sedimentary Geology 134: 275-286.

Mietto, P. & Manfrin, S. (1995): La successione delle faune ad ammonoidi al limite Ladinico-Carnico (Sudalpino, Italia). - Ann. Univ. Ferrara, Sci. Terra 5 (suppl.): 13-35.

Mojsisovics, E. von (1879): Die Dolomit-Riffe von Südtirol und Venetien. – Beiträge zur Bildungsgeschichten der Alpen, 1-552, Wien.

Mundil, R., Pàlfy J., Renne P. & Brack P. (2010): The Triassic timescale: new constraints and a review of geochronological date. – In: S.G. Lucas (eds.) The Triassic timescale, Geol. Soc. Spec., London.

Neri, C., Gianolla, P., Furlanis, S., Caputo, R. & Bosellini, A. (2007): Note illustrative della Carta Geologica d'Italia. Foglio Cortina d'Ampezzo 029. Scala 1:50.000. - Servizio Geologico d'Italia, 200 pp.

Neri, C., Mastandrea, A., Laghi, G., Baracca, A. & Russo, F. (1994): New biostratigraphic data on the S. Cassiano Formation around Sella Platform (Dolomites, Italy). - Paleopelagos 4: 13-21.

Richthofen, F., von (1860): Geognostische Beschreibung der Umgegend von Predazzo, Sanct Cassian und der Seisser Alpe in Südtirol. - Perthes, Gotha.

Rossi, P.L., Viel, G & Simboli, G. (1977): Significato paleogeografico e magmatico-tettonico della serie vulcanica vulcano-clastica ladinica superiore nell'area del Monte Civetta. - Boll. Soc. Geol. It. 95 (1976): 433-458.

Russo, F., Neri, C., Mastandrea, A. & Baracca, A. (1997): The Mud Mound nature of the Cassian Platform margins of the Dolomites. A case history: the Cipit boulders from Punta Grohmann (Sasso Piatto Massif, Northern Italy). - Facies 36: 25-36.

Sacerdoti, M. & Sommavilla, E. (1962): Pillowlave, ialoclastiti e altre formazioni vulcanoclastiche nella Regione Dolomitica occidentale. - Studi Trent. Sc. Nat. 39: 423-473.

Schönborn, G. (1999): Balancing cross section with kinematic constraints: The Dolomites (northern Italy). – Tectonics 18(3): 527-545.

Stefani, M., Brack, P., Gianolla, P., Keim, L., Maurer, F., Neri, C., Preto, N., Riva, A., Roghi, G. & Russo, F. (2004): Triassic carbonate platforms of the Dolomites: carbonate production, relative sea-level fluctuations and the shaping of the depositional architecture. - In: M. Stefani (ed.), Triassic carbonate platforms of the Dolomites: carbonate production, relative sea-level fluctuations and the shaping of the depositional architecture fieldbook - 32dn Int. Geol. Congr.: 1-44.

Urlichs, M. (1994): Trachyceras Laube 1896 (Ammonoidea) aus dem Unterkarn (Obertrias) der Dolomiten (Italien). – Stuttgarter Beiträge für Naturkunde , Serie B, 217: 1–55.

Wissmann, H.L. & Münster, G.G. von (1841): Beiträge zur Geognosie und Petrefacten-Kunde des Südöstlichen Tirol's vorzuglich der Schichten von St. Cassian. – Beitr. Petrefacten-Kunde 4: 1-152, Bayreuth.

Viel, G. (1979): Litostratigrafia ladinica: una revisione. Ricostruzione paleogeografica e paleostrutturale dell'area Dolomitico-Cadorina (Alpi Meridionali). Parte I e II. – Riv. It. Paleont. Strat. 85/1: 85-125 and 85/2: 297-352.

Wolf, K.H. (1965): Gradational sedimentary products of calcareous algae. – Sedimentology 5: 1-37.

Manuscript submitted: 20.6.2011
Revised manuscript accepted: 18.10.2011

Geo.Alp, Vol. 8, S. 76–118, 2011

A 4-DAY GEOLOGICAL FIELD TRIP IN THE WESTERN DOLOMITES

Rainer Brandner[1] & Lorenz Keim[2]

With 28 Figures

[1] Institut für Geologie & Paläontologie, Universität Innsbruck, Innrain 52, A-6020 Innsbruck;
E-mail address: Rainer.Brandner@uibk.ac.at

[2] Amt für Geologie & Baustoffprüfung/Ufficio Geologia e prove materiali, Autonome Provinz Bozen – Südtirol/Provincia Autonoma di Bolzano-Alto Adige, Eggentalerstr./Via Val d'Ega 48, I-39053 Kardaun/Cardano;
E-mail address: Lorenz.Keim@provinz.bz.it

Introduction and geological setting of the Dolomites

The Dolomite Mountains are known for their spectacular seismic scale outcrops showing Triassic carbonate platforms and build-ups preserved with their clinoforms and slope facies in primary transition to adjacent basinal areas. The juxtaposition of Middle and Upper Triassic reefs and basins are preserved due to the lack of strong tectonic deformation and is strengthened by erosion to form the extraordinary landscape as seen today. Since the outstanding studies of Richthofen (1860) and Mojsisovics (1879), who correctly recognized the primary geometries of the build-ups ("Überguss-Schichtung") in transition to the basins, the Dolomites are the type area for heteropic facies developments. Bosellini (1984) presented the first modern synthesis of depositional geometries of the build-ups. Regional sequence stratigraphy was firmly established with the revision of the chronostratigraphic framework by Brack & Rieber (1993), De Zanche et al. (1993) and Mietto & Manfrin (1995). In addition, a better understanding was developed of progradation and retrogradation geometries of carbonate platform development in context with sea level changes (Gianolla et al., 1998, with further references). A new 1:25.000 scale geological map (Geologische Karte der Westlichen Dolomiten) was provided in 2007 for the whole area of the Western Dolomites on the basis of extensive field work and detailed stratigraphic investigations and structural analyses.

The Dolomites are part of the south alpine retro wedge of the Alpine chain. The Neogene S-vergent thrust- and fold belt is located south of the Periadriatic Lineament (Pustertal Fault), east of the Giudicaria fault system and north of the Valsugana thrust (Fig. 1). All these faults are inherited structures which were remobilized at different times since their installation in the Early Permian (see below). Within this framework of major faults, the Dolomites form a Neogene pop-up structure with only weak tectonic deformation (Doglioni, 1987). North of the Pustertal Line, more exactly north of the hinge of the Tauern Window antiform, Austroalpine and Penninic nappes are thrusted toward the north in the Paleogene.

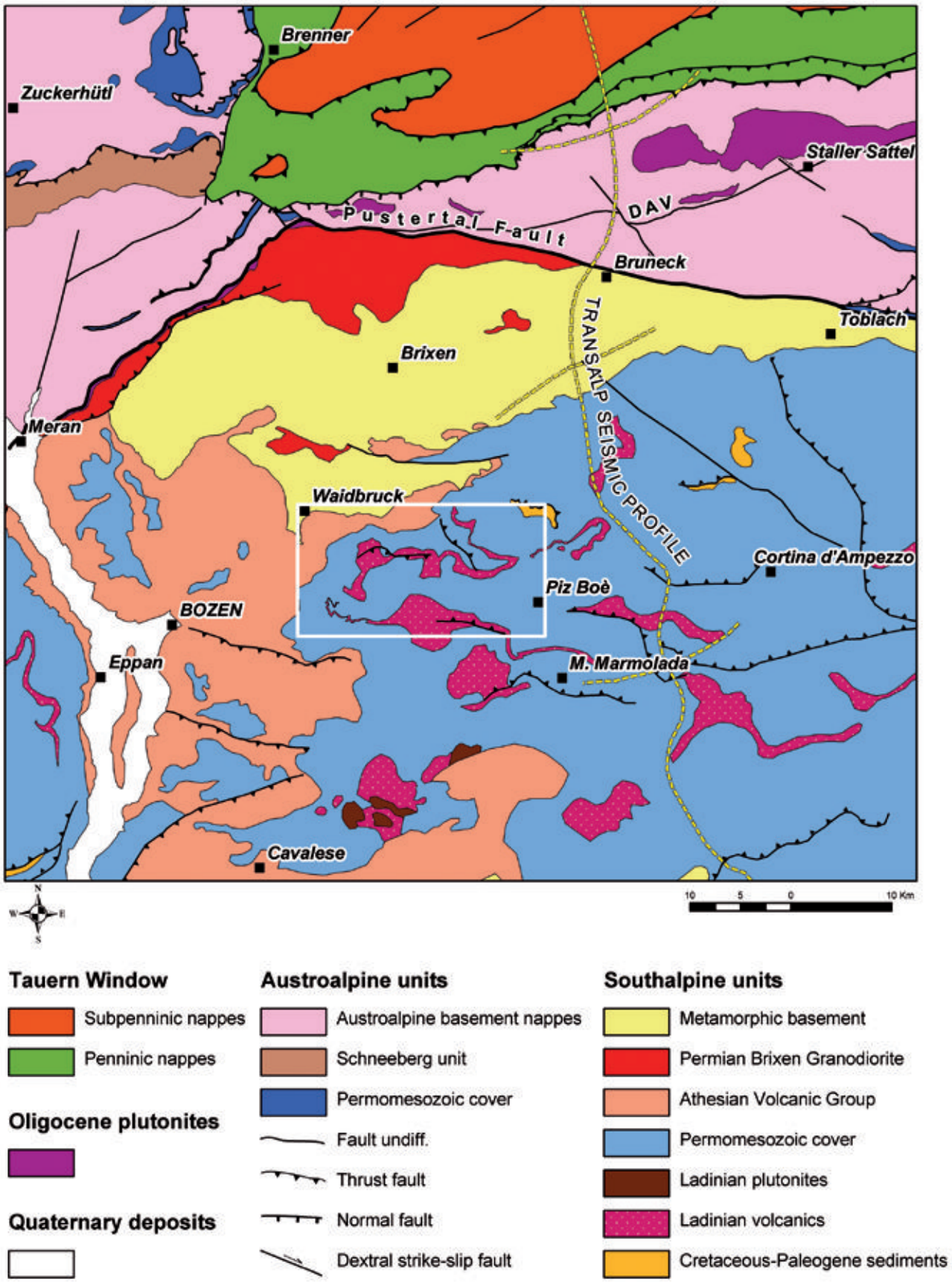

Fig. 1: Regional geologic overview with location of the excursion area in the Dolomites (rectangular).

Both, Austroalpine and Southalpine units are part of the passive continental margin of the Apulia microplate with a comparable geodynamic development since the Lower Permian. Early continental rifting processes associated with the break-up of Pangea during the Lower and Middle Permian gave way to the stepwise propagation of the Neo-Tethys from SE. Pulses of distinct rifting tectonics in the Dolomites in the Early Permian and Middle Triassic are closely associated with voluminous plutonic and volcanic rocks deposited largely in the same place. Both, Permian and Triassic magmatic rocks display typical calc-alkaline trends and the geochemical and isotopic composition indicate that the melts originated from the interaction of upper mantle and lower crust (Barth et al., 1993, Visonà et al., 2007). The marked orogenic signature is not compatible with the conventional rifting model. But also for the subduction related model, proposed by Castellarin et al. (1988), unequivocal geological field evidences in the Southern Alps and surroundings are still missing. Nevertheless, in many plate reconstructions we still find a Triassic active margin in prolongation of the closing Paleotethys south of the Southern Alps (e. g. Stampfli & Borel, 2002). New paleomagnetic data advocate an intra-Pangea dextral megashear system of >2.000 km to avoid the crustal misfit between Gondwana and Laurasia in the Early Permian (Muttoni et al., 2003). Within this scenario, lithosphere-scale extension enables mantle melt injections in the lower crust to generate hybridisation of magmas (Schaltegger & Brack, 2007). This model represents a good possibility to unravel the large-scale geodynamic context of Permian and Triassic particularities of the Southern Alps.

Permian and Triassic rifting tectonics are more intensive in the Southalpine realm than in the Austroalpine, where during this time period magmatism and volcanism are nearly absent. This different evolution requires a transcurrent shearing system in between the two realms to facilitate different stretching of the lithosphere. Therefore, we assume already for the Permo-Triassic time span a forerunner of the differentiation of Apulia N and Apulia S, separated by a Paleo-Insubric Line, which proposed Schmid et al. (2004) for the Jurassic.

The Permo-Triassic succession of the Dolomites can be subdivided into three tectonically controlled 2nd order megacycles, which are superposed by 3rd order cycles (sequences) and cycles of higher order (e. g. Werfen Fm.):

1. Early Permian volcanic deposits with intercalated fluvio-lacustrine sediments of the Athesian Volcanic Group enclose ca. 10 Ma from 285 to 275 Ma (Marocchi et al., 2008). The up to 3 km thick sequence rests on a basal conglomerate, covering the Variscan crystalline basement by a main unconformity and was deposited in the Bozen/Bolzano intracontinental basin.

2. After a marked stratigraphic gap of ca. 10 Ma, the Gröden/Val Gardena alluvial red beds were deposited on top of the volcanic group as well as on top of the Variscan basement. With the cooling of the crust, sedimentation of Gröden sandstone was very spacious and shallow marine deposits of the Bellerophon Fm and Werfen Fm prograded stepwise westward on a very gentle ramp. This second megacycle ends with Lower Anisian shallow-water carbonates of the Lower Sarldolomite.

3. A second period of rifting starts in the Middle/Upper Anisian with strong block tilting in several phases followed by the "Middle Triassic thermal event" in the Ladinian. Strong subsidence created space for the upward growth of buildups and carbonate platforms adjacent to up to 800 m deep marine basinal areas. Ladinian volcanics infilled basinal depressions and onlapped carbonate platform slopes. With the waning of rifting activity and volcanism thermal subsidence controlled once more the sedimentary development with spacious progradation of carbonate platforms. Minor pulses of rifting still occurred in the Upper Carnian, but in the Norian the accentuate relief was levelled out by the spacious carbonate platform of the Dolomia Principale/Hauptdolomit.

During the Upper Triassic and Jurassic the Southalpine and Austroalpine domains were involved in a new system of rifting processes (Bertotti et al., 1993). Starting from the Atlantic with the Central Atlantic Magmatic Province (CAMP) at the end of the Triassic, the Atlantic propagated north-eastward to form the Alpine Tethys, i.e. the Ligurian/Penninic Ocean (Frizon de Lamotte et al., 2011). Apulia was now surrounded by two different domains, the "Neo-Tethys" in the east and the "Alpine Tethys" in the west, thus forming a terrane or a microcontinent. The Southern Alps with the Dolomites in their heart have been in-

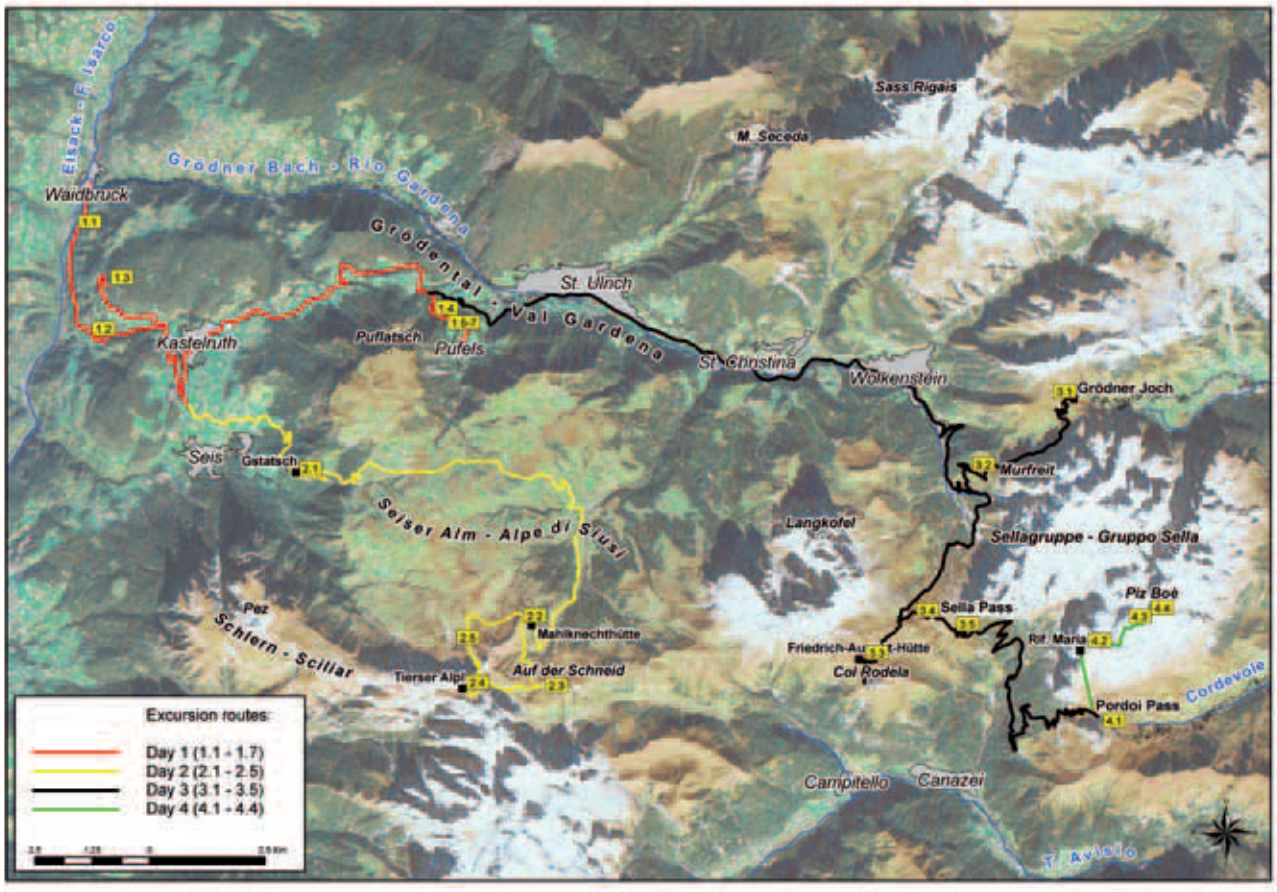

Fig. 2: Satellite image of the Dolomites with location of the four-day excursion routes.

volved in various processes related to these two rifting systems for a long period of time lasting from the Early Permian to the Upper Cretaceous.

The above mentioned three megacycles are superposed by the global mass extinction events at the Permian Triassic boundary (PTB), in the Carnian and at the Triassic Jurassic boundary (TJB). All three events strongly affected the reef growth and the carbonate factory, especially the PTB and the Carnian event effectively controlled the sedimentary development in the Dolomites.

The convergent tectonics of the Southalpine is, however, quite different from that of the Austroalpine: W- to NW-vergent thrusting and folding started in the Austroalpine just in the Late Jurassic with the closing of the Meliata Ocean in the SE (Gawlick et al., 1999) heralding the eoalpine orogenesis during the Late Cretaceous (for an comprehensive overview see Schmid et al., 2004). These eoalpine compressive events with metamorphism, do not have any record in the Southalpine, and thus require a kind of kinematic decoupling from the Austroalpine. Froitzheim et al. (2011) propose a sinistral strike-slip zone as a Paleo-Insubric Line, boardering the Austroalpine nappe stack with Late Cretaceous extensional Gosau basins toward the south. The only indication of eoalpine orogenesis nearby the Southalpine is documented by a drastic change in the Upper Cretaceous marine sedimentation in the still existing extensional basins with the input of siliciclastics, Flysch-like deposits with rare chrome spinell (Castellarin et al., 2006).

During the Paleogene compressional deformation occurred and the Dolomites became a foreland basin, a process related to the Dinaric post-collisional orogeny. Predominantly the eastern Dolomites have been affected by a WSW- to SW-vergent thin-skinned thrust belt (Doglioni, 1987). Toward NE (Comelico, Carnia) also the crystalline basement was involved in the frontal ramp tectonics (Castellarin et al., 2004, 2006).

With the Neogene Valsugana structural system, i.e. the alpine retrowedge, the Venetian basin beca-

me the foreland of the Dolomites. Strong overthrusts in a SSE direction are indicated by uplifting of the hanging wall of the Valsugana thrust of approximately 4 km in the upper Miocene (Castellarin et al., 2004, with references). Remnants of the Oligocene/Miocene coastline are preserved at ca. 2.600 m altitude at the southern flank of Monte Parei in the Eastern Dolomites (Keim & Stingl, 2000).

The four-day excursion focuses on the geodynamic and stratigraphic evolution of the Permian– Triassic and presents with its spectacular outcrops the most representative key sections of the Western Dolomites (Fig. 2). Triassic extensional vs. alpine compressional tectonics of the Col Rodela imbricate zone as well as the "Gipfelüberschiebungen" (= summit thrusts), i. e. Dinaric thrusts on top of the Triassic Sella atoll-reef, Raibl Group, Hauptdolomit and Lower Jurassic drowning of the shallow-water platform, are further impressive targets of the excursion.

DAY 1

The Permian volcanic event and the upper Permian to lower Triassic stratigraphic succession

The Bozen/Bolzano basin, filled by a succession of up to 3 km thick volcanics and intercalated sediments, documents the development of a new tensional regime in the interior of Pangea after the end of Variscan orogeny. The fundamental plate boundary reorganisation is seen in the context of the above mentioned intra-Pangea dextral megashear system at the transition of an Early Permian Pangea "B" to a Late Permian Pangea "A" configuration (see Muttoni et al., 2003), contemporary to the opening of the Neotethys Ocean.

The thick volcanic sequence, in the older literature known as "Bozner Quarzporphyr", ranges from basaltic andesites to rhyolithes and spans a period lasting from ca. 285 Ma to 275 Ma. The sequence is now defined as Athesian Volcanic Group (AVG) (see Carta Geologica d'Italia, 2007, Marocchi et al., 2008). High-precision extrusion ages combined with detailed field mapping over extended areas of the AVG were provided by Morelli et al. (2007) and Marocchi et al. (2008). Mapping of several newly established and well-dated volcanic stratigraphic units enables for the first time the reconstruction of the three-dimensional emplacement history within the strongly tectonically influenced basin development.

The Bozen/Bolzano basin is confined by a system of NNE and ESE striking, normal or transtensive faults. The most prominent faults are the Giudicarie fault in the west, the Pustertal fault in the north, the Calisio line in the southwest and the Valsugana line in the southeast (Fig. 3). All these Permian paleo-lines were reactivated several times later on, but at different deformation regimes. The Lower Permian age of similar striking faults of other volcanic basins is shown by the fact that these faults are sealed with intercalated sediments or volcanic formations (Brandner et al., 2007, Marocchi et al., 2008). Detailed field mapping indicates half-graben geometries, for instance, in the area of Waidbruck-Villnöß and Meran 2000 with block-tilting toward NW. With the new geochronological data of the volcanic sequence it is now possible to recognize a temporal polarity within the Permian fault pattern (Marocchi et al., 2008), i.e. a younging trend of the volcanic formations from the northwestern margin of the basin to the central part in the southwest. These data imply, together with the half graben geometries, an opening trend of the basin in a NW–SE direction. Because of the geometries of the Lower Permian fault pattern, a transtensional opening of the basin would only be possible in a sinistral shearing system, which is in contrast with the timing of plate tectonic models of Muttoni et al. (2003) and Cassinis et al. (2011). At this point it is essential to mention, that the Bozen/Bolzano volcanic basin formation does not correspond to the first transtensional event in the Southern Alps. In the Carnic Alps, the up to 2000 m thick filling of the transtensional Naßfeld/Pramollo basin, with the mixed siliciclastic-carbonate sediments of the Auernig, Rattendorf and Trogkofel Groups, spanning a time period from the Upper Carboniferous to the Artinskian in the Early Permian (Venturini, 1991, Krainer et al., 2009), occurs i.e. circa 20 Ma earlier than the Bozen/Bolzano megacycle. Thus, we speculate, that the basic change in plate kinematics took place within the period of Lower Permian magmatism that largely affected Paleo-Europe.

The AVG is subdivided into a lower part with mainly andesitic and rhyodacitic volcanic products and an rhyolithic upper part. The change of the geochemical composition is closely related to a volcano-tectonic collapse. Cogenetic subvolcanic rhyodacitic intrusions along fractures are described by Morelli et al. (2007) near Terlan/Terlano. Five kilometres to the south, a second important collapse fracture is mentioned by the authors, producing a considerable depression. Ac-

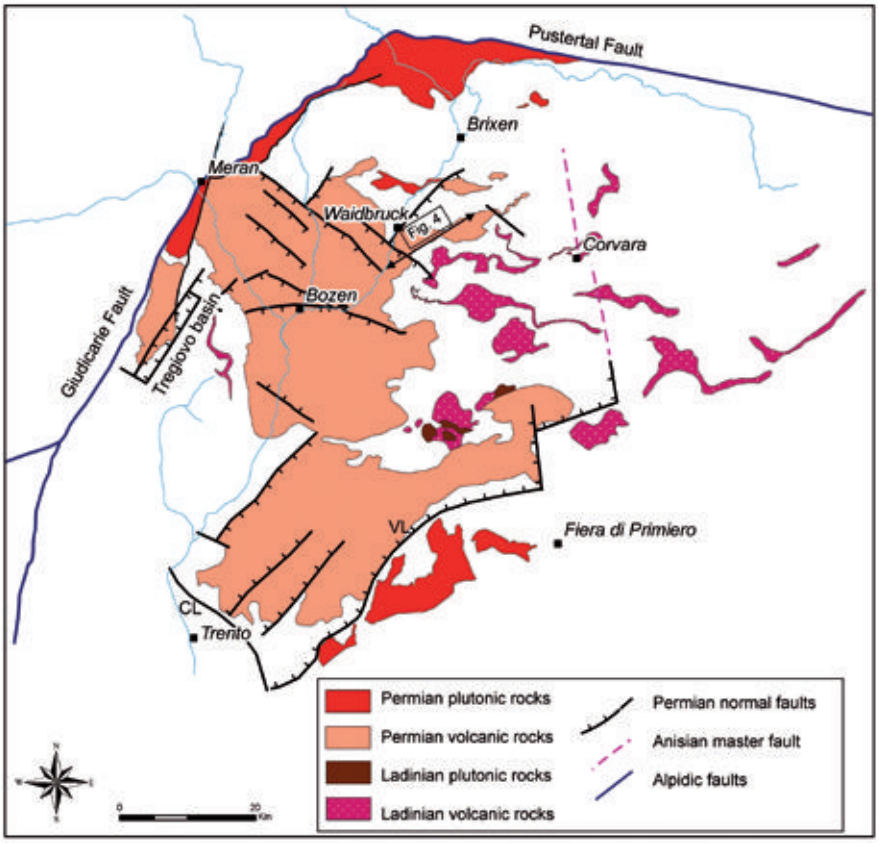

Fig. 3: (a) Distribution of present-day Permian and Ladinian plutonic and volcanic rocks. The formation of Permian volcanics seems to be connected to synvolcanic extensional tectonics with NW-SE and NE-SW trending faults with half graben geometries. Configuration of the Permian faults could be related to an overall sinistral megashear associated with the beginning of the opening of the Neo-Tethyan Ocean in the Far East. Data on Permian faults based on own field mapping, Carta Geologica d'Italia (2007, sheet "Appiano-Eppan"), Carta Geologica d'Italia (2010, sheet "Merano-Meran"), Selli (1998) and Morelli, C. (pers. comm., 2011). The Ladinian magmatites in the Dolomites are located close to the Permian ones – thus a genetic connection, i.e. a similar uplifted position of the mantle as in the Permian, could be proposed. The Anisian master fault serves as an example and shows the inheritance of the Permian fault pattern in the Triassic and Jurassic. CL = Calisio paleo-line, VL = Val Sugana paleo-line (modified after Selli, 1998).

cording to Morelli et al. (2007) more than 1000 m of pyroclastic flow deposits accumulated, i.e. ignimbrites of the Auer/Ora Formation. A similar scenario can be observed along the road from Waidbruck/Ponte Gardena to Kastelruth/Castelrotto at stop 1.2 with the collapse escarpment of the WNW–ESE striking Bundschuh normal fault (Figs. 4, 5). We recognize here the sealing of the fault with ignimbrites of the Auer/Ora Formation (Brandner et al., 2007). The volcanic activity is interrupted at different stratigraphic levels marked by alluvial conglomerates, sandstones and lacustrine deposits with plant remains (Hartkopf-Fröder et al., 2001).

The volcano-sedimentary Lower Permian megasequence is unconformably overlain by the spacious cover of continental clastic deposits of the Gröden/Val Gardena Fm., which forms the basis of the 2nd megacycle and is devoid of volcanics. Thermal subsidence dominated the sedimentary development of this cycle, which is evident by widespread interfingering of continental and shallow-marine facies. The general marine transgression of the Neotethys to the west took place in several third-order sequences ranging from coastal plain environments with sabkha evaporates to shallow-shelf carbonates of the Bellerophon Fm. After the end Permian mass extinction mixed shallow-marine carbonates and terrigenous sediments of the Werfen Fm. are characterised by the long lasting biogenic recovery, lacking carbonate producing organisms. The first carbonate bank produced by calcareous algae is of Lower Anisian age (Lower Sarl/Serla Fm) and forms the top of the 2 megacycle.

Excursion route

Stops 1.1–1.3 are located along the classic geological section at Waidbruck/Ponte Gardena on the road to Kastelruth/Castelrotto crossing the whole sequence from the basal conglomerate, volcanoclastic sediments, andesitic and dacitic block lavas to rhyodacitic and rhyolithic ignimbrites.

Stops 1.4 to 1.7 are dedicated to the Permian-Triassic sequence of the Pufels/Bulla key-section along the abandoned road to Pufels/Bulla (Fig. 2).

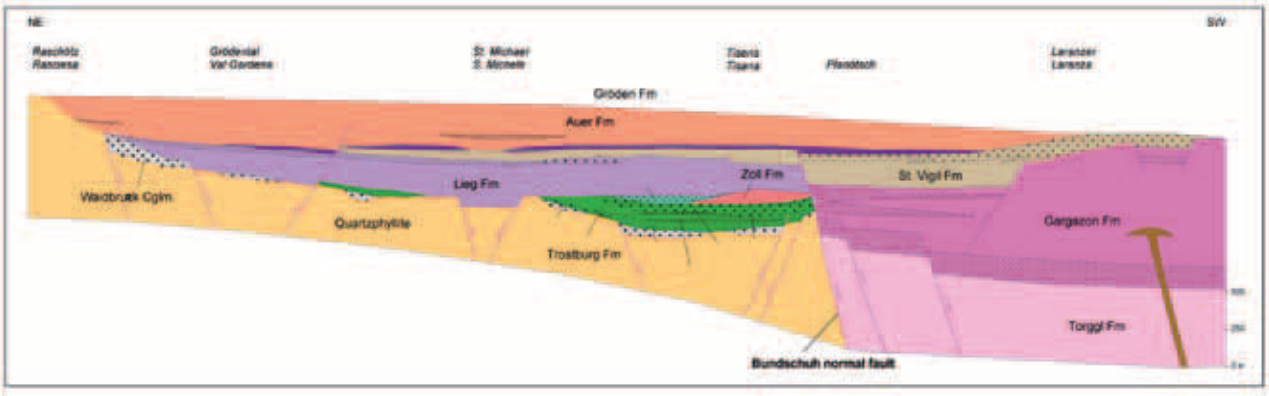

Fig. 4: Schematic lithostratigraphic model of the Permian Athesian Volcanic Group east of the Eisack valley, based on Geologische Karte der Westlichen Dolomiten 1:25.000 (2007) and Brandner et al. (2007). The location of the schematic section is shown in Fig. 3.

Stop 1.1 – Waidbruck/Ponte Gardena Conglomerate

The classic geological section along the road to Kastelruth/Castelrotto starts with the well-known outcrop of the Waidbruck/Ponte Gardena Conglomerate at the basis of the volcanics of the AVG (Fig. 4). The unconformable contact with the underlying crystalline basement is covered by Quaternary debris. The thickness of the basal conglomerate differs strongly, in some places it reaches 50 m, while at others the conglomerate is lacking. Geological field mapping showed an abrupt pinching out of the conglomerates along NW-SE and NE-SW striking Permian normal faults.

Krainer (1989) studied the section in detail (Fig. 6) and recognized three lithofacies types: (1) massive, poorly sorted and matrix-rich conglomerates with a matrix-supported grain fabric, (2) crudely bedded, clast-supported conglomerates filling up to 1 m deep erosive channels and (3) fine-grained, cross bedded conglomerates, filling smaller channels. The conglomerates consist of poorly rounded clasts of rocks of the crystalline basement, predominantly quartz phyllite and better rounded quartz pebbles. The quartz pebbles and grains are covered by a reddish thin film of hematite indicating semiarid to arid climatic conditions. Mature quartz pebbles with a long transportation history and angular, immature phyllite pebbles are mixed in the poorly sorted debris flow sediments. They testify, in combination with the poorly sorted channel fills, an ephemeral stream environment with wadi channels. Higher up in the section, the amount of volcanic pebbles and sandstones increases to turn into a ca. 70 m thick pyroclastic/volcanic sequence with block lavas, tuffs, explosion breccias, irregularly intercalated in the lava flows (Di Battistini et al., 1989). Fluvial conglomerates with quartz pebbles and sporadic metamorphic clasts from the basement are locally interbedded. The mixed volcaniclastic/volcanic-terrigenous sequence is overlain by 60–80 m thick, finely crystalline andesitic lavas (Trostburg Fm., Brandner et al., 2007). Visonà et al. (2007) determined from this lava flow a SHRIMP U-Pb zircon age of 290.7+/-3 Ma indicating that the andesitic lavas of the northern region preceded the general onset of the volcanism of the AVG with 284.9+/-1.9 Ma (Marocchi et al., 2008) in the Etsch/Adige valley.

Stop 1.2 – First turn of the road, near the locality Zoll: the Bundschuh fault, a Permian normal fault

The Bundschuh normal fault is situated in a small valley in between the farmsteads Planötsch and Bundschuh (Figs. 4, 5). The Permian age of the fault is expressed by its sealing with rhyolithic ignimbrites of the Auer/Ora Fm at the top of the AVG. The fault has been reactivated insignificantly several times later on. The Bundschuh fault crosses the Eisack/Isarco valley in WNW-ESE direction and delimits in the lower section the crystalline basement toward thick sequences of ignimbrites of the Gargazon and Torggl Fms in the hanging wall located in the south. The remarkable difference in the thickness of the fluvial sediments of the St. Vigil Fm of about 70 m on both sides of the fault is interpreted by levelling of the strong relief created by faulting.

The Bundschuh fault and the Villnöß/Funes paleofault mark together with the Meran 2000 fault system the northern margin of the Lower Permian Bozen/Bolzano basin.

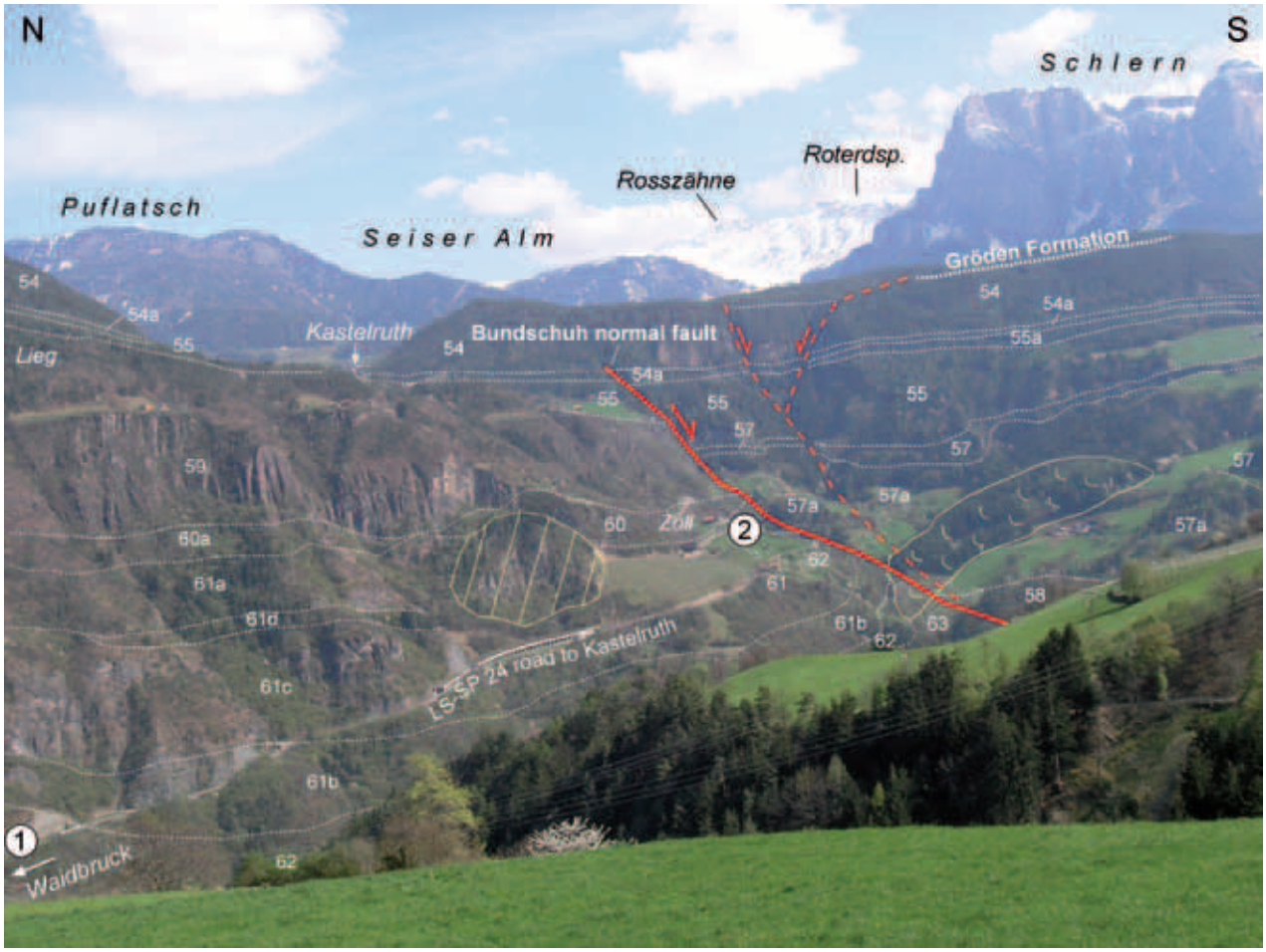

Fig. 5: Panoramic view of the Permian volcanics between Waidbruck/Ponte Gardena and Kastelruth/Castelrotto. A major upper Permian syn-volcanic, WNW-ESE running, steep normal fault between Bundschuh-Planötsch is present. This fault also causes the abrupt thickness change of the epiclastic sediments of the St. Vigil Fm. Numbers correspond to the facies model of Fig. 4. (after Brandner et al., 2007). Numbers 1 and 2 = excursion stops.

Stop 1.3 – Tisens, little quarry near Lieg Inn: typical succession at the base of the Auer/Ora ignimbrite formation.

The section starts along the access road with a sedimentary sequence of the St. Vigil Fm with sandstones and conglomerates of reworked volcanic rocks, randomly also quartz grains and phyllites occur of the crystalline basin. The sandstones are cross bedded and are arranged in small channels with graded channel fillings typical for point bar sequences. A 2 m thick sandstone bank marks the top of the sequence. After a non exposed part in the outcrop a black vitrophyric rhyolithic tuff of 8–12 m thickness follows at the base of red coloured ignimbrites of the Auer/Ora Fm. The whole volcanic succession is exposed in a quarry. The vitrophyre is known in the older literature as "Pechsteinporphyr von Tisens" and is still used as building and décor stone. The vitrophyre is characterized by nearly unaltered glass (a petrographic peculiarity for an age of 275 Ma) in the groundmass, which is responsible for the black colour. Eutaxitic microstructures and perlithic fracturation can be observed under the microscope, as well as scattered crystals of quartz, sanidine, plagioclase and biotite (Mostler, 1982, Bargossi et al., 1998).

The vitrophyre is overlain with a sharp boundary by red rhyolithic ignimbrites of the Auer/Ora Fm. The petrographic composition and structure are similar to the vitrophyre, the difference is only the altered, red coloured groundmass. Intercalated are aphyric, red and black lithoclasts. Typical are juvenile aphanitic inclusions with flame structures ("fiamme"). The sharp boundary with the yellowish horizon on top of the vitrophyre is interpreted by Mostler (1982) and Bargossi et al. (1998) as a weathering horizon (spherical weathering).

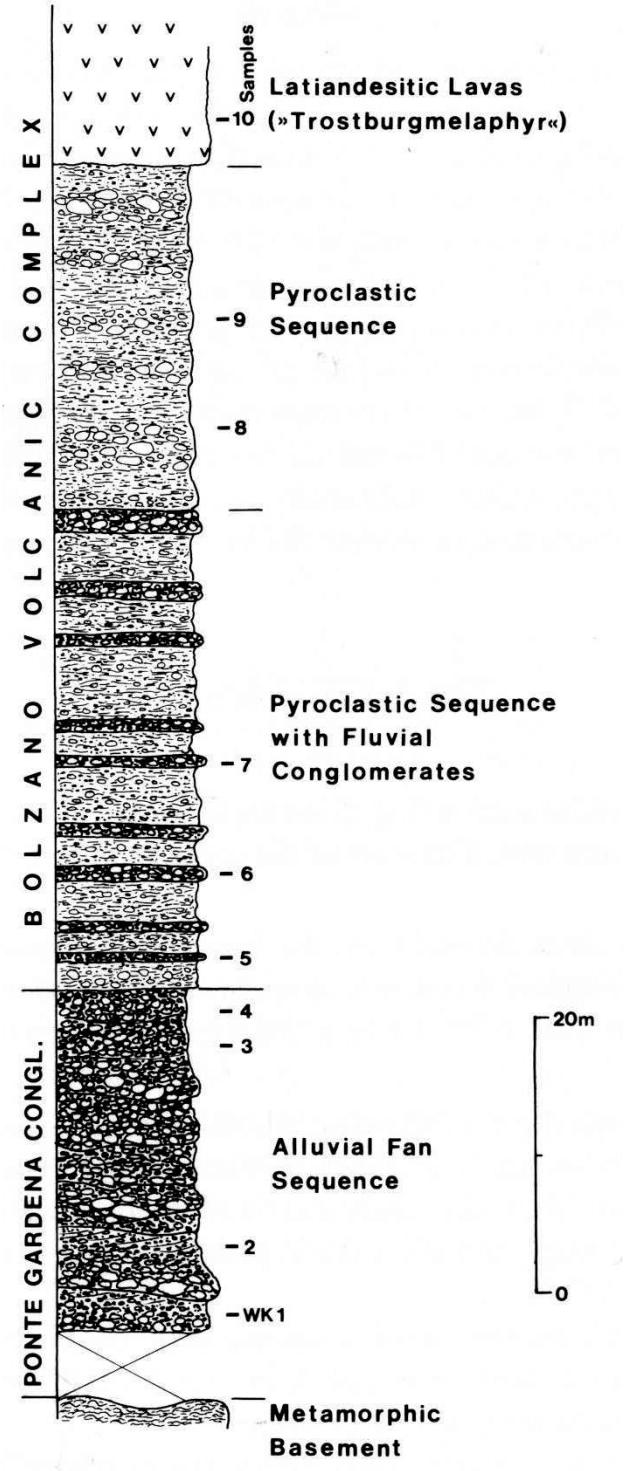

Fig. 6: Measured section of the Ponte Gardena (Waidbruck) Conglomerate and the lower part of the volcanic sequence along the road from Waidbruck to Kastelruth, after Krainer (1989). Reworked clasts of the Ponte Gardena (Waidbruck) Conglomerate consist essentially of quartz phyllite of the underlying metamorphic basement. Upsection, these conglomerates are gradually replaced by conglomerates and sandstones with abundant and well rounded volcanic clasts.

The Pufels/Bulla road section: from the Permian-Triassic Boundary (PTB) to the Induan-Olenekian Boundary (IOB)[1]

[1] The following chapter is basically a reproduction of the published field guide by Brandner et al. (2009).

General remarks

The Pufels/Bulla section offers an excellent opportunity to study the Permian-Triassic boundary (PTB) and the Lower Triassic Werfen facies and stratigraphy in a nearly continuous section that reaches from the PTB to the Induan/Olenekian boundary (IOB) located within the Campill Member (Fig. 7). Based on this key-section at Pufels/Bulla we want to stimulate the discussion on questions of the "system earth", i.e. genetically related correlations of lithofacies, sea-level changes, anoxia and stable carbon and sulphur isotope curves. Magnetostratigraphy enables a direct comparison with continental sedimentary sequences of the German Zechstein and Buntsandstein to understand sequence stratigraphy, cycles and regional climatic influences.

The Pufels/Bulla section is well known for its excellent outcrop quality as well as findings of conodonts constraining the Upper Permian, PTB and Lower Triassic succession. Investigations on lithostratigraphy and biostratigraphy have been carried out by Mostler (1982), Perri (1991) and Farabegoli & Perri (1998). Integrated studies of lithostratigraphy, magnetostratigraphy and chemostratigraphy have been carried out by Scholger et al. (2000), Korte & Kozur (2005), Korte et al. (2005), Farabegoli et al. (2007) and Horacek et al. (2007a). A comprehensive review is given by Posenato (2008).

Lithostratigraphy and depositional environments

The shallow marine sediments of the topmost Bellerophon Fm and Werfen Fm were deposited on a very gentle, NW–SE extending ramp. The coastal plain environment of the upper Gröden Fm was present in the west while a shallow marine, mid and outer ramp environment of the Bellerophon Fm could be found in the east. The Bellerophon Fm shows several cycles representing 3rd order sequences within a general westward prograding sedimentary wedge. The over-

lying Werfen Formation consists of a strongly varying sequence of mixed terrigenous siliciclastic and carbonatic lithofacies, organized in T/R-cycles of different order and frequency. These 3rd order depositional sequences (see De Zanche et al., 1993, Gianolla et al., 1998) are composed of 4th order cycles of storm layers (thickening or thinning upward) and may have been orbitally forced. For detailed descriptions of lithology and biostratigraphy see Broglio Loriga et al. (1983). The PTB mass extinction of carbonate producing organisms prevented the evolution of a rimmed shelf area during the entire Lower Triassic. After this exceptionally long lasting recovery period of reefal buildups in the whole Tethys area, the first appearance of reef building organisms occurred in the lower Middle Triassic, the nearby situated Olang/Valdaora Dolomites (Bechstädt & Brandner, 1970).

The lack of reefal buildups and binding organisms may have caused the extreme mobility of vast amounts of loose carbonate and siliciclastic sediments that have been removed repeatedly by storm-dominated, high-energy events. These processes generated a storm-dominated stratification pattern that characterises the specific Werfen facies. Applying the concept of proximality of storm effects (Aigner, 1985), i. e. the basinward decrease of storm-waves and storm-induced currents, we tried to interpret relative sea-level changes from the stratigraphic record. Proximal and distal tempestite layers are arranged in shallowing-upward cycles (parasequences) but also in deepening-upward cycles depending on their position within the depositional sequences. However, numbers of cycles and cycle stacking patterns vary from section to section according to the position on ramp. The main control for these sedimentary variations seems to be the ratio between accommodation space and sediment supply, which follows the variable position of the base level (see base level concept from Wheeler, 1964). Variations in base level determine the geometry of progradational, aggradational and retrogradational stacking patterns of the individual sedimentary cycles. Base level, however, does not automatically correspond to sea level.

Reviewing the published data of magnetostratigraphy and chemostratigraphy, calibrated with bio-chronostratigraphy, Posenato (2008) assigned radiometric ages to the Lower Triassic sequence of the western Dolomites. Assuming that the duration from PTB to IOB is roughly 1.3 Ma, the total sediment thickness of 200 m in the Pufels section results in a sedimentation rate of 1 m/6.5 ka, uncorrected for compaction. This rather high sedimentation rate not only suggests a high frequency of storm events (hurricanes), but also stresses the exceptional environmental conditions during this period and may indicate a lack of dense vegetation in the hinterland.

Since the 19th century several attempts have been made to subdivide the Werfen beds into mapable lithostratigraphic units: (1) in a first step, Wissmannn, 1841 (lit. cit. in Posenato, 2008) made a simple subdivision according to the grey and red colours of the interbedded marls in Seisser Schichten and Campiler Schichten; (2) Recent research in sedimentology and biostratigraphy by Bosellini (1968), Broglio Loriga et al. (1983, 1990) and others enabled a division of the Werfen Formation – still an informal unit – into 9 members (Tesero, Mazzin, Andraz, Siusi/Seis, Gastropodenoolith, Campill, Val Badia, Cencenighe, San Lucano) which correspond *pro parte* to depositional sequences (De Zanche et al., 1993). In general, the Werfen Formation is characterized by subtidal sediments, but intra- to supratidal levels with evaporitic intercalations are present within the Andraz, Gastropodenoolith, the base of Val Badia, Cencenighe and San Lucano members.

Stratigraphic terminology

The historical lithostratigraphic units "Seiser Schichten" and "Campiler Schichten" are now considered members (Siusi/Seis Mb ("Siusi" is the Italian translation of the German name of the village Seis) and Campill Mb) but with different usage of the lower and upper boundaries depending on the individual research groups. This mismatch of lithostratigraphic definitions has been ignored by some authors especially from outside of Italy, which resulted in wrong and confusing correlations of biostratigraphy, magneto- and chemostratigraphy (for further information see the review of Posenato, 2008).

Due to relative sea-level changes, facies belts shift on the gentle ramp in time and space, with the consequence that lithologies are arranged in cycles and therefore are repetitive. In such a situation it is rather obvious, that members as lithostratigraphic units also shift in time. Hence the defined boundaries of the members are not always isochronous. More stratigraphic studies, which are independent of local

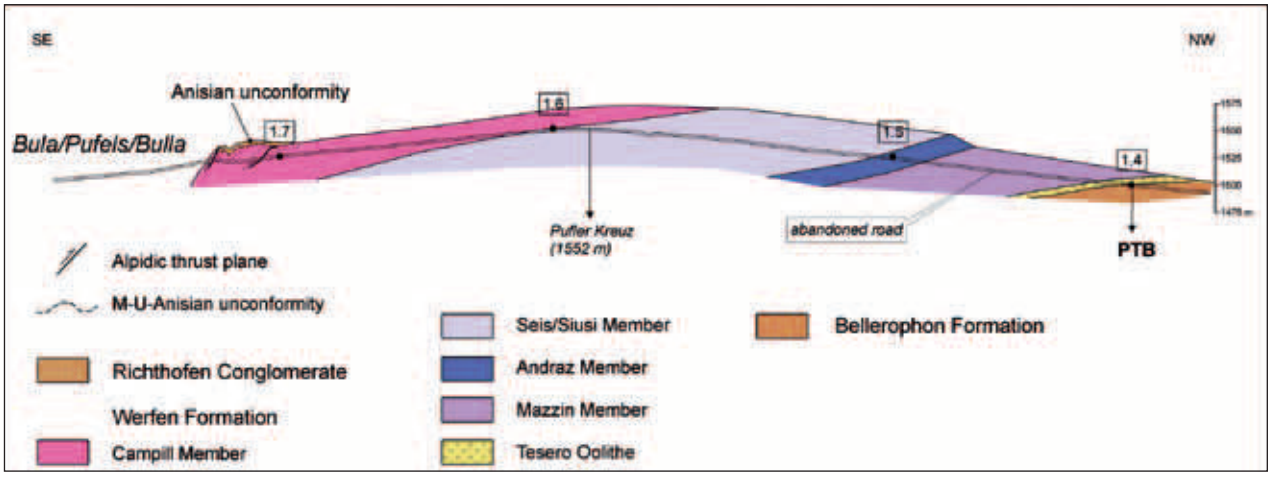

Fig. 7: Geological cross section along the abandoned road to Pufels/Bulla with location of the single excursion stops (1.4–1.7). PTB = Permian-Triassic Boundary (after Brandner et al., 2009).

facies developments, such as magnetostratigraphy and chemostratigraphy, are needed for a better understanding of the sedimentary evolution and correlation of the successions.

Practicality for field mapping: detailed lithostratigraphic divisions are important for 3-D understanding of palaeogeography, but also for the resolution of tectonic structures. By mapping large areas in the eastern and western Dolomites we always encountered the problem of the correct determination of the "Gastropodenoolith Member", particularly in areas with isolated outcrops or tectonic disturbances. This member is characterised by a high lateral variability in facies and thickness (Broglio Loriga et al., 1990) with storm layers of oolithic grainstones with microgastropods, and occasionally intraformational conglomerates ("*Kokensches Konglomerat*"). As these lithotypes occur in different positions in the Seis/Siusi and Campill Mbs, the boundaries of the "Gastropodenoolith Member" have been defined differently depending on the authors. For geologic mapping in the field we used a practicable solution by defining the lower boundary of the Campill Mb at the appearance of the first observable sandstone- or calcareous sandstone layers (unit D on top of the Siusi Mb defined by Broglio Loriga et al., 1990). This terrigenous input marks a distinct break in the sedimentary development of the Werfen Formation and has a very wide palaeogeographical distribution. The stronger clastic input in the overall marine Werfen Fm is genetically correlatable with the boundaries between Unterer/Oberer Alpiner Buntsandstein in the Austroalpine (Krainer, 1987) and Lower/Middle Buntsandstein of Central Germany (Szurlies et al., 2003). The term "Gastropodenoolith" will be used only as remarkable facies type but not as an individual lithostratigraphic unit (see Geologische Karte der Westlichen Dolomiten, 2007).

The Pufels/Bulla road section exposes the whole sequence from the PTB to the supposed IOB, i. e. uppermost Bellerophon Fm and Werfen Fm with Tesero Mb, Mazzin Mb, Andraz Mb, Seis Mb and lower Campill Mb. Younger members of the Werfen Fm are lacking in this area due to block tilting and erosion during the Upper Anisian (Fig. 7).

Stop 1.4 – Permian/Triassic Boundary

Bellerophon Fm: the outcrop at the starting point of the section only shows the top of the formation with gray calcareous dolomite mudstones, and with vertical open tubes, interpreted as root traces (Fig. 8a). The dolomites belong to the top of the *"Ostracod and peritidal dolomite unit"* described by Farabogoli et al. (2007). They are covered by 4-cm thick, orange to green coloured marls, which probably represent a hiatus that represents a sequence boundary. The sequence "Ind 1" starts with a sequence consisting of dm bedded, grey to dark grey fossiliferous packstones that are intercalated with irregular cm-thick layers of black carbonaceous marlstones. Bedding planes are wavy due to strong bioturbation. This 155 cm thick sequence is termed *Bulla Mb* (Farabegoli et al., 2007).

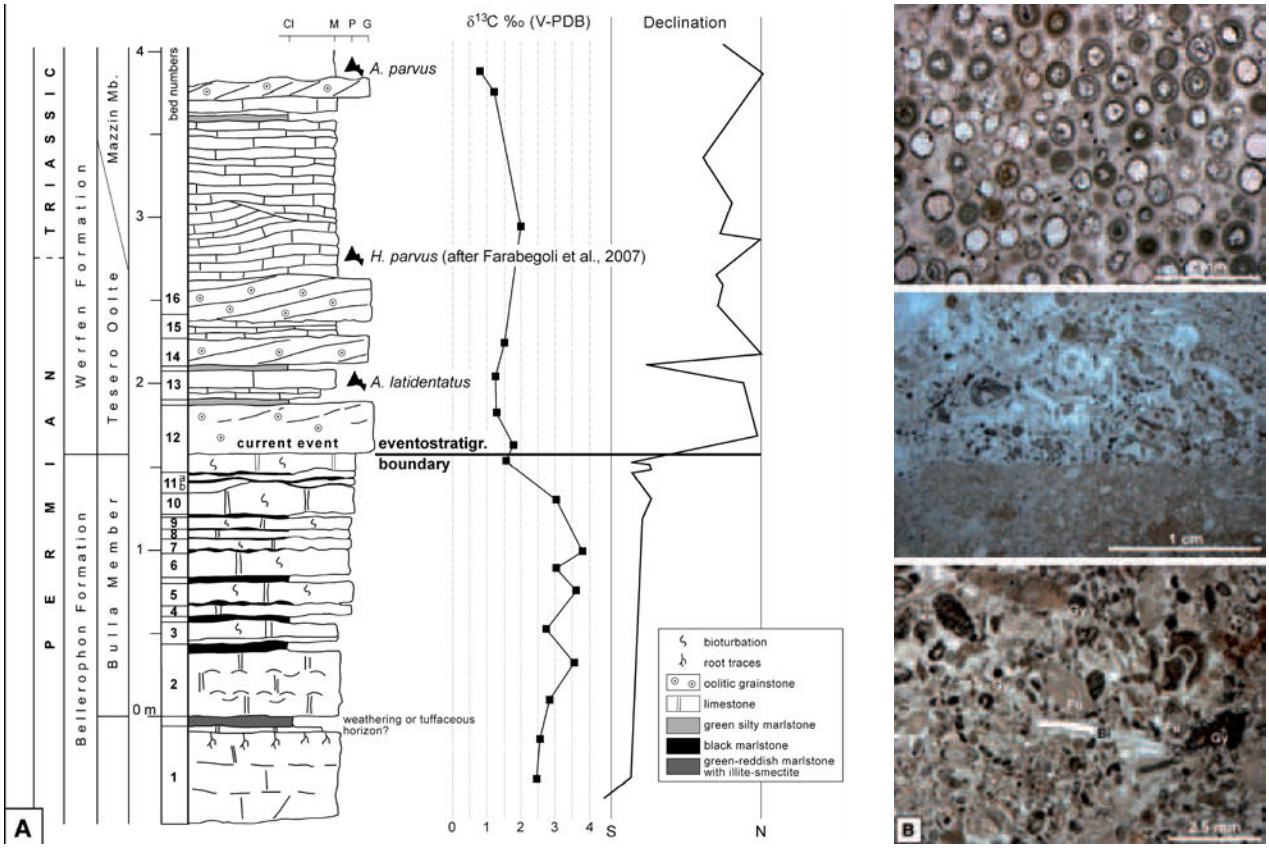

Fig. 8: The Perm-Triassic Boundary: (a) detailed measured section of the PTB with litho-, bio-, chemo- and magnetostratigraphy. Conodonts and position of the PTB after Mostler (1982) and Farabegoli et al. (2007), magnetic declination after Scholger et al. (2000); (b) Three thin-section photomicrographs from the uppermost Bellerophon Formation and the lowermost Werfen Formation. The lower thin section shows a fossil rich, skeletal packstone with typical fusulinids (Fu), red algae (gymnocods, Gy) and bivalves (Bi). The middle thin section shows a variably sharp contact between the fossiliferous packstone to a grainstone along a firm ground. An increase of hydrodynamic energy is documented by outwash of mud and reworking of intraclastic grains. Only a part of the grains is reworked (e. g. fusulinids). Contrary to Farabegoli et al. (2007) we do not see evidence for subaerial exposure. The uppermost image shows a typical oolitic grainstone from the Tesero Oolite (after Brandner et al., 2009).

Werfen Fm: The Werfen Fm starts with the *Tesero Oolite Mb* within bed number 12 of the detailed section (Fig. 8a). Fossiliferous packstones are overlain with a sharp contact by well washed, fossiliferous grainstones, 4 to 5 cm thick (Fig. 8b), grading to grainstones with superficial ooids (5 cm thick bed) and cross bedded oolites (20 cm thick bed) on the top of the beds. The detailed description of this important environmental change was made possible by sampling the entire 40 cm thick bed in order to prepare a polished slab comprising the entire bed and 5 large thin sections. In contrast to the black carbonaceous marlstone layers of the Bulla Member, centimetre intercalations in the Tesero Oolite Member are composed of greenish terrigenous silty marlstones.

With the Tesero Oolite, at the base of the Lower Triassic Werfen Formation, we observe a fast, several tens of kilometres, westward shift of the shoreline that shows a typical onlap configuration, i. e. transgression and not regression as described from other areas in the world. The topmost Bellerophon Formation (cycle A in Brandner, 1988; Bulla Member *sensu* Farabegoli et al., 2007) and the Tesero Oolite record severe environmental changes at the event stratigraphic boundary of the PTB and includes profound biotic extinctions, which coincide more or less with the well known negative carbon isotope excursion (Fig. 8a). The event-stratigraphic boundary of PTB is situated ca. 1.3 m below the FAD of the conodont *Hindeodus parvus*, defining the base of the Triassic (see Mostler, 1982 and Fig. 3 in Farabegoli et al., 2007).

The transition from fossiliferous packstones of the Bellerophon Fm to the barren grainstones of the Tesero Oolite is characterized by a stepwise increase in the hydrodynamic energy (see bed 12, Fig. 8a and "current event" of Brandner, 1988). These steps are recorded in three 4–5 cm thick storm layers without a significant unconformity or signs of subaerial exposure. Petrographic evidence suggests friable-cemented firm grounds on the sea floor. Borings show only poorly defined walls (Fig. 8b). The uneven surface of the firmground only shows little erosion by storm waves. There is no evidence for vadose diagenesis. For a different interpretation see Farabegoli et al. (2007).

On the contrary, ooids are not leached (such as the oomoldic porosity of the Miami Oolite) but have nuclei of calcite crystals and sparry calcite cortices encrusted by micritic laminae. Calcite crystals show borings of endolithic algal filaments underlining their primary precipitation on the sea floor. Further investigations are needed to verify the possible primary low-magnesium calcite precipitation on the Permian-Triassic sea floor. The factors known to control the precipitation of calcium, i. e. low Mg/Ca ratios and faster growth rates (Chuodens-Sánchez & González, 2009), would shed an interesting light on the assumed unusual seawater chemistry at the PTB.

Some ooids contain coatings of finely dispersed pyrite, but pyrite is also common in intergranular positions (in agreement with Wignall & Hallam, 1992, Bond & Wignall, 2010). Enhanced oxygen depletion in the surface water may have been caused by global warming and ocean heating (Shaffer et al., 2009). These processes would lead to an increase in alkalinity within a reducing, subtidal environment. The drop of the carbon isotope curve correlating with the Tesero Oolite may indicate an increase of isotopically depleted bicarbonate ions in seawater caused by the activity of sulphate reducing bacteria in a stratified ocean (Tethys as a "giant Black Sea", see Korte et al., 2004, Horacek et al., 2007b). An increase in the amount of HCO_3^- forces precipitation of calcite on the sea bottom. The synchronous rise of ^{34}S in correlative sections nearby (Seis/Siusi, Newton et al., 2004 and Tramin/Termeno, Brandner, 1988, Horacek et al., 2010) supports this model. Carbonate seafloor crusts and fans and special types of oolites and oncolites are widespread in different levels of the Lower Triassic and are often connected to perturbations of the carbon isotope curve (Pruss et al., 2006, Horacek et al., 2007a, b).

Synchronously to the pronounced increase in hydrodynamic energy in the shallow water environment at the event-stratigraphic boundary of the PTB, an increase in humidity and freshwater discharge is documented at the beginning of the continental Buntsandstein facies. This interpretation is based on the magnetostratigraphic correlation of the Pufels/Bulla section and sections of the continental facies realm of the Germanic Trias (Szurlies et al., 2003, Hug & Gaupp, 2006).

Mazzin Member

The contact of the Tesero Oolite to the Mazzin Member is transitional (Figs. 8a, 9); some beds of Tesero Oolite occur intercalated within dm-bedded, nearly unfossiliferous grey limestones (structurless mudstones, sometimes microbial structures). The oolite intercalations are interpreted as sand waves or sheets of ooid sand accumulating in a mid to outer ramp position. They are fed by about 10 meter thick sand bars which are preserved in the depositional environment as a barrier island and outcrop in the Tramin/Termeno section, about 40 km SW of Pufels (Brandner et al., 2009). The repeated migration of oolitic sand to the shelf area may have been controlled by cyclic sea-level lowstands and storm-dominated transport. Oolitic grainstone layers disappear upward in the section, emphasizing the transgressive trend of the depositional sequence.

A very characteristic lithotype that occurs in the middle part of the section are "streaked" mudstones: beds of grey limestones or marly limestones with low content of silty quartz and micas with mm- to cm thick planar laminae of graded bioclastic packstones (mostly ostracods). They are interpreted as distal storm layers. Streaked mudstones alternate with structureless, bioturbated mudstones generating meter-scaled symmetrical cycles. Mudstones with strong bioturbation correspond to the time-equivalent vermicular limestones in Iranian sections (e. g. Horacek et al., 2007), or the Lower Anisian "Wurstelkalke" in the Austroalpine realm.

The upper part of the section shows an increase in terrigenous input. Meter-scale cycles with thickening storm layers of bioclastic packstones are capped by greenish marlstones suggesting a shallowing-up trend (Fig. 9). This trend results in the predominance of multicoloured laminated siltstone with wave ripples and mud crack structures at the top of the depositional sequence (Ind 1).

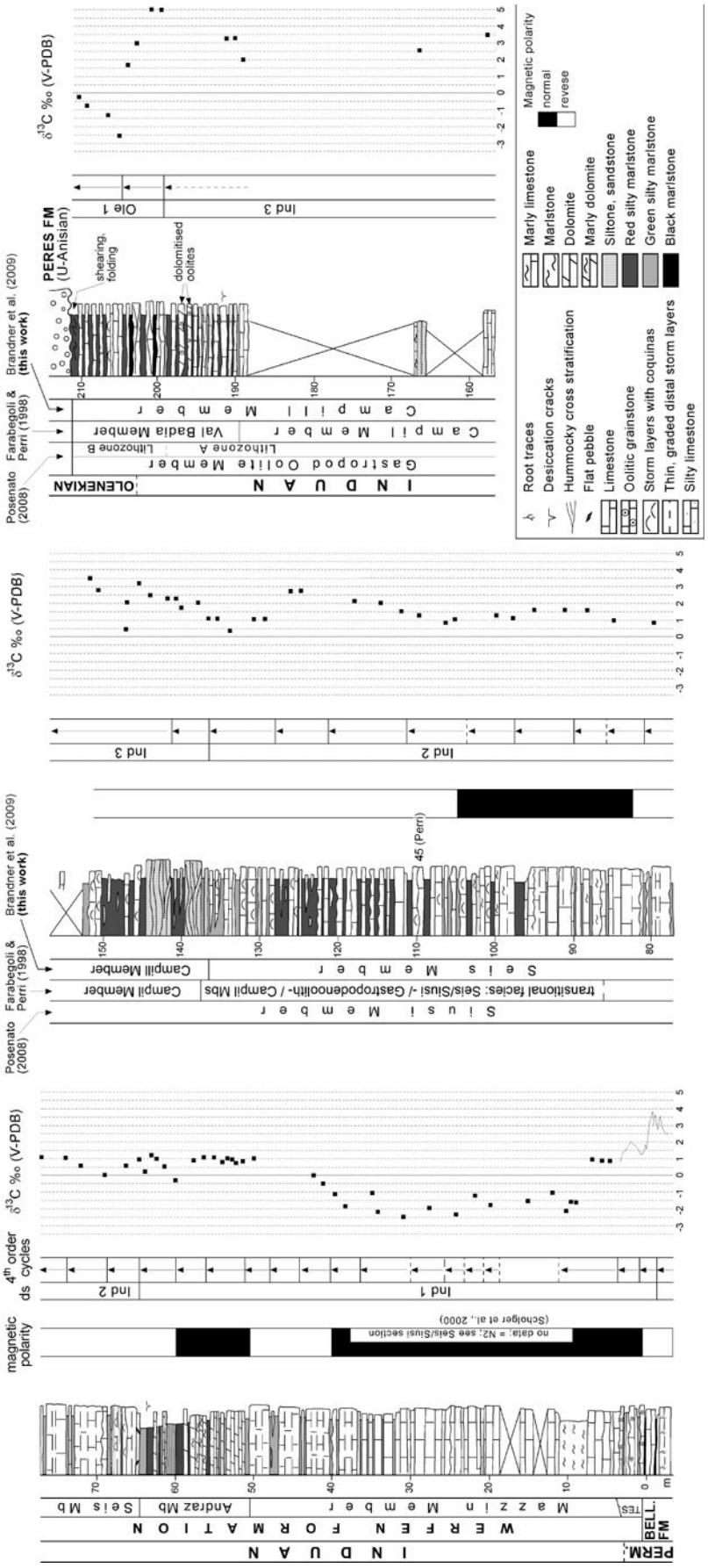

Fig. 9: Measured section through the Werfen Formation along the abandoned road to Pufels/Bulla. The top of the section shows alpine ramp folds which can be restored bed by bed. Upper Anisian conglomerates unconformably overlie the lower part of the Campill Member recording upper Anisian uplift and erosion (after Brandner et al., 2009).

Stop 1.5 – Supratidal/subtidal facies

Andraz Member

The peritidal unit consists of a cyclic alternation of marly-silty dolomites, locally cellular, laminated silty marls and siltstones with a typical mud-flat facies. As there is no clear interruption in the sequence, we propose that progradation of the coastal tidal flat facies rather than a distinct drop of the sea level formed this sequence.

New artificial outcrops of the Andraz Member (this unit is usually completely covered) that were excavated along the abandoned road and those that were made during the construction of the gallery of the new road to Pufels enabled the measurement of a detailed section and high-resolution sampling for magnetostratigraphy and carbon isotope analyses (Fig. 9).

Seis/Siusi Member

The Seis Member is a sequence of interbedded limestones and silty marlstones with a greenish colour in the lower and reddish one in the upper part. The ubiquitous content of terrigenous quartz and micas, always in the same silt grain size, reveal an air blown silt transport from the hinterland in the west. Limestone beds show textures typical for tempestites. In general they consist of graded litho- and bioclastic packstones and wackestones (often shell tempestites) with bed thicknesses ranging between centimetres and a few decimetres. The base of the beds mostly is sharp and erosional, scours and gutter casts are present. Wave-ripples with wavelengths up to 100 cm are common often causing a lenticular shape of the beds. Hummocky cross stratification occurs at the base of the rippled beds.

A special lithotype is the "Gastropodenoolith". Individual tempestite beds consist of reddish grainstones and packstones with oolites and microgastropodes (often with internal sediments or ferroan dolomite spar fillings and glauconite which do not correspond to the matrix of the packstones). Another one is the "Kokensches Konglomerat", an old term used by German authors, which consists of a conglomerate with flat pebbles. Both lithologies are handled as "leading facies types" for the Gastropod Oolite Member. Unfortunately both types are to be found in the lower and upper part of the Seis Member as well as in the Campill Member, complicating the definition of the Gastropod Oolite Member (see above).

Tempestite proximality (thick-bedded tempestites are more proximal (= shallower) than thinner bedded tempestites (= deeper)) enables the grouping of beds in thickening- or thinning upward cycles on the scale of few meters (Fig. 9). The lithofacies comprise both the upper shoreface and the offshore environment. Hummocky cross stratification and gutter casts indicate the lower shoreface facies and offshore facies of a high-energy type of coast (Fig. 10).

The Seis Member overlies the Andraz Member with a well-preserved erosional unconformity which is interpreted as SB at the base of the depositional sequence Ind 2 (Fig. 9). The sequence starts with a transgressional package of well-bedded tempestites characterized by rip up clasts (flat pebbles), microgastropodes and glauconite.

The onset of reddish marlstone in the upper part of the member signalizes a better oxidation of the sea bottom, which may be a consequence of a lower sedimentation rate or better circulation of bottom water. Reddish marlstones in the upper part of the Seis Member are distributed in the western and eastern Dolomites, but their isochronous onset is not demonstrated. Toward the boundary with the Campill Member the predominance of offshore facies in the cycles shifts once more to a shoreface facies with thickening of shell tempestites and scour fillings.

Biostratigraphic remarks: The Seis/Siusi Member in the Dolomites is known for the abundance of *Claraia* specimens defining the *Claraia Zone* (Fig. 11). The subzones with *Cl. wangi-griesbachi, C. clarai* and *C. aurita* occur in the upper Mazzin, lower and upper Seis members (Broglio Loriga et al., 1990, Posenato, 2008). In the Pufels/Bulla sections several findings of *Claraia* specimens have been documented by Mostler (1982).

Stop 1.6 – Siliciclastic input, climate signal

Campill Member

The start of the Campill Member is defined here with the first distinct occurrence of quartz/mica sandstones. Half meter- to meter-thick calcareous sandstone beds with hummocky cross stratification and a remarkable glauconite accumulation represent the transgressive phase of sequence Ind 3. The beds

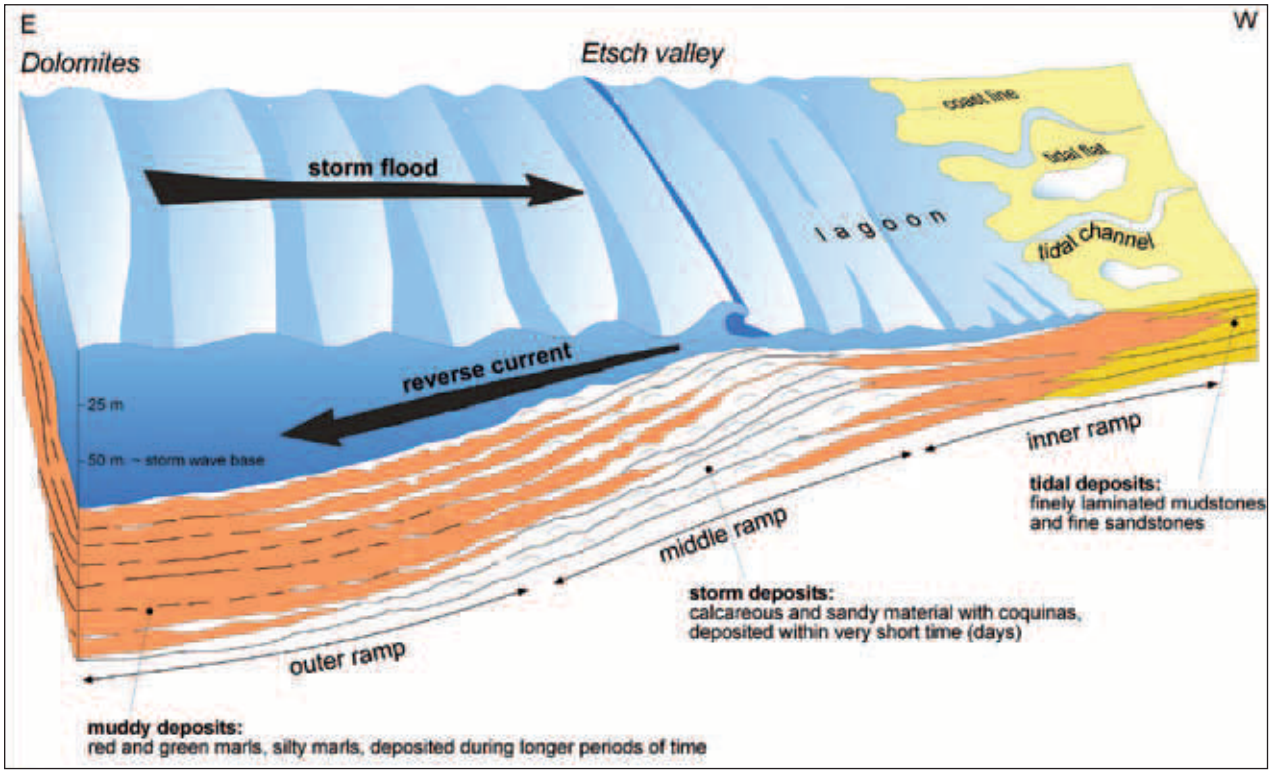

Fig. 10: Schematic model for the deposition of the Werfen Formation on an east-dipping ramp. Sedimentation is essentially controlled by storms; the coast line is supposed to be far to the west near the Como Lake. Mud deposits, now red and green marls, alternate with layers of sand with bivalve and gastropod shells. Each limestone bed is the product of a storm event and is deposited within some days. Storms generate energy-rich, seafloor-touching waves, which, especially in the coastal zone, are eroding and swirling up the mud and sand on the seafloor. Consequently, bivalve and gastropod shells are washed out and enriched sepa¬rately forming coquina beds (see Fig. 11) (after Brandner & Keim, 2011).

grade to thinner bedded storm layers (bioclastic shell tempestites) forming thinning upward cycles on the scale of several meters (Fig. 9). U-shaped burrows interpreted as *Diplocraterium* burrows, microripples and wrinkle structures are remarkable sedimentary structures in this part of the section. Most typical are "Kinneyia" structures, mm-scale winding ridges resembling small-scale interference ripples. After Porada & Bouougri (2007) these structures formed underneath microbial mats and are usually preserved on flat upper surfaces of siltstone or sandstone beds.

From ca. 152 m to 186 m section along the road is mostly covered. The next outcrops at the top of the section show some folding and ramp folds, but exact balancing of the stratigraphy by retrodeformation is possible.

The last 20 meters of the section are important for two reasons: (1) a prominent change is present in facies development from peritidal to subtidal offshore environment, and (2) this change is accompanied by a strong negative shift in the carbon isotope curve which is correlatable to the proposed GSSP section of the Induan-Olenekian Boundary in Mud (Spiti, Himalaya) (Krystyn et al., 2007). Peritidal cycles are made up of greenish to reddish silty and sandy marls with wave ripples and mud cracks alternating with dm-bedded silty bioclastic limestones and a few yellowish oolitic dolomites and marly dolomites. Posenato (2008) termed this unit "lithozone A" of the Gastropod Oolite Mb in the definition of Broglio Loriga et al. (1990). Two thinning upward cycles with some dm-thick amalgamated hummocky cross-stratified silty limestone beds at their base represent the transgressive phase of sequence "Ole 1" (accepting the strong negative carbon isotope excursion as a proxy for the IOB). The background sedimentation is still composed of red silty and sandy marlstones. Rare dark gray to black laminated marlstones may indicate short intervals of decreasing oxygen at the sea bottom.

The road section ends with the upper Anisian erosional unconformity on top of the lower part of the Campill Member. Upper Anisian Conglomerates (Voltago-/Richthofen Conglomerate) directly overlie red siltstones, sandstones and silty marls.

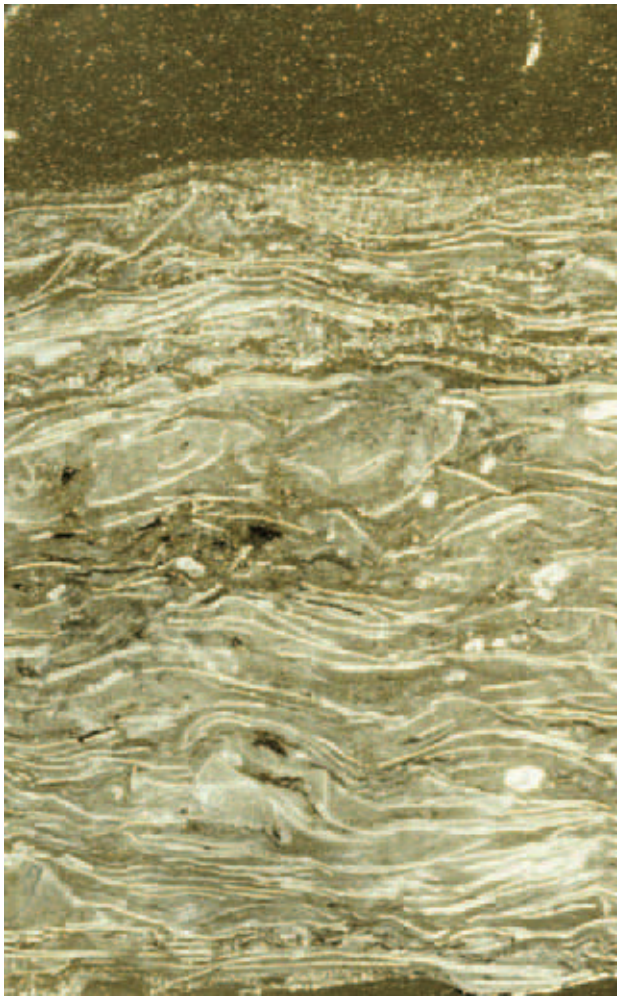

Fig. 11: Thin section photomicrographs of typical tempestite beds with grading and coquinas with *Claraia clarai* (after Brandner & Keim, 2011).

Summary

The lithostratigraphic and sedimentologic study has enabled the identification of meter-scale transgressive-regressive cycles (parasequences) in peritidal to subtidal depositional environments. Associations of the parasequences constitute, with varying stacking patterns, four depositional sequences that may have regional significance as shown by Horacek et al. (2007) who carefully correlated the stratigraphy of several sections in the Dolomites and Iran (). The main excursions of the carbon isotope curve can be correlated to sequence stratigraphic boundaries: (1) transgressive systems tract (TST) of sequence Ind 1; (2) TST of Ole 1 (see also Krystyn et al., 2007); and (3) the TST at the base of the Val Badia Member (not preserved in the Pufels section). This would imply that the profound changes in the global carbon cycle in the Lower Triassic are forced by eustatic sea-level changes. The TSTs of the sequences Ind 2 and Ind 3 are not clearly mirrored by the carbon isotope curve at Pufels.

Only in the transition towards more terrigenous input, i.e. at the base of the Campill Member, irregularities in the trend of the carbon isotope curve are present. More conspicuous is a negative shift in the Iranian sections (Horacek et al. 2007). On the other hand, the regional importance of the terrigenous input signal is evidenced by the magnetostratigraphic correlation with the continental facies of the German Triassic. Equivalent to the terrigenous Campill event in the Southalpine and the Upper Buntsandstein in the Austroalpine, the Volpriehausen Formation at the base of the Middle Buntsandstein starts with the first basin-wide influx of coarse grained sands (Szurlies, 2004). These distinct breaks in sedimentation style indicate a climate change to a more humid environment with increased rainfall and continental runoff.

Stop 1.7 – The Pufels/Bulla overthrust

This point offers a unique panorama of the Pufels overthrust – an alpidic structure due to N-S compression (Fig. 12). The whole pile of rocks, comprising the sequence between Außerraschötz and Piz Culac, is tilted towards the south. However, from Piz Culac to Col dala Dodesc the whole succession between the Bellerophon Fm and the Ladinian lavas is tectonically repeated.

The Pufels (Bulla) overthrust originated from a sheared, overturned syncline: the Contrin Dolomite southwest of Piz Culac shows this folding structure very clearly. Due to gradual compression the S-shaped folding was finally cut through. The whole upper rock package moved further to the north leading to the above cited repetition of the succession.

The basal shear plane of the Pufels thrust probably runs at the border between the Gröden and Bellerophon Fms and subsequently ascends the Werfen Fm presumably to the Schlern Dolomite, which is not preserved in the area.

The Pufels thrust is temporarily connected to the so-called "Val Sugana phase"; this deformation phase was active in the Southern Alps from 13 to 7 million years ago and caused the strongest uplift of the Dolomite Mountains (Castellarin & Cantelli, 2000).

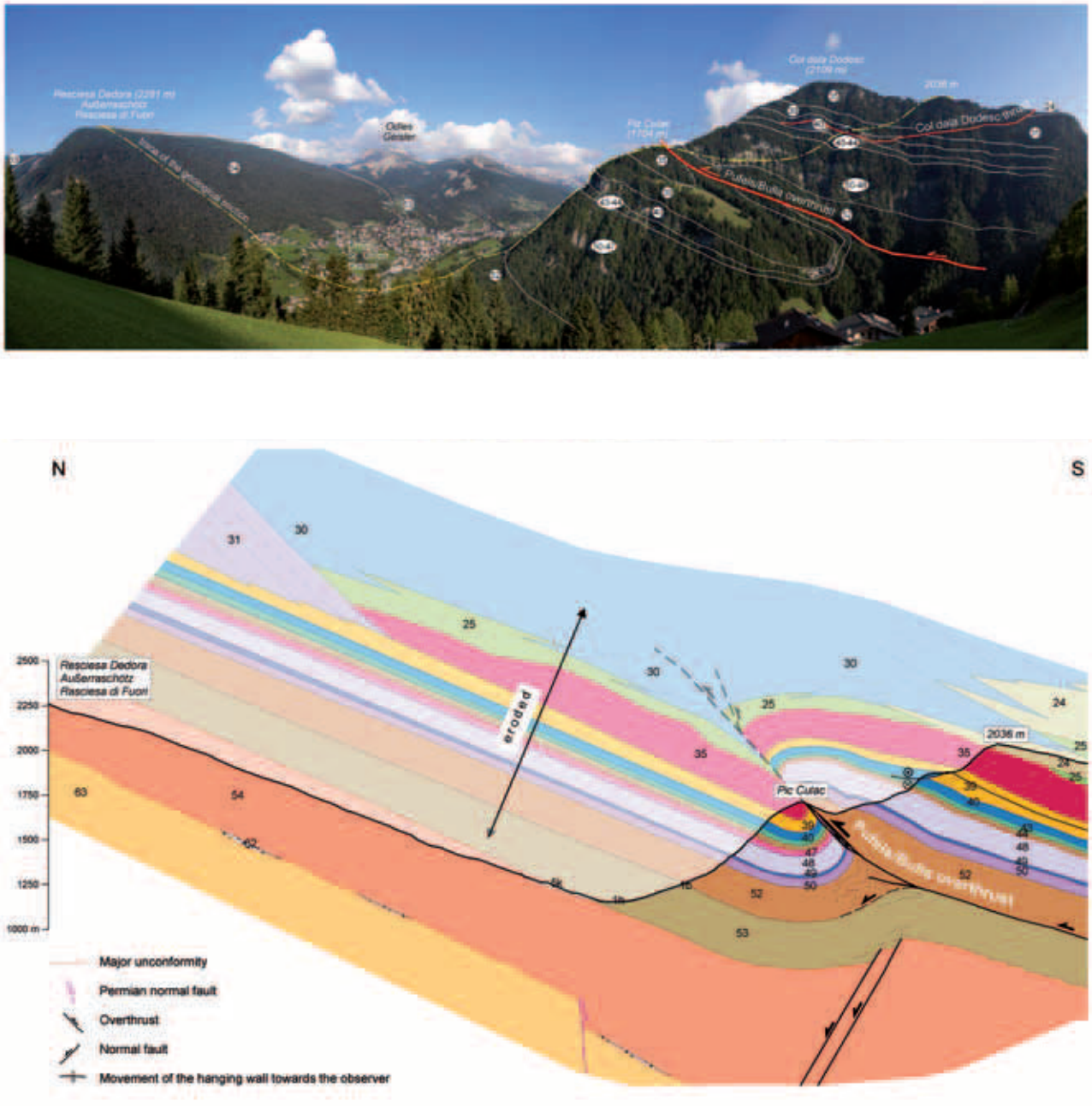

Fig. 12: Geological cross section of the N-vergent Pufels/Bulla overthrust, which developed from the sheared syncline at Piz Culac. The virtual extension of the cross section in the air shows the south dipping clinoforms of the Geisler/Odles on the upper left side. 63 = Southalpine metamorphic Basement, 62 = Waidbruck Conglomerate., 54 = ignimbrites undifferentiated of the Athesian Volcanic Group, 53 = Gröden Fm, 52 = Bellerophon Fm, 50 = Mazzin Mb, 49 = Andraz Mb, 48 = Seis/Siusi Mb, 47 = Campill Mb, 44 = Peres Fm (Voltago/Richthofen Conglomerate), 43 = Morbiac Fm, 40 = Contrin Fm, 39 = Buchenstein Fm, 35 = lavas, 25 = Wengen Fm, 24 = St. Cassian Fm, 5k = till, 1h = alluvial deposits, 1b = talus deposits (after Brandner & Keim, 2011, based on Geologische Karte der Westlichen Dolomiten 1:25.000 (2007)). Foto: H. Rier.

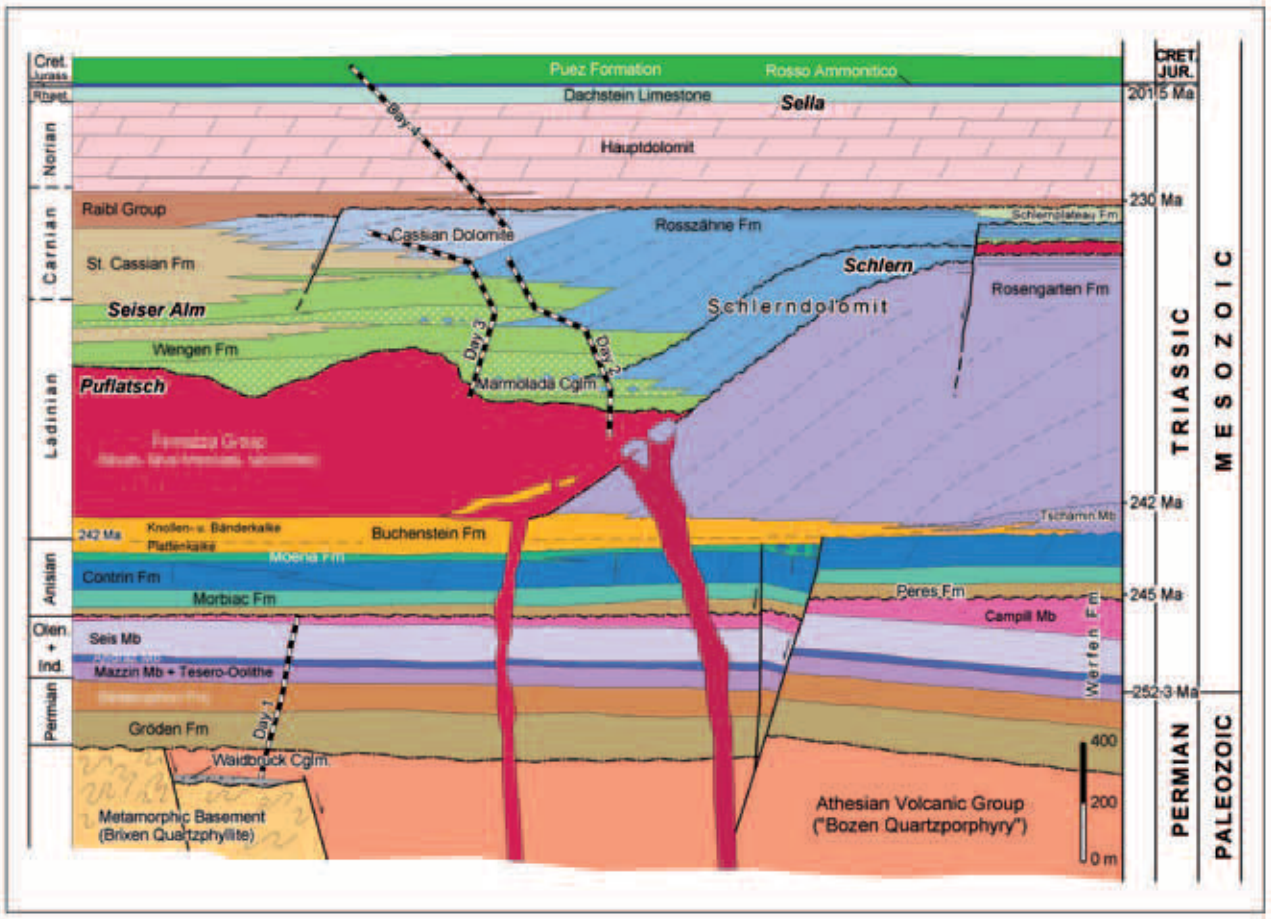

Fig. 13: Lithostratigraphic model for the Permo-Mesozoic succession of the Western Dolomites (modified after Brandner et al., 2007).

DAY 2

Middle and Upper Triassic successions at the NE margin of the Schlern/Sciliar platform and in the Seiser Alm/Alpe di Siusi basin

General remarks on the Middle and Upper Triassic stratigraphy

In the Ladinian the Schlern/Rosengarten carbonate platform forms the primary sedimentary margin of an extended carbonate platform spreading further towards the west on the Trento swell. The platform margins are typically characterized by 30–35° steep clinoforms (= "Überguss-Schichtung" *sensu* Mojsisovics, 1879) with progradation directions towards the NE and the SE. Large parts of this platform are eroded away – some remnants are preserved on the Mendel/Mendola situated to the SW of Bozen/Bolzano. In the adjacent basin, located in the east, pelagic sediments of the Buchenstein Fm were deposited. The platform slope as well as the basinal deposits became buried under a thick sequence of volcanic rocks during the late Ladinian (Longobardian, *Archelaus* zone, see Brandner et al., 1991, Brack et al., 2005) and thus unmistakably confirm the primary lateral change of the different facies. Basinal deposits, ca. 50 m in thickness, are time-equivalent to a ca. 800 m thick series of platform deposits. Based on this difference in relief, the water depth of the Buchenstein basin at the end of the pre-volcanic platform growth could be estimated to be ca. 800 m – such a reliable estimate would not be possible with common bathymetric criteria. Figure 13 shows a lithostratigraphic model for the Permo-Cretaceous succession of the Western Dolomites; Figure 14 shows a chronostratigraphic framework for the Triassic formations.

The focus of the actual field excursion mainly lies on the stratigraphic evolution at the slope-to-basin transition, the geometries of the sedimentary successions with their onlap and downlap structures as well as the resulting sequence stratigraphic implications of a mixed carbonate/volcanic and volcanicla-

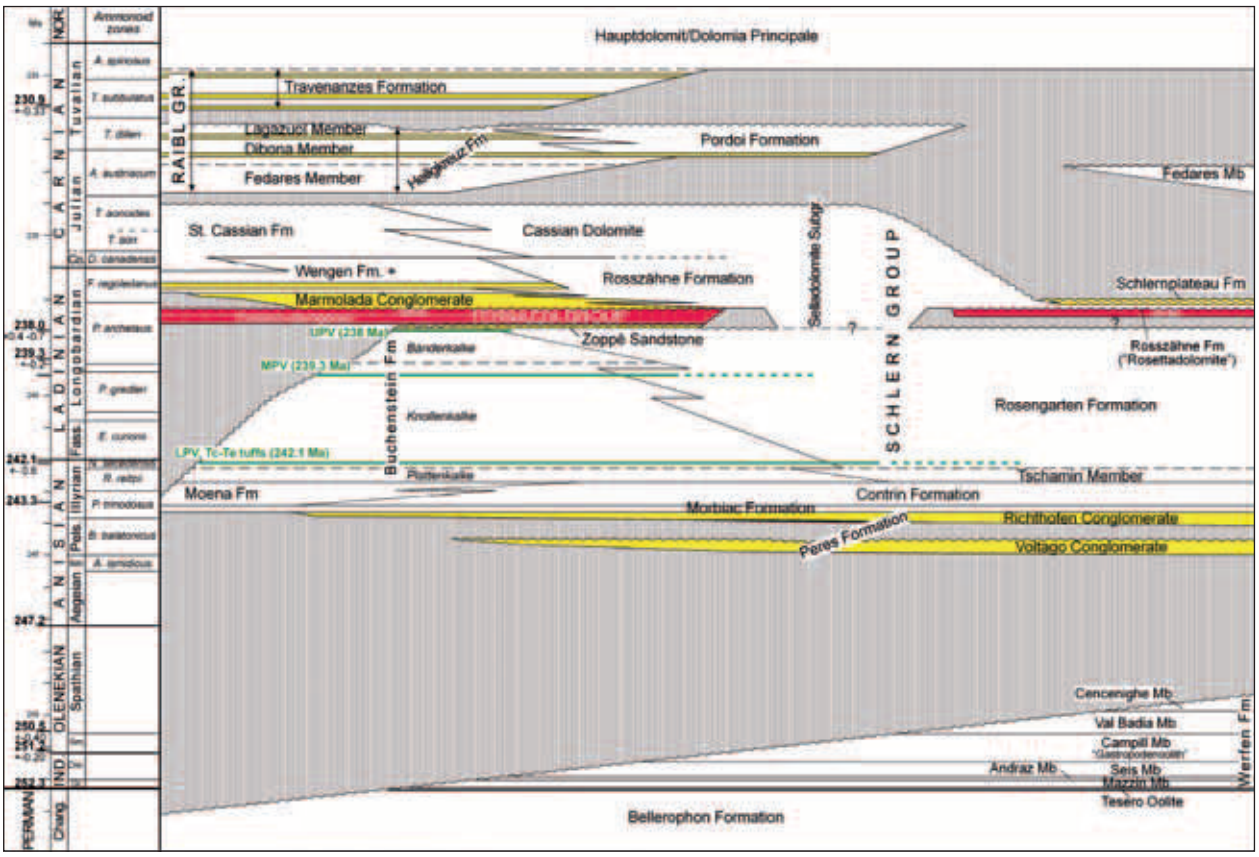

Fig. 14: Chronostratigraphic framework for the Triassic succession of the western Dolomites. LPV, MPV, UPV = Lower, middle and upper Pietra Verde (see Brack et al., 2005). Radiometric ages taken from Mundil et al. (2010). The main siliciclastic intervals are shown in yellow color.

stic depositional realm. The tectonically undeformed large-scale outcrops of the slope-to-basin transition zone can be easily compared with seismic sections and thus may help in the interpretation of seismic lines. So straightforward the outcrop situations are, however, so different are the geological interpretations of the patterns seen (see Bosellini, 1984, Sarg, 1988, Brandner 1991, Yose, 1991).

The underground of the platform-to-basin ensemble is well exposed in the well-known section in the Frötschbach/Rio Freddo situated at the northern flank of the Schlern. Here, the sedimentary succession starts with the Lower Triassic Seis/Siusi and Campill Mb. of the Werfen Fm, which is unconformably overlain by Anisian conglomerates of the Peres Fm, comparable with the Pufels/Bulla road section. This Anisian unconformity is widespread in the entire Western Dolomites and the succeeding conglomerates overlie the Upper Permian Bellerophon in the east (ca. Badia valley) and the Lower Anisian Lower Sarldolomit in the west (Etsch/Adige valley). Based on this erosional cut from young to old a block tilting of a ca. 75 km wide crustal segment with an uplift of ca. 350 m in the east was postulated (Brandner, 1984). This block rotation occurred in three individual phases during the Late Anisian and is interpreted as a new extensional rift tectonics after the Lower Permian.

The 3rd order depositional sequences after this major unconformity in the Western Dolomites are controlled by tectonics, independently form possible eustatic sea-level fluctuations. The genetically connected transgressive-regressive succession above the Anisian unconformity include the continental-marginal marine Peres Fm and the shallow marine Morbiac and Contrin Fms. The three units form a classical depositional sequence ("An 4") with LST, TST and HST. The top of this sequence is again bordered by an unconformity related to extensional tectonics. The carbonate banks of the Contrin Fm break up locally and form megabreccias along extensional faults. The resulting depressions and cavities were filled by anoxic, finely laminated sediments (Moena Fm).

The created submarine relief by this Late Anisian extensional tectonics has as determining influence on the following carbonate platform development of the

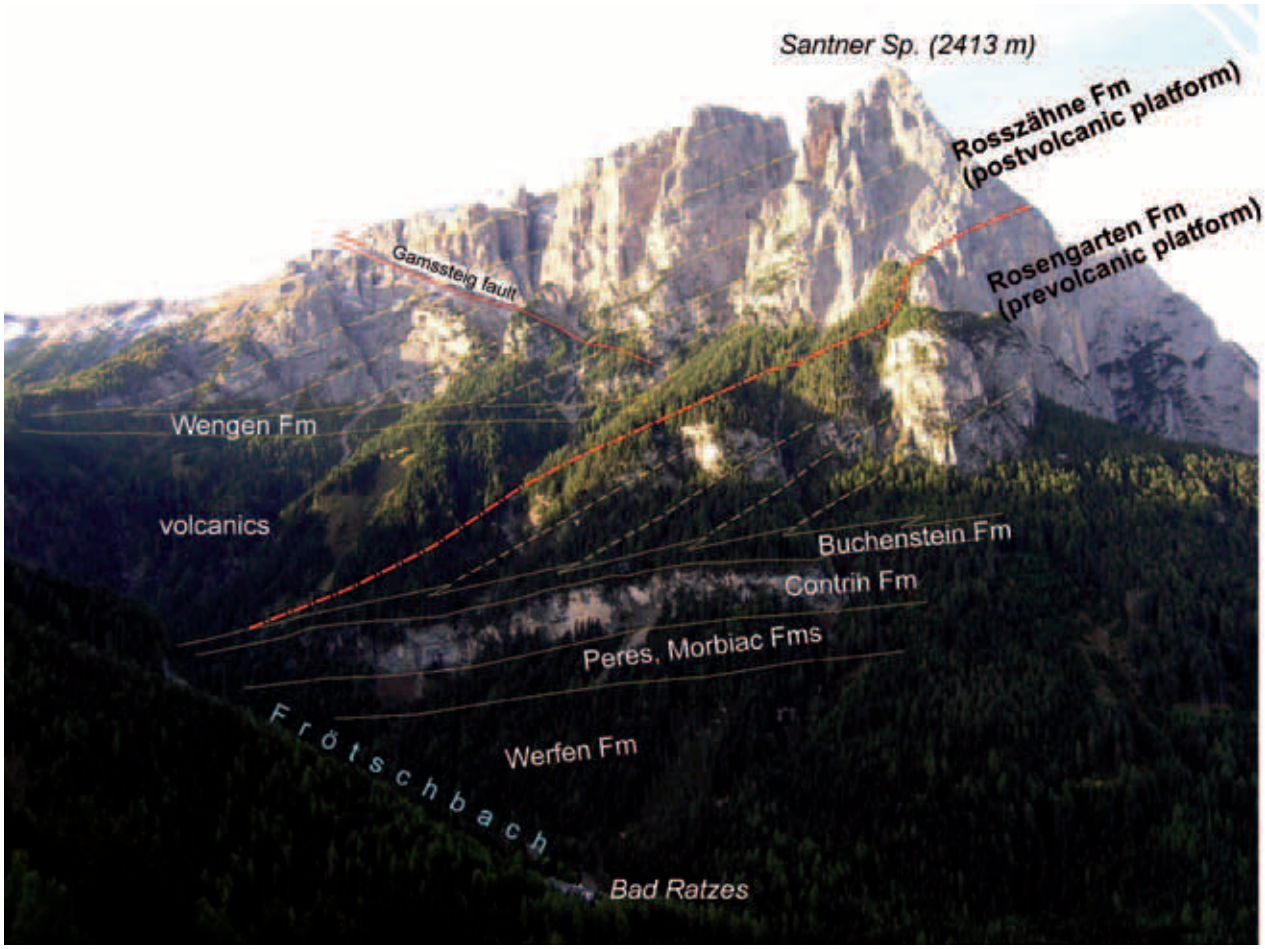

Fig. 15: Panoramic view on the north-eastern flank of the Schlern showing the excellently preserved, seismic-scale platform-to-basin transition of the Anisian to Ladinain carbonate platform. Depositional sequences are bordered by 3rd order unconformities (stippled lines).

Schlern/Sciliar-Rosengarten/Catinaccio. The nucleus of this carbonate platform is situated in the area of the Vajolettürme – a pre-existing high zone of this area that goes back to Permian rift tectonics ("Tiers/Tires Paleo-fault"). After an initial aggradation stage the platform prograded towards the NE, the Seiser Alm/Alpe di Siusi, as well as towards the SE forming the spectacular clinoform geometries exposed at the Rosengarten Group. Maurer (1999) succeeded in calculating the vertical and lateral growth rates of the Anisian-Ladinian platform. Biostratigraphic and radiometric ages of the sediments of the basinal Buchenstein Fm, which interfingers with the clinoforms, indicate an initial vertical platform growth of 600–700 m within the *Reitzi* and *Secedensis* zones (Late Anisian, see Brack et al., 2005). In a later stage, the *Curionii* zone (Early Ladinian), the platform switched to strong progradation, which lasted until the *Archelaus* zone (Late Ladinian), after which the Buchenstein basin and the clinoforms became buried under a thick volcanic sequence. The total thickness of the platform edifice is in the order of 850 m – the stratigraphic top is eroded –, the distance over which progradation took place ca. 5,5 km. Similar values can be assumed for the Schlern/Sciliar platform.

The lowermost deposits of the Buchenstein Fm, the so-called *Plattenkalke*, consist of finely laminated, bituminous limestones with radiolarian micrites that interfinger with the gently dipping slope deposits of the Tschamin-Member. This unit consists of dolomitized, reefal grainstones with stromatactoid cavities. The postulated interfingering zone is located near the drowning structural high zone at the Vajolettürme. The gently dipping slope of the Tschamin Mb is overlain by steep clinoforms of the Rosengarten Fm marking the start of the progradational phase at the transition from the TST to the HTS. In the basinal succession this change of sedimentation style is shown by the transition from the *Plattenkalke* to the *Knollenkalke* of the Buchenstein Fm. The succee-

ding *Bänderkalke* show a coarsening-upward trend with overlying toe-of-slope breccias beds, and corresponds to a rapid progradational phase during the late HST. The volcanics of the Fernazza Group above show different thicknesses and are characterized by a distinct relief at the top. The volcanics devide the carbonate platforms of the Schlern Group into the pre-volcanic Rosengarten Fm and the post-volcanic Rosszähne Fm and Cassian Dolomite. For a diverse stratigraphic terminology, however, see Carta Geologica d'Italia (1972, 1977), Brondi et al. (1976), Bosellini (1984), and De Zanche et al. (1993). At the north face of the Schlern/Sciliar the volcanics wedge out on the lower/middle platform slope (Figs. 13, 15); upslope the clinoforms of the post-volcanic Rosszähne Fm directly overly those of the pre-volcanic Rosengarten Fm without any recognizable interruption. The post-volcanic basinal deposits of the Wengen Fm are locally characterized by strong gravity sheddings of volcaniclastic and epiclastic sediments (Marmolada Conglomerate), which probably derived from a volcanic island near the Marmolada (Bosellini, 1996).

In the interfingering zone of the Wengen Fm with the Rosszähne Fm at the north-eastern flank of the Schlern/Sciliar and at the Mahlknechtwand three distinct progradational cycles of reef tongues with intercalated volcanoclastic sandstones and conglomerates are present. Within the single cyclothems the amount of volcanic detritus decreases gradually upsection and becomes almost absent at the transition to the St. Cassian Fm. At this time the relief of the debris delivering volcanic hinterland is almost levelled out and re-flooded of this area occurs again as a consequence of the general subsidence after the Mid-Triassic rifting period. The rather complex, but intriguing interactions between subsidence, sea-level fluctuations and sediment input from two contrasting sources (carbonate platform vs. volcanic island) into the marine basin are discussed on the second day at the Mahlknechtwand (Stop 2.2).

At the platform top itself (Schlern/Sciliar plateau) there was hardly any accommodation space available and several subaerial exposures with karst and soil formation (iron ore) were formed. After a further depositional gap in the Lower Carnian sedimentation proceeded in some shallow-marine depressions with the deposition of thin black marls and shales of the Raibl Group (Fedares Mb) and finally the Norian Hauptdolomit/Dolomia Principale.

Excursion route

From Bula/Pufels to Seiser Alm/Alpe di Siusi to the Mahlknechthütte/Rif. Molignon by bus, then hiking to the Mahlknecht cliff, walk to Auf der Schneid/Cresta Alpe di Siusi, walk to Tierser Alpl Hütte, Rosszahnscharte/Forc. di Denti di Terra Rossa, walk down to the Wiedner Woadn and back to Mahlknechthütte.

Stop 2.1 – Gasthof Gstatsch

General Explanation of the panorama at the NE-flank of the Schlern (Fig. 15). The interruption of the carbonate platform development by the intercalation of Upper Ladinian volcanics is clearly visible. The volcanic rocks form an onlap onto the paleoslope of the Rosengarten Fm (Schlern Group) and wedge out towards the SW. Contemporaneous, thinner layers of volcanics are present on the platform top as well (not visible from here). The growth of the post-volcanic platform started directly on top of the pre-volcanic one without any distinct unconformity in between. Therefore we assume that the interruption of the platform growth was only of minor duration. The post-volcanic platform (Rosszähne Fm) is characterized by a stronger progradational geometry compared to the pre-volcanic Rosengarten Fm. At the platform top there is hardly any accommodation space available for aggradation. The major part of the Schlern massif consists of the pre-volcanic Rosengarten Formation. Due to the rapid fill of the ca. 800 m deep Buchenstein basin by a ca. 450 m thick volcanic sequence – towards the SE the thickness of the volcanics increases with the formation of islands (eroded) in the area of the Marmolada – the former submarine topography was completely remodeled. This topographic change led also to profound changes of the sedimentation pattern.

Stop 2.2 – Mahlknechthütte/Rif. Molignon

This spectacular outcrop of the Mahlknecht wall shows the sedimentation on the slope and toe-of-slope of the Rosszähne reef. A varicoloured succession of megabreccias, calcarenites, volcaniclastic sandstones and conglomerates (Marmolada Conglomerate) directly overlie well-preserved pillow lavas that occur on top of the thick volcanic sequence,

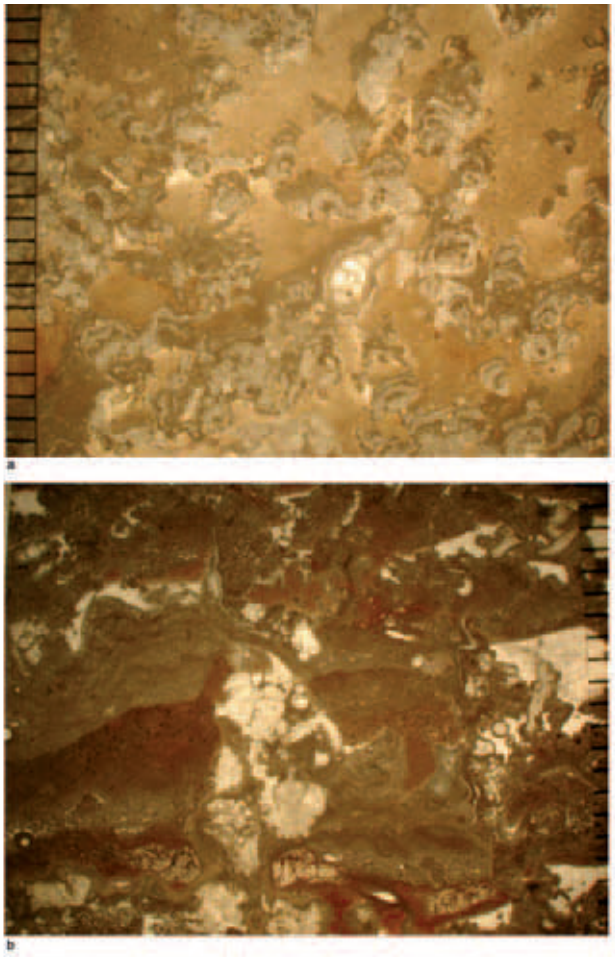

Fig. 16: Thin section photomicrographs of Cipit boulders from the Mahlknechtwand: (a) Thrombolitic boundstone with Tubiphytes and microbial encrustations and large cavities filled with internal sediment; (b) Boundstone with clotted peloidal micrite, festooned crusts, *Tubiphytes*, botryoidal cements and various generations of tilted geopetal sediment infills. Scale in mm.

which itself succeeds the Buchenstein Fm and the Rosengarten Fms.

In the interstitial pores and cooling cracks of the pillows locally radiolarian micrites with sponge spiculae occur. These remnants of pelagic deposits correspond to a ca. 20 m thick succession of the lowermost Wengen Fm in a similar facies in the Tschapid creek, located ca. 2.5 km to the west, with conodonts and *Daonellae* of the Longobardian substage (*Archelaus* zone, Brandner, 1991). The thickness variation results from an onlap geometry onto the very irregular, ca. NW-dipping surface of the volcanics. The sedimentary succession is dominated by megabreccias with the so-called "Cipit boulders". They result from high-density, clast-supported gravitative debris flows, and formed the distinct relief of the outer surface of the debris stream. The Cipit boulders exhibit very well-preserved depositional fabrics and shells, partially still with their original aragonite composition. Thus the growth fabrics and reef building organisms can be studied in detail in these rocks. The dominating constituents are bindstones and baffle-stones with peloidal micite crusts, various festooned crusts as well as masses of *Tubiphytes* and other microproblematica (Brandner et al., 1991). Corals, calcareous sponge bafflestones or oncolites, which could have derived from the platform margin, are rare. Most of the limestone boulders originate from the middle and upper slope (Brandner et al., 1991, Flügel, 1991). Growth cavities of centimetre - to decimetre-size that are filled with internal sediments in various phases (tilted geopetals), and fibrous and botryoidal cements are common (Fig. 16). These microbial boundstones were indurated upon formation and combined with syndepositional cementation these processes resulted in the formation of semi-stabilized clinoforms. The formation of breccias and megabreccias tongues calls for multiphase gravitational mass movements with repeated encrustation and cementation. The single clasts or boulders may consist of other, smaller breccia clasts, i.e. the overall fabric is that of breccias within other breccias with a trend of enlargement of the clasts. These data point to multiple interactions of platform shedding, *in situ* carbonate precipitation and microbial encrustation on the clinoforms, geopetal infill, early cementation, breccia formation due to oversteepening or seismic shocks, microbial encrustation and stabilization, cementation, geopetal infill, renewed brecciation, and so on (Fig. 17). Moving down slope, the thickness of the breccia beds increases significantly. Isolated megabreccias at the toe-of-slope and the proximal basin, known as Cipit boulders, are therefore not the product of erosion of the platform margin commonly related to sea-level lowstands. None of the Cipit boulders shows dissolution pores or vadose cements, indicative of subaerial exposition. We postulate that the main reasons for the gravitative mass movements of the prograding reef tongues are the different rheological characteristics and thus the instability of the slope succession: the rapidly cemented carbonate breccia beds overlie water-saturated volcaniclastic sediments which were not yet cemented. This alternation reduces distinctly the shear strength and any earthquake may lead to the downslope sliding of the rigid carbonate layers ("hard" on "soft") along a discrete shear surface (= clinostratification). At the frontal side of the mass movement body the carbo-

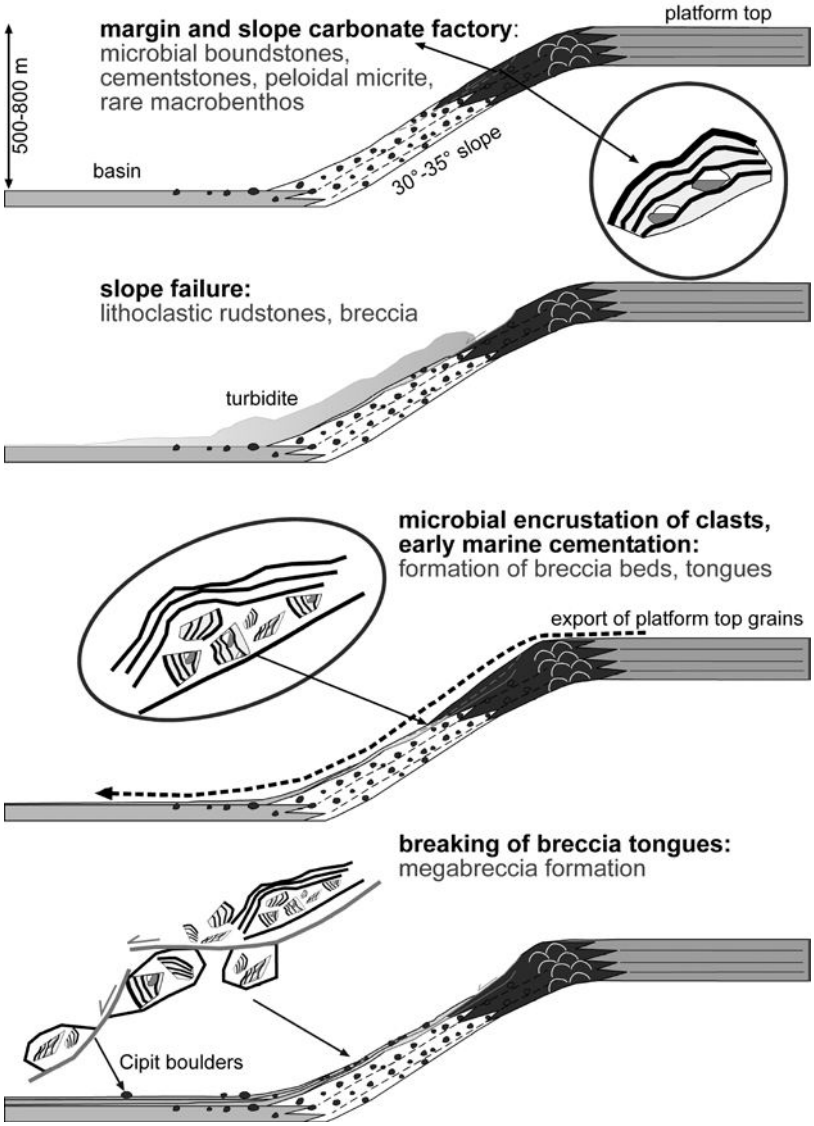

Fig. 17: Schematic model for steeply dipping, prograding carbonate slopes. The formation of breccias and megabreccias on the slope requires multiple interactions of platform shedding, *in situ* carbonate precipitation and microbial encrustation, geopetal infill, early cementation, break up of already hardened sediments by gravitational mass-movements that were triggered by oversteepening or seismic shocks, followed by renewed encrustation and cementation, etc. The clinostratification corresponds partially to discrete submarine shear planes.

nate banks turn into single boulders (Fig. 17). In the distal part the megabreccias turn into dm bedded calciturbidites with shallow-water derived grains. Ooids and coated grains testify their provenance from the flooded platform top.

Well-bedded sedimentary intervals with volcaniclastic detritus overlie the platform tongues and form an onlap geometry onto the paleo-slope (see also Stop 2.3). The succession is made up of sandstones and conglomerates as channel fills (Marmolada Conglomerate). They are epiclastic sediments with well-rounded pebbles originating from fluvial transport. Their actual position on the lower reef slope and in the deep basin resulted from gravitative redeposition. The volcaniclastic intervals are repeatedly interbedded with the reef tongues, but not by chance. The carbonate/volcaniclastic succession shows a certain rhythmicity, whose control mechanisms are still a matter of debate. The peculiarity of the depositional environment is the different provenance of the sediments: the carbonates were formed on the Rosszähne platform itself, whereas the volcaniclastic sediments were transported from a far away situated volcanic island (surroundings of Marmolada?). The regularity in the sedimentary successions suggests that sea-level fluctuations were the controlling parameter. There is, however, no consensus whether the megabreccias together with the Cipit boulders were formed during a sea-level lowstand (LST) or highstand (HST) (see Yose, 1991). We postulate that more arguments are in favor of the transport of the volcaniclastics during a sea-level lowstand, whereas the progradation of the reef tongues with shallow water grains (oolites) occurred during sea-level highstands.

Fig. 18: Panoramic view from "Auf der Schneid" (Cresta di Siusi) to the Rosszähne and Mahlknechtwall showing the interfingering between prograding reef slope deposits of the Rosszähne Fm (Rz1, 2) and volcaniclastic sandstones and conglomerates (V1). Wedging-out of volcaniclastics onto the upper carbonate slope (= onlap) as well as the succeeding downlap surface (DLS) of reef tongue 2 are clearly visible. The natural cut of the Mahlknechtwand runs obliquely to the depositional dip of the clinoforms, therefore the true dip-angle is steeper. V = volcanics (Fernazza Group) which cover the paleo-slope of the pre-volcanic Rosengarten Fm (Ro) to the south of the Tierser Alpl (after Brandner et al., 2007).

Stop 2.3 – Auf der Schneid/Cresta di Siusi

Panorama of the seismic-scale outcrops of the entire slope domain of the post-volcanic Rosszähne platform (Fig. 18). The wedging out of the volcaniclastic sequence onto the post-volcanic carbonate slope at the transition to red beds at the Roterd Sp./Cima di Terra Rossa, which may reflect intermittent subaerial exposure of the platform top, is clearly visible. Above it follows the downlap surface of the prograding Rosszähne reef tongues of the early highstand. South of the Tieser Alpl the onlap of the volcanics is well exposed within the Rosengarten massif. The steeply dipping Tierser Alpl fault does not significantly disturb the platform geometry and the stratigraphic successions.

Stop 2.4 – Tierser Alpl Hütte and Rosszahn Scharte

General explanation of the spectacular panorama and of the isolated Langkofel/Plattkofel carbonate platform with its W dipping paleoslope. Between the Rosengarten/Schlern and the Langkofel/Plattkofel reef a narrow seaway can be assumed, but its actual extension does not correspond exactly to the original, Triassic, one: during the Alpine deformation the Langkofel/Plattkofel platform was sheared off its underground and thrusted towards the north.

At the Rosszahn Scharte the ca. 30° steep N dipping paleoslope with the above described phenomena of gravitative submarine sliding of carbonate banks and megabreccia formation can be observed (Fig. 19). The later dolomitization of the entire carbonate platform and slope – the exact timing is not known, but a first stage of dolomitization during the Ladinian during subaerial exposure and a second one during burial seem plausible – affected only the still connected carbonate tongues, which were permeable for dolomitization fluids. The further transported boulders in the basin were isolated by the fine grained sedimentary matrix and thus escaped the dolomitization.

Stop 2.5 – above Wiedner Woadn

Exemplary outcrop in a little gully: Marmolada Conglomerate and volcaniclastic sandstones form an onlap onto the steeply dipping paleoslope of the Rosszähne carbonate platform.

Fig. 19: Outcrop photo of steeply N-dipping clinoforms west of the Rosszahn Scharte with typical slope breccia tongues.

DAY 3

Geology of the Sella platform and Col Rodela

Introduction

The third day is dedicated to the Sella massif as well as to the Col Rodela. The Sella Group, one of the most prominent mountains of the Dolomites, is located in the central Dolomites and is orographically bordered by the four, well-known passes: the Gröden/Gardena Pass (2121 m) in the north, the Campolongo Pass (1875 m) in the east, the Pordoi Pass (2239 m) in the south and the Sella Pass (2244 m) in the west (Fig. 2). From a geological point of view, the Sella massif can be subdivided into two parts: (1) a lower one that consists of the Late Ladinian to Early Carnian carbonate platform in the strict sense; (2) an upper one that essentially comprises the Norian Hauptdolomite and a thin cover of Rhaetian to Cretaceous sediments. These two major carbonate bodies are separated by the Carnian "Raibl beds", forming the typical recessively weathering ledge at the outer rim of the massif. The lower carbonate edifice consists of postvolcanic, platform and flank deposits (Selladolomite Subgroup: Rosszähne Fm and Cassian Dolomite) and exhibits excellently-preserved, steep clinoforms (ca. 35°) on all sides. It exhibits a sub-round shape in plan view, measures 7–8 km in diameter and interfingers on all sides with basinal sediments of the Wengen and St. Cassian Formations, respectively. This atoll-like geometry of the Sella platform thus has become one of the classical examples in the study of large-scale depositional geometries of isolated carbonate platforms (Leonardi & Rossi, 1957, Bosellini, 1984, Kenter, 1990, Bosellini & Neri, 1991, Keim & Schlager, 1999, 2001).

The growth of the Sella platform came to a standstill in the Early Carnian and was subsequently covered by a sequence of mixed carbonate-siliciclastic deposits, the "Raibl beds" *Auct.*, hereafter termed Pordoi Formation. It consists of volcanoclastic sandstones at the base, followed by peritidal dolomites interbedded with marlstones. The sedimentation pattern of the Pordoi Fm was strongly influenced by synsedimentary tectonics (Doglioni, 1992, Keim & Brandner, 2001). Extensional tectonics led to local fissures, block-tilting, graben structures and breccia deposits. Towards the centre of the mountain, the thickness of the Pordoi Fm decreases distinctly and is locally reduced to zero.

The upper part of the Sella is formed by the well-bedded Hauptdolomit/Dolomia Principale, an approx. 250 m thick succession of peritidal deposits, which are overlain by some tens of meters of Rhaethian Dachstein limestone. At the summit of the Sella, the Piz Boè (3152 m), the stratigraphic succession terminates with red nodular limestones (Ammonitico Rosso, Jurassic) and hemipelagic marlstones (Puez Marls, Cretaceous, see Fig. 13).

Lithostratigraphy of the Sella platform

The lithostratigraphic units used in this guidebook follow the "Geologische Karte der Westlichen Dolomiten – Carta geologica delle Dolomiti Occidentali 1:25.000". The lithostratigraphic terms of the Ladinian-Carnian deposits differ in some way from the names used so far in this region (e.g. Carta geologica d'Italia, F. "Marmolada", 1977, Bosellini, 1991):

Basinal sediments: Wengen Fm, St. Cassian Fm: lithologic interfingering of each other.

Carbonate platform: Selladolomite Subgroup: postvolcanic Schlerndolomite undifferentiated; locally the Selladolomite can be subdivided into an older platform, termed Rosszähne Fm (like at the Schlern massif, see day 2), which interfingers with the Wengen Fm, and a younger platform, the Cassian Dolomite, which interfingers with the St. Cassian Formation. The "Gardena Megabreccia" *sensu* Bosellini & Neri (1991) belongs to the Rosszähne Formation.

Post-carbonate platform sediments: Pordoi Formation (the former "Raibl beds").

Biostratigraphy

The biostratigraphic data are derived from various basinal sections (Wengen and St. Cassian Fms.) around the Sella and from the Pordoi Fm. overlying the platform top. Ammonoid faunas (Reithofer, 1928, Mietto & Manfrin, 1995, Mietto et al., 2008) obtained from the basinal successions indicate an Upper Ladinian (*Regoledanus* Zone) to Lower Carnian age. The topmost part of the section above the so-called "Gardena Megabreccia" to the south of the Gardena Pass (Col de Frea) was assigned by Mietto & Manfrin (1995) to the *Daxatina* cf. *canadensis* subzo-

ne, nowadays termed *Canadensis* zone = base of the Carnian stage (Broglio Loriga et al., 1999, Mietto et al., 2008). Conodonts of the Wengen and St. Cassian Fms (Mastandrea et al., 1997) around the Sella (*Budurovignathus* group) belong to the *diebeli* assemblage zone *sensu* Krystyn (1983), which corresponds to the standard *Regoledanus* zone (Upper Ladinian).

The youngest basinal deposits, time-equivalent to the final platform growth, are exposed at the eastern side of the Sella, at the foot of Crep de Munt. A preliminary pollen study from dark marls of the St. Cassian Fm, showed a rich fauna containing among others the taxa *Concentricisporites* cf. *bianulatus* and *Gordonispora fossulata* (Keim & Roghi, 2006). These findings confirm a Lower Carnian age (Julian 1/II = *aonoides* zone). Pollen from the uppermost Pordoi Fm at Piccolo Pordoi, just a few metres below the Hauptdolomit (Dolomia Principale) contained the taxa *Vallasporites ignacii, Duplicisporites verrucatus, Pseudoenzonalasporites summus, Patinasporites densus, P.* cf. *densus, Ovalipollis pseudoalatus, Camarozonosporites* cf. *rudis* and *Hevizipollenites* sp.. This association indicates a late Julian age (*Austriacum* zone) and thus correlates with the basal Heiligkreuz Fm. in the eastern Dolomites. Thus a major stratigraphic gap, which probably occupies most of the Tuvalian, has to be assumed to exist between the topmost Pordoi Fm and the overlying Hauptdolomit.

Alpine tectonic deformation

Alpine deformation of the Sella Group is rather weak and thus the Triassic submarine paleo-topography is still well preserved. The oldest, pre-alpine deformation patterns are Carnian extensional structures with numerous, nearly N-S trending fissures, grabens and halfgrabens, which became sealed by the Norian Hauptdolomite (Doglioni, 1992, Keim & Brandner, 2001). These structures are present all around the Sella massif, but especially at the E-side. The most conspicuous alpine deformation structures are also exposed at the eastern side with overthrusts in a ramp-flat system (Doglioni, 1985, 1992) leading to the so-called "Gipfelüberschiebung" (summit thrusts) at Piz Boè; here the Rhaetian Dachstein limestone, the Jurassic Ammonnitico Rosso and the Cretaceous Puezmarls are strongly folded and overthrusted by several slices of Hauptdolomit. This deformation is of Paleogene age and was correlated with the Dinaric, W-vergent compression (Doglioni, 1992). The succession at the northern part of the Sella was folded along the E-W trending Plan-Grödnerjoch/Passo Gardena anticline and was tilted towards the south by 15°–20°. The Sella S-side is involved into the E-W running Padon anticline and thus the succession is tilted towards the north.

Additionally, the entire Sella massif is dissected by numerous NE-SW and NW-SE running transcurrent faults, the most prominent one is the sinistral strike slip fault along the Val de Mesdì to the Pordoi Pass.

Platform-basin transition: geometry and sedimentology

The entire platform shows pervasive dolomitization. In contrast to the hundreds of meters thick clinoforms, the topset beds at the outer rim of the Sella reach only some tens of meters. Towards the centre of the Sella the thickness of the topsets increases considerably. Based on the height of the clinoforms, the thickness of the Selladolomite Subgroup ranges between 400 to 700 m. The transition between topsets and steep slope occurs within tens of meters. The clinoforms show a primary depositional angle of 30–35° and interfinger on all sides with basinal deposits (Bosellini, 1984). Intensive downslope transport is indicated by debris aprons at the toe of the clinoforms; they consist of turbidites, debris-flow breccias and swarms of meter-size boulders (Bosellini & Neri, 1991, Mastandrea et al., 1997). In addition, the basins were fed with volcanoclastics (conglomerates, sandstones, siltstones) and terrigenous mud.

The topsets show horizontal, planar bedding with bed-thicknesses between 0.1 and 1 m. Occasionally, patches of cross-bedded are¬ni¬tes as well as meter-size tepees occur (e.g. in Val de Mesdì). At Pisciadù, within the topsets coral colonies of the type *Thecosmilia* have been found in growth position. The content of skeletal grains from the measured section at Pisciadù is generally less than 5% and consists predominately of echinoderm debris, bivalves, foraminifera, dasycladacean and solenoporacean fragments, *Tubiphytes?*, cyanophyta, such as *Rivularia*, *Cayeuxia* or *Hedstroemia* and uncertain sphinctozoan sponges (Keim & Schlager, 2001). The skeletal grains in most cases are totally recrystallized and often show micritic encrustations. The most striking observation is the presence of automicrite facies in all different platform domains, although the amount varies considerably (Keim & Schlager, 1999, 2001). Most of the samples from the margin-upper slope consist of automicritic boundstones with large cement-filled cavities in-between ("evinosponges"-like structures).

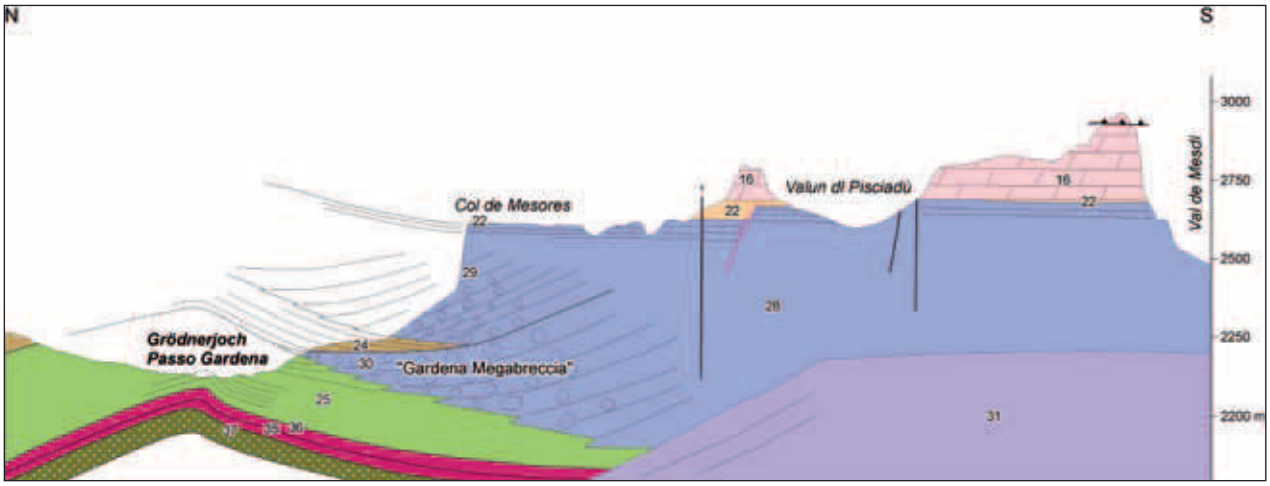

Fig. 20: The geological situation at Grödner Joch/Passo Gardena: (a) The geological cross section illustrates the antiformal deformed lower slope megabreccias ("Gardena megabreccia") and basinal deposits during alpine tectonics along the E-W trending Plan-Grödner Joch/Passo Gardena anticline; (b) close up view of the "Gardena megabreccia" (= Rosszähne Fm) wedging out in the basinal sediments of the Wengen Formation. See text for explanation. 37 = "Caotico eterogeneo", 35 = lava, 37 = Hyaloclastites, 31 = pre-volcanic Schlerndolomite (Rosengarten Fm), 30 = post-volcanic Schlerndolomite (Rosszähne Fm), 29 = Cassian Dolomite, 28 = Selladolomite Subgroup (post-volcanic platform carbonates undiff.), 25 = Wengen Fm, 24 = St. Cassian Fm, 22 = Pordoi Fm ("Raibl beds"), 16 = Hauptdolomit/Dolomia Principale.

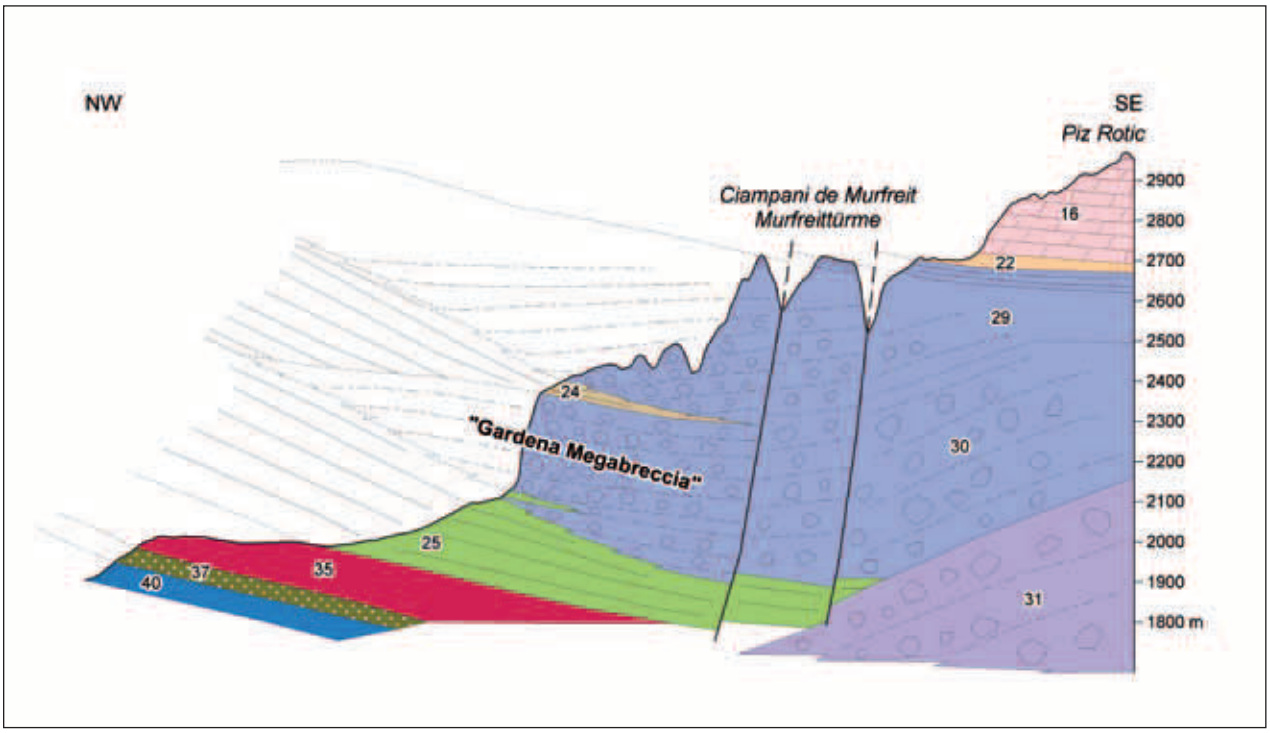

Fig. 21: Geologic cross section at Campani de Murfreit. Alpine antiformal deformation of the entire stratigraphic succession up to the Norian Hauptdolomite clearly shown. 40 = Contrin Fm; for a detailed legend see Fig. 20.

Skeletal grains from the margin-upper slope may include *Tubiphytes*, *Macrotubus*, *Girvanella*, serpulids?, and occasionally some bivalve filaments, ostracods and gastropods. The high cement content of the samples comprises mainly fibrous cements in the form of botryoids or even druses. All cements are altered to dolomite. Fibrous cements are inclusion-rich and may form cm-thick isopachous layers. The volumetrically most important cement type are isopachous layers of former radiaxial fibrous calcites. The breccia tongues of the lower slope contain abundant boulders up to several m in diameter. The planar shape and steep angle of the clinoforms, however, indicate that the large-scale geometry of the slope was controlled by non-cohesive layers of sand and rubble piled up to the angle of repose (Kenter, 1990, Keim & Schlager, 1999, 2001, Schlager & Reijmer, 2009).

Excursion route

During the excursion, we will approach the Sella from the Gardena Valley and continue in a counterclockwise direction. From the Gardena Pass we will pass the Sella Pass, walk to Col Rodela, turn back to the Sella Pass, and then proceed to the Pordoi Pass.

Stop 3.1 – Grödnerjoch/Passo Gardena

The N-front of the Sella platform, including the outcrops at Meisules dala Biesces/Murfreit, is one of the most controversial examples in terms of depositional geometries (e.g. Leondari & Rossi, 1957, Bosellini, 1982, Bosellini & Neri, 1991). The platform shows a subdivision which is twofold (Fig. 20): (1) a lower unit, the so-called "Gardena Megabreccia" (Bosellini, 1982, Bosellini & Neri, 1991), which is covered by basinal sediments (Wengen and St. Cassian Fms.) and (2) an upper unit, composed of steeply inclined slope deposits and thin flat-lying top-set beds of the Sella platform proper (Cassian Dolomite). The megabreccia body is distinctly stratified: at Gardena Pass the beds are nearly horizontal, at Meisules/Murfreit, however, the boulder beds dip with ca. 20° to SE. The same dip angle is present in the underlying Wengen Fm and also in the platform-top sediments at the Meislues/Murfreit Towers (Fig. 21). Locally, the basinal St. Cassian Fm between the "Gardena Megabreccia" and the above lying Cassian Dolomite wedge out, causing the two units to be weld together. The thickness of the "Gardena Megabreccia" varies between about 200 m at Meisules/Murfreit and zero at the Gardena Pass. At Gardena Pass, the megabreccia tongues pinch out by interfingering with the basinal Wengen Formation and outrunner blocks ("Cipit boulders") which are clearly visible in the basin sediments. The "Gardena Megabreccia" mainly consists of tongues of boulders with diameters of up to several meters and intercalations of some dm-thick beds of calciturbidites. The boulders are largely composed of automicritic boundstones, with microproblematica like *Tubiphytes*, scarce metazoans (sponges, corals), peloidal to skeletal packstones and cement-filled cavities (Russo, in Bosellini & Neri, 1991). The "Gardena Megabreccia" was interpreted by Bosellini (1982) and Bosellini & Neri (1991) as channelized megabreccia as the result of multiple collapses of a "pre-existing carbonate platform, rather than a buildup". De Zanche & Gianolla (1995) regarded it as the lowstand prograding complex of their Car1 depositional sequence.

We do not share these interpretations and regard the "Gardena Megabreccia" as folded lower slope breccia tongues of the Rosszähne Fm (Keim & Neri, 2004, Brandner et al., 2007). The strong thickness variation (0–200 m) of the megabreccia body is related to the oblique erosive cut of the proximal-distal parts of these lower slope deposits. The variation of the dip-angle of the megabreccia (flat-lying, SE-dip) is the result of alpine tectonic deformation along the ca. E-W trending Plan-Grödnerjoch anticline: the former N-dipping, lower slope deposits, which interfinger with the basinal sediments of the Wengen Fm were tilted by 15–30° and are actually part of the southern limb of the above mentioned Plan-Grödnerjoch/Passo Gardena anticline.

In the surroundings of the Grödnerjoch/Passo Gardena, the Cassian Dolomite situated above the "Gardena Megabreccia" does not show this tilting and is characterized by the classical 30–35° steep clinoforms and horizontal lying topsets. At this location the folded part of the platform and slope has simply been eroded away (Fig. 20). Further to the SW, however, at the Murfreit Towers, the topset beds of the Cassian Dolomite, the overlying Carnian Pordoi Fm ("Raibl beds") as well as the Norian Hauptdolomite are tilted 15–20° towards the S-SE (Fig. 21). These data clearly point to folding at the N-NW side of the Sella Group during alpine deformation.

Stop 3.2 – Hotel Gerhard, at the foot of Meisules dala Biesces

This short stop on the road again impressively shows the tilted Rosszähne Fm ("Gardena Megabreccia") with distinctly SE dipping breccia beds (Fig. 21); this alpine folding with formation of the Plan-Grödnerjoch/Passo Gardena anticline affected also the younger stratigraphic units including the Hauptdolomite. Furthermore, the facies interfingering of the lower slope breccias and the basinal sediments of the Wengen Fm is clearly expressed by the alternation of calciturbidites, marls, sandstones and a ca. 20 m thick dolomitized limestone breccia tongue.

From Sella Pass to Col Rodela: geological introduction

The area of Col Rodela is one of the most interesting examples in the Dolomites that allows for a controversial interpretation of stratigraphy and tectonics. At the southern flank of Col Rodela a highly complex, repeated series of successions of the upper Permian Bellerophon Fm and the upper Ladinian "Caotico eterogeneo" are present. It is one of the areas, where ca. 30 years ago the idea of Middle Triassic compressional or transpressional tectonics with folding and overthrusting was born (e.g. Pisa et al., 1980, Castellarin et al., 1982, 1988, Doglioni, 1987). According to these authors this tectonic model is essentially based on two field observations: (1) at Col Rodela the tectonic sheet stacks are sealed by the undisturbed upper Ladinian Marmolada Conglomerate, and (2) in the Valle di San Nicolò south of Col Rodela the evaporitic Bellerophon Fm is strongly folded and cross-cut by volcanic dikes. Therefore, the folds, which were believed to result from compressional tectonics, predate the volcanic event.

But ca. 20 years later, Castellarin et al. (1998, 2004) abandoned the model of Ladinian compressional tectonics at Col Rodela and re-interpreted the entire sheet stack as a diapiric mélange in connection with the formation of breccias and megabreccias

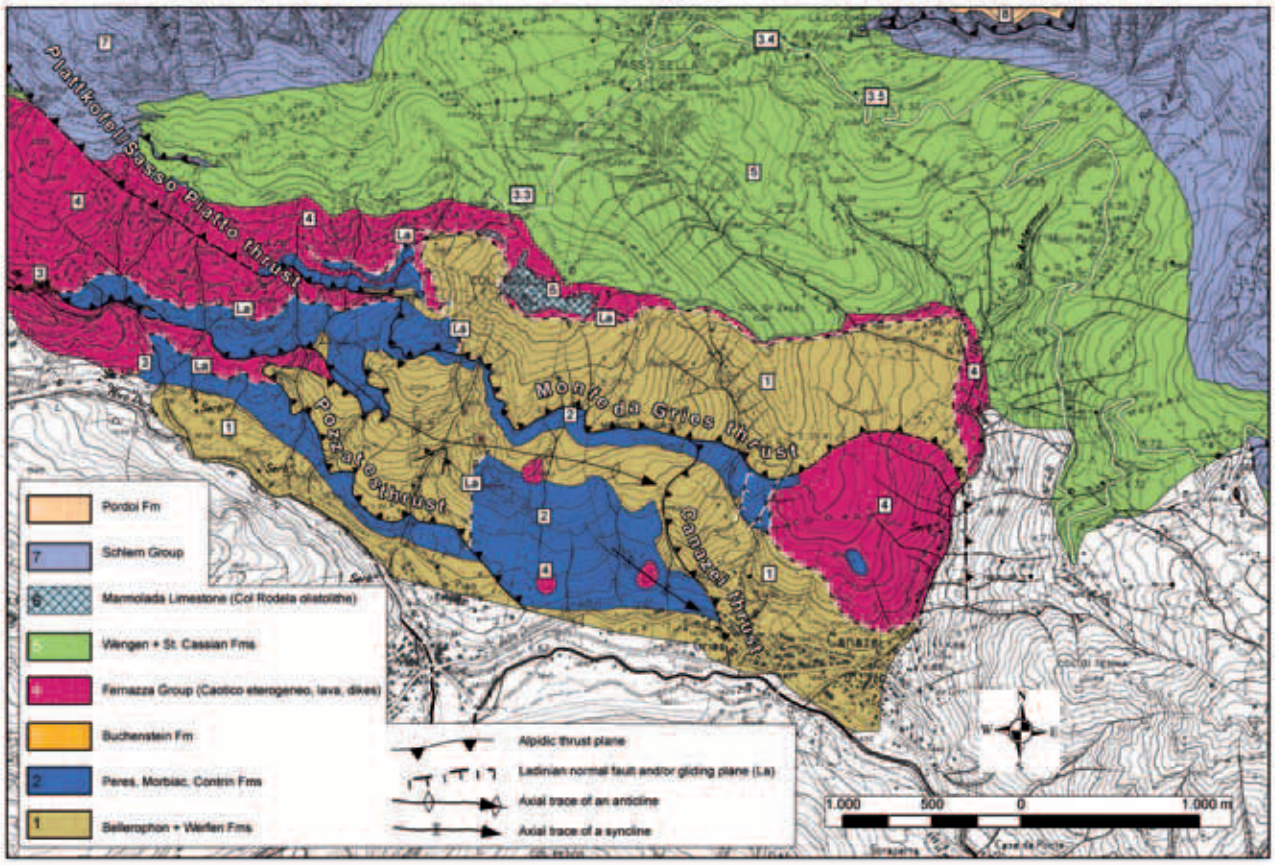

Fig. 22: Simplified tectonic map of the area between Canazei (Val di Fassa) and Col Rodela, based on the Geologische Karte der Westlichen Dolomiten 1:25.000 (2007). Tectonic repetition of the stratigraphic succession is caused by a two-phased alpine, an early and a late Dinaric deformation phase.

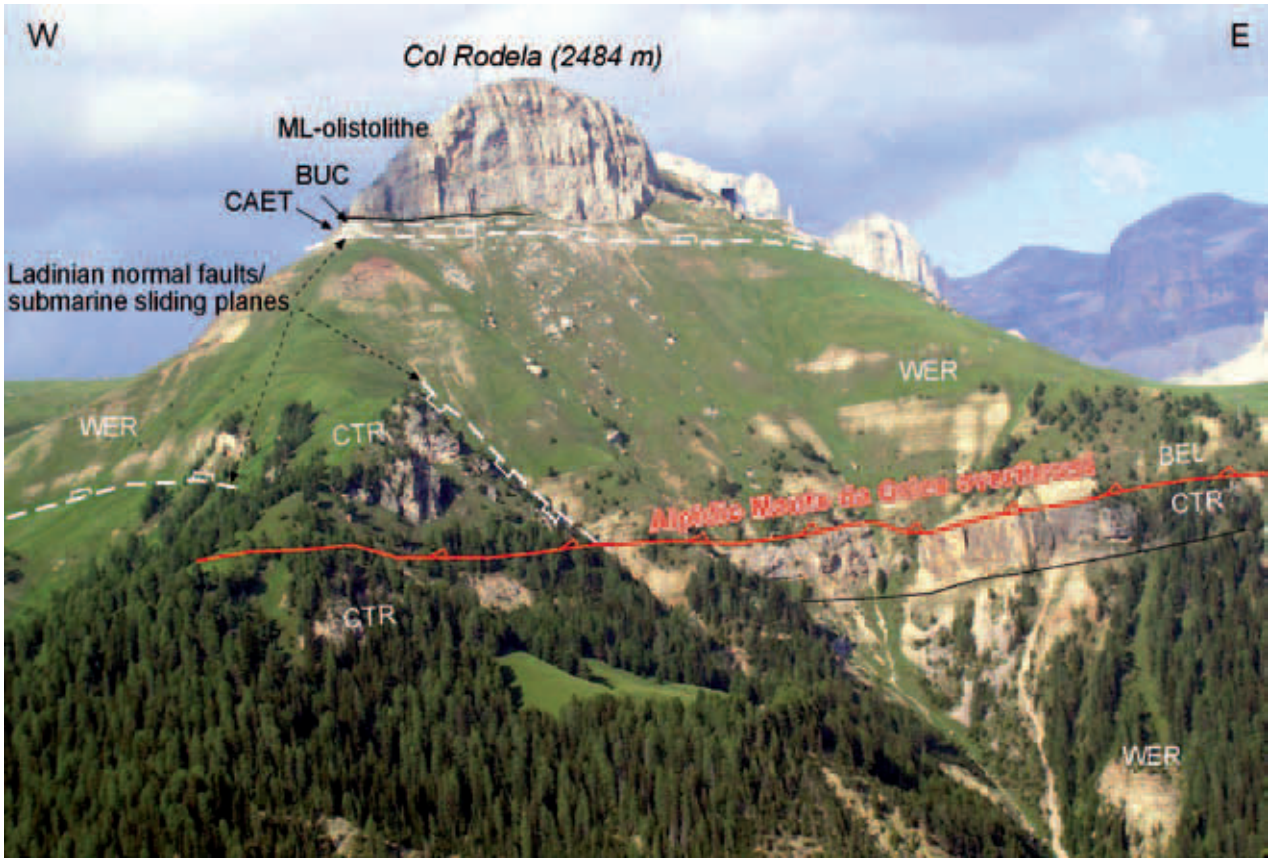

Fig. 23: Panoramic view of the southern flank of Col Rodela with outline of the most important tectonic structures. BEL = Bellerophon Fm, WER = Werfen Fm, CTR = Contrin Fm, CAET = "Caotico eterogeneo", BUC = Buchenstein Fm, ML = Marmolada Limestone (olistolithe).

of the "Caotico eterogeneo". Only extensional faults were regarded to represent Ladinian faults.

In the course of our geologic mapping project of the Western Dolomites also the area between Campitello and Col Rodela has been mapped again (Geologische Karte der Westlichen Dolomiten, 2007). Based on these new field data we reached the following conclusions: (1) confirmation of various Ladinian, synsedimentary normal faults with formation of the "Caotico eterogeneo" and (2) two-phase alpidic compressional tectonics with folding and thrust structures (Fig. 22).

Stop 3.3 – August-Friedrich-Hütte

This stop offers a good view to the N- and W-side of Col Rodela and invites the visitor to discuss its tectono-stratigraphic setting. The Col Rodela (2484 m) itself consists of a ca. 100 m thick remnant of Anisian-Ladinian reef slope limestone (Marmolada limestone) with some meter thick coeval basinal sediments (Buchenstein Fm) at its base (Figs. 23, 24). This reef-slope-basin pair is underlain by some meter thick polymict breccias of the "Caotico eterogeno", which themselves rest on the Lower Triassic Campill Member (Werfen Formation). The "Caotico eterogeneo" essentially consists of submarine scarp megabreccias and mass flow deposits. The Marmolada limestone of Col Rodela is a giant block inside the "Caotico eterogeneo" (Mutschlechner, 1935, Pisa et al., 1980, Bosellini et al., 1982, Castellarin et al., 1988, 1998, 2004). The entire succession is overlain by upper Ladinain lavas breccias, lavas and by the Marmolada Conglomerate (Wengen Formation) and dips with ca. 15–30° towards the NE. The boundary surface between the Campill Mb. and the breccias of the "Caotico eterogeneo" is interpreted herein as a Ladinian extensional fault or as a submarine sliding plane, respectively (Fig. 23). The stratigraphic loss at this boundary includes the Anisian conglomerates (Peres Fm) and the above following transgressive deposits of the Morbiac and Contrin Formations with a total thickness of about 100 m. Since the bounda-

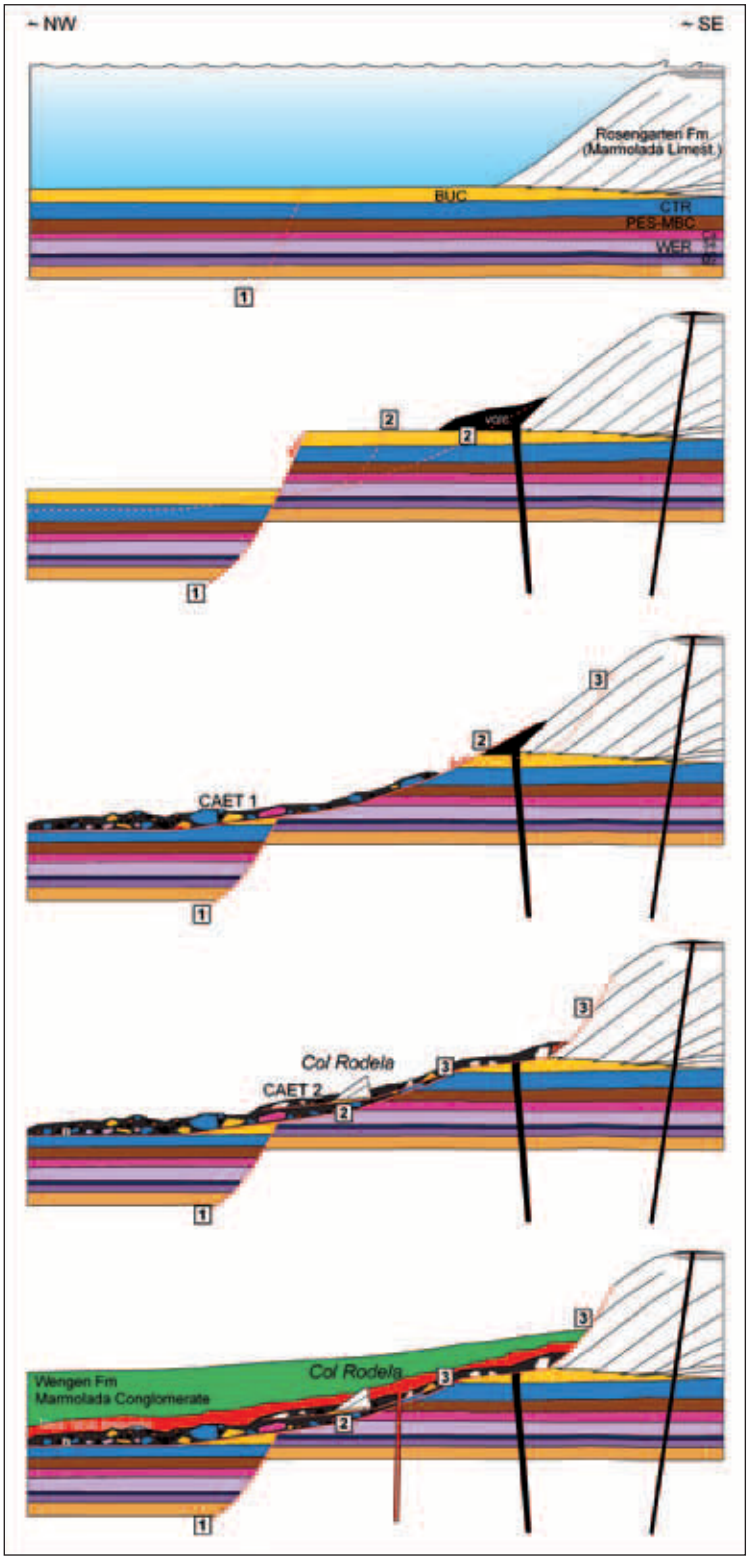

Fig. 24: Schematic model for the development of the "Caotico eterogeneo" for the area of Col Rodela during the Late Ladinian. The formation of breccias and megabreccias with reworking of sediments down to the Werfen Fm requires multiple extensional tectonic processes with steep and flat lying normal faults and/or gliding planes in connection with the volcanic activity. The breccias and megabreccias resulted essentially from submarine mass flow deposits. The presence of Ladinian normal faults combined with a complex stratigraphic succession of the "Caotico eterogeneo" with local olistoliths complicates the interpretation of the succession at the southern flank of Col Rodela. Alpidic thrust planes cut through various stratigraphic levels and younger rocks, which were downfaulted during the late Ladinian, may have been thrusted over older rocks during the alpine (Dinaric) deformation.

ry surface between the Campill Mb and the "Caotico eterogeneo" is a rather stratiform surface over considerable distances, the dip angle of the inferred Ladinian extensional fault or submarine sliding planes, must have been very gentle or nearly horizontal, at least in the surroundings of Col Rodela (Fig. 24). However, further to the N/NW, another steep normal fault must have existed in order to create the necessary space for the submarine gliding mass. This extensional tectonic process was multiphased and obviously related to the contemporaneous basic volcanism/magmatism in the central western Dolomites (Val di Fassa, Gröden/Val Gardena). The breccias and megabreccias of the "Caotico eterogeneo" with reworked clasts and blocks of Lower Triassic to Ladinian successions including reworked volcanic clasts are the response to this volcano-tectonics.

Alpine tectonic deformation

The repetitions of the sedimentary successions at the southern flank of Col Rodela are interpreted herein as a two phased Dinaric (Paleogene) WSW and SW directed thrust tectonics and folding. The new mapping (Fig. 22) shows three slices, the Campitello slice in the footwall, the Elbetina slice in the middle and the Rodela slice in the hanging wall. All three slices comprise incomplete sequences spanning from Bellerophon Fm, operating as lower detachment, to the Contrin Fm and the heterogenous Fernazza Group ("Caotico eterogeneo"). The thicknesses are variable due to Upper Anisian and Ladinian normal faulting and erosion. The Pozzates thrust with the Canazei branch thrust are interpreted as early Dinaric top to the WSW thrust planes which were folded subsequently by the late Dinaric SW–NE compression. In the roof of the antiformal deformed slice stack the Monte da Gries thrust brings up the Rodela slice. Due to Ladinian normal faulting, volcanic rocks of the footwall slice are overthrusted by similar volcanoclastic sequences in the hangingwall Rodela slice above Canazei. Therefore it is difficult to recognize the trace of the thrust plane toward the SE. The whole duplex structure is gently dipping to the E and disappears therefore below the thick sequence of the Fernazza Group, Wengen and St. Cassian Fms to the east of Canazei.

Stop 3.4 – Sella Pass

At this stop the facies interfingering in the basinal deposits (Wengen and St. Cassian Fms) as well as the W-dipping clinoforms of the Sella platform can be observed. The basinal deposits are characterized by a alternation of volcaniclastic and carbonate dominated successions (Fig. 25). The entire succession has been described by Bosellini & Neri (1991) and Mastandrea et al. (1997). The typical dark coloured marls, shales, sandstones and fine conglomerates with typical intercalated Cipit boulders of the Wengen Fm are replaced upsection by beige marls and light coloured calcarenites of the St. Cassian Fm. direct at the Hotel Maria Flora. This carbonate rich interval is about 40 m thick and is again covered by volcaniclastic sandstones and conglomerates of the Wengen Fm, ca. 50 m thick; this clastic interval is overlain essentially by calcarenites, rudstones and breccia beds of the prograding platform. This upper part of the St. Cassian Fm contains one more volcaniclastic layer, ca. 2 m thickness, which occurs just below the "Locomotiva" (Fig. 25). This lithofacies variation in the basin is the response to a different amount of clastic input derived from a volcanic hinterland and carbonate grains that were exported by the producing carbonate platform. This variation in sediment input to the basins may be governed by sea-level fluctuations, climatic or tectonic processes that resulted in the interfingering between Wengen and St. Cassian Fm. The final dominance of light coloured marls and calcarenites of the St. Cassian Fm goes hand in hand with the complete flooding of the debris delivering volcanic island, supposed to be located in the area west of Marmolada.

The W-dipping clinoforms of the Cassian Dolomite (Selladolomite Subgroup) are distinctly flattening out towards the basin and their dip angle decreases in the progradational direction from about 30° in the Val Lasties to 20° at the Sella towers (Kenter, 1990). The topsets are only 10–20 m thick; the transition zone to the steeply dipping clinoforms is rather massive to structureless.

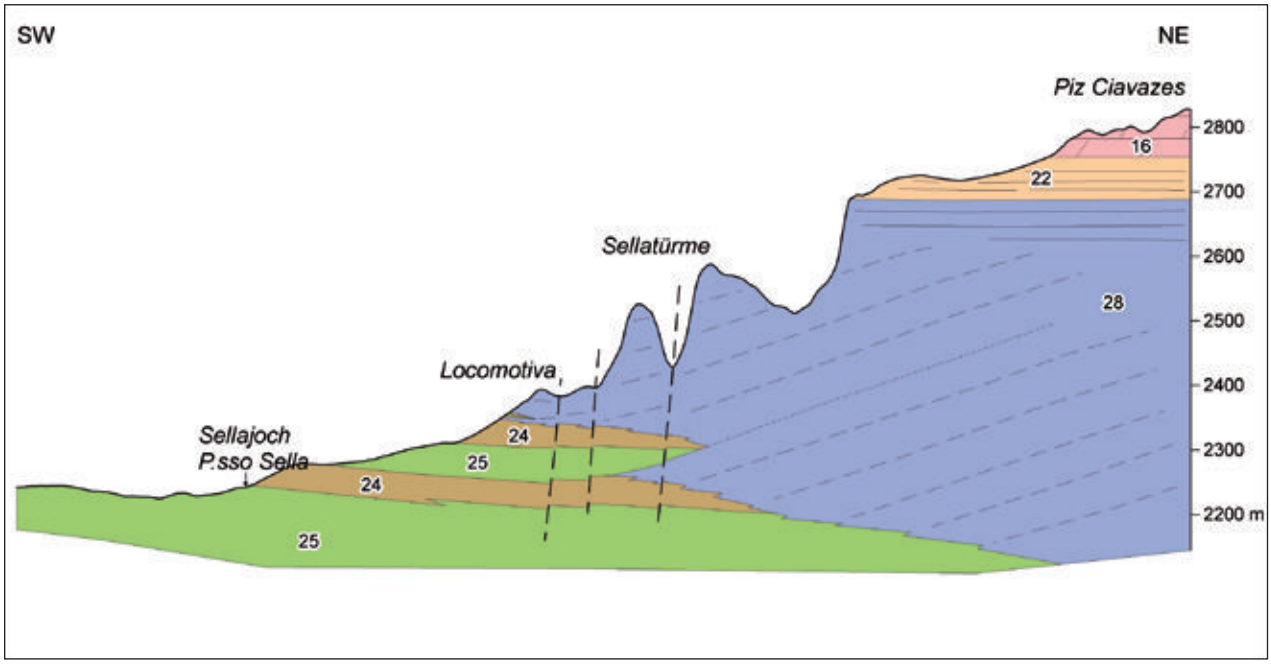

Fig. 25: Interpretative cross section between Piz Ciavaces and Passo Sella. The subdivision of the platform and slope deposits into the Rosszähne Fm and Cassian Dolomite, such as at the Grödner Joch/Passo Gardena, is not possible here. Therefore the term Selladolomite-Subgroup is used. The two-fold repetition of the Wengen and St. Cassian Fms originates from the different input of carbonate vs. volcaniclastic material into the basin. 25 = Wengen Fm (incl. Marmolada Conglomerate), 24 = St. Cassian Fm, 28 = Selladolomite Subgroup, 22 = Pordoi Fm, 16 = Hauptdolomit/Dolomia Principale.

Stop 3.5 – road curve just below the Sella Pass

This stop offers an excellent panoramic view of the WNW-exposed wall of Sass Pordoi, shows topsets and clinoforms of the Selladolomite Subgroup, and gives some insights into the nucleus of the Sella platform in the Val Lasties. In addition, the thinning out of the Pordoi Fm towards the centre of the platform, the overlying stratified Hauptdolomite as well as the youngest sediments at Piz Boè can be observed.

DAY 4

Stratigraphy and tectonics at the southern side of the Sella Group

Excursion route

This day is dedicated to the general geology at the Pordoi Pass itself and to the tectonic deformation at the summit Piz Boè (3152 m). From the Pordoi Pass we ascent to Sas Pordoi by cable car, walk to the Piz Boè (3152 m), and turn back to Sas Pordoi und descend by cable car. The Sass Pordoi and Piz Boè offer one of the most spectacular panoramic views over the entire Dolomites.

Stop 4.1 – Pordoi Pass

The area of the Pordoi Pass represents a Carnian seaway between the S-prograding Sella platform flanks in the north and the N-prograding Sas Becè platform located in the south. Actually, the lowermost clinoforms of both platforms are separated by a narrow basin zone of ca. 330 m width only. This distance, however, probably was shortened by alpine, N-S-directed compressional tectonics (Fig. 26). Additionally, the NE-SW running sinistral strike slip fault of the Val de Mesdì passes just west of the Pordoi Pass and has caused the formation of intense fracture zones within the Cassian Dolomite. The basinal sediments of the St. Cassian Fm are rather badly exposed and consist of beige-brown marls and calcarenites and occasionally some Cipit boulders. Beds of the St. Cassian Fm dip ca. 20–30° towards the north as a result of the above mentioned alpine deformation. Therefore also the actual dip angle of clinoforms of Sas Becè is too steep with respect to their original

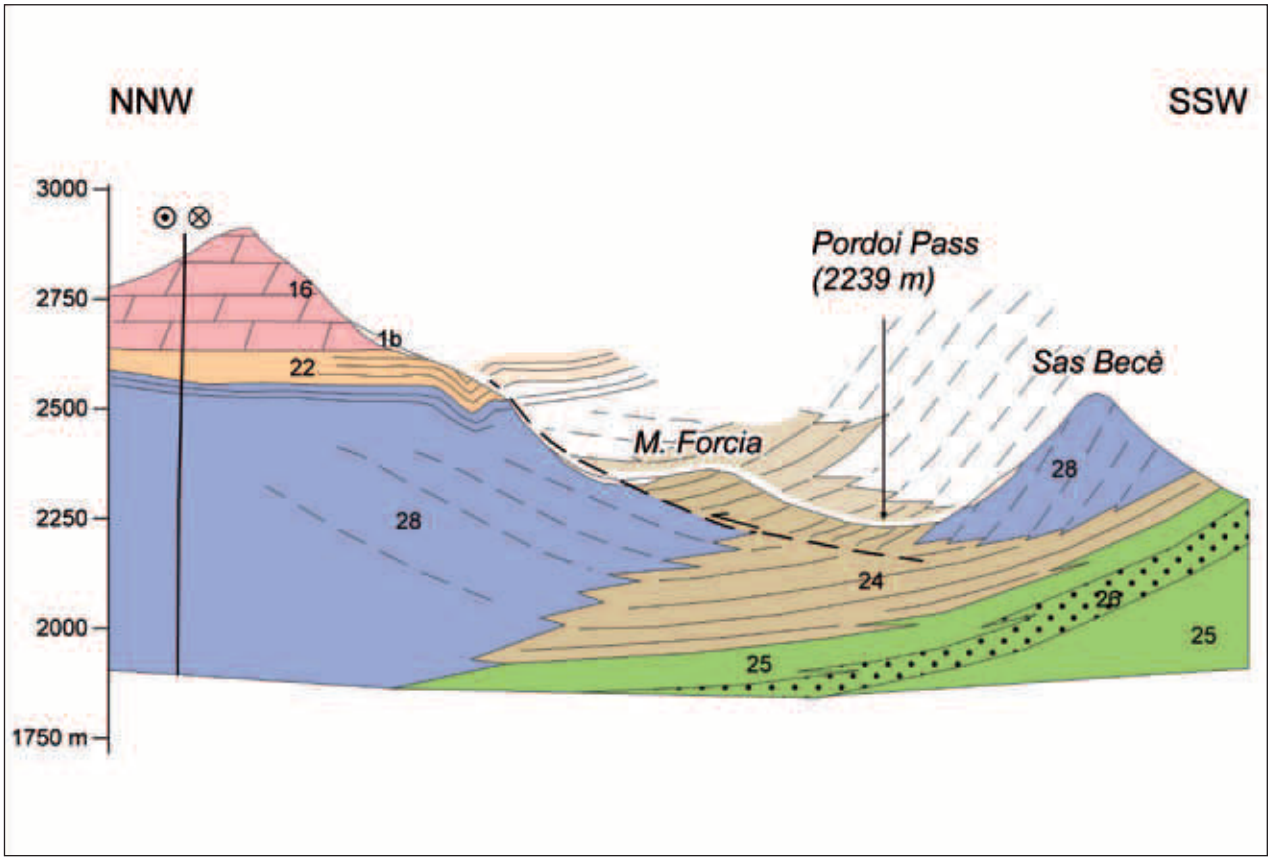

Fig. 26: Interpretative N-S cross section across Passo Pordoi. See text for explanation. 28 = Selladolomite Subgroup, 26 = Marmolada Conglomerate, 25 = Wengen Fm,, 24 = St. Cassian Fm, 22 = Pordoi Fm, 16 = Hauptdolomit/Dolomia Principale, 1b = talus deposits.

depositional angle. North of the Pordoi Pass, the basinal sediments of the St. Cassian Fm cover the entire area to the M. Forcia (2356 m). This is the highest point with basinal sediments at the S-side of the Sella platform, but unfortunately, the contact with the above lying platform dolomites is not exposed. The outcrop at M. Forcia is located about 140 m higher than the interfingering zone between clinoforms and basinal sediments exposed NW and ENE of the Pordoi Pass. This difference in height can been explained in two ways: (1) an onlap geometry of the St. Cassian Fm onto the clinoforms during standstill of platform growth and thus basin filling or (2) N-vergent overthrusting of the St. Cassian Fm, possibly over the S-dipping clinoforms. Based on the actual state of knowledge, we prefer a combination of both mechanisms (Fig. 26).

The ascent to Sas Pordoi by cable car offers unique views on the platform geometry with steep clinoforms and topsets as well as the sharply overlying Pordoi Fm and the Hauptdolomit/Dolomia Principale.

Stop 4.2 – Sas Pordoi and walk to Piz Boè

The spectacular panoramic view at Sas Pordoi (2950 m) enables to see most of the prominent Triassic carbonate platforms in the Dolomites. Along the trail to Piz Boè, the Norian Hauptdolomite with its typical peritidal cyclothemes can be observed. The basic cycles include a subtidal unit of dolomicrites with gastropods and megalodontid bivalves, an intertidal unit with laminated, stromatholitic layers with fenestral fabrics and bird's eyes, and, occasionally, a thin supratidal unit composed of teepee structures, intraclastic breccias, desiccation cracks and greenish dolomitized mudstones. In the upper part of the Hauptdolomit the frequency of intraclast breccias and subaerial exposure surfaces increases. At the base of the overlying Dachstein Limestone a distinct level, ca. 80 cm thick, of intraclast breccias with black pebbles is present. The Dachstein Limestone is about 40 m thick and consists of some decimeter thick calcareous beds interbedded with green marls.

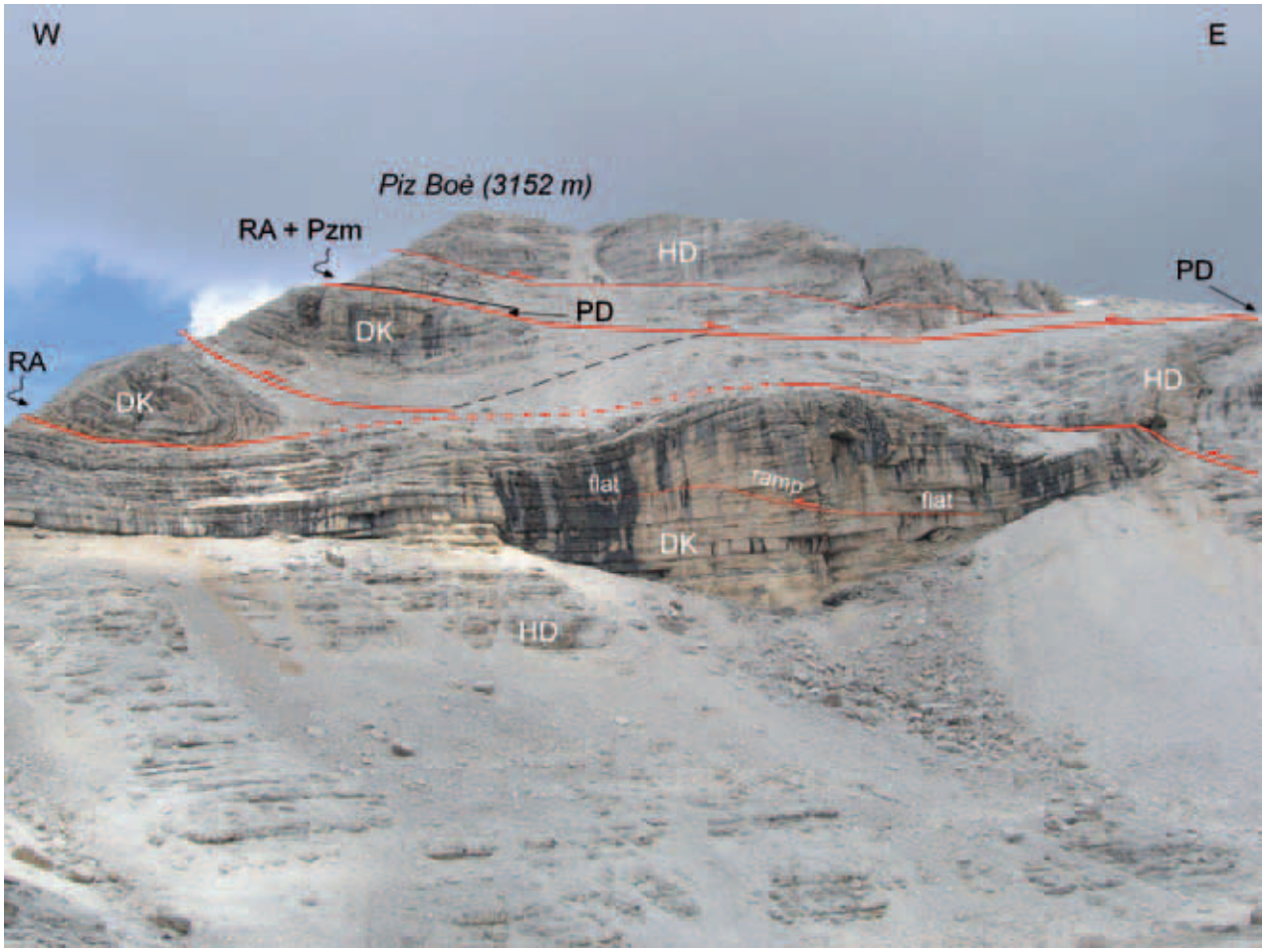

Fig. 27: Foto and line drawings of the southern flank at Piz Boè showing a stack of W vergent thrust slices. PD = Pordoi Fm, HD = Hauptdolomite, DK = Dachstein Limestone, RA = Rosso Ammonitico, Pzm = Puez Marls.

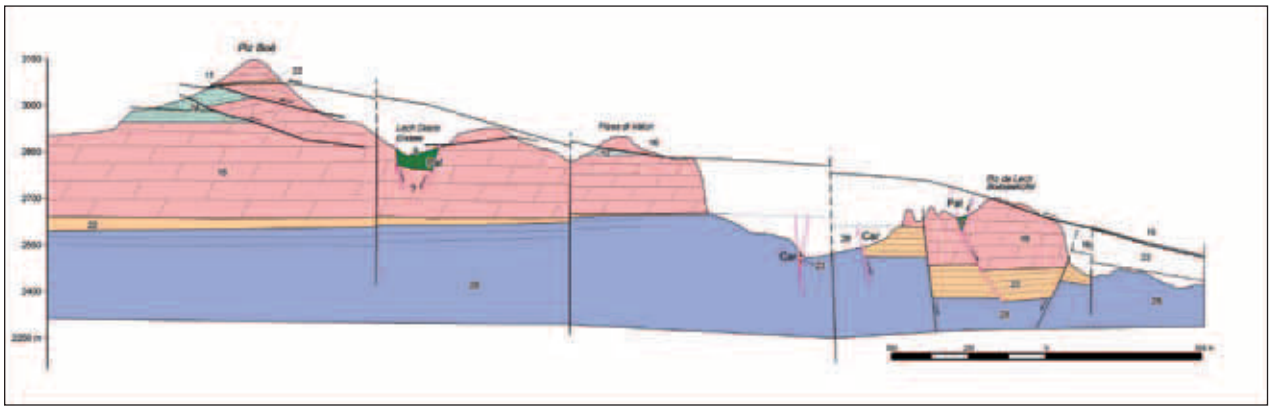

Fig. 28: Geologic cross section of the Piz Boè-Piz da Lech overthrust sub-parallel to the Dinaric NE-SW directed compression. The footwall is dissected by numerous steeply dipping normal faults of Carnian (Car) and late Cretaceous?-Paleogene (Pal) age associated with the formation of graben structures. Note the strong thickness variation of the Carnian Pordoi Fm ("Raibl beds"). At Pizes dl Valun the thickness of the Hauptdolomit/Dolomia Principale is distinctly reduced due to an erosional surface of probably Jurassic age. Based on this cross section the transport width of the uppermost slice of Hauptdolomit from the eastern side of Piz da Lech to Piz Boè can estimated to be at least 3 km.
28 = Selladolomite Subgroup (= Cassian Dolomite in the present case), 22 = Pordoi Fm, 23 = breccias (Pordoi Fm), 16 = Hauptdolomit/ Dolomia Principale, 14 = Dachstein Limestone, 12 = Gardenacia Fm (breccias, dolosparites), 11 = Rosso Ammonitico, 9 = Puez Marls.

The succession was described in detail by Bosellini & Broglio Loriga (1965), and contains locally abundant foraminifera, among others the age diagnostic *Triasina hantkeni* (Maizon) for the late Triassic (Rhaetian).

Piz Boè summit thrust – some general remarks

The thrust structures at the summit of the Sella Group, the so-called "Gipfelüberschiebungen" (= summit thrust) at Piz Boè, were described already 100 years ago by Ogilvie Gordon (1910). Generally spoken, several slices of Hauptdolomit/Dolomia Principale are thrusted over the Rhaetian Dachstein Limestone, the Jurassic Rosso Ammonitico and the Cretaceous Puez Marls. A first detailed geological map and description of these structures was presented by Reithofer (1928). Doglioni (1985, 1990) re-interpreted the thrust structures by applying modern structural analyses as "Klippen" of an eroded, WSW-directed Dinaric overthrust in a ramp-flat system. Most of the hanging wall of the ramp at the eastern slope of the Sella is now eroded. Doglioni (1990) presented a detailed geological map of the Piz Boè area and calculated a total shortening by the overthrusts of ca. 0.7 km based on balanced cross sections. According to the author the thrust plane is irregular along the strike and shows lateral and oblique ramps. Along these ramps fold-bend folding is common with ENE to E-W trending axes. As such, these fold-bend fold axes trend in the direction of the maximum, Dinaric compression (ENE-WSW) and should not be confused with another perpendicular tectonic phase (Doglioni, 1990).

Based on our geological mapping we agree mostly with the observations and interpretations made by Doglioni (1985, 1990), but question some of his cross sections, since he did not recognize or neglected the presence of slices of the Pordoi Fm ("Raibl beds") at the base of the ENE dipping, main thrust plane.

Stop 4.3 – Southern flank of Piz Boè

From this viewpoint some of the main tectonic structures can be observed: the Piz Boè overthrust consist of several (3–4) thrust planes, which are clearly related to the WSW to SW directed, Dinaric compression. A classical ramp-flat geometry of the thrust plane as well as an overturned, NW-SE trending syncline in the Dachstein Limestone is well visible (Fig. 27, see also Doglioni, 1985, 1990). The presence of slices of the Pordoi Fm at the base of the overthrusted Hauptdolomit/Dolomia Principale wedge suggests that the basal shear plane of the main thrust plane is located within the Pordoi Formation further to the east – an area, which today is completely eroded away (Fig. 28). Interestingly, none of such slices of the Pordoi Fm are present along this Dinaric thrust plane at Piz da Lec, which is the prolongation of the Piz Boè overthrust to the NE (Doglioni, 1985, 1990; see Fig. 28). Thus we assume that the shortening along of the Piz Boè summit thrust is by far greater than the calculated 0.7 km of Doglioni (1990). At Piz da Lac, the Dinaric thrust plane shows a distinct ramp-flat geometry within the Hauptdolomit/Dolomia Principale and cuts an older, ca. N-S trending graben structure in the Hauptdolomit/Dolomia Principale with down faulted Cretacous Puez Marls (Doglioni, 1992). A similar graben structure with down faulted Puez Marls crops out at the Eissee/Lago Gelato at the E-side of Piz Boè. At the eastern flank of Piz Boè, Dinaric thrust planes and intense folding of the Jurassic-Cretaceous sediments are well developed between Cresta Strenta and Piz Lech Dlace/Eisseespitze.

Stop 4.4 – Piz Boè (3152 m)

The summit of the Sella Group offers a unique panoramic view over the entire Dolomites and some more insights on the complex tectonic structures on the eastern side of Piz Boè.

Acknowledgements

Thanks to John Reijmer (VU University Amsterdam and TU Delft) for critically reading the text and Karl Krainer (Univ. Innsbruck) for editorial handling.

References

Aigner, T. (1985): Storm depositional systems. - Lectures Notes in Earth Sciences 3, 175 p, Springer.

Bargossi, G.M., Rottura, A., Vernia, L., Visonà, D. & Tranne, C.A. (1998): Guida all'escursione sul Distretto Vulcanico Atesino e sulle plutoniti di Bressanone-Chiusa e Cima d'Asta. - Mem. Soc. Geol. It., 53: 23-41, Roma.

Barth, S., Oberli, F., Meier, M., Blattner, P., Bargossi, G. M., & Di Battisti, G. (1993): The evolution of a calc-alcaline basic to silicic magma system: geochemical and Rb-Sr, Sm-Nd, and 18O/16O isotopic evidence from the late Hercynian Atesina-Cima d'Asta volcanic-plutonic complex, Northern Italy. – Geochim. Cosmochim. Acta 57: 4285-4300.

Bechstädt, T. & Brandner, R. (1970): Das Anis zwischen St. Vigil und dem Höhlensteintal (Pragser und Olanger Dolomiten, Südtirol). - Festband d. Geol. Inst., 300-Jahr-Feier Univ. Innsbruck, 9-101, Innsbruck.

Bertotti, G., Picotti, V., Bernoulli, D. & Castellarin, A. (1993): From rifting to drifting: Tectonic evolution of the South-Alpine upper crust from the Triassic tot he Early Cretaceous. - Sedimentary Geology, 86: 53-76, doi: 10.1016/0037-0738(93)90133-P.

Bond, D.P.G. & Wignall, P.B. (2010): Pyrite framboid study of marine Permian–Triassic boundary sections: A complex anoxic event and its relationship to contemporaneous mass extinction. - GSA Bulletin, 122: 1265-1279.

Bosellini, A. (1968): Paleogeologia pre-anisica delle Dolomiti centrosettentrionali. - Atti Accad. Naz. Lincei, Mem. Cl. Sci. Fis. Mat. Nat., Sez. 9 (8): 1–33.

Bosellini, A. (1982): Geologia dei Passi dolomitici circostanti il Gruppo di Sella. - In: Castellarin, A. & Vai. G.B. (Eds) Guida alla Geologia del Sudalpino centro-orientale. Guide geologiche regionali della Soc. Geol. It., 267-272, Bologna.

Bosellini, A. (1984): Progradation geometries of carbonate platforms: example from the Triassic of the Dolomites, Northern Italy. - Sedimentology, 32:1-24.

Bosellini (1991): Geology of the Dolomites. An introduction. - Dolomieu Conference on Carbonate Platforms and Dolomitization. Ortisei (Italy), 43 pp.

Bosellini, A. (1996): Geologia delle Dolomiti. - Athesia, 192 pp, Bozen.

Bosellini, A. & Broglio Loriga, C. (1965): Gli „Strati a *Triasina*" nel Gruppo di Sella (Dolomiti Occidentali). - Mem. Geol. Pal. Univ. Ferrara, Fasc. II, N. 6/1: 159-190, Ferrara.

Bosellini, A. & Neri, C. (1991): The Sella Platform (Upper Triassic, Dolomites). - Dolomieu Conference on Carbonate Platforms and Dolomitization, Guidebook Excursion B, 30 pp, Ortisei (Italy).

Bosellini, A., Castellarin, A., Doglioni, C., Guy, F., Lucchini, F., Perri Cristina, M., Rossi, P.L., Simboli, G. & Sommavilla, E. (1982): Magmatismo e tettonica nel Trias delle Dolomiti. - In: Castellarin, A. & Vai, G.B. (Eds) Guida alla Geologia del Sudalpino Centro-Orientale. Soc. Geolog. Italiana, 189-210, Bologna

Brack, P., & Rieber, H. (1993): Towards a better definition of the Anisian/Ladinian boundary: new biostratigraphic data and correlations of boundary sections from the Southern Alps. – Eclogae Geol. Helv., 86 (2): 415-527.

Brack, P., Rieber, H. & Nicora, A. & Mundil, R. (2005): The Global boundary Stratotype Section and Point (GSSP) of the Ladinian Stage (Middle Triassic) at Bagolino (Southern Alps, Northern Italy) and its implications for the Triassic time scale. - Episodes, 28 (4): 233-244.

Brandner, R. (1984): Meeresspiegelschwankungen und Tektonik in der Trias der NW-Tethys. - Jb. Geol. B.-A., 126: 435-475, Wien.

Brandner, R. (1988): The Permian-Triassic Boundary in the Dolomites (Southern Alps, Italy), San Antonio Section. - Ber. Geol. B.-A., 15: 49-56, Wien.

Brandner, R. (1991): Geological Setting and Stratigraphy of the Schlern-Rosengarten Buildup and Seiser Alm Basin. - In: Brandner, R., Flügel, E., Koch, R. & Yose, L.A (Eds.) The Northern Margin of the Schlern/Sciliar-Rosengarten/Catinaccio Platform. Dolomieu Conference on Carbonate Platforms and Dolomitization, Guidebook Excursion A, Ortisei (Italy), 61 pp.

Brandner, R. & Keim, L. (2011): Geotrail Bula - Pufels - Bulla. - Amt für Geologie & Baustoffprüfung/Ufficio Geologia e prove materiali, Autonome Provinz Bozen-Südtirol/Provincia Autonoma di Bolzano-Alto Adige, 44 pp.

Brandner, R., Flügel, E. & Senowbari-Daryan, B. (1991): Biotic and microfacies criteria of carbonate slope builders: implications for the reconstruction of source areas (Middle Triassic: Mahlknecht Cliff, Dolomites). - Facies, 25: 279-296, Erlangen.

Brandner, R., Gruber, A. & Keim, L. (2007): Geologie der Westlichen Dolomiten: von der Geburt der Neotethys im Perm zu Karbonatplattformen, Becken und Vulkaniten der Trias. Geo.Alp, 4: 95-121, Innsbruck-Bozen.

Brandner, R., Horaceck, M., Keim, L. & Scholger, R. (2009): The Pufels/Bulla road section: deciphering environmental changes across the Permian-Triassic to the Olenekian by integrated litho-, magneto- and isotope stratigraphy. A field trip guide. - Geo. Alp, 6: 116-132, Innsbruck-Bozen.

Broglio Loriga, C., Masetti, D. & Neri, C. (1983): La Formazione di Werfen (Scitico) delle Dolomiti occidentali: sedimentologia e biostratigrafia. - Riv. Ital. Paleont., 88 (4): 501-598, Milano.

Broglio Loriga, C., Goczan, F., Haas, J., Lenner, K., Neri, C., Scheffer, A.O., Posenato, R., Szabo, I. & Mark, A.T. (1990): The Lower Triassic sequences of the Dolomites (Italy) and Trasnsdanubian Mid-Mountains (Hungary) and their correlation. - Mem. Sc. Geol. Padova, 42: 41-103, Padova.

Broglio Loriga, C., Cirilli, S., De Zanche, V., Di Bari, D., Gianolla, P., Laghi, G. F., Lowrie, W., Manfrin, S., Mastradrea, A., Mietto, P., Muttoni, G., Neri, C., Posenato, R., Reichichi, M., Rettori, R., & Roghi, G. (1999): The Prati di Stuores/Stuores Wiesen Section (Dolomites Italy): a candidate Global Stratotype Section and Point for the base of the Carnian stage. - Riv. It. Paleont. Strat., 105: 37-78, Milano

Brondi, A., Fuganti, A., Lunz, L., Mittempergher, M, Murara, G., Nardin, N., Nascimben, P., Perna, G., Rossi, D., Scudeler Baccelle, L., Sommavilla, E. & Zipoli, G. (1976): Commento al foglio geologico 027 Bolzanao, scala 1:50.000 (ed. 1973). - Studi Trent. Sc. Nat., 53: 109-218, Trento.

Carta Geol. d'Italia (1972): Servizio geologico d'Italia, Foglio 025 "Bolzano", 1:50000, Firenze.

Carta Geol. d'Italia (1977): Servizio geologico d'Italia, Foglio 028 "La Marmolada", 1:50000, Firenze.

Carta Geol. d'Italia (2007): ISPRA - Servizio geologico d'Italia, Foglio 026 "Appiano-Eppan", 1:50000, Roma.

Carta Geol. d'Italia (2010): ISPRA - Servizio geologico d'Italia, Foglio 013 "Merano-Meran", 1:50000, Roma.

Cassinis, G., Perotti, C.R. & Ronchi, A. (2011): Permian continental basins in the Southern Alps (Italy) and peri-mediterranean correlations. – Int. J. Earth Sc. (Geol. Rundschau), DOI 10.1007/s00531-011-0642-6.

Castellarin, A. & Cantelli, L. (2000): Neo-Alpine evolution of the Southern Eastern Alps: Journal of Geodynamics, 30: 251–274.

Castellarin, A., Guy, F. & Selli, L. (1982) Geologia dei dintorni del Passo di S. Nicolò e dalla Valle di Contrin (Dolomiti). – In: Castellarin, A. & Vai. G.B. (Eds) Guida alla Geologia del Sudalpino centro-orientale. Guide geologiche regionali della Soc. Geol. It., 231-242, Bologna.

Castellarin, A., Lucchini, F.A., Rossi, P.L., Selli, L. & Simboli, G. (1988): The Middle Triassic magmatic-tectonic arc development in the Southern Alps. - Tectonophysics, 146: 79-89.

Castellarin, A., Selli, L., Picotti, V. & Cantelli, L. (1998): Tettonismo e diapirismo medio triassico delle Dolomiti. - Mem. Soc. Geol. It., 53: 145-169, Roma.

Castellarin, A., Cantelli, L., Picotti, V. & Selli, L. (2004): Structure of the Italian Dolomites, partilally along the southern section of the Transalp profile. - 32nd International Geological Congress, Florence (Italy), Field Trip Guide Book – P54, 40 pp, Firenze.

Castellarin, A., Nicolich, R., Fantoni, R., Cantelli, L., Sella, M. & Selli, L. (2006): Structure of the lithosphere beneath the Eastern Alps (southern sector of the TRANSALP transect). - Tectonophysics, 414: 259-282.

Chuodens-Sánchez , V. de & González, L. A. (2009): Calcite and Aragonite precipitation under controlled instantaneous supersaturation: elucidating the role of $CaCO_3$ saturation state and Mg/Ca ratio on calcium carbonate polymorphism. – J. Sed. Res., 79: 363-376.

De Zanche, V. & Gianolla, P. (1995): Litostratigrafia al limite Ladinico-Carnico (Sudalpino orientale). Ann. Univ. Ferrara, Sci. Terra, 5 (suppl.): 41-48, Ferrara.

De Zanche, V., Gianolla, P., Mietto, P., Siorpaes, C. & Vail, P. R. (1993): Triassic sequence stratigraphy in the Dolomites (Italy). - Mem. Sci. Geol., 45: 1-27, Padova.

Di Battistini, G., Gallo, F., Riammetti, F. & Vernia, L. (1989) Permian Andesites from Val d'Isarco and Val di Funes volcanic sequence (Bolzano, northern Italy). Miner. Petrogr. Acta, 32: 133-147, Bologna.

Doglioni, C. (1985): The overthrusts in the Dolomites: ramp-flat systems. Eclog. Geol. Helv., 78: 335-350, Basel.

Doglioni C. (1987): Tectonics of the Dolomites (Southern Alps-Northern Italy). J. Struct. Geol., 9: 181-193.

Doglioni, C. (1990): Anatomy of an overthrust. Annales Tectonicae, 4: 68-82.

Doglioni, C. (1992): Relationships between Mesozoic extensional tectonics, stratigraphy and Alpine inversion in the Southern Alps. Eclog. Geol. Helv., 85: 105-126, Basel.

Farabegoli, E. & Perri, C. M. (1998): Permian/Triassic boundary and Early Triassic of the Bulla section (Southern Alps, Italy): lithostratigraphy, facies and conodont biostratigraphy. - Giornale di Geologia, 60 (Spec. Issue ECOS VII Southern Alps Field Trip Guidebook): 292-311.

Farabegoli, E., Perri, C. M. & Posenato, R. (2007): Environmental and biotic changes across the Permian-Triassic boundary in western Tethys: The Bulla parastratotype, Italy. - Global and Planetary Change, 55: 109-135.

Flügel, E. (1991) Environmental analysis of allochthonous carbonate blocks and autochthonous mounds at the northern margin of the Schlern-Rosengarten (Sciliar-Catinaccio) platform. - In: Brandner, R., Flügel, E., Koch, R. & Yose, L.A. (Eds) The Northern Margin of the Schlern/Sciliar-Rosengarten/Catinaccio Platform. Dolomieu Conference on Carbonate Platforms and Dolomitization, Guidebook Excursion A, 41-55 pp, Ortisei, Italy.

Froitzheim, N., Weber, S., Nagel, T. J., Ibele, T. & Furrer, H. (2011): Late Cretaceous extension overprinting a steep belt in the Northern Calcareous Alps (Schesaplana, Rätikon, Switzerland and Austria): Int. J. Earth Sci. (Geologische Rundschau), DOI 10.1007/s00531-011-0717-4.

Frizon de Lamotte, D., Raulin, C., Mouchot, N., Wrobel-Daveau, J. C., Blanpied, C., & Ringenbach, J.-C. (2011): The southernmost margin of the Tethys realm during the Mesozoic and Cenozoic: Initial geometry and timing of the inversion processes. – Tectonics, 30, TC3002, doi: 1029/2010TC002691.

Gawlick, H.-J., Frisch, W., Vecsei, A., Steiger, T. & Böhm, F. (1999): The change from rifting to thrusting in the Northern Calcareous Alps as recorded in Jurassic sediments. - Geologische Rundschau, 87: 644–657.

Geologische Karte der Westlichen Dolomiten 1:25.000. (2007): Autonome Provinz Bozen – Südtirol. - Amt für Geologie u. Baustoffprüfung, Bozen/Kardaun.

Gianolla, P., De Zanche, V. & Mietto, P. (1998): Triassic sequence stratigraphie in the Southern Alps (Northern Italy): definition of sequences and basin evolution. - SEPM Special Publication, 60: 719-747.

Hartkopf-Fröder, C. Wood, G.D. & Krainer, K. (2001): Palynology of the Permian Bolzano Volcanic Complex, Southern Alps, Italy, part 1: miospore preservation, quantitative spore color and quantitative fluorescence microscopy. In: Goodman, D.K. & Clarke, R.T. (Eds.) Proceedings of the IX International Palynological Congress, Houston, Texas, U.S.A., 1996. – Am. Ass. Strat. Palynolog. Found: 79-97.

Horacek, M., Brandner, R. & Abart, R. (2007a): Carbon isotope record of the P/T boundary and the Lower Triassic in the Southern Alps: evidence for rapid changes in storage of organic carbon; correlation with magnetostratigraphy and biostratigraphy. - Palaeogeography, Palaeoclimatology, Palaeoecology, 252: 347-354.

Horacek, M., Richoz, S., Brandner, R., Krystyn, L., Spötl, C. (2007b): Evidence for recurrent changes in Lower Triassic oceanic circulation of the Tethys: The $\delta^{13}C$ record from marine sections in Iran. - Palaeogeography, Palaeoclimatology, Palaeoecology, 252: 355-369.

Horacek, M., Povoden, E., Richoz, S. & Brandner, R. (2010): High-resolution carbon isotope changes, litho- and magnetostratigraphy across Permian-Triassic Boundary sections in the Dolomites, N-Italy. New constraints for global correlation. - Palaeogeography, Palaeoclimatology, Palaeoecology, 290: 58-64.

Hug, N. & Gaupp, R. (2006): Palaeogeographic reconstruction in red beds by means of genetically related correlation: results from the upper Zechstein (Late Permian). - Z. dt. Ges. Geowiss., 157(1): 107-120.

Keim, L. & Schlager, W. (1999): Automicrite Facies on Steep Slopes (Triassic, Dolomites, Italy). - Facies, 41: 15-26, Erlangen.

Keim, L. & Stingl, V. (2000): Lithostratigraphy and Facies architecture of the Oligocene conglomerates at Monte Parei (Fanes, Dolomites, Italy). – Riv. It. Strat. Paleont., 106: 123-132, Milano.

Keim, L. & Brandner, R. (2001): Facies interfingering and synsedimentary tectonics on late Ladinian-early Carnian carbonate platforms (Dolomites, Italy). - Int. J. Earth Sciences (Geol. Rundsch.), 90: 813-830.

Keim, L. & Schlager, W. (2001): Quantitative compositional analyses of a Triassic carbonate platform (Southern Alps, Italy). - Sediment. Geol., 139: 261–283.

Keim, L. & Neri, C. (2004): The Sella Platform. - In: Stefani, M., Brack, P., Gianolla, P., Keim, L., Maurer, F., Neri, C., Preto, N., Riva, A., Roghi, G. & Russo, F.: Triassic carbonate platforms of the Dolomites: carbonate production, relative sea-level fluctuations and the shaping of the depositional architecture. 32nd International Geological Congress, Florence (Italy), Field Trip Guide Book – P44, 25-33, Firenze.

Keim, L. & Roghi, G. (2006): The age of the Sella platform (Triassic, Dolomites): new insights from palynological studies. - Pangeo Austria, Innsbruck University Press, 140-141, Innsbruck.

Kenter, J.A.M. (1990): Carbonate platform flanks: slope angle and sediment fabric. - Sedimentology, 37: 777-794.

Korte, C. & Kozur, H. W. (2005): Carbon isotope stratigraphy across the Permian/Triassic boundary at Jolfa (NW-Iran), Peitlerkofel (Sas de Pütia, Sas de Putia), Pufels (Bula, Bulla), Tesero (all three Southern Alps, Italy) and Gerennavár (Bükk Mts., Hungary). - Journal of Alpine Geology/Mitt. Ges. Geol. Bergbaustud. Österr., 47: 119-135.

Korte, C., Kozur, H. W., Joachimsky, M. M., Strauss, H., Veizer, J. & Schwark, L. (2004): Carbon, sulfur, and strontium isotope records, organic geochemistry and biostratigraphy across the Permian/Triassic boundary in Abadeh, Iran. - Int. J. Earth Sci. (Geol. Rdsch.), 93: 565-581.

Korte, C., Kozur, H. W. & Veizer, J. (2005): $\delta^{13}C$ and $\delta^{18}O$ values of Triassic brachiopods and carbonate rocks as proxies for coeval seawater and palaeotemperature. - Palaeogeography, Palaeoclimatology, Palaeoecology, 226: 287-306.

Krainer, K. (1987): Zusammensetzung und fazielle Entwicklung des Alpinen Buntsandsteins und der Werfener Schichten im westlichen Drauzug (Kärnten/ Osttirol).- Jb. Geol. B.-A, 130: 61-91, Wien.

Krainer, K. (1989): Composition and evolution of Lower Permian molasse sediments (Ponte Gardena Conglomerate) at the base of the Bolzano Volcanic Complex, Southern Alps (N Italy). - N. Jb. Geol. Paläont. Mh., 7: 400-424, Stuttgart.

Krainer, K. Sanders, D. & Schaffhauser, M. (2009): Early Permian Shelf Margin Retreat and Carbonate Deposition, Zweikofel Massif, Carnic Alps (Austria). – Austrian Journal of Earth Sciences, 102/2: 134-148.

Krystyn, L. (1983) Das Epidaurus-Profil (Griechenland) – ein Beitrag zur Conodonten-Standardzonierung des tethyalen Ladin und Unterkarn. Schriftenr. Erdwiss. Komm. Österreich. Akad. Wiss., 5: 231-258.

Krystyn, L., Richoz, S. & Bhargava, O. N., (2007): The Induan-Olenekian Boundary (IOB) – an update of the candidate GSSP section M04. - Albertiana, 36: 33-45.

Leonardi, P. & Rossi D. (1957): La scogliera coralligena del Sella nelle Dolomiti Occidentali. - Ann. Univ. Ferrara, Sci. Terra, 3: 1-26, Ferrara.

Marocchi, M., Morelli, C., Mair, V., Klötzli, U. & Bargossi, G. M. (2008): Evolution of Large Silicic Magma Systems: New U-Pb Zircon Data on the NW Permian Athesian Volcanic Group (Southern Alps, Italy). - The Journal of Geology, 116: 480-498.

Mastandrea, A., Neri, C. & Russo, F. (1997): Conodont biostratigraphy of the S. Cassiano Formation surrounding the Sella Massif (Dolomites, Italy): implications for sequence stratigraphic models of the Triassic of the Southern Alps. - Riv. Ital. Paleont. Strat., 103: 39-52, Milano.

Maurer, F. (1999): Wachstumsanalyse einer mitteltriassischen Karbonatplattform in den westlichen Dolomiten (Südalpen). - Ecl. Geolog. Helv., 92: 361-378, Basel.

Mietto, P. & Manfrin, S. (1995): La successione delle faune ad ammonoidi al limite Ladinico-Carnico (Sudalpino, Italia). - Ann. Univ. Ferrara, 5 (Suppl.): 13-35, Ferrara.

Mietto, P., Manfrin, S., Preto, N. & Gianolla, P. (2008): Selected ammonoid fauna from Prati di

Stuores/Stuores Wiesen and related sections across the Ladinian-Carnian boundary (Southern Alps, Italy). - Riv. It. Strat. Paleont., 114 (3): 377-429, Milano.

Mojsisovics, E.M. von (1879): Die Dolomit-Riffe von Südtirol und Venetien: Beiträge zur Bildungsgeschichte der Alpen. - A. Hölder, 551 pp, Wien.

Morelli, C., Bargossi, G.M., Mair, V., Marocchi, M. & Moretti, A. (2007): The Lower Permian volcanics along the Etsch valley from Meran to Auer (Bozen). - Mitt. Österr. Miner. Ges., 153: 195-218.

Mostler, H. (1982): Bozener Quarzporphyr und Werfener Schichten. - In: Mostler, H. (Ed.), Exkursionsführer zur 4. Jahrestagung der Österreichischen Geologischen Gesellschaft, 43-79, Innsbruck.

Mundil, R., Pàlfi, J., Renne, P.R. & Brack, P. (2010): The Triassic timescale: new constraints and a review of geochronological data. - In: Lucas, S.G. (ed) The Triassic Timescale. Geol. Soc. London Spec. Publ., 334: 41-60, London.

Mutschlechner, G. (1935): Geologie der Langkofelgruppe. Jb. Geol. B-A, 85: 21-49, Wien.

Muttoni, G., Kent, D.V., Garzanti, E., Brack, P., Abrahamsen, N. & Gaetani, M. (2003): Early Permian Pangea „B" to Late Permian Pangea „A". - Earth and Planetary Science Letters, 215: 379-394.

Newton, R. J., Pevitt, E. L., Wignall, P.B. & Bottrell, S. H. (2004): Large shifts in the isotopic composition of seawater sulphate across the Permo-Triassic boundary in northern Italy. - Earth and Planetary Science Letters, 218: 331-345.

Ogilvie Gordon, M.M. (1910) Die Überschiebung am Gipfel des Sellamassivs in Südtirol. – Verh. der k. u. k. Geol. Reichsanst., Wien.

Perri, C. M. (1991): Conodont biostratigraphy of the Werfen Formation (Lower Triassic), Southern Alps, Italy. - Boll. Soc. Pal. Ital., 30/1: 23-45.

Pisa, G., Castellarin, A., Lucchini, F., Rossi, P.L., Simboli, G., Bosellini, A. and Sommavilla, E.

(1980): Middle Triassic magmatism in Southern Alps. I. A review of general data in the Dolomites. - Riv. Ital. Paleontol. Stratigr., 85: 1093-1110, Milano.

Porada, H. & Bouougri, H. (2007): Wrinkle structures – a critical review. - Earth Science Reviews, 81: 199-215.

Posenato, R. (2008): Global correlations of mid Early Triassic events: The Induan/Olenekian boundary in the Dolomites (Italy). - Earth Science Reviews, 91: 93-105.

Pruss, S. B., Bottjer, D. J., Corsetti, F. A. & Baud, A. (2006): A global marine sedimentary response to the end-Permian mass extenction: Examples from southern Turkey and western United States. - Earth Science Reviews, 78: 193-206.

Reithofer, O. (1928): Geologie der Sellagruppe (Südtiroler Dolomiten). - Jb. Geol. B.-A., 78: 529-580, Wien.

Richthofen, F. v. (1860): Geognostische Beschreibung der Umgebung von Predazzo, Sanct Cassian und der Seisser Alpe in Süd-Tirol. Perthes Gotha.

Sarg, J.F. (1988): Carbonate Sequence Stratigraphy. - In: C.K. Wilgus, B.S. Hastings, C.G.S.C,

Kendall, H.W. Posamentier, C.A. Ross & J.C. Van Wagoner (Eds) Sea level changes: an integrated approach. SEPM Spec. Publ. 42: 155-182.

Schlager, W. & Reijmer, J.J.G. (2009): Carbonate platform slopes of the Alpine Triassic and the Neogene - a comparison. – Austrian Journal of Earth Sciences, 102: 4-14, Vienna.

Schaltegger, U. & Brack, P. (2007): Crustal-scale magmatic systems during intracontinental strike-slip tectonics: U, Pb and Hf isotopic constraints from Permian magmatic rocks of the Southern Alps. - Int. J. Earth Sci (Geol Rundsch), 96: 1131-1151.

Schmid, S.M., Fügenschuh, B., Kissling, E. & Schuster, R. (2004): Tectonic map and overall architecture of the Alpine orogen. - Eclogae Geol. Helv., 97: 93-117.

Scholger, R., Mauritsch, H. J. & Brandner, R. (2000): Permian-Triassic boundary magnetostratigraphy from the Southern Alps (Italy). - Earth and Planetary Science Letters, 176: 495-508.

Selli, L. (1998): Il lineamento della Valsugana fra Trento e Cima d'Asta: cinematica neogenica ed eredità strutturali permo-mesozoiche nel quadro evolutivo del Subalpino Orientale (NE-Italia). - Mem. Soc. Geol. It., 53: 503-541, Roma.

Shaffer, G., Olsen, S. M. & Pederson, O. P. (2009): Long-term ocean oxygen depletion in response to carbon dioxide emissions from fossil fluids. - Nature Geoscience, 2: 105-109.

Stampfli, G.M. & Borel, G.D. (2002): A plate tectonic model for the Paleozoic and Mesozoic constrained by dynamic plate boundaries and restored synthetic oceanic isochrons. Earth and Planetary Science Letters, 196 (1): 17–33.

Szurlies, M. (2004): Magnetostratigraphy: the key to a global correlation of the classic Germanic Trias-case study Volpriehausen Formation (Middle Buntsandstein), Central Germany. - Earth and Planetary Science Letters, 227: 395-410.

Szurlies, M., Bachmann, G. H., Menning, M., Nowaczyk, N. R. & Käding, K. C. (2003): Magnetostratigraphy and high-resolution lithostratigraphy of the Permian-Triassic boundary interval in Central Germany. - Earth and Planetary Science Letters, 212: 263-278.

Venturini, C. (1991): Introduction to the geology of the Pramollo Basin (Carnic Alps) and its surroundings. - Giorn. Geologia, sr. 3, 53: 13-47.

Visonà, D., Fioretti, A. M., Poli, M. E., Zanferrari, A. & Fanning, M.(2007): U-Pb SHRIMP zircon dating of andesite from the Dolomite area (NE Italy): geochronological evidence for the early onset of Permian Volcanism in the eastern part oft he Southern Alps. - Swiss J. Geosci. 100: 313-324.

Wheeler, H. E. (1964): Baselevel, lithosphere Surface, and Time-Stratigraphy. - Geol. Soc. Amer. Bull., 75: 599-610.

Wignall, P. B. & Hallam, T. (1992): Anoxia as a cause of the Permian/Triassic mass extinction: facies evidence from northern Italy and the western United States. Palaeogeography, Palaeoclimatology, Palaeoecology 93: 21-46.

Yose, L.A. (1991): Sequence stratigraphy of mixed carbonate/volcaniclastic slope deposits flanking the Sciliar (Schlern) – Catinaccio buildup, Dolomites, Italy. - In: Brandner, R., Flügel, E., Koch, R. & Yose, L.A (Eds.) The Northern Margin of the Schlern/Sciliar-Rosengarten/Catinaccio Platform. Dolomieu Conference on Carbonate Platforms and Dolomitization, Guidebook Excursion A, Ortisei (Italy), 71-39 pp.

Manuscript submitted: 14.11.2011
Manuscript accepted: 17.11.2011

Geo.Alp, Vol. 8, S. 120–121, 2011

WORKSHOP ON THE CASSIAN BEDS (UPPER TRIASSIC)

28. - 29. Juli 2011
Naturmuseum Südtirol, Bozen

Extendend abstracts

Im Folgenden werden sieben erweiterte Kurzfassungen des Workshops abgedruckt.

Vom 28. bis 29. Juli 2011 fand im Naturmuseum Südtirol (Bozen) ein Workshop zu den Cassianer Schichten mit anschließender Exkursion auf den Stuores Wiesen südlich von St. Cassian (Hochabtei) statt. Die Organisation dieser Tagung lag in den Händen von Evelyn Kustatscher (Naturmuseum Südtirol), Lorenz Keim (Amt für Geologie & Baustoffprüfung, Autonome Provinz Bozen – Südtirol) und Piero Gianolla (Univ. Ferrara). Ziel des Workshops war es, die vielen Forschergruppen, die sich mit unterschiedlichsten Aspekten der Cassianer Schichten beschäftigen, an einen runden Tisch zu laden und möglicher Weise gemeinsame Projekte auszuarbeiten. Es nahmen 26 Geologen und Paläontologen aus sechs Ländern (Italien (16), Deutschland (6), Österreich (1), Polen (1), Holland (1) und Israel (1)) teil. Am Vormittag des 28. Juli fanden elf Vorträge und drei Posterpräsentationen statt, am Nachmittag wurde am runden Tisch über zukünftige Forschungsvorhaben zu den Cassianer Schichten diskutiert. Alle Beteiligen waren der Meinung, dass eine engere Zusammenarbeit zwischen Paläontologen, Stratigraphen und Sedimentologen nötig sei.
Die Exkursion am 29. Juli, die von P. Gianolla, A. Riva und M. Urlichs geleitet wurde, führte zu den klassischen Aufschlüssen der Cassianer Schichten an den Südabhängen der Stuores Wiesen, südlich von St. Cassian, Typlokalität der gleichnamigen Schichten und des von der International Commission on Stratigraphy ratifizierten GSSP der Ladin/Karn-Grenze. Nach lebhafter Diskussion der stratigraphischen Einordnung der Beckensedimente aus Vulkanoklastika, Kalk- und Mergelabfolgen (Wengen- vs. St.-Cassian-Formation) führte M. Urlichs (Stuttgart) zu seinen ab den 1970er Jahren detailliert studierten Fossilfundstellen der Cassianer Schichten. Viele dieser Fundstellen sind zwar von mäßiger Aufschlussqualität, liefern aber noch immer zahlreiche Fundstücke. Die Exkursionsteilnehmer suchten jedenfalls gemäß der „superficial sampling method" eifrig nach fossilen Kostbarkeiten.
Alle waren unisono der Meinung, dass die Schönheit und der geologische Aufbau der Dolomiten zu Recht mit der Aufnahme in die Liste des UNESCO-Weltnaturerbes belohnt worden seien.

Lorenz Keim und Evelyn Kustatscher

Fig. 1
Round-Table-Diskussion am Nachmittag im Naturmuseum Südtirol, Bozen.

Fig. 2
Erläuterungen von P. Gianolla zum Ladin/Karn-GSSP am Südhang der Stuores Wiesen (Provinz Belluno).

Fig. 3
Fossilsuche in den Cassianer Schichten, Stuores Wiesen (Hochabtei, Südtirol).

Geo.Alp, Vol. 8, S. 122–127, 2011

VERTEBRATE FAUNA FROM THE SAN CASSIANO FORMATION (EARLY CARNIAN) OF THE DOLOMITES REGION

Massimo Bernardi[1], Marco Avanzini[1] and Fabrizio Bizzarini[2]

With 3 Figures and 1 Table

[1] Museo delle Scienze, via Calepina 14, I-38122 Trento
[2] Museo Civico di Rovereto, Borgo S. Caterina 41, I-38068 Rovereto

1. Introduction

The basinal San Cassiano Formation (early Carnian) mainly consist of marls, micrites and oolitic-bioclastic calciturbidites. These sediments are heteropic with the prograding Cassian platforms and derive from the erosion of volcanic rocks and from the precipitation of carbonates exported from the platforms (Keim & Neri, 2005 and references therein).

Where the Formation is well represented, as in the area of Prati di Stuores (Stuores Wiesen), Sett Sass, Forcella Giau it has yielded an extraordinary invertebrate fossil fauna which has been studied since the XIX century (e.g., Münster, 1834). Being extremely diverse, and excellently preserved (aragonite is often still preserved in the thin shells) the San Cassiano invertebrate fauna is one of the best known of the whole Mesozoic (Fürsich & Wendt, 1977). This heavily contrasts with the paucity of vertebrate findings which is also highlighted by the almost complete absence of published papers on the topic (but see Boni, 1941, Bizzarini et al., 2001). Here we provide an updated check-list of historical and new vertebrate findings focusing on their bearing on the palaeoecology of San Cassiano Formation Biota.

Note that we are not considering the vertebrate remains that were found in the overlying Heiligkreuz Formation (mid-late Carnian) (e.g., Sirna et al., 1994; Bizzarini & Rottonara, 1997; Dalla Vecchia & Avanzini, 2002) among which is, most notably, the famous *Metoposaurus sanctecrucis* (Koken, 1913) despite the not always clear distinction between San Cassiano and Heiligkreuz formations in historical collections.

2. Vertebrate palaeontology

2.1 New findings

The new specimens described here have been collected near the Sief Pass (Badia Valley, Bolzano Province), just below and slightly East to the famous Richthofen Riff. The Carnian platforms are there clearly documented by the two main prograding carbonate systems: the Lower Cassian Dolomite, to which correspond the Richthofen Reef ridge, and the Upper Cassian Dolomite, which constitutes the Sett Sass. In the area of the Pass, above the Wengen (La Valle) volcanoclastic Formation, the San Cassiano Formation crops out. Although the specimens were not found in situ, the lithology of the matrix clearly suggests that the fossil bearing level is part of the San Cassiano Formation. In the outcrop, several bi-

oclastic calciruditic levels, bounded by finer-grained levels (possibly documenting turbiditic events) near the base of the Formation were identified as possible correspectives.

Systematic palaeontology

Class Chondrichthyes Huxley, 1880
Cohort Euselachii Hay, 1902
Superfamily Hybodontoidea Owen, 1846
Family Acrodontidae Casier, 1959
Genus *Acrodus* Agassiz, 1838

Acrodus sp. **(Fig. 1)**

The specimens are two domed, finely ornamented tooth crowns. Teeth are strongly arched in labial and lingual views. At least one lateral cusplet was clearly present although only half is preserved. A single, well marked longitudinal ridge runs across the crown. The crown is projected lingually. The ornamentation is finely reticulate. Crown is separated from the root by a band of vertical ridges. No expanded lingual torus is

Fig. 1: The two *Acrodus* sp. teeth found at the base of the Richthofen Riff, near the Sieff camp (BZ). *Acrodus* represent a new taxon for the San Cassiano association.

visible on the root. The root is high and perforate by numerous, randomly placed, foramina.

Studied teeth are very similar to those of other sharks such as *Acrononemus* Rieppel, 1982 or even *Asteracanthus* Agassiz 1837 and most of the characters that enable a clear distinction of these genera are found on the finspine and cranium. Nevertheless listed characters allow to confidently attribute the specimens to the genus *Acrodus* Agassiz, 1838. Given the fragmentary nature of the studied material we prefer to leave the determination in open nomenclature.

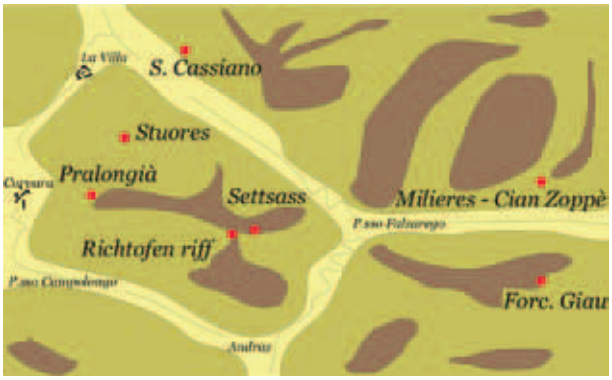

Fig. 2: Simplified location map of the fossiliferous outcrops (red dots) where vertebrate remains have been documented to date, Dolomites region, NE Italy.

2.2 Previous findings

The few studies listing vertebrate findings from the San Cassiano Formation have reported of fragmentary remains only (Figure 2). The here reported check-list (Table 1) is mainly based on the studies published by Wissmann and Münster (1841), Klipstein (1843-1845), Boni (1941), Broglio Loriga (1967), Sirna et al. (1994), Bizzarrini et al. (2001), and integrated with personal observations and new findings. Notably, specialists of invertebrates have sometimes found rare vertebrate remains both in their surface and bulk samples (e.g., fish otolithes and shark teeth, comm. pers. Alexander Nützel and Hans Hagdorn, 2011), but no further study has ever been conducted.

The determination of some of the listed specimens, especially those described in the past centuries, should be considered cautiously because of the fragmentary nature of the specimens, mainly represented by isolated teeth and body fragments with scales, and because a full revision of the material has not yet been completed.

3. The San Cassiano biota

The autoecology of the listed taxa deduced both from present-day equivalents and from previously described biotas, enables to reconstruct the broad scale characteristics of the San Cassiano ecosystem. The shelled invertebrate fauna could have sustained the diet of the classical Triassic shallow water durophagous reptiles, the placodonts, as well as neopetigian *Colobodus*. The strong and rounded teeth of this perleidiform were placed on the mandibles and

Reptilia	Archosauriformes	Archosauria indet.	Stuores Wald/Bosco di Stuores (Bizzarini et al., 2001)
	Sauropterygia		
	Nothosauria	Nothosauridae indet.	Stuores Wald/Bosco di Stuores (Bizzarini et al., 2001)
		Nothosaurus sp.	Wissmann and Münster (1841)
	Placodontia	Placodontia indet.	?Pralongià and Stuores Wald/Bosco di Stuores (Boni, 1941; Bizzarini et al., 2001)
		Placochelys sp.	San Cassiano and Forcella Settsass (Broglio Loriga 1967; Bizzarini et al., 2001)
		Cyamodontoidea indet.	Stuores Wald/Bosco di Stuores (Bizzarini et al. 2001)
Chondrichthyes			
	Elasmobranchii	Paleobatidae indet.	Forcella Giau, Milieres-Cian Zoppè
		Paleobates sp.	Stuores Wald/Bosco di Stuores (Bizzarini et al., 2001)
		Hybodontidae indet. *Hybodus* sp.	Forcella Giau, Milieres-Cian Zoppè Stuores Wald/Bosco di Stuores (Bizzarini et al., 2001)
		Hybodus hexagonus *Acrodus* sp.	San Cassiano (Broglio Loriga, 1967) Richthofen Riff, this work
Osteichthyes			
	Perleidiformes		
	Colobodontidae	*Colobodus bronni*	Pralongià, San Cassiano and Stuores Wald/Bosco di Stuores, Forcella Giau (Boni, 1941; Broglio Loriga, 1967; Bizzarini et al., 2001; Bizzarini M., 1979)

Table 1: Check-list of the vertebrates remains form the San Cassiano Formation with their finding localities. Note that the taxonomic status of the genus *Colobodus* is very confused (see Gardiner & Schaeffer, 1989; Mutter, 2004, and references therein).

on the palatine molariformes suggesting that *Colobodus* was a durofagous fish which could easily crush even thickly shelled invertebrates. The well represented shark population was dominated by euryhaline bottom-dwelling selachians as *Palaeobates* sp. which fed mainly on benthos. *Acrodus* sp. was itself a bottom-dwelling shark that probably had a mixed diet constituted of fish, hard-shelled molluscs and crustacea (Cappetta, 1987; Rees & Underwood, 2008). *Hybodus* sp. possesses a heterodont dentition with the predominantly 'clutchingtype' teeth of a piscivorous animal (Cappetta, 1987). The shallow water nothosaurs were fish and squid eaters; Bizzarini et al. (2001) estimated that the *Nothosaur* sp. found in the Stuores Wald/Bosco di Stuores locality could have been up to four meters in length. This would have possibly given the sauropterygian *Nothosaur* the position of top-predator in the San Cassiano biota, possibly together with the indetermined archosaur (here figured as a phytosaur based on similar findings in the Heiligkreuz Formation described by Dalla Vecchia and Avanzini, 2002).

Despite quantitatively and qualitatively scarce the here listed findings document the high trophic (feeding) levels of a well developed shallow water ecosystem. Most if not all the remains are thus interpreted as allochthonous. The complexity of the reconstructed food web is shown in Figure 3. Lower parts of the food chains are dominated by the well known bivalves, gastropods and cephalopods, besides there are durophagous fish and reptiles, followed by the top predators, animals that fed on fishes and small predatory reptiles.

Faunal composition is in particular similar to those documented in age-equivalent deposits from other regions of Europe. The most notable difference with other Middle-Late Triassic vertebrate marine associations from Europe is the absence of the classical Triassic top predators as *Saurichthys* or *Mixosaurus.* This latter has however been reported from the overlying mid-late Carnian Heiligkreuz Formation by Koken (1913). The paucity of the collected material leaves the question open for future findings and analysis.

This brief review of the vertebrate fauna of the San Cassian Formation aims to contribute to a better understanding of the ecology of a World-wide reference palaeoecosystem.

4. Acknowledgments

The authors wish to thank A. Nützel and H. Hagdorn for constructive discussions, A. Kroh for access to the collection of the Naturhistorisches Museum Wien. F.M. Petti and M. Zandonati for assistance with the figures. We are also indebted with E. Borghi who found the specimens. This research was supported by Museo delle Scienze, Trento.

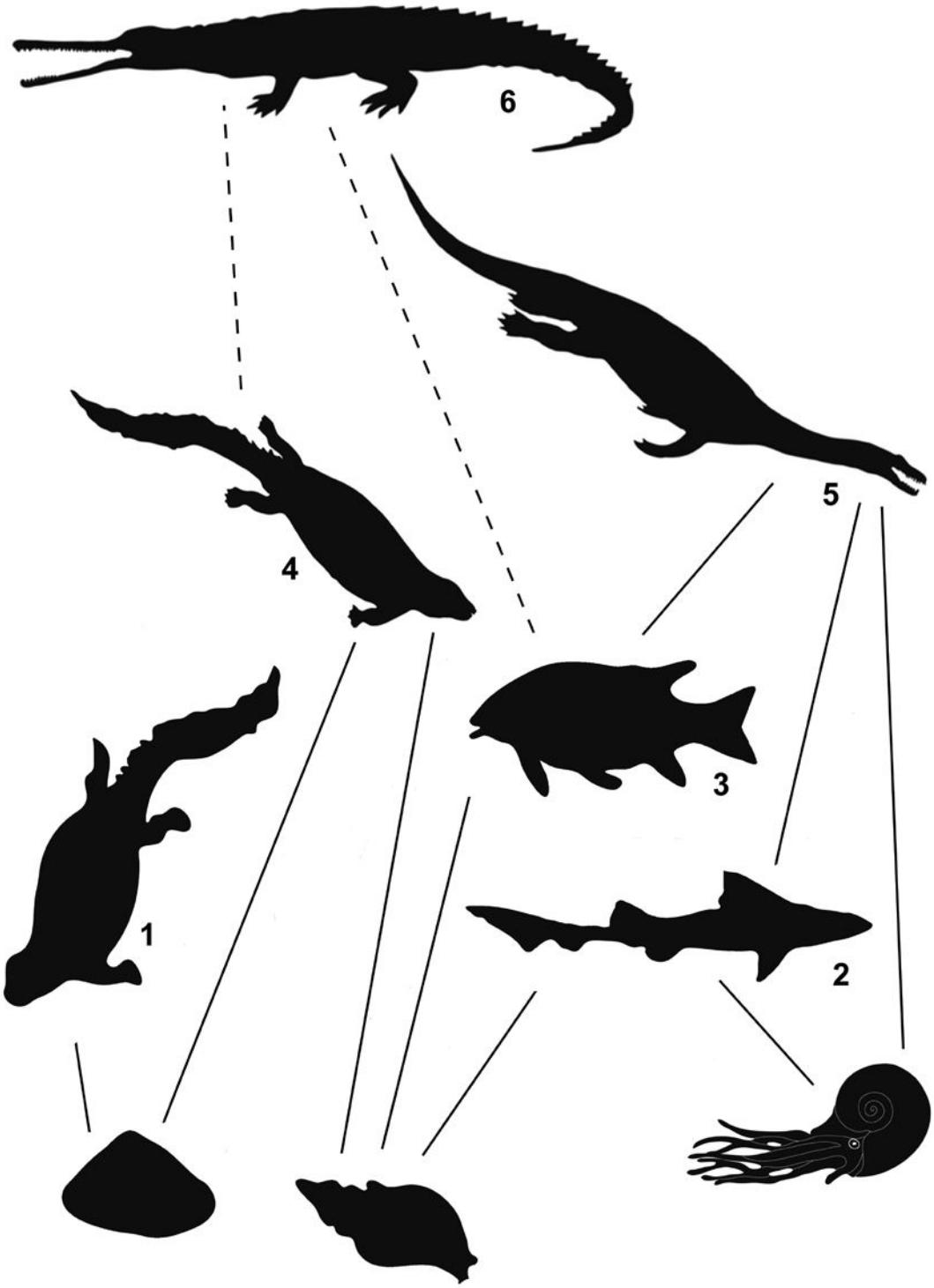

Fig. 3: Food web of the San Cassiano biota, showing assumed interactions among the key components of the marine fauna. 1 *Placochelys*, 2 *Paleobates*, 3 *Colobodus*, 4 Cyamodontidea, 5 *Nothosaur*, 6 *Archosaur* (?phytosaur).

5. References

Bizzarini, F., Prosser F., Prosser G., Prosser, I. (2001): Osservazioni preliminari sui resti di vertebrati della formazione di S. Cassiano del Bosco di Stuores (Dolomiti nord-orientali). - Ann. Mus. Civ. Rov., 17: 137-148.

Bizzarini F. & Rottonara, E. (1997): La tanatocenosi a vertebrati delle Heiligenkreuzschichten in alta Val Badia-Dolomiti. - Boll. Mus. civ. St. nat. Venezia, 47: 307-316.

Bizzarini, M. (1979): Note paleontologiche sulle Dolomiti orientali. - Ass. Paleontologica "M. Gortani", Portogruaro.

Boni, A. (1941): Notizie paleontologiche su San Cassiano. - Riv. Ital. Paleont e Stratigr. 47: 9-28.

Broglio Loriga, C. (1967): Elenco dei fossili degli strati di S. Cassiano. – In: Leonardi P. (ed.): Le Dolomiti - Geologia dei monti tra l'Isarco e il Piave 1: 298-310.

Cappetta, H. (1987): Chondrichthyes II. - In: Schultze H.-P. (ed.): Handbook of Paleoichthyology, Vol. 3B, 193 pp., Gustav Fischer Verlag, Stuttgart, New York.

Dalla Vecchia, F.M. & Avanzini, M. (2002): New findings of isolated remains of Triassic reptiles from Northeastern Italy. - Boll. Soc. Pal. It., 41: 215-235.

Fürsich, F.T. & Wendt, J. (1977): Biostratinomy and palaeoecology of the Cassian Formation (Triassic) of the Southern Alps. - Palaeogeog. Palaeoclimatol. Palaeoecol., 22: 257-323.

Gardiner, B.G. & Schaeffer, B. (1989): Interrelationships of lower actinopterygian fishes. - Zool. J. Lin. Soc., 97: 135-87.

Keim, L. & Neri, C. (2005): Formazione di S. Cassiano. - In: Cita Sironi, M.B., Abbate, E., Balini, M., Conti, M.A., Falorni, P., Germani, D., Groppelli, G., Manetti, P. & Petti, F.M. (eds.): Carta Geologica d'Italia - 1:50.000, Catalogo delle Formazioni, Unità tradizionali. Quaderni serie III, 7, Fascicolo VI., pp. 49-55, APAT, Dipartimento Difesa del Suolo, Servizio Geologico d'Italia.

Klipstein, A. (1843-1845): Beiträge zur geologischen Kenntnis der östlichen Alpen. Giessen.

Koken, E. (1913): Beiträge zur Kenntnis der Schichten von Heiligenkreuz (Abteital, Südtirol). - Abh. Geol. Reichsanst. Wien, 16/4: 1-56.

Münster, G. (1834): Über das Kalkmergel-Lager von St. Cassian in Tyrol und die darin vorkommenden Ceratiten. - N. Jahrb. Min., Geol. Paläont., 1834: 1-15.

Mutter, R.J. (2004): The "perleidiform" family Colobodontidae: A review. In: Arratia, G., Tintori, A. (eds.): Mesozoic Fishes 3 – Systematics, Paleoenvironments and Biodiversity, pp. 197-208, Verlag Dr. Friedrich Pfeil, München, Germany.

Rees, J. & Underwood, C. (2008): Hybodont sharks of the English Bathonian and Callovian (Middle Jurassic). – Palaeontology, 51: 117-147.

Sirna, G., Dalla Vecchia, F.M., Muscio, G., Piccoli, G. (1994): Catalogue of Paleozoic and Mesozoic Vertebrates and vertebrate localities of the Tre Venezie area (North Eastern Italy). - Mem. Sci. Geol., 46: 255-281.

Wissmann, H.L. & Münster, G. von (1841): Beiträge zur Geognosie und Petrefactenkunde des südöstlichen Tirols vorzüglich der Schichten von St. Cassian. - Beiträge zur Petrefactenkunde, 4: 1-152.

Geo.Alp, Vol. 8, S. 128–135, 2011

BENTHIC CRINOIDS FROM THE TRIASSIC CASSIAN FORMATION OF THE DOLOMITES

Hans Hagdorn

With 2 Plates

Muschelkalkmuseum, Schlossstraße 11, 74653 Ingelfingen, Germany
Email: encrinus@hagdorn-ingelfingen.de

The marls of the late Ladinian/early Carnian Cassian Formation have been painstakingly searched for more than 170 years for the beautifully preserved fossils that make this Fossillagerstätte one of the richest treasure troves of Mesozoic invertebrates. Its crinoid fauna is the most diverse Triassic fauna known from the western Tethys. However, unlike the obrutional conservation lagerstätten in the late Anisian/early Ladinian germanotype Muschelkalk, which has much less diverse crinoid faunas, articulated skeletons are extremely rare in the Cassian Formation. This is due to a relatively long transport from their original habitat to the area of deposition. Hence, the variety of crinoid sclerites forms a puzzle with many parts is still missing.

Most of the taxa established during the last 170 years are based on fragmentary material, mostly columnals, many of which are of limited diagnostic value and cannot be unequivocally attributed to a genus or even a species. For Count Münster (1834) cylindrical columnals similar to *Encrinus liliiformis* gave evidence for a Muschelkalk (Triassic) age of the Cassian Formation. Subsequently the Cassian crinoids were described within the classical monographs (Münster, 1841; Klipstein, 1845; Laube, 1864, 1865). New taxa were added by Bather (1909), Leonardi & Lovo (1950) and Zardini (1974), most of them as a result of Rinaldo Zardini´s collecting activity around Cortina d´ Ampezzo. Hagdorn (1988, 2004) started to subdivide the order Encrinida. However, a revision of the entire fauna is still a desideratum, especially in respect of its worldwide importance for the post-Palaeozoic crinoid radiation and mid Carnian extinction (Simms, 1990; Hagdorn, 2011).

This paper presents (1) a first step towards a revision of the Cassian benthic crinoids (the planktonic and benthic microcrinoids excluded), (2) evidence of their possible biostratigraphic value and (3) a first data set of their palaeogeographic distribution and relation to Eastern Tethyan faunas of this time interval.

At present, the following taxa can be distinguished:

Order Holocrinida	Family Tollmannicrinidae	
	Tollmannicrinus quinqueradiatus	rare columnals
Order Encrinida	Family Encrinidae	
	Encrinus sp. indet.	2 crowns, isolated sclerites
	Chelocrinus cassianus	a few crowns, many cups, isolated sclerites
	Cassianocrinus varians	a few crowns, many cups, isolated sclerites
	Zardinicrinus granulosus	1 crown, many cups, isolated sclerites
	Zardinicrinus tuberculatus	a few cups, isolated sclerites
	Family Traumatocrinidae	
	Traumatocrinus sp. indet.	a few columnals
	Family Ainigmacrinidae	
	Ainigmacrinus calyconodalis	a few cups, several calyconodals
Order Isocrinida	Family Isocrinidae	
	Tyrolecrinus tyrolensis	1 cup, 1 basal circle, columnals
	Balanocrinus subcrenatus	rare columnals
	Laevigatocrinus laevigatus	1 stem fragment, rare columnals
	"Isocrinus" propinquus	2 cups, columnals
	"Isocrinus" apetalus	rare columnals
	"Isocrinus" venustus	columnals
Order Millericrinida (?)	Family indet.	
	"Encrinus" cancellistriatus	columnals

As demonstrated by Bizzarini et al. (1989) and Broglio Loriga et al. (1999) for the planktonic microcrinoids, a faunistic succession can also be observed within the benthic crinoid faunas of the late Ladinian/Carnian sediments in the Dolomites. While Encrinida are rather common from the Ladinian Pachycardientuffe of the Seiser Alm and at the type locality of the Cassian Formation around Pralongia (Stuores Wiesen) up to the outcrops at Richthofenriff (Forcella Settsass), the outcrops along the Falzarego Road, near Lake Misurina, and on Seelandalm yielded no Encrinida and only a restricted number of Isocrinida species. This distribution reflects a major cut in the phylogeny of the post-Palaeozoic crinoids marked by the extinction of order Encrinida between *aonoides* and *austriacum* biozones (Simms, 1990; Hagdorn, 2011).

Thus, establishment of a Ladinian/Carnian crinoid biozonation for the Western Tethys on the base of abundant and easily determinable sclerites could serve as an additional, fairly high-resolving biochronological tool for such sediments that are poor in ammonoids or conodonts. For this purpose, the Dolomites are certainly the best place to start with. However, more bed-by-bed collecting will be necessary.

Moreover, this could be a second step towards a crinoid biochronology covering the entire Triassic that would continue the Anisian crinoid biochronology established by Hagdorn & Głuchowski (1993) and Hagdorn et al. (1997) downsection and upsection. Finally, analyses of biostratigraphically well dated crinoid faunas from other parts of the Tethys could serve for a reconstruction of a palaeobiogegraphical scenario.

Plates 1 and 2 aim to give photographic pictures of the type specimens that are housed in different European collections. As a good deal of this historical material was bought from cattle herds, specified locality data are not available. These specimens are mostly labelled "Cassianer Schichten, St. Cassian". Otherwise, locality data are given in the captions. Type and figured material of Cassian crinoids are deposited in the following collections

NHML	Natural History Museum London (originals of Klipstein 1843 – 1845)
BSP	Bayerische Staatssammlung für Paläontologie München (originals of Münster 1841)
GBA	Geologische Bundesanstalt Wien (originals of Laube 1865)
IGPT	Institut für Geologie und Paläontologie Tübingen (originals of Quenstedt 1874 – 1876)
MB	Museum für Naturkunde an der Humboldt Universität zu Berlin (originals Laube 1861)
MHI	Muschelkalkmuseum Ingelfingen (as yet unpublished material)
NHMW	Naturhistorisches Museum Wien (originals of Laube 1861)
SMNS	Staatliches Museum für Naturkunde Stuttgart (originals of Hagdorn 1983, 1988)

Acknowledgements

I should like to thank for loan of specimens Drs. A. Kroh, Wien, D. Lewis, London, A. Liebau, Tübingen, E. Pietrzeniuk and Ch. Neumann, Berlin, M. Urlichs, Stuttgart, W. Werner and A. Nützel, München.

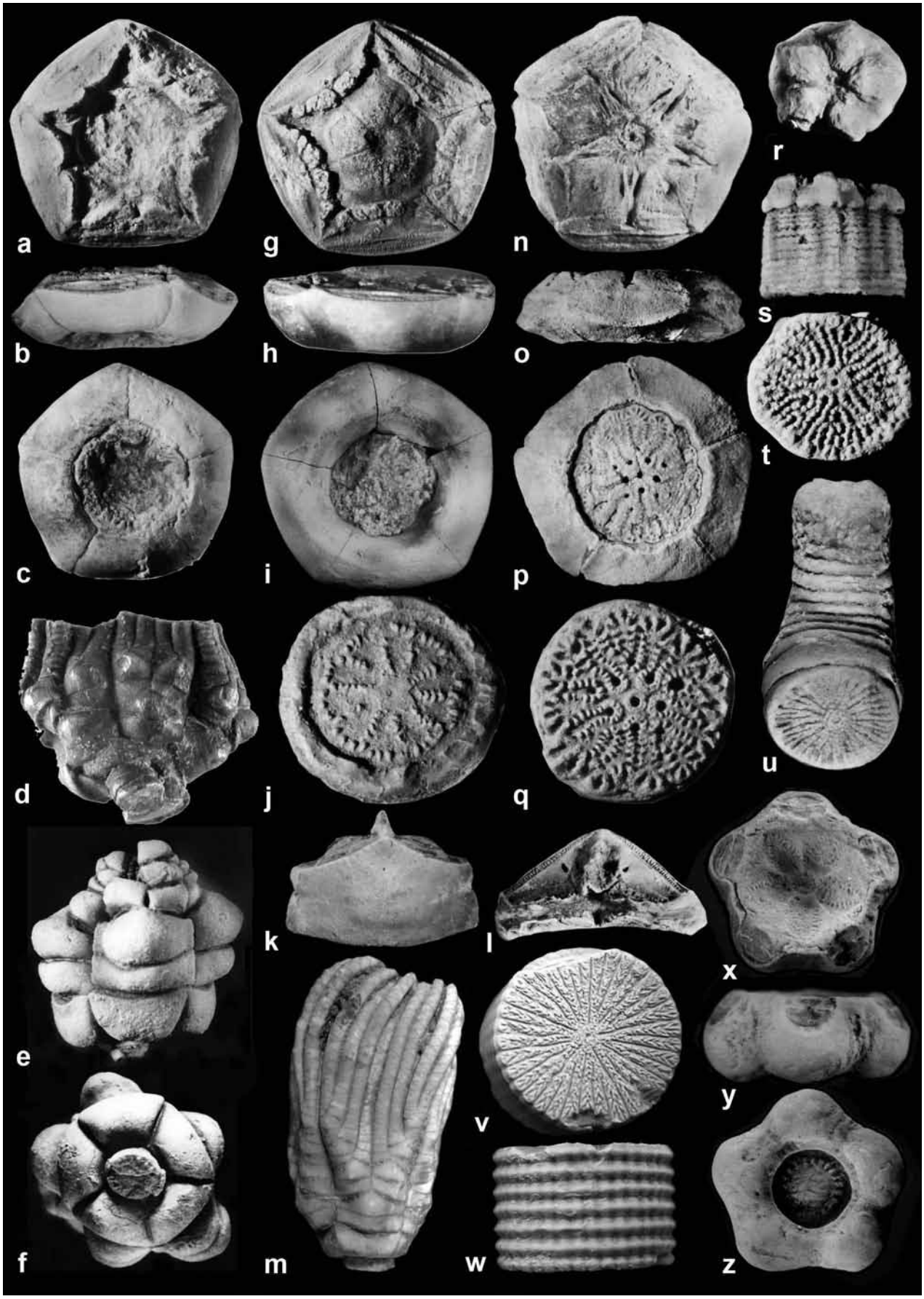
a
b
c
d
e
f
g
h
i
j
k
l
m
n
o
p
q
r
s
t
u
v
w
x
y
z

Plate 1: Encrinida.
a – d ***Chelocrinus cassianus*** **(Laube, 1864);**
a – c cup, orig. *Encrinus liliiformis* v. Münster 1841, pl. 5, fig. 6, BSPM 1877 X 1020; width 11 mm;
d crown, orig. *Encrinus cassianus*, holotype, Laube 1865, pl. 8a, fig. 1, MB uncatalogued; width 27 mm.
e – f ***Encrinus*** **sp. indet.;** crown, orig. *Encrinus cassianus*, Quenstedt 1874 – 1876, pl. 107, fig. 8, IGPT Qu. Ast. u. Encr. Tab. 107, fig. 8; width of cup 11 mm.
g – m *Cassianocrinus varians* **(v. Münster, 1841);**
g – i cup, orig. *Encrinus varians*, v. Münster 1841, lectotype, pl. 5, fig. 8, BSP 1877 X 1013; width 18 mm;
j proximal columnal, orig. v. Münster 1841, syntype, pl. 5, fig. 10 a, BSP 1877 X 1026; width 11,5 mm;
k – l primibrachials 1 + 2 axillary, orig. *Encrinus liliiformis* v. Münster 1841, pl. 5, fig. 7 c,d, BSP 1877 X 1025; width 14 mm;
m crown, orig. *Encrinus (Cassianocrinus) tetarakontadactylus* Laube, 1865, holotype, pl. 8b, fig. 1 – 3, NHMW 1865/IX/130; length 22,5 mm.
n – u ***Zardinicrinus granulosus*** **(Münster, 1834);**
n – p cup, orig. *Encrinus granulosus* (v. Münster, 1834), lectotype, v. Münster 1841, pl. 5, fig. 19, BSP 1877 X 1015; width 12,5 mm;
q pluricolumnal, syntype, v. Münster 1841, pl. 5, fig. 14, BSP 1877 X 1023; width 6 mm;
r – t proximal pluricolumnal with basal circle, syntype, v. Münster 1841, pl. 5, fig. 16, width 7 mm, BSP 1877 X 1010;
u distal pluricolumnal, syntype, v. Münster 1841, pl. 5, fig. 13 b, BSP 1877 X 1022; length 11 mm.
v – w ***Traumatocrinus*** **sp. indet.,** pluricolumnal, NHMW uncatalogued; width 8,7 mm.
x – z ***Ainigmacrinus calyconodalis*** **Hagdorn, 1988,** calyconodal, holotype, "Becken vom *subcrenatus*?" orig. v. Münster 1841, pl. 4, fig. 10, BSP AS VII 563; width 10,8 mm.

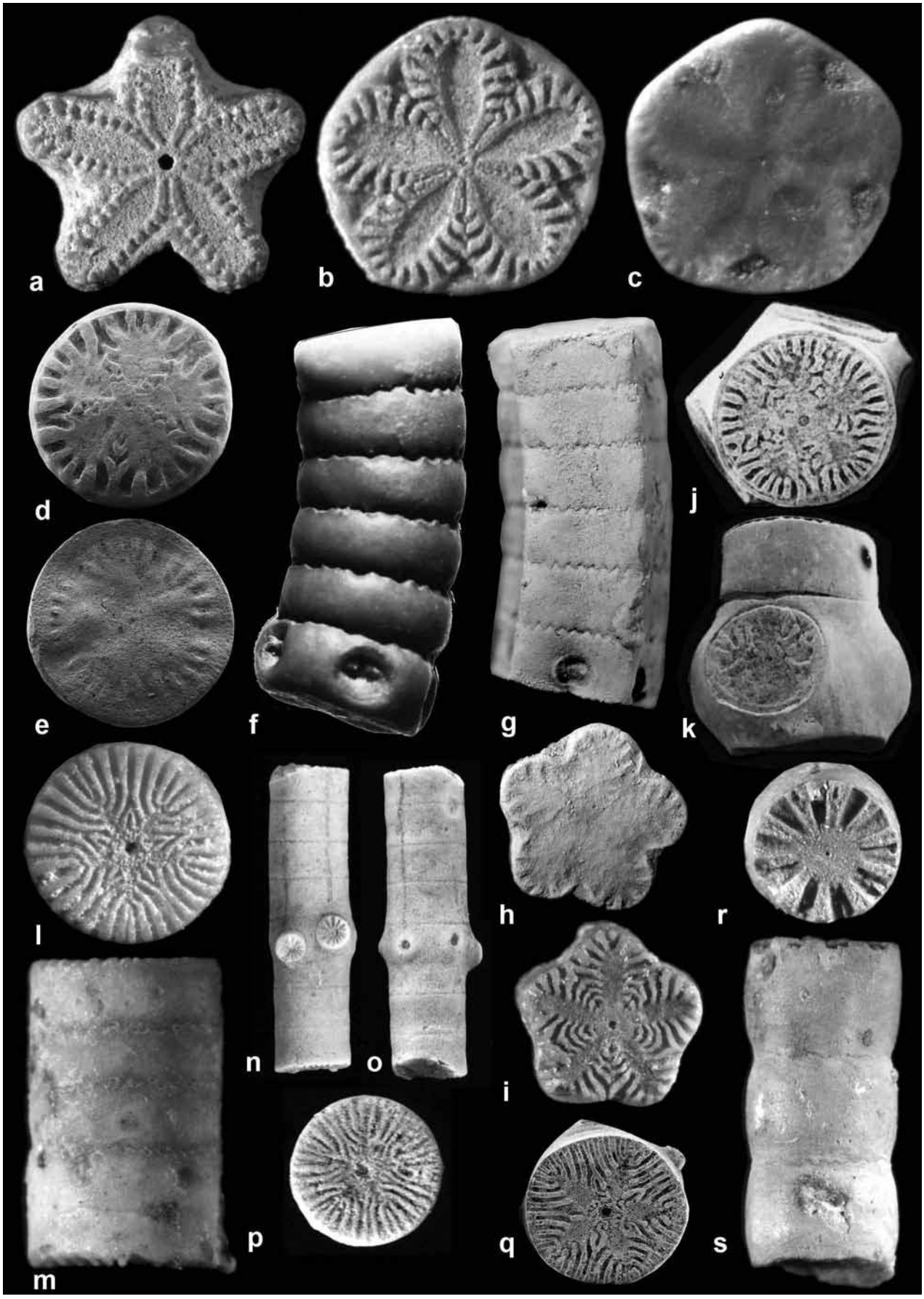
a
b
c
d
e
f
g
j
k
l
m
n
o
h
r
i
p
q
s

Plate 2: Isocrinida, Millericrinida.
a – c ***"Isocrinus" propinquus*** **v. Münster, 1834,** Stuores Wiesen; a proximal nodal, MHI 2063/1; width 5 mm; **b** internodal, MHI 2063/2; width 5,3 mm;
c hyponodal with synostosial articulation facet, MHI 2063/3; width 5,9 mm.
d – f ***Balanocrinus subcrenatus*** **(v. Münster, 1841);**
d pluricolumnal, internodal facet, Stuores Wiesen, Unterkarn, orig. Hagdorn 1983, fig. 1 a, SMNS 26337; width 4,5 mm;
e internodal, orig. Hagdorn 1983, fig. 1 b, Stuores Wiesen, SMNS 26338, width 4,5 mm;
f pluricolumnal, SMNS 26337; length 12 mm.
g – i ***Tyrolecrinus tyrolensis*** **(Laube, 1865);**
g – h pluricolumnal, synostosial lower nodal facet, holotype, orig. Laube 1865, GBA 1865/3/83; length 5 mm; **i** internodal, Seelandalm, MHI 2064/1; width 3,9 mm.
j – k ***Laevigatocrinus laevigatus*** **(Münster, 1841),** pluricolumnal with nodal, internodal facet, lectotype, orig. v. Münster 1841, pl. 4, fig. 7 b, g, BSP AS VII 912, width 5 mm;
l – m ***"Isocrinus" apetalus*** **Zardini 1976,** pluricolumnal, Forcella Giau; MHI 2065/1; width 3 mm;
n – q ***"Isocrinus" venustus*** **(Klipstein, 1845);**
n – p pluricolumnal, internodal facet enlarged, holotype, orig. Pentacrinus venustus Klipstein, 1845, NHML 75860; length 11 mm;
q pluricolumnal, internodal facet, Stuores Wiesen; MHI 2066; width 1,6 mm.
r – s ***"Encrinus" cancellistriatus*** **Bather, 1909,** pluricolumnal, Seelandalm; MHI 2067; width 3,5 mm.

References

Bather, F. A. (1909): Triassic echinoderms of Bakony. – Resultate der wissenschaftlichen Erforschung des Balatonsees, 1/1.Teil, Anhang Paläontologie des Balatonsees 1: 288 S., Hölzel, Wien.

Bizzarini, F., Laghi, G. F., Nicosia, U., Russo, F. (1989): Distribuzione stratigrafica dei Microcrinoidi (Echinodermata) nella Formazione di S. Casiano (Triassico Superiore, Dolomiti): Studio preliminare. – Atti Soc. Nat. Mat. di Modena, 120: 1-14, 4 figs., 3 pls.; Modena.

Broglio Loriga, C., Cirilli, S., De Zanche, V., Di Bari, D., Gianolla, P., Laghi, G., Manfrin, S., Mastandrea, A., Mietto, P., Muttoni, G., Neri, C., Posenato, R., Rechichi, M. C., Rettori, R., Roghi, G. (1999): The Prati di Stuores/Stuores Wiesen Section (Dolomites, Italy): a candidate Global Stratotype and Point for the bese of the Carnian stage. – Riv. Ital. Paleont. Strat., 105 (1): 37-78.

Hagdorn, H. (1983): *Holocrinus doreckae* n. sp. aus dem Oberen Muschelkalk und die Entwicklung von Sollbruchstellen der Isocrinida. – N. Jahrb. Geol. Paläont., Monatsh., 1983 (6): 345-368.

Hagdorn, H. (1988): *Ainigmacrinus calyconodalis* n. g. n. sp., eine ungewöhnliche Seelilie aus der Obertrias der Dolomiten. – N. Jahrb. Geol. Paläont., Monatsh., 1988 (2): 71-96.

Hagdorn, H. (2004): *Cassianocrinus varians* (Münster, 1841) aus der Cassian-Formation (Trias, Oberladin/Unterkarn) der Dolomiten – ein Bindeglied zwischen Encrinidae und Traumatocrinidae (Crinoidea, Articulata). – Ann. Naturhist. Mus. Wien, 105 A: 231-255.

Hagdorn, H. (2011): The Triassic – Crucial period of post-Paleozoic crinoid diversification. – Swiss Journ. Palaeont., 130 (1): 91-112.

Hagdorn, H., Głuchowski, E. (1993): Palaeobiogeography and Stratigraphy of Muschelkalk Echinoderms (Crinoidea, Echinoidea) in Upper Silesia – In: Hagdorn, H. & Seilacher, A. (Ed.), Muschelkalk. Schöntaler Symposium 1991 (= Sonderbände der Gesellschaft für Naturkunde in Württemberg), 2: 165-176, Goldschneck, Korb.

Hagdorn, H., Konrad, G., Török, A. (1997): Crinoids from the Muschelkalk of the Mecsek Mountains and their stratigraphical significance. – Acta Geol. Hung., 40 (4): 391-410.

Klipstein, A. (1843-1845): Beiträge zur geologischen Kenntnis der östlichen Alpen. – 311 S., Heyer, Giessen. [die dritte Lieferung mit den Seiten 241-311 und den Tafeln 16-20 ist 1845 erschienen].

Laube, G. C. (1864): Über *Encrinus cassianus* Lbe. und dessen Verhältnisse zu bekannten Encriniten. – Jahrb. k.-k. geol. Reichsanst., 14: 207-208.

Laube, G. C. (1865): Die Fauna der Schichten von St. Cassian. Ein Beitrag zur Paläontologie der Alpinen Trias. I Abtheilung. Spongitarien, Corallen, Echiniden und Crinoiden. – Denksch. k. Akad. Wissensch., math.-naturwiss. Classe, 24: 223-296.

Leonardi, P., Lovo, M. (1950): Nuove forme di echinodermi della fauna cassiana di Cortina d'Ampezzo. – Studi Trent. Scien. nat., 27: 3-10.

Münster, G. Graf zu (1834): Über das Kalkmergel-Lager von St. Cassian in Tyrol und die darin vorkommenden Ceratiten. – N. Jahrb. Geol., Geogn., Geol. Petrefaktenk., 1834: 1-15.

Münster, G. Graf zu (1841): Beschreibung und Abbildung der in den Kalkmergelschichten von St. Cassian gefundenen Versteinerungen. – In: Wissmann, H.L. & Münster, G. (Eds.), unter Mitwirkung des Dr. Braun. Beiträge zur Petrefacten-Kunde 4: 25-147, Bayreuth.

Quenstedt, F.A. (1874-1876): Petrefaktenkunde Deutschlands. 1. Abt. 4. Band Echinodermen. Die Asteriden und Encriniden nebst Cysti- und Blastoiden. – VIII, 742 S. Nebst Atlas von 25 Tafeln, Fues, Leipzig.

Simms, M. J. (1990a): Crinoid diversity and the Triassic/Jurassic boundary. – Cahiers Université Catholique Lyon, Sér. Scient., 3: 67-77.

Zardini, R. (1976): Fossili di Cortina. Atlante degli echinodermi cassiani (Trias medio-superiore) della regione dolomitica attorno a Cortina d´Ampezzo. – 28 S., Foto Ghedina, Cortina d´Ampezzo.

Geo.Alp, Vol. 8, S. 136–140, 2011

ECHINOIDS FROM THE TRIASSIC OF ST. CASSIAN – A REVIEW

Andreas Kroh

With 1 Figure and 1 Table

Natural History Museum Vienna, Department of Geology & Palaeontology, Burgring 7, 1010 Vienna, Austria;
e-mail: andreas.kroh@nhm-wien.ac.at

Introduction

The end-Permian mass extinction event severely affected most echinoderm groups and caused the loss of all but a few selected survivor clades (Twitchett & Oji 2005), resulting in a severe evolutionary bottleneck. In echinoids, however, biodiversity was low during the Late Permian already and only one genus is known to have survived the end-Permian crisis (*Miocidaris* – Kier 1965; Smith & Hollingworth 1990). Data from lantern supports, however, indicate that at least two echinoid lineages passed from the Permian to the Triassic (Kier 1984) and it is from these two that the morphological diversity of all post-Palaeozoic sea urchins derives. One of the two survivor lineages were the miocidarids, which have lantern supports formed from interambulacral protrusions termed apophyses and which evolved into modern cidaroids. The other lineage lacks apophyses and possibly is the ancestor of all euechinoids.

Recovery after the mass extinction occurred at different times in echinoderms (Twitchett & Oji 2005). While crinoids and ophiuroids seem to have recovered relatively rapidly (Twitchett & Oji 2005; Chen & McNamara 2006; Hagdorn 2011), echinoids are exceedingly rare in the Early and Mid-Triassic. A significant evolutionary radiation did not occur before the Carnian in echinoids. From the Early Triassic just two echinoid species are known, both of which appear to be stem-group cidaroids related to the P/T-survivor *Miocidaris*. Unlike most modern forms they are construed from imbricating plates producing a flexible rather than a rigid corona. The mid-Triassic fossil record of echinoids is similarly poor. Only three species are known, all of them stem-group cidaroids. In the Late Triassic echinoids become much more diverse and new clades appear (modern-type cidaroids, triadocidarids and pedinids in the Carnian, pseudodiadematids in the Rhaetian). Ignoring the Cassian Beds echinoids five species are known from Carnian strata, eight from the Norian and four from the Rhaetian (Kier 1977; Smith 1994; Hagdorn 1995).

In total 99 echinoid taxa have been reported from Triassic strata worldwide, 44 of which are based on isolated spines (based on Smith 1990, with updates from Kroh 2010). A considerable number of additional species are based on indeterminate test fragment. Only 5 species are known from articulated specimens preserving coronal fragments, spines and lantern elements. Spine-based taxa artificially double the observed palaeobiodiversity and establishing species on such material is thus problematic. Echinoid spines can be very distinct and easily recognizable, but radically different types may occur on a single individual, especially in cidaroids (as e.g. in extant histocidarids which have smooth aboral spines and coarse saw-tooth edged oral spines). The association of isolated spines and corona material, however, is important for unravelling the phylogenetic position of Triassic echinoids.

The Triassic echinoid fauna is heavily biased in several ways. First of all there is a strong geographical bias (Smith 1990, 1994), with 80% of the corona-based species having been described from Europe. Another bias concerns preservation potential: as shown by Smith (2007) Triassic echinoids are much more prone to disarticulation than their Jurassic successors, owing to a high proportion of species with fully or partially imbricate corona in the Triassic, whereas the test of younger forms usually is firmly sutured. Few Triassic echinoids are thus preserved as complete coronas, let alone as articulated specimens. The effects of these biases are further amplified by a skewed rock record, where terrestrial deposits dominate during much of the Triassic, whereas in the Jurassic marine deposits are much more widespread (Smith 2007).

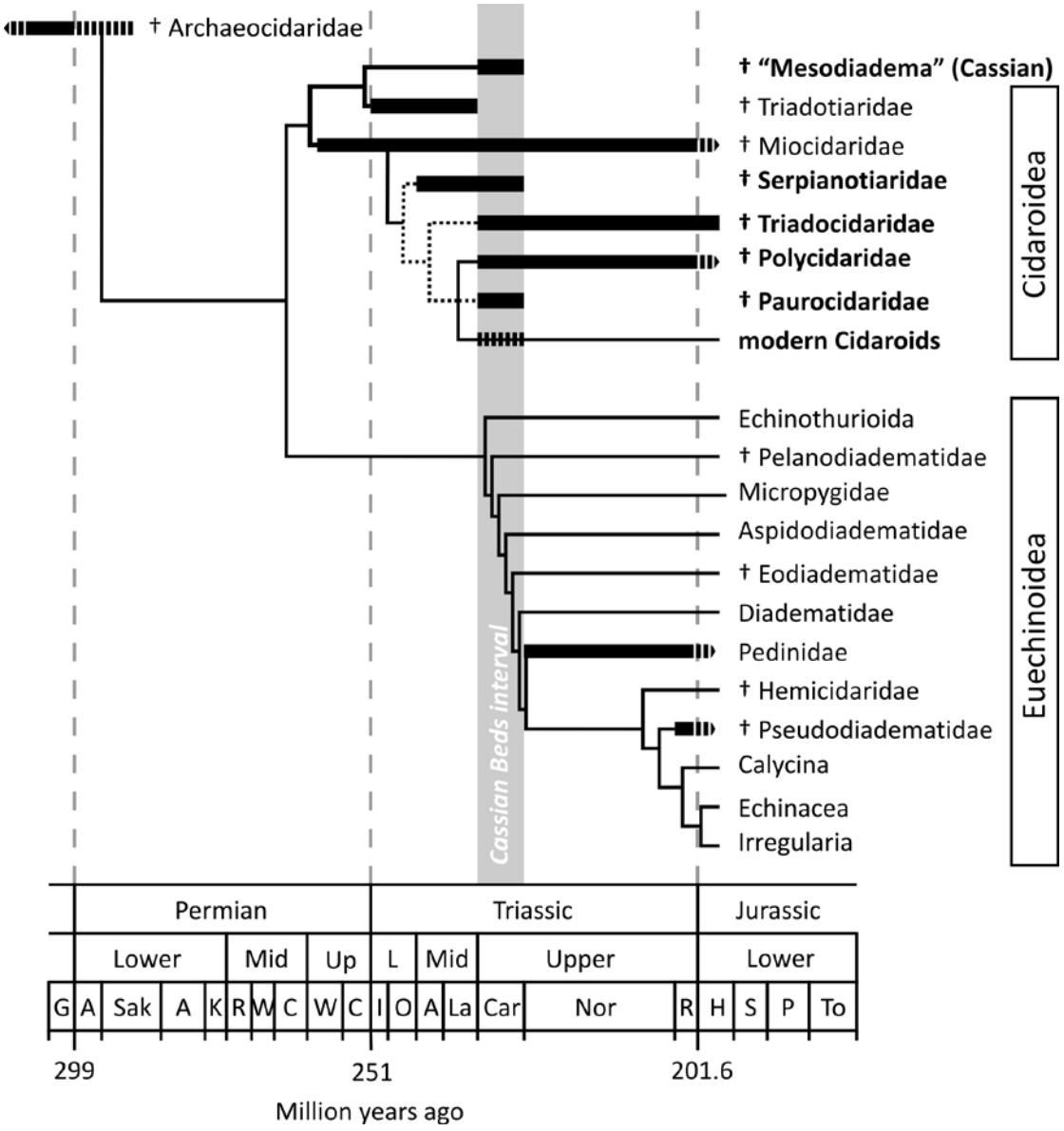

Fig. 1: Phylogenetic relationship between Triassic echinoids and their immediate successors (modified from Kroh & Smith 2010: fig. 5A). Massive black bars represent actual taxon ranges on stage level (data from Hagdorn 1995; Smith 1990, 2005 and references therein). Hatched bars are uncertain distributions and thin stippled lines represent ambiguous relationship (*Serpianotiaris* was found to be a primitive euechinoid representative by Smith 1994, 2007). Taxa in bold font are represented in the Cassian Beds (excluding taxa based on spines or indeterminate test fragments). Extinct taxa are marked by a dagger symbol.

Echinoids from the Cassian Beds

The Cassian Beds contain the largest and most important echinoid fauna of Triassic age worldwide. More than 70 nominal taxa have been described from these deposits, 20 of which were considered valid upon critical revision by Kier (1977, 1984) and Smith (1990). Recently additional, new material was described by Vadet (1999a, b), providing supplementary data on lantern elements and introducing six new genera and three new species. The fauna contains both "old-fashioned" stem-group cidaroids, as well as modern type cidaroids and the short lived triadocidarid clade (Table 1). The latter are cidaroid-like, but lack lantern supports and possibly are not part of the crown group (Kroh & Smith 2010). Despite the considerable attention received in the past, the echinoid fauna of the Cassian Beds, however, is far

from being fully investigated. Numerous additional taxa (10+) are known from small fragments only and were, in part, named in open nomenclature by Kier (1977, 1984). Among these rare un-named specimens are some of the very first ancestors of non-cidaroid echinoids, including the oldest ambulacral lantern supports (auricles) and the first example of ambulacral compound plating (Kier, 1984). Both features are major innovations characterizing regular euechinoids and the Cassian Bed examples might represent missing links between Early Jurassic modern-type euechinoids and their Triassic ancestors.

Additionally, the Cassian fauna contains the minute enigmatic echinoid *Tiarechinus princeps* Neumayr, 1881. This species shows curious constructional features and can currently not be confidently placed anywhere in the echinoid tree. Its test structure is unique among Post-Palaeozoic echinoids in having just four plates in each interambulacrum, with a single adoral element and three upper elements. It has been described in detail by both Lovén (1883) and Kier (1977) but its strange morphology provides little clue as to what its closest relatives might be. Known specimens likely are juveniles (although their gonopores are already open) and future finds of larger specimens hopefully will help to resolve the taxonomic affinities of this taxon.

Future prospects

It is envisioned that bulk-sampling might be a key to a better understanding and broader knowledge of the Cassian Beds echinoid fauna. Specimens available today largely were hand-picked from weathered surfaces and are usually not associated with detailed geographic and stratigraphic information. Consequently detached spines and lantern parts can usually not be referred to specific taxa known from test fragments. Such element associations, however, would likely considerably increase our knowledge on the Cassian echinoids and their phylogenetic significance. A further, as yet completely unexplored field in relation to the Cassian Beds, is represented by echinoid pedicellariae. Recently published results (Mostler 2009) have shown that pedicellariae of Middle to Late Triassic age may be preserved in excellent quality. Moreover, that they show a much higher morphological diversity than expected. Pending proper sampling techniques are employed, such high-quality preservation seems likely in the Cassian Beds too. Pedicellariae evolved in an arms race against pest and parasites (Coppard et al. 2010) and underwent a major radiation in the Early Mesozoic. Today these structures are important features for species-level taxonomy and an improved knowledge on their early diversification is much needed.

stem-group Cidaroida

1 *Leurocidaris montanaro* (Zardini, 1973)
2 *„Mesodiadema" marginatum* Bather, 1909
3 *„Mesodiadema"* sp.

Serpianotiaridae

4 *Serpianotiaris* sp.

Polycidaridae

5 *Paracidaris subcoronata* (Münster in Wissmann & Münster, 1841)
6 *Polycidaris regularis* (Münster in Wissmann & Münster, 1841)
7 *Zbindenicidaris subcoronata* (Münster, 1844)

Cidaroida

Paurocidaridae

8 *Paurocidaris adrianae* (Zardini, 1973)
9 *Paurocidaris rinbianchi* (Zardini, 1973)

?Cidaridae

10 *Triassicidaris ampezzana* (Zardini, 1973)

Incertis sedis

11 *Tiarechinus princeps* Neumayr, 1881

Triadocidaridae

12 *Levicidaris furlani* Kier, 1984
13 *Levicidaris pfaifferi* Kier, 1984
14 *Levicidaris zardinia* Kier, 1977
15 *Megaporocidaris mariana* Kier, 1977
16 *Mikrocidaris pentagona* (Münster in Wissmann & Münster, 1841)
17 *Triadocidaris giauensis* (Zardini, 1973)
18 *Triadocidaris subsimilis* (Münster in Wissmann & Münster, 1841)
19 *Triadocidaris venusta* (Münster in Wissmann & Münster, 1841)
20 *Triadocidaris* sp. A
21 *Triadocidaris* sp. B
22 *Zardinechinus giulinii* Kier, 1984
23 *Zardinechinus lancedelli* (Zardini, 1973)
24 *Zardinechinus suessi* (Laube, 1865)

Table 1: Echinoid fauna of the Cassian Beds (from Zardini 1973; Kier 1977, 1984; Vadet 1999a, b; Smith 1990, 1994,2005). Spine-based taxa and species established for undiagnostic fragments have been omitted. Note that "Mesodiadema" of the Cassian Beds is not congeneric with the Early Jurassic type of the genus (see Smith & Anzalone 2000)

References

Chen, Z. Q. & McNamara, K. J. (2006): End-Permian extinction and subsequent recovery of the Ophiuroidea (Echinodermata). – Palaeogeogr., Palaeoclimatol., Palaeoecol., 236/3–4: 321–344.

Coppard et al. 2010, S. E., Kroh, A., Smith, A. B. (2010): The evolution of pedicellariae in echinoids: an arms race against pests and parasites. – Acta Zool. doi: 10.1111/j.1463-6395.2010.00487.x

Hagdorn, H. (1995): Die Seeigel des germanischen oberen Muschelkalks. – Geol. Paläont. Mitt. Innsbruck, 20: 245–281.

Hagdorn, H. (2011): Triassic: the crucial period of post-Palaeozoic crinoid diversification. – Swiss J. Palaeont., 130/1: 91–112.

Kier, P. M. (1965): Evolutionary trends in Paleozoic echinoids. – J. Paleont., 39/3: 436–465.

Kier, P. M. (1977): Triassic echinoids. – Smiths. Contr. Paleobiol., 30: iv+1–88.

Kier, P. M. (1984): Echinoids from the Triassic (St. Cassian) of Italy, their lantern supports, and a revised phylogeny of Triassic echinoids. – Smiths. Contr. Paleobiol., 56: iii+1–41.

Kroh, A. (2010): Index of Living and Fossil Echinoids 1971-2008. – Ann. Naturhist. Mus. Wien, Ser. A, 112: 195–470.

Kroh, A. & Smith, A. B. (2010): The phylogeny and classification of post-Palaeozoic echinoids. – J. Syst. Palaeont., 8/2: 147–212.

Lovén, S. (1883): On *Pourtalesia*, a genus of Echinoidea. – Kong. Svenska Vetenskaps-Akad. Handl., n. ser., 19/7: 1–95.

Mostler, H. (2009): Pedicellarien spät-Norischer Echiniden aus der Hallstätter Tiefschwellen-Fazies, Nördliche Kalkalpen. – Geo.Alp, 6: 19–52.

Neumayr, M. (1881): Morphologische Studien über fossile Echinodermen. – Sitzber. Kaiserl. Akad. Wiss., Math.-naturwiss. Cl., Abt. I, 84/1: 143–176.

Smith, A. B. (1990): Echinoid evolution from the Triassic to Lower Jurassic. – Cahiers Univ. Cath. Lyon, Ser. Sci., 3: 79–117.

Smith, A. B. (1994): Triassic echinoids from Peru. – Palaeontogr. (A), 233/1–6: 177–202.

Smith, A. B. (editor) 2005. The Echinoid Directory. World Wide Web electronic publication. http://www.nhm.ac.uk/research-curation/projects/echinoid-directory/index [accessed 01/07/2011].

Smith, A. B. (2007): Intrinsic versus extrinsic biases in the fossil record: contrasting the fossil record of echinoids in the Triassic and early Jurassic using sampling data, phylogenetic analysis, and molecular clocks. – Paleobiol., 33/2: 310–323.

Smith, A. B. & Anzalone, L. (2000): *Loriolella*, a key taxon for understanding the early evolution of irregular echinoids. – Palaeont., 43/2: 303–324.

Smith, A. B. & Hollingworth, N. T. J. (1990): Tooth structure and phylogeny of the Upper Permian echinoid *Miocidaris keyserlingi*. – Proc. Yorkshire Geol. Soc., 48/1: 47–60 .

Twitchett, R. J. & Oji, T. (2005): The Early Triassic recovery of echinoderms. – C. R. Palevol, 4/6-7: 463–474.

Vadet, A. (1999a): Revision des echinides de Saint Cassian et evolution des echinides post-carboniferes 1. – Mem. Soc. Acad. Boulonnais, 20/1: 1–60.

Vadet, A. (1999b): Revision des echinides de Saint Cassian et evolution des echinides post-carboniferes 2. – Mem. Soc. Acad. Boulonnais, 20/2: 61–116.

Geo.Alp, Vol. 8, S. 142–145, 2011

TYPE SPECIMENS FROM THE CASSIAN BEDS IN THE COLLECTION OF THE NHM VIENNA

Andreas Kroh, Thomas Nichterl & Alexander Lukeneder

With 2 Figures and 1 Table

Natural History Museum Vienna, Department of Geology & Palaeontology, Burgring 7, 1010 Vienna, Austria;
e–mail: andreas.kroh@nhm–wien.ac.at, thomas.nichterl@nhm–wien.ac.at, alexander.lukeneder@nhm–wien.ac.at

Introduction

The collection of the Natural History Museum Vienna (NHMW) contains abundant material from the Triassic deposits cropping out in the vicinity of St. Cassian, South Tyrol (Italy). In total the collection contains more than 50 drawers of material including numerous types and figured specimens. Unfortunately, most of the material is accompanied by vague locality information only, being attributed to "St. Cassian" or "Stuores Mergel". We have reason to assume that the majority of these specimens come from the region of the Carnian candidate type section at "Stuores Wiesen" in the neighbourhood of Pralongià, SW of San Cassiano. Numerous other localities, however, are documented in the collection as well (Tab. 1).

Origin of the collection

Most of the Cassian Bed specimens of the NHMW were collected during the 19th century. Major acquisitions were made in 1842 (donated by the physician Rinna von Sarenbach, Vienna), 1847 (bought from the mineral dealer Dr. Baader, Heidelberg), 1864 (donated by the Geological Survey of Austria, Vienna), 1865 (exchange with L. Liebner, Innsbruck), 1884 (bought from collectors J. Ninz, J. Ploner and B. Canins, St. Cassian) and 1897 (bought from collector J. Ploner, St. Cassian). A few additional specimens were acquired in the early 20th century from the heirs of Austrian fossil collectors (1926: Dr. Heinrich, Bischofshofen; 1928: Carl Eckhart, Vienna).

Research history

In the 1860s Gustav Carl Laube (* 9.1.1839 Teplitz, Bohemia; † 12.4.1923 Prag) was briefly employed at the Hof–Mineralienkabinett in Wien (today the Natural History Museum Vienna) and at the k. & k. Polytechnisches Intitut, a precursor of the Vienna University of Technology. During this time he studied the material of the Cassian Beds housed at these institutions, as well as the material kept at the Geologische Reichsanstalt (today the Geological Survey of Austria). Comparing these specimens with Münster's type material housed in Munich (at the Bavarian State Collection for Palaeontology) he critically revised the complete invertebrate fauna of the Cassian Beds, synonymising many of the species previously established by Münster and Klipstein. His results were published in a series of papers in the Denkschriften der k. & k. Akademie der Wissenschaften during the years 1865 to 1870.

Laube's material and additional Cassian specimens present in the NHM Vienna collection formed the basis for many subsequent studies (Fig. 1). These focussed mainly on the gastropod fauna of the Cassian Beds, e.g. Kittl (1891, 1892, 1894), Bandel (1991, 1992, 1993a, b, 1994, 1995) and Schwardt (1992).

Cassian bed type material

Currently the NHM Vienna collection contains 162 holotypes, 16 paratypes, 96 syntypes, 502 figured specimens and 40 lots of reference specimens from the Cassian Beds (Fig 2A). Most of the types and reference specimens are gastropods (544 lots), followed

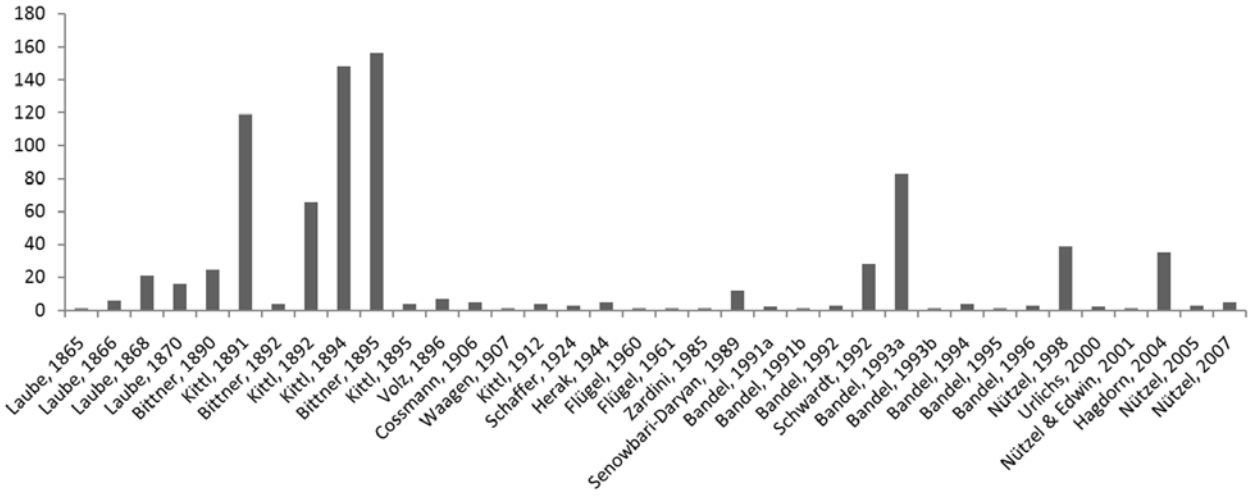

Fig. 1: Number of type and figured specimens in the NHMW collection per publication.

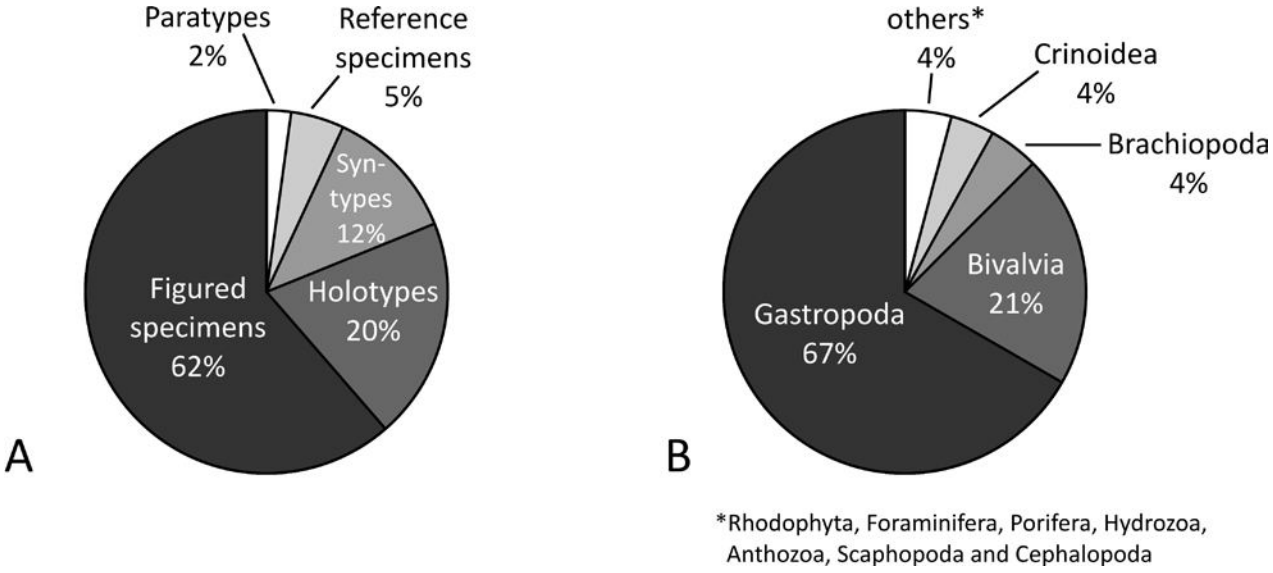

Fig. 2: Proportions of type figured and reference specimens (A) and their systematic provenance (B).

by bivalves (171 lots), crinoids (35 lots), brachiopods (32 lots), sponges (16 lots) and other groups (18 lots) (Fig. 2B). Additionally, abundant non–type material from the Cassian Beds is available for study at the NHM Vienna. Although some of the latter have been determined, the large majority remains unstudied so far.

Information on the type and reference specimens is available via the OeTyp–Website (http://www.oeaw.ac.at/oetyp/palhome.htm). The OeTyp–Project is a joint effort of the Austrian Academy of Sciences (Commission for the Palaeontological and Stratigraphical Research of Austria) and the Natural History Museum Vienna to provide data on palaeontological types, figured specimens and reference material in Austrian collections. Currently the database contains more than 70,000 animal and plant fossils. Regular updates are provided as further published fossil material is included.

Cassian bed localities in the NHMW collection
Andráz-Piere
Coldo Oi
Covara
Falzarego
Grones
Heilig Kreuz
La Fraina
Livinalongo, near Buchenstein (Castell-Berg)
Poroloi
Pré di Medesch, near Lavarella
Prelongei
Preromang
Ridma
Romerlo, near Cortina
Schlern
Schluderbach
Seelandalpe
Set Sass
St. Cassian
St. Vigil
Stern
Stuores, near Badia
Tofana
Valparola
Wengen

Tab. 1: List of Cassian bed localities represented in the NHM collection. The names are provided as stated on the labels. Localities represented by single or very few specimens only are not listed.

References

Bandel, K. (1991a): Schlitzbandschnecken mit perlmutteriger Schale aus den triassischen St. Cassian–Schichten der Dolomiten. – Ann. Naturhist. Mus. Wien, 92A: 1–53.

Bandel, K. (1991b): Über triassische "Loxonematoidea" und ihre Beziehungen zu rezenten und palaeozoischen Schnecken. – Paläont. Z., 65/3–4: 239–268

Bandel, K. (1992): Ueber Caenogastropoda der Cassianer Schichten (Obertrias) der Dolomiten (Italien) und ihre taxonomische Bewertung. – Mitt. Geol. Palaeont. Inst. Univ. Hamburg, 73: 37–97.

Bandel, K. (1993a): Trochomorpha (Archaeogastropoda) aus den St. Cassian–Schichten (Dolomiten, Mittlere Trias). – Ann. Naturhist. Mus. Wien, Ser. A., 95: 1–99.

Bandel, K. (1993b): Caenogastropoda during Mesozoic times. – Scripta Geol., Spec. Issue, 2: 7–56.

Bandel, K. (1994): Triassic Euthyneura (Gastropoda) from St. Cassian Formation (Italian Alps) with a discussion on the evolution of the Heterostropha. – Freiberger Forschungsh., C452: 79–100.

Bandel, K. (1995): Mathildoidea (Gastropoda, Heterostropha) from the Late Triassic St. Cassian Formation. – Scripta Geol., 111: 1–83.

Bandel, K. (1996): Some heterostrophic gastropods from Triassic St. Cassian Formation with a discussion of the classification of the Allogastropoda. – Paläont. Z., 70/3–4: 325–365.

Bittner, A. (1890): Brachiopoden der alpinen Trias. – Abh. k. k. Geol. Reichsanst., 14: 1–320.

Bittner, A. (1892): Brachiopoden der alpinen Trias. Nachtrag I. – Abh. k. k. Geol. Reichsanst., 17/2: 1–39.

Bittner, A. (1895): Lamellibranchiaten der Alpine Trias, I. Theil: Revision der Lamellibranchiaten von St. Cassian. – Abh. k. k. Geol. Reichsanst., 18/1: 1–236

Cossmann, M. (1906): Essais de paléoconchologie comparée, Vol. 7: 261 p., 14 pl. – Paris.

Flügel, E. (1960): *Cassianostroma* n. gen., die erste Hydrozoe aus den Cassianer-Schichten (Ober–Ladin) der Suedalpen. – N. Jb. Geol. Palaeont. Mh., 1960: 49–59.

Flügel, E. (1961): Algen (Solenoporaceen) aus den Cassianer-Schichten (Ober-Ladin) der Südalpen. – N. Jb. Geol. Paläont. Mh., 1961: 339–345.

Hagdorn, H. (2004): *Cassianocrinus varians* (Münster, (1841) aus der Cassian–Formation (Trias, Oberladin/Unterkarn) der Dolomiten – ein Bindeglied zwischen Encrinidae und Traumatocrinidae (Crinoidea, Articulata). – Ann. Naturhist. Mus. Wien, Ser. A, 105: 231–255.

Herak, M. (1944): Zur Kenntnis triadischer Kalkschwämme (Sycones). – N. Jb. Min. Geol. Paläont., Abt. B, 60: 107–135.

Kittl, E. (1891): Die Gastropoden der Schichten von St. Cassian der suedalpinen Trias. 1. Teil. – Ann. k. k. Naturhist. Hofmus. Wien., 6: 166–262.

Kittl, E. (1892): Die Gastropoden der Schichten von St. Cassian der suedalpinen Trias. 2. Teil. – Ann. k. k. Naturhist. Hofmus. Wien, 7/1–2: 35–97.

Kittl, E. (1894): Die Gastropoden der Schichten von St. Cassian der suedalpinen Trias. 3. Teil. – Ann. k. k. Naturhist. Hofmus. Wien, 9/2: 143–277.

Kittl, E. (1895): Die triadischen Gastropoden der Marmolata und verwandter Fundstellen in den weissen Riffkalken Südtirols. – Jb. k. k. Geol. Reichsanst., 44/1: 99–182.

Kittl, E. (1912): Materialien zu einer Monographie der Halobiidae und Monotidae der Trias. – Resultate wiss. Erforsch. Balatonsee 1/1, Paläont. Anh., 2/4: 1–229.

Laube, G. C. (1865): Die Fauna der Schichten von St. Cassian. Ein Beitrag zur Palaeontologie der alpinen Trias. – Denkschr. k. Akad. Wiss. math. –naturwiss. Cl., 24: 223–296.

Laube, G. C. (1866): Die Fauna der Schichten von St. Cassian. Ein Beitrag zur Palaeontologie der alpinen Trias. –Denkschr. k. Akad. Wiss. math. –naturwiss. Cl., 2. Abt., 25: 1–76.

Laube, G. C. (1868): Die Fauna der Schichten von St. Cassian. Ein Beitrag zur Palaeontologie der alpinen Trias. III. Abtheilung. Gastropoden. I. Hälfte. – Denkschr. k. Akad. Wiss. math. –naturwiss. Cl., 28/2: 29–94.

Laube, G. C. (1870): Die Fauna der Schichten von St. Cassian. Ein Beitrag zur Palaeontologie der alpinen Trias. IV. Abtheilung. Gastropoden. II. Hälfte. – Denkschr. k. Akad. Wiss. math. –naturwiss. Cl., 30/2: 1–48.

Nützel, A. (1998): Über die Stammesgeschichte der Ptenoglossa (Gastropoda). – Berlin. Geowiss. Abh. (E), 26: 1–229.

Nützel, A. (2005): A new Early Triassic gastropod genus and the recovery of gastropods from the Permian/Triassic extinction – Acta Palaeont. Polonica, 50/1: 19–24.

Nützel, A. (2007): Two new caenogastropod genera from the Late Triassic Cassian Formation. – Zitteliana, 47: 55–60.

Nützel, A. & Erwin, D. H. (2001): New Late Triassic Gastropods from the Wallowa Terrane (Idaho) and their biogeographic Significance. – Facies, 45: 87–92.

Schaffer, F. X. (1924): Lehrbuch der Geologie. 2. Teil. Grundzüge der historischen Geologie (Geschichte der Erde, Formationskunde). 1.–3. Aufl. – 628 pp., F. Deuticke, Leipzig & Wien.

Schwardt, A. (1992): Revision der *Wortheniella*–Gruppe (Archaeogastropoda) der Cassianer Schichten (Trias, Dolomiten). – Ann. Naturhist. Mus. Wien, Ser. A, 94: 23–57.

Senowbari–Daryan, B. (1989): Spicula in segmentierten Schwämmen. – Berlin. Geowiss. Abh., (A) 106: 473–515.

Urlichs, M. (2000): *Germanonautilus* (Nautiloidea) aus dem Unterkarnium der Dolomiten (Obertrias, Italien). – Stuttgarter Beitr. Naturk., Ser. B (Geol. Paläont.), 291: 1–13.

Volz, W. (1896): Die Korallen der Schichten von St. Cassian in Sued–Tirol. In: Frech, F. & Volz, W. Die Korallenfauna der Trias. – Palaeontogr., 43: 1–124, Stuttgart. [material largerly at the GBA]

Waagen, L. (1907): Die Lamellibranchiaten der Pachycardientuffe der Seiser Alm nebst vergleichenden paläontologischen und phylogenetischen Studien. (Fortsetzung, II. Teil, zu A. Bittner, Lamellibranchiaten der alpinen Trias). – Abh. k. k. Geol. Reichsanst., 18/2: 1–180.

Zardini, R. (1985): Fossili Cassiani (Trias Medio–Superiore). Primo aggiornamento all'Atlante dei Bivalvi e secondo aggiornamento all'Atlante Gasteropodi della formazione di S. Cassiano raccolti nella regione Dolomitica attorno a Cortina D'Ampezzo. – 17 pp., Ghedina, Cortina d'Ampezzo.

Geo.Alp, Vol. 8, S. 146–155, 2011

PLANT FOSSILS IN THE CASSIAN BEDS AND OTHER CARNIAN FORMATIONS OF THE SOUTHERN ALPS (ITALY)

Evelyn Kustatscher[1], Fabrizio Bizzarrini[2] & Guido Roghi[3]

Mit 16 Abbildungen und 3 Tabellen

[1] Naturmuseum Südtirol, Bindergasse 1, 39100 Bozen, Italy
[2] C/o Museo Civico di Rovereto, Borgo S. Caterina 41, I-38068 Rovereto
[3] Istituto di Geoscienze e Georisorse-CNR-Sezione di Padova, c/o Dipartimento di Geoscienze, Università degli Studi di Padova, Padova, Italy.

Introduction

Triassic macrofloras in the Southern Alps are rare, and the majority of literature data is devoted to Ladinian plants. The first plant remain from the Southern Alps, a not better defined "fern fragment", has been illustrated by Wissmann and Münster (1841). Later, several authors mentioned and figured plant fossils from the so-called "Buchensteiner Schichten", "Wengener Schichten" and *"alpiner Muschelkalk"* of the Dolomites (e.g., Mojsisovics, 1879; Ogilvie Gordon, 1927, 1934; Leonardi, 1953; for an overview see Wachtler & van Konijnenburg-van Cittert, 2000). Only Koken (1913) indicated badly preserved plant remains from the Heiligkreuz Schichten without describing or figuring them. Outside the Dolomites, only two more localities rich in Triassic plant remains were known: the Anisian flora of Recoaro (e.g., De Zigno, 1862; Schenk, 1868) and the Carnian flora of Raibl/Cave del Predil (e.g., Bronn, 1858; Schenk, 1866-7, Stur, 1868, 1885).
In the last few years several outcrops were found, yielding well-preserved plant fossils, some of them are Carnian in age such as Dogna in the Julian Alps, Stuores near Corvara, Heiligkreuz near Badia and Rifugio Dibona section near Cortina in the Dolomites. These floras, together with the Raibl flora, give a nice overview on the Carnian floras of the Southern Alps.

The floras

2.1 Heiligkreuz (Dolomites)

The plant remains from Heiligkreuz were collected from the horizon described by Bosellini as Strati di Santa Croce (Bosellini e Largaiolli, 1965): The plant remains belong to the Heiligkreuz Formation which means a Carnian (late Julian - early Tuvalian) age. The Tanatocenosis of the strata with the plant fossils contains *Unionites munsteri* and *Ptychostoma pleurotomoides* as well as *Renngartenella sanctaecrucis*. Two specimens represent leaf sheets (up to 53 mm long and 16 mm wide) with the typical fused leaf teeth belonging to *Equisetites* (Pl. 1, Fig. 1). Seven plant fragments were collected from this site. Small conifer shoot fragments are up to 30 mm long and 10 mm wide (Pl. 1, Fig. 2). The leaves are rhomboidal (4.5 x 3.5 mm) with distinct costae.

2.2. Stuores Wiesen (Dolomites)

The plant remains from Stuores were collected during an excavation of a nothosaurid skeleton in a calcareous layer of the San Cassian Formation. This gives the flora an early Carnian (Julian) age. Disarticulated mollusks were also found as well as teeth of other vertebrates such as *Cymadontoidea*, *Colobodus*, *Hybodus* and *Paleobates* (Bizzarini et al., 2001).

Fig. 1: Location of the various plant localities in the Dolomites.

Small conifer shoot fragments are up to 65 mm long and 9.5 mm wide (Pl. 1, Fig. 3). The leaves are rhomboidal (4.5 x 3.5 mm) with distinct costae.

2.3. Dogna (Julian Alps)

The flora from Dogna in the Julian Alps has been collected from the Rio del Lago Formation and is, thus, also early Carnian in age (Roghi et al., 2006a). Preliminary studies had permitted to distinct at least six different taxa. A few stem impressions (45 mm long and up to 2 mm wide) with distinct vascular bundles belong to equisetalean stem fragments. A few frond fragments belong to the fern genus *Danaeopsis* Heer ex Schimper 1869. The fragments (up to 20 mm long and 35 mm wide) are characterized by secondary veins arising acutely (50°) from the stout midrib, forking at least once near the midrib (Pl. 1, Fig. 4). The almost complete absence of anastomosing veins near the margin and a low number of vein bifurcations within the lamina suggests a resemblance with the species *D. angustifolia* (Kustatscher et al., submitted). Several frond fragments belong to *Ptilozamites sandbergeri* (Schenk) Kustatscher & Van Konijnenburg-van Cittert, 2007 (Pl. 1, Fig. 5). This seed fern is characterized by simple pinnate leaves, up to 120 mm long and 30 mm wide. The axis is slightly striate (2-4 mm), the sub-rectangular to sub-triangulate pinnules (6-22 mm long and 3-8 mm wide) are inserted perpendicularly and with an expanded basis. Each pinna displays 6–8 parallel veins, and a distinct margin.

The most abundant group are the conifers with at least three different taxa distinguished by their leaf shape and cuticles (Roghi et al., 2006a). The first type (Pl. 2, Fig. 3) is characterized by up to 15 cm long and 3-4 cm wide shoots covered by spirally arranged rhomboidal leaves (7-8.5 mm long and 4-6 mm wide). The leaves are too strongly carbonised to yield cuticles. This taxon resembles the specimens described by Dobruskina et al. (2001, pl. 15, figs. 1-3) as *Voltzia haueri* Stur.

The second conifer type (Pl. 2, Fig. 1) has smaller shoots (up to 4 cm long and 1 cm wide), bearing more delicate leaves (2-2.5 x 3-3.5 mm) with a rhomboidal shape and an obtuse apex. The thick cuticle shows stomata arranged in short rows. The walls of the 4-6 subsidiary cells are thickened on the inner side, while the large papillae cover partially the stomatal pit resembling the cheirolepidiaceous. The last type consists of up to 10 cm long and 0.6 cm wide shoot fragments with slightly falcate, spirally and closely arranged leaves (3.5-4 mm long and 2.5 mm wide) (Pl. 2. Fig. 2). The dicyclic stomata with circles of 8-10 thickened subsidiary cells are arranged in short longitudinal rows. Papillae cover the stomatal pit.

2.4. Rifugio Dibona (Dolomites)

The flora of Dibona is mostly famous because of the amber drops which were found, partly together with plant remains, in the sediments of the Heiligkreuz Formation, being thus of upper Carnian age. Macroremains are seldom found in the sediments. They belong to equisetalean stem fragments and conifer shoots (Pl. 2, Fig. 4) probably of the genus *Voltzia*. Of particular interest are the dispersed leaves (Pl. 2, Fig. 5) that have been found in the same horizon of the amber drops. Those are wide triangular to rhomboidal in shape, with an obtuse apex (4.5-6 x 3-4.5 mm). The stomata are arranged in short rows and are characterized by a circle of 4-6 subsidiary cells.

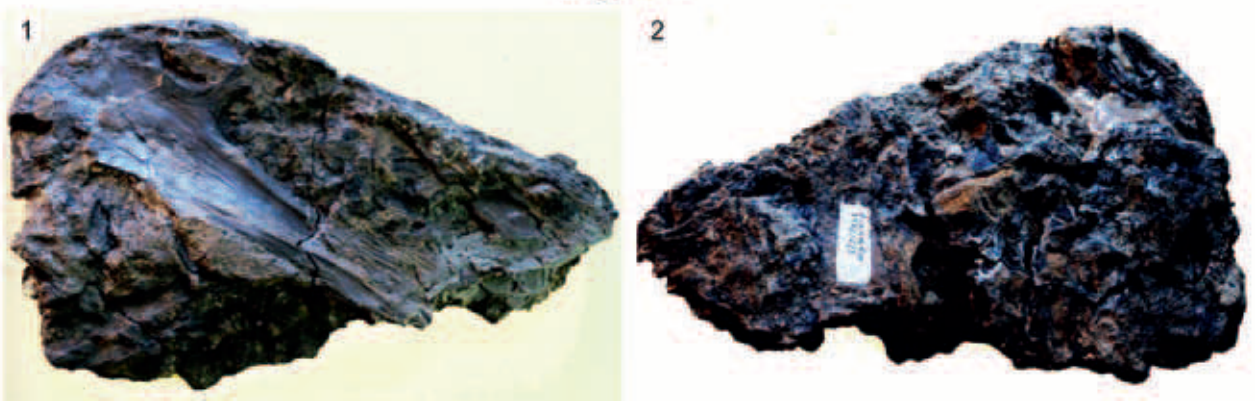

Fig. 2: Charcoal fragments on the back of *Metoposaurus santacrucii* Koken 1913.

2.5. Raibl/Cave del Predil (Julian Alps)

The flora from Raibl is, together with those from Lunz and Neuewelt, one of the most famous Upper Triassic (Carnian) floras in the Alps. It has been attributed to the lower part of the Raibl Formation, corresponding to the Predil Limestone (De Zanche et al., 2000), belonging thus to the lower Carnian. The flora has been studied mostly in the second half of the 19th century (e.g., Bronn, 1858; Schenk, 1866-7, Stur, 1868, 1885); lately Dobruskina et al. (2001) published an overview on the flora, consisting of circa 600-650 specimens.

According to the literature this flora is nicely diversified. The horsetails are represented by *Equisetites arenaceus* (Jaeger) Schenk 1864 although in literature *Calamites raiblensis* Schenk 1865 and *Equisetites strigatum* Stur 1885 are mentioned as well. The latter corresponds to *Phylladelphia strigata* Bronn 1858, an enigmatic fossil (for more details see Kustatscher & Van Konijnenburg-van Cittert, 2008) (Pl.2, Fig. 9). The ferns are represented by frond fragments of taxa well represented in Middle Triassic floras such as *Neuropteridium grandifolium* (Schimper et Mougeot) Compter 1883, *Neuropteridium elegans* (Brongniart) Schimper 1869, *Chiropteris lacerata* (Quenstedt) Rühle von Lilienstern 1931, *Cladophlebis ruetimeyeri* (Heer) Leonardi 1953 (Pl. 2, Fig. 8) and perhaps *Cladophlebis leuthardtii* Leonardi 1953. *Ptilozamites sandbergeri* (Schenk) Kustatscher & Van Konijnenburg-van Cittert, 2007 (Pl. 3, Fig. 2) is numerous. The cycads are represented by *Sphenozamites bronnii* (Schenk) Passoni et al. 2003 (Pl. 3, Fig. 3); probably *Pterophyllum giganteum* Schenk 1865 and *Pterophyllum longifolium* Stur 1885 fall also within its variability. Some entire-leaved cycads might belong to the genus *Macrotaeniopteris* or *Bjuvia*. The conifers are the most abundant group of the flora and several species have been created for this flora such as *Voltzia haueri* Stur 1885, *Voltzia raiblensis* Stur 1885 (Pl. 3, Fig. 6) and *Cephalotaxites raiblensis* Stur 1885. *Pelourdea vogesiaca* (Schimper et Mougeot) Seward 1917 (Pl. 3, Fig. 5) is also abundant in this flora. A modern taxonomic revision of this flora (in progress) will permit to understand how diversified this flora is.

2.6. Additional plant remains

Charcoalified wood, seeds and small conifer shoots have been also collected from Pralongià (com. pers., Helmut Buratti, 2011), Misurina (com. pers., Alexander Nützel, 2011). Additionally, the *Metoposaurus santacrucii* of Koken (1913) shows on the backside of the sample a high frequency of charcoal fragments (Fig. 2). Late Carnian plant remains are also known from Lastoni di Formin in the Dolomites (Heiligkreuz Formation) (Roghi et al., 2006a). Also in this case, the plant remains belong mostly to the conifers (mainly as isolated leaves) while some other fragments belong probably to the sphenophytes.

Acknowledgements

We wish to thank Alexander Lukeneder and Andreas Kroh (Naturhistorisches Museum Wien) and Irene Zorn and Barbara Meller (Austrian Geological Survey) for the help during the study of the Raibl flora. The project "Taxonomic revision of the Carnian (Upper Triassic) conifers from the historical Raibl flora from Northern Italy " (AT-TAF-2999) received funding through SYNTHESYS, which is made available by the European Community - Research Infrastructure Action under the FP6 „Structuring the European Research Area" Programme.

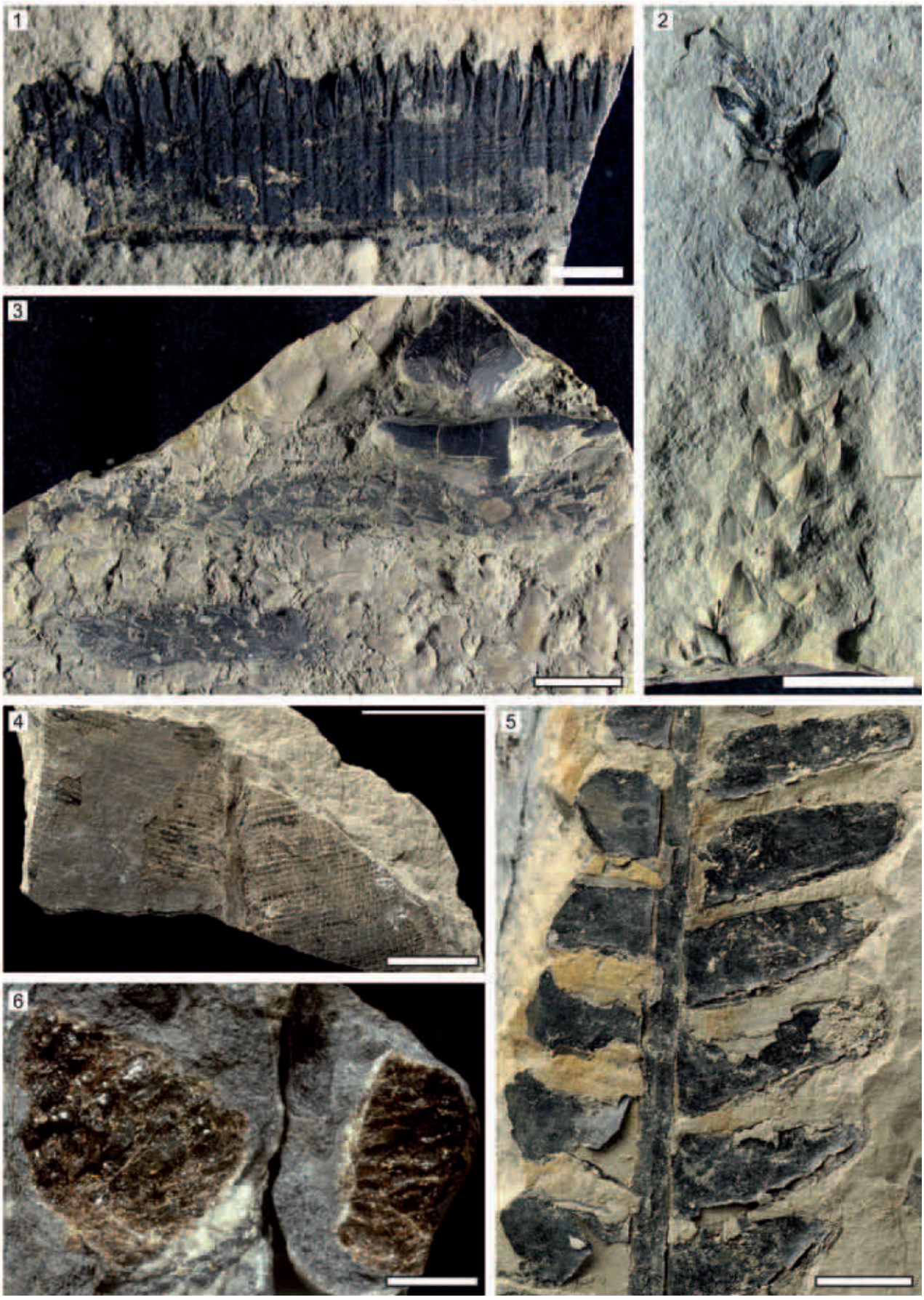
1
2
3
4
5
6

Plate 1 (scale = 1 cm if not indicated differently)

Fig. 1: *Equisetites* sp., leaf sheet, Heiligkreuz, Heiligkreuz Formation.
Fig. 2: *Voltzia* sp., shoot fragment, Heiligkreuz, Heiligkreuz Formation.
Fig. 3: *Voltzia* sp., shoot fragments together with bone fragments, Stuores, San Cassian Formation.
Fig. 4: *Danaeopsis angustifolia* (Kustatscher et al., submitted), frond fragment, Dogna, Rio del Lago Formation (CHIUT 107).
Fig. 5: *Ptilozamites sandbergeri* (Schenk) Kustatscher & Van Konijnenburg-van Cittert, 2007 frond fragment, Dogna, Rio del Lago Formation (CHIUT 104).
Fig. 6: Amber fragment, Dogna, Rio del Lago Formation.


1
2
3
4
5
8
9
6
7

Plate 2 (scale = 1 cm if not indicated differently)

Fig. 1: *Brachyphyllum* sp., shoot fragment, Dogna, Rio del Lago Formation (CHIUT 14), scale = 0.5 mm.
Fig. 2: Shoot of the conifer taxon 3, Dogna, Rio del Lago Formation (CHIUT 11), scale = 0.5 mm.
Fig. 3: *Voltzia* sp., shoot fragment, Dogna, Rio del Lago Formation (CHIUT 84).
Fig. 4: Shoot of the conifer taxon 3, Dogna, Rio del Lago Formation (CHIUT 11), scale = 0.5 mm.
Fig. 5: Dispersed leaves and amber drops from the paleosoil, Dogna, Rio del Lago Formation.
Fig. 6: conifer dwarf shoot, Dibona, Heiligkreuz Formation, scale = 0.5 mm.
Fig. 7: seed, Dibona, Heiligkreuz Formation, scale = 0.5 mm.
Fig. 8: *Cladophlebis ruetimeyeri* (Heer) Leonardi 1953, frond fragment, Raibl/Cave del Predil, Raibl Formation (GBA 2007-072-0012).
Fig. 9: *Phylladelphia strigata* Bronn 1858, enigmatic fossil, Raibl/Cave del Predil, Raibl Formation (NHM 1866 XL 464).


1
2
3
4
5
6

Plate 3 (scale = 1 cm if not indicated differently)

Fig. 1: *Equisetites* sp., Raibl/Cave del Predil, Raibl Formation (NHM 1887 IX 68).

Fig. 2: *Ptilozamites sandbergeri* (Schenk) Kustatscher & Van Konijnenburg-van Cittert, 2007, frond fragment, Raibl/Cave del Predil, Raibl Formation (GBA 2005-0008-004).

Fig. 3: *Sphenozamites bronnii* (Schenk) Passoni et al. 2003, leaf fragment, Raibl/Cave del Predil, Raibl Formation (GBA 2007-072-0060).

Fig. 4: *Voltzia* sp., shoot fragment, Raibl/Cave del Predil, Raibl Formation (GBA 1986-2-06).

Fig. 5: *Pelourdea vogesiaca* (Schimper et Mougeot) Seward 1917, leaf fragment, Raibl/Cave del Predil, Raibl Formation (NHM 2007B0003-0017).

Fig. 6: *Voltzia raiblensis* Stur 1885, shoot fragment, Raibl/Cave del Predil, Raibl Formation (NHM 1864 LII 39).

References

Bechstädt, T.H. & Brandner, R. (1970): Das Anis zwischen St. Vigil und dem Höhlensteintal (Pragser und Olanger Dolomiten, Südtirol). – Festband des Geologischen Institutes, 300-Jahr-Feier Universität Innsbruck, 9-103.

Bizzarini, F., Prosser, G. & Prosser, I. (2001): Osservazioni preliminari sui resti di vertebrati della formazione di S. Cassiano del Bosco di Stuores (Dolomiti nord-orientali). - Ann. Mus. Civ. Rovereto, 17: 137-148.

Bosellini A. & Largaiolli T. (1965): Contributo alla conocenza degli strati di S. Croce (Val Badia - Dolomiti). – Stud. Trent. Sci. Nat., Sez. A, 42: 5-12.

Bronn, H. G. (1858): Beiträge zur triasische Fauna und Flora der bituminösen Schiefer von Raibl, nebst Anhang über die Kurr'sche Sippe Chiropteris aus dem Lettekohlen-Sandstein. - N. Jahrb. Min., Geogn., Geol. Petrefactenk, 1: 1-63.

Calligaris, R. (1986): Geologia della Val di Braies e segnalazione di nuovo località fossilifere a vegetali nel Ladinico superiore. - Atti Museo Civ. St. Nat., 24(1): 1-64.

De Zigno, M.E. (1862): Sulle piante fossili del Trias di Recoaro raccolte dal Prof. A. Massalongo. - Mem. Ist. Ven. Sc. Lett. Arti, 11: 1-32.

Dobruskina, I.A., Jurkovsek B., Kolar Jurkovsek, T. (2001): Upper Triassic Flora from „Raibl beds" of Julian Alps (Italy) in Karavanke Mts. (Slovenia). - Geologija, 44(2): 263-290.

Koken, E. (1913): Beiträge zur Kenntnis der Schichten- von Heiligkreuz (Abteital, Südtirol). - Abh. k.k. geol. Reichsanst., 15: 1-43.

Kustatscher, E. & Van Konijnenburg-van Cittert, J.H.A. (2008): Considerations on *Phylladelphia strigata* Bronn from the historical Raibl flora (Carnian, lower Upper Triassic, Italy). - Geo.Alp, 5: 69-81.

Kustatscher, E., Van Konijnenburg-van Cittert, J.H.A., Roghi, G. (2010): Macrofloras and palynomorphs as possible proxies for palaeoclimatic and palaeoecological studies: A case study of Kühwiesenkopf / Monte Prà della Vacca (Olang Dolomites, N-Italy). - Palaeogeol., Palaeoclimatol., Palaeoecol., 291(1-2): 71-80.

Leonardi, P. (1953): Flora continentale Ladinica delle Dolomiti. - Mem. Ist. Geol. Min., 18: 1-22.

Mojsisovics, E. (1879): Die Dolomit-Riffe von Südtirol und Venetien: Beiträge zur Bildungsgeschichte der Alpen. - 551 pp., A. Hölder Verlag, Wien.

Ogilvie Gordon, M.M. (1927): Das Grödner-, Fassa- und Enneberggebiet in den Südtiroler Dolomiten. - Abh. Geol. Bundesanst., 24(2): 1-376.

Roghi G., Kustatscher E., Van Konijnenburg-van Cittert, J.H.A. (2006a): Late Triassic Plant from Julian Alps (Italy). - Boll. Soc. Paleont. It., 45 (1): 133-140.

Roghi, G., Ragazzi, E., Gianolla, P. (2006b): Triassic amber of the Southern Alps. - Palaios, 21: 143-154.

Schenk, A. (1866-7): Über die Flora der schwarzen Schiefer von Raibl. - Würzb. Naturwissensch. Zeitsch., 6: 10-20.

Schenk, A. (1866-7): Über die Flora der schwarzen Schiefer von Raibl. - Würzb. Naturwissensch. Zeitsch., 6: 10-20.

Schenk, A. (1868): Über die Pflanzenreste des Muschelkalk von Recoaro. - Geogn.- paläontol. Beitr., 2(1): 58-87.

Stur, D. (1868): Beiträge zur Kenntnis der geologischen Verhältnisse der Umgebung von Raibl und Kaltwasser. - Jb. geol. Reichsanst., 18: 71-122.

Stur, D. (1885): Die obertriadische Flora der Lunzer-Schichten und des bituminösen Schiefers von Raibl. - Sitzungsber. Kais. Akad. Wiss. Wien, Math Naturw. Kl., Abt. 1, 88(1): 93-103.

Stur, D. (1885): Die obertriadische Flora der Lunzer-Schichten und des bituminösen Schiefers von Raibl. - Sitzungsber. Kais. Akad. Wiss. Wien, Math Naturw. Kl., Abt. 1, 88(1): 93-103.

Wachtler, M., Van Konijnenburg - Van Cittert, J.H.A. (2000): The fossil flora of the Wengen Formation (Ladinian) in the Dolomites (Italy). – Beitr. Paläont., 25: 105-141.

Wissmann, H.L., Münster, G. Graf von (1841): Beiträge zur Geognosie und Petrefactenkunde des südöstlichen Tirol's vorzüglich der Schichten von St. Cassian. - 152 pp., Buchner'sche Buchhandlung, Bayreuth.

Geo.Alp, Vol. 8, S. 156–162, 2011

MICROBIALITES AS PRIMARY BUILDERS OF THE LADINIAN – CARNIAN PLATFORMS IN THE DOLOMITES: BIOGEOCHEMICAL CHARACTERIZATION

Tosti, Fabio[1], Guido, Adriano[1], Demasi, Fabio[1], Mastandrea, Adelaide[1], Naccarato, Attilio[2], Tagarelli, Antonio[2], Russo, Franco[1]

With 4 Figures

[1] Dipartimento di Scienze della Terra, Universitàdella Calabria, Via BucciCubo 15b, 87036 Rende (CS), Italy.
[2] Dipartimento di Chimica, Universitàdella Calabria, Via BucciCubo 12c, 87036 Rende (CS), Italy.

Introduction

The importance of automicrites or microbialites is well known in carbonate platform and reefal environments throughout Earth history (Reitner, 1993; Camoin et al., 1999). During the Proterozoic and early Palaeozoic, microbial carbonate mounds and reef-like structures were the world's first large-scale biotic constructions (Riding, 1991; Flügel et al., 1993; Riding & Awramik, 2000). From the late Palaeozoic onward, skeletal framebuilders, always associated with microbialites and microbially induced cements, played a leading role in constructing carbonate platforms. The ratio of microbialites to skeletal metazoans during geological time is characterized by phases in which microbialites greatly prevail, as in stressed environments or in the immediate aftermath of biological crises, and phases of equal coexistence of the two components (Webb, 1996; Russo et al., 1997, 1998; 2000; Kiessling et al., 2002; Riding, 2002; Russo, 2005).
An important example is constituted by the carbonate successions belonging to the Wengen and S. Cassiano formations, located in the Eastern Dolomites, Punta Grohmann, Sassolungo (Bz) (Fig. 1).
The Punta Grohmann section is one of the most classical Late Ladinian – Early Carnian basin successions of the Dolomites, described in several important papers (Ogilvie-Gordon, 1927; Leonardi, 1967; ScudelerBaccelle, 1971; Russo et al., 1997; Gianolla et al., 1998; Gianolla & Neri, 2007).
Many levels, occurring within this succession, contain gravity-displaced carbonate olistoliths, the so-called *„Cipit boulders"* of Richthofen (1860). They are fed to the basin by coeval prograding Cassian carbonate platforms (Assereto et al., 1977; Bosellini, 1984) or, in some cases, by pre-existing buildups undergoing erosion. While these platforms are completely dolomitized, generally the changes did not affect the Cipit boulders, because they are embedded in a marly matrix impermeable to diagenetic fluids (Biddle,1981; Russo et al., 1991). Therefore, the olistoliths and, in general, the gravity-resedimented carbonates occurring within the basin deposits, represent the unique evidence of the original fabric and texture of the ancient carbonate platform margin/ upper slope (Fürsich & Wendt, 1977; Fois & Gaetani, 1981; Biddle,1981; Brandner et al., 1991).
To corroborate the microbialitic model proposed by Russo et al. (1997) for the Late Ladinian – Carnian platform buildups, together with classical micro- and nanomorphological studies and EDS microanalyses we carried out detailed biogeochemical analyses on organic matter extracted from selected samples of carbonate boulders in order to confirm the role of microbialites as "primary builders" in the sense that they are syndepositionally cemented and dominate volumetrically the bioconstruction.

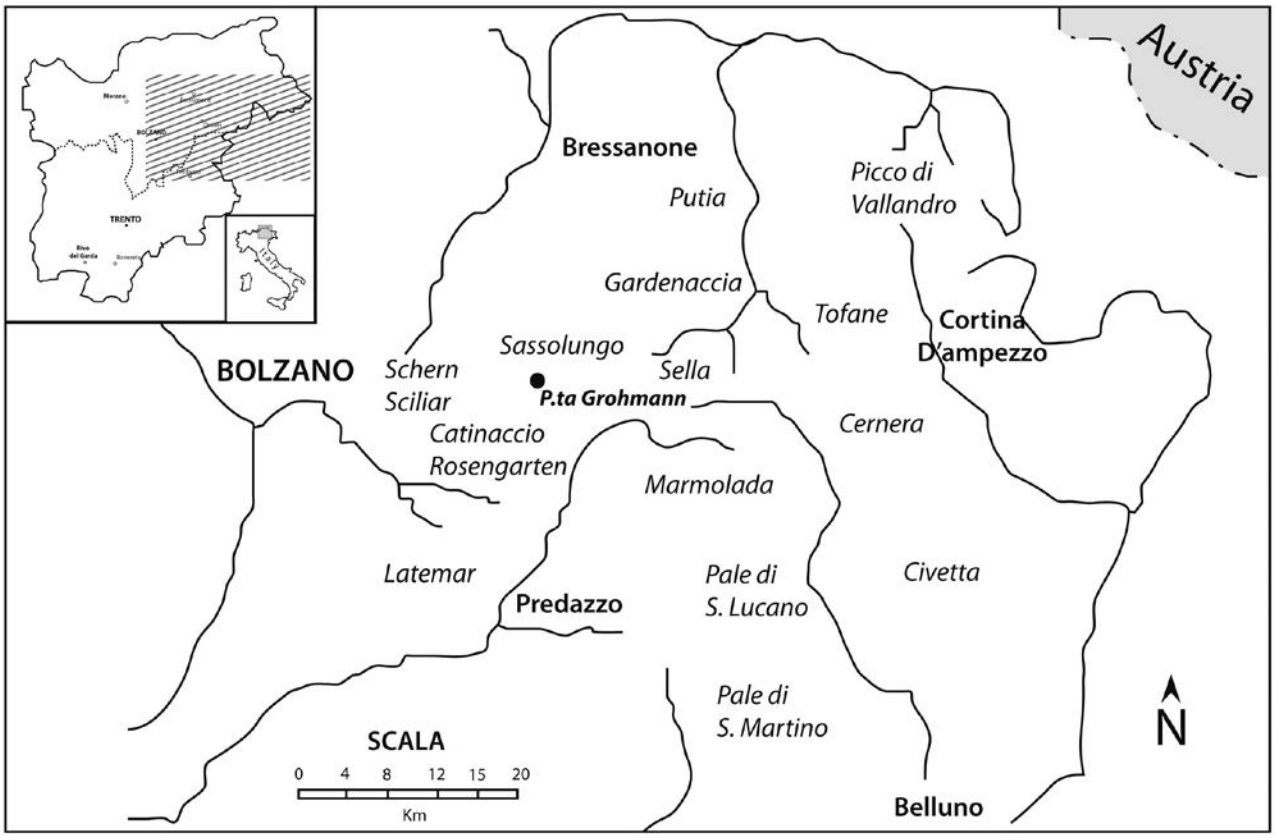

Fig. 1: Location map of Punta Grohmann (Sassolungo, BZ).

Sample Location

A stratigraphic scheme of the Punta Grohmann section is represented in Figure 2. The studied boulders are indicated with labels from U1 to U5 and have been sampled from two different sedimentary settings: unit c (olistolith fed by dismantling of a previous platform), unit d (swarm of Cipit boulders inserted randomly in the S. Cassiano succession). The third unit, labeled "e" in figure 2 is characterized by two coarsening upward cycles at the toe-of-slope, recording the progradation of an active platform, yielded samples not well preserved and unsuitable to be studied for the organic matter content.

Methods

The micro and nanomorphological analyses were performed using optical, UV fluorescence and scanning electron microscope (SEM) observations. Geochemical characterization was carried out with energy-dispersive X-ray spectrometer (EDS).

Organic matter characterization was made up in selected samples. They were grounded to a fine powder and organic compounds extracted using a mixture of solvents by ultrasonication. Total lipid extracts were fractionated by column chromatography into polar and apolar compounds. These hydrocarbon fractions were analyzed by Fourier Transform–Infrared Spectroscopy (FT-IR), in order to obtain a first global characterization of organic functional groups, and then by Gas Chromatography coupled to Mass Spectrometer (GC–MS), to detect and recognize specific macromolecules (biomarkers).

Results and Discussion

Microfacies are constituted on average by 15% of bioclasts, 10% of detrital micrite, 50% of microbialites, and 25% of cements. The bioclasts belong to metazoans, mainly stromatoporoids and inozoa, microproblematica (e.g. *Tubiphytes obscurus*, *Macrotubus babai*, *Plexoramea cerebriformis*), skeletal cyanobacteria (e.g. *Cladogirvanella cipitensis*), and rarely fragments of bivalves, gastropods and echino-

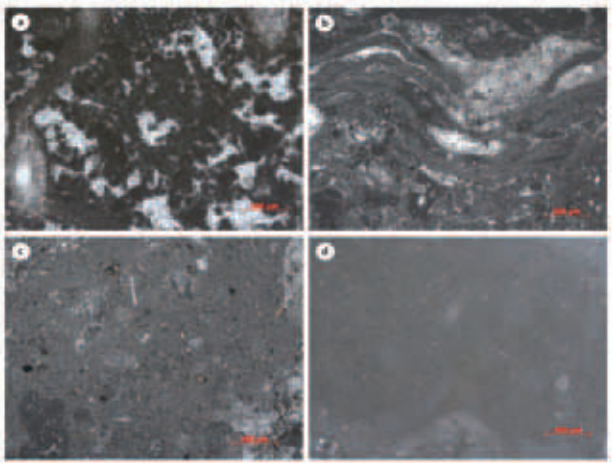

Fig. 3: Different types of micrites in the Punta Grohmann samples: a) thrombolitic micrite; b) stromatolitic micrite; c) detrital micrite; d) aphanitic micrite.

derms. The microbialites or automicrites, exhibit both dense microcrystalline (aphanitic) or peloidal microfabric, and sometimes are organized in stromatolitic laminae or thrombolitic fabric. Early cements are represented by botryoidal and fibrous infilling vugs and stromatactis-like cavities and late cements of ferroan blocky sparry calcite.

The distribution of organic matter remains was detected on the base of epifluorescence observations which revealed very bright fluorescence in the peloidal micrite.

Therefore, FT-IR and GC-MS analyses were carried out on total lipid extracts from this type of micrite. They revealed the presence of stretching C=C vibrations attributable to alkene and/or unsaturated carboxylic acids. GC-MS investigations indicated the presence of extended hopane series, short chain methyl-steranes (C_{22}, C_{23}), straight chain saturated (C_{14}, C_{16}), monounsaturated ($C_{17:1}$, $C_{18:1}$), and diunsaturated($C_{18:2}$) carboxylic fatty acids (Fig. 3).

The carboxylic acid pattern and pentacyclicterpanes series, recorded in the studied micrite, is similar to that found in microbial mats (Thiel et al., 1997; Ourisson et al., 1987; Brocks & Summons, 2004). Actually, straight chain saturated (C_{14}, C_{16}), monounsaturated ($C_{16:1}$, $C_{18:1}$) carboxylic acids and diunsaturated $C_{18:2}$ acids are also known as typical bacterial components (Kenyon et al., 1972; Cohen & Vonshak, 1991; Merrit et al., 1991; Thiel et al., 1997; Peters et al., 2005). Pentacyclicterpanes of the C_{27} to C_{31} extended hopane series are diagnostic of the bacteria domain. Biological precursors of extended hopanes, the bacteriohopanepolyols, likely have the physiological function of membrane rigidifiers in bacteria, a role in eukarya fulfilled by sterols (Ourisson et al., 1987; Brocks & Summons, 2004).

Although some authors suggested that thermal degradation of regular steranes (C_{27}–C_{29}) could be responsible for the formation of C_{21} and C_{22} short chain steranes (Huang *et al.*, 1994), 4-Methyl and 4,4-dimethyl steroids have been identified in cultures of methanotrophic bacteria (Bouvier et al., 1976; Schouten et al., 2000)

Conclusions

The Cipit boulders from the Punta Grohmann section contain automicrites analogous to those described in Reitner & Neuweiler (1995). These carbonate olistoliths are characterized by skeletal cyanobacteria and microproblematica, with a minor contribution by sponges, embedded in a large amount of stromatolitic and/or clotted peloidal micrite (Russo et al., 1997). Biomarker data confirmed the presence of bacteria/cyanobacteria communities during platform deposition, indicating that microbes have played a prominent role in the genesis of these carbonates. These communities created the chemical conditions that triggered the induced precipitation of great volumes of syndepositionally-cemented automicrites, which stabilized the carbonate bodies controlling their depositional geometries. Although following the Dunham classification (1962) these carbonates should be considered as "wackestone", the very early cementation of microbialites, confirmed by the presence of bacterial biomarkers and the steep depositional geometries suggest that Punta Grohmann carbonates must be classified as "boundstone" in which the bioconstructor role is played by microbialites.

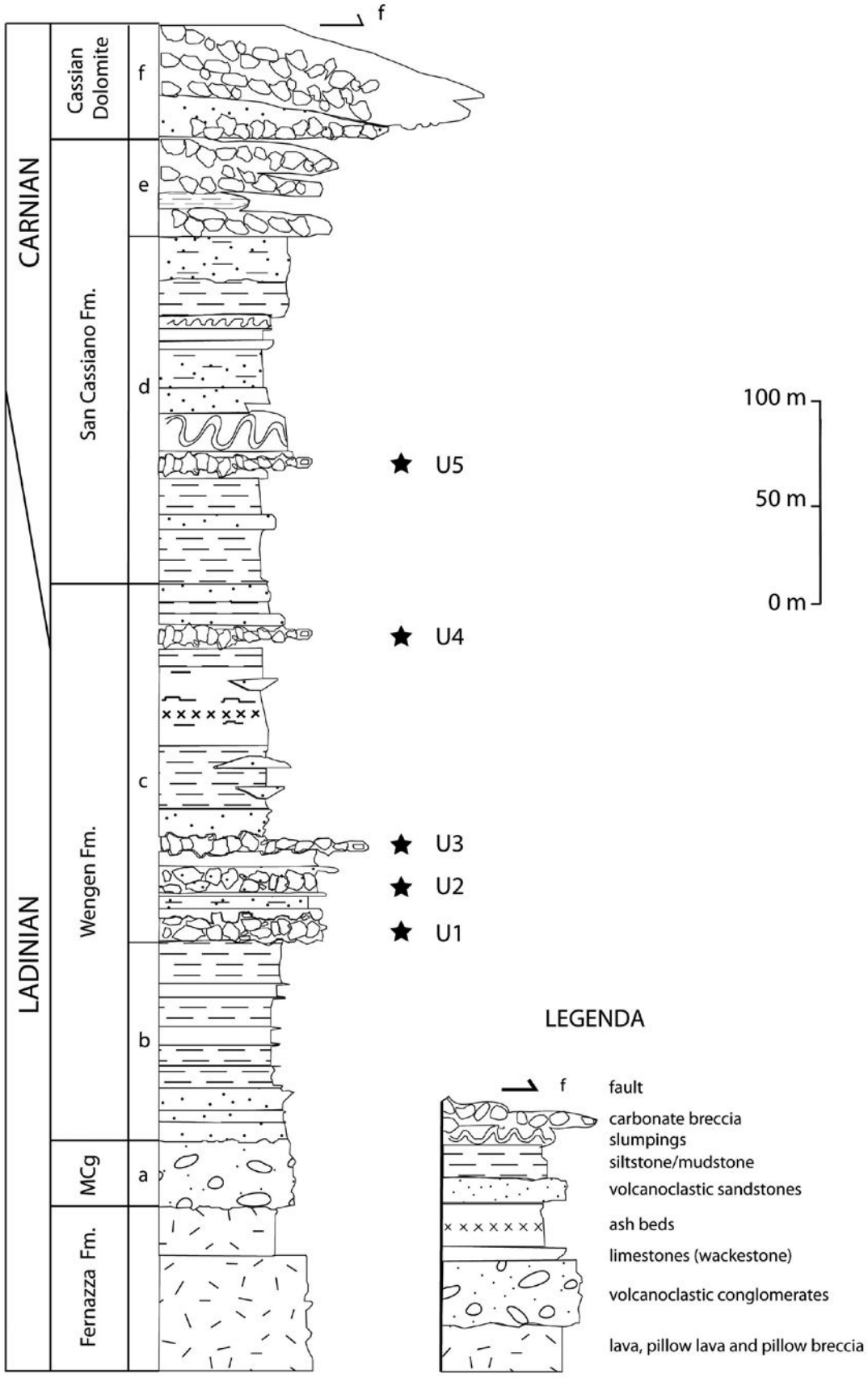

Fig. 2: Stratigraphic log of the studied section (modified from Russo et al., 1997).

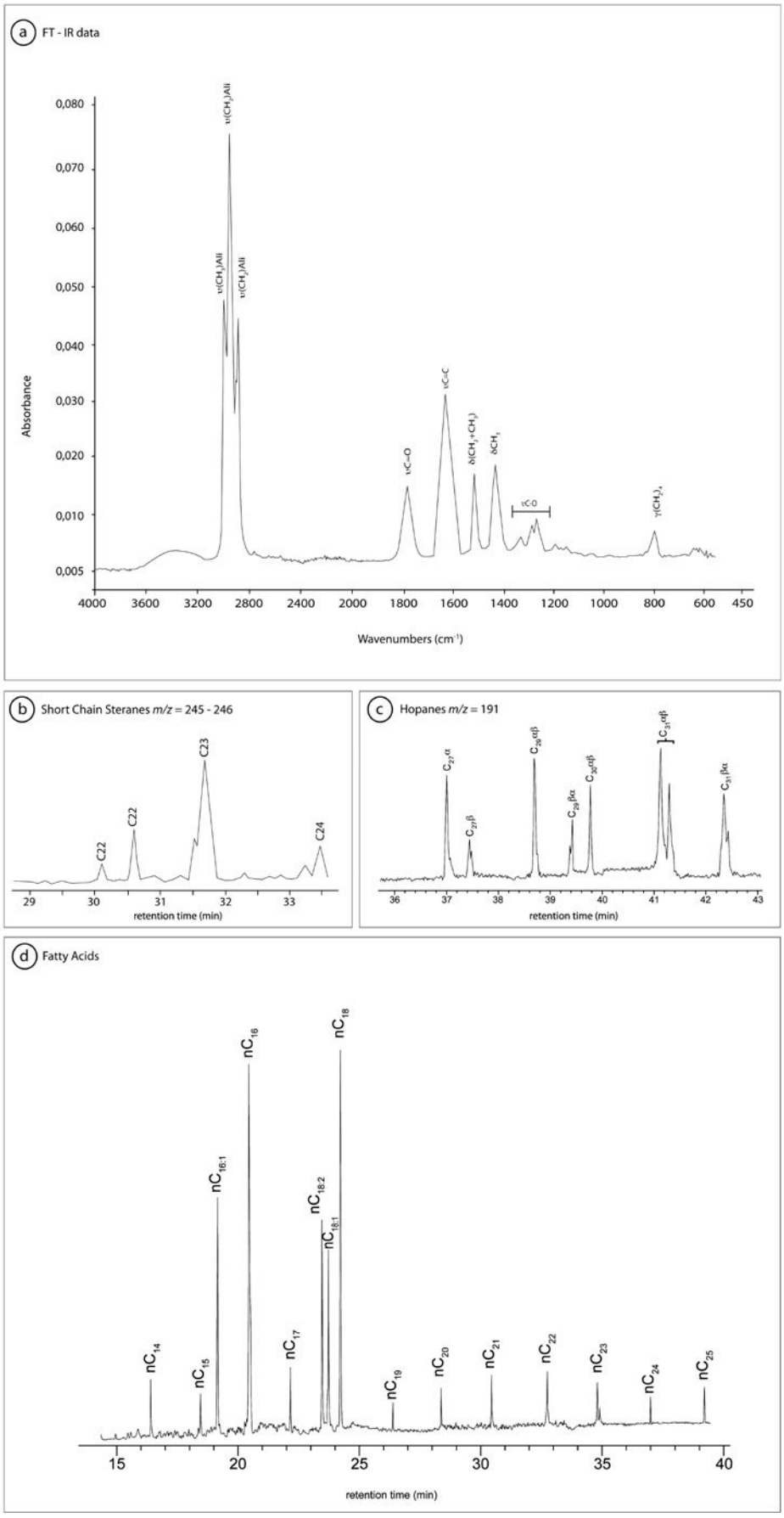

Fig. 4: FT-IR and GC-MS results of a selected sample showing functional groups and specific biomarkers of bacteria:
a)FT-IR spectrum on total lipid extracts;
b) Short chain steranes;
c) Hopanes;
d) Fatty acids distribution.

References

Assereto, R., Brusca, A., Gaetani, M., Jadoul, F. (1977): Le mineralizzazioni Pb-Zn nel Triassico delle Dolomiti: quadro geologico ed interpretazione genetica. – L'Industria Mineraria, 28: 367-402.

Biddle, K.T. (1981): The basinal Cipit boulders: indicators of Middle to Upper Triassic buildup margins, Dolomite Alps, Italy. – Riv. Ital. Paleont. Strat., 86: 779-794.

Bosellini, A., (1984): Progradation geometries of carbonate platform: example from the Triassic of the Dolomites, Northern Italy. – Sedimentology, 31: 1–24.

Bouvier, P., Rohmer, M., Benveniste, P., Ourisson, G. (1976): $\Delta^{8\,(14)}$ Steroids in the bacterium *Methylococcus capsulatus.* - Biochemistry, 159: 267–271.

Brandner, R., Flügel, E., Koch, R., Yose, L.A. (1991): The Nothern Margin of the Schlern/Sciliar – Rosengarten/Catinaccio Platform. - Dolomieu Conference on Carbonate Platform and Dolomitization, Field Guide Book, Ortisei/St. Urlich, Italy, Guidebook Excursion A, 1-61.

Brocks, J. J. & Summons, R. E. (2004): Sedimentary hydrocarbons, biomarkers for early life. - In: Schlesinger, W.H. (ed.): Treatise on Geochemistry. - Biogeochemistry, 63-115, Elsevier Pergamon, Oxford.

Camoin, G. F., Gautret, P., Montaggioni, L. F., Cabioch, G. (1999): Nature and environmental significance of microbialites in Quaternary reefs: the Tahiti paradox. - Sed. Geol., 126: 271–304.

Cohen, Z. & Vonshak, A. (1991): Fatty acid composition of Spirulina and Spirulina-like cyanobacteria in relation to their chemotaxonomy. - Phytochem., 3130: 205–206.

Dunham (1962): Classification of carbonate rocks according to depositional texture. - In: Ham, W. E. (ed.): Classification of carbonate rocks. - American Association of Petroleum Geologists Memoir, 108-121.

Flügel, E., Hillmer, G., Scholz, J. (1993): Microbial carbonates and reefs: an introduction. - Facies, 29: 1–2.

Fois, E. & Gaetani, M. (1981): The northern margin of the Civetta buildup. Evolution during the Ladinian and the Carnian. - Riv. It. Paleont. Strat., 86, 3: 469-542.

Fürsich, F.T. & Wendt, J. (1977): Biostratinomy and Palaeoecology of the Cassian Formation (Triassic) of the Southern Alps. - Palaeogeogr, Palaeoclimatol, Palaeoecol, 22: 257-323

Gianolla, P., De Zanche, V., Mietto, P. (1998): Triassic Sequence Stratigraphy in the Southern Alps. Definition of sequences and basin evolution. - In: De Graciansky, P.C., Hardenbol, J., Jacquin, T., Vail, P.R., Ulmer-Scholle, D. (eds.): Mesozoic- Cenozoic Sequence Stratigraphy of European Basins. - SEPM Special Publication, 60: 723-751.

Gianolla., P. & Neri, C. (2007): Formazione di Wengen. – In: Cita Sironi, M.B., Abbate, E., Balini, M. Conti, M.A., Falorni, P., Germani, D., Groppelli, G., Manetti, P., Petti, F.M. Carta Geologicad'Italia – 1:50.000, Catalogo delleFormazioni – Unitàtradizionali (2), QUADERNI serie III, 7/VIII, S.E.L.C.A., Firenze, 111-124.

Huang, D.F., Zhang, D.J., Li, J., (1994): The origin of 4-methylsteranes and pregnanes from Tertiary strata in the Qaidam Basin, northwest China. - Geochemistry 22: 343–348.

Kenyon, C. (1972): Fatty acid composition of unicellular strains of blue-green algae. - J. Bacteriol. 109: 827–834.

Kiessling, W., Flügel, E., Golonka, J. (2002): From patterns to processes: the future of reef research. - In: Kiessling, W., Flügel, E., Golonka, J. (eds.): Phanerozoic Reef Patterns. - SEPM Spec. Publ., 72: 735–743.

Leonardi, P. (1967): Le Dolomiti. Geologia dei Monti tra Isarco e Piave. - 1019 pp., Manfrini Ed., Rovereto.

Merrit, M. V., Rosenstein, S. P., Lojl, C., Chou, R. H., Allen, M.M. (1991): A comparison of the major lipid classes and fatty acid composition of marine unicellular cyanobacteria with freshwater species. - Arch. Microbiol. 155: 107–113.

Ogilvie-Gordon, M.M. (1927): Das Grödner-, Fassa- und Enneberggebiet in den SüdtirolerDolomiten. – Abh. Geol. Bundesanst., 24 (2): 1-376.

Ourisson, G., Rohmer, M., Poralla, K. (1987): Prokaryotic hopanoids and other polyterpenroid sterol surrogates. – Ann. Rev. Microbiol., 41: 301-334.

Peters, K.E., Walters, C.C., Moldowan, J.M. (2005): The Biomarker Guide: Second Edition. – 1155 pp., Cambridge University Press, Cambridge.

Reitner, J. (1993): Modern cryptic microbialite/metazoan facies from Lizard Island (Great Barrier Reef, Australia), formation and concepts. - Facies, 29: 3–40.

Reitner, J. & Neuweiler, F. (1995): Mud Mounds: a polygenetic spectrum of fine-grained carbonate buildups. - Facies, 32: 1–69.

Richthofen, F. & Freiherr von (1860): GeognostischeBeschreibung der Umgebung von Predazzo, Sanct Cassian und der Seisser Alpe. - 327 pp., J. PerthesVerlag, Gotha.

Riding, R. (1991): Classification of microbial carbonates. - In: Riding, R. (ed.): Calcareous Algae and Stromatolites, 21– 51, Springer-Verlag, Berlin.

Riding, R. (2002): Structure and composition of organic reefs and carbonate mud mounds: concepts and categories. - Earth- Sci. Rev., 58: 163–231.

Riding, R. & Awramik, S.M. (2000): Microbial Sediments. - Springer-Verlag, Heidelberg

Russo, F. (2005): Biofacies evolution in the Triassic platforms of the Dolomites, Italy. - 33–44, Ann. Univ. Ferrara, volume speciale.

Russo, F., Mastandrea, A., Neri, C. (1998): Le comunità-costruttricidellepiattaformetriassichedelle Dolomiti. - Mem. Soc. Geol. It., 53.

Russo, F., Neri, C., Mastandrea, A., Laghi, F.G. (1991): Depositional and Diagenetic History of the Alpe di Specie (Seelandalpe) Fauna (Carnian, Northeastern Dolomites). - Facies, 25: 187-210,.

Russo, F., Neri, C., Mastandrea, A., Baracca, A. (1997): The mud mound nature of the Cassian Platform Margins of the Dolomites A case history: the Cipit boulders from Punta Grohmann (SassoPiatto Massif, northern Italy). - Facies, 36: 25–36.

Russo, F., Mastandrea, A., Stefani, M., Neri, C. (2000): Carbonate facies dominated by syndepositional cements: a key component of middle Triassic platforms. The Marmolada case history (Dolomites, Italy).- Facies, 42: 211–226.

Schouten, S., Bowman,J.P., Rijpstra, W.I.C., Sinninghe-Damsté, J.S. (2000): Sterols in a psychrophilic methanotroph, Methylosphaerahansonii. - FEMS Microbiology Letters, 186: 193–195.

ScudelerBaccelle, L. (1971): La serie ladino-carnicaalla base della Punta Grohmann (Gruppo del Sassolungo, DolomitiOccidentali). Strutturesedimentarie e petrologiadellafaciescarbonatica. - Mem. Geopaleont. Univ. Ferrara, 3 (1), Ferrara.

Thiel, V., Merz-Preiß, M., Reitner, J., Michaelis, W. (1997): Biomarker studies on microbial carbonates: extractable lipids of a calcifying cyanobacterial mat (Everglades, USA). - Facies 36: 163–172.

Webb, G.E. (1996): Was Phanerozoic reef history controlled by the distribution of non-enzymatically secreted reef carbonates (microbial carbonate and biologically induced cement?). - Sedimentology, 43: 947–971.

Geo.Alp, Vol. 8, S. 164–169, 2011

STUNTING IN INVERTEBRATES FROM THE TYPE AREA OF THE CASSIAN FORMATION (EARLY CARNIAN) OF THE DOLOMITES (ITALY)

Max Urlichs

With 2 Figures

Staatliches Museum für Naturkunde Stuttgart, Rosenstein 1, 70191 Stuttgart.

Abstract

Stunting is described to occur in the bivalves *Palaeonucula strigilata* and *Prosoleptus lineatus*, the gastropod *Rhaphistomella radians*, and the brachiopods *Koninckina leonhardi* and *Camerothyris subangusta*, all from the Cassian Formation (Early Carnian, Dolomites). The high percentage of framboidal and finely dispersed pyrite in beds with stunting indicates reduced live conditions at the sea bottom. The occurrence of stunting correlates to the end of transgressive cycles, when stagnation took place at the end of the prograding of the neighbouring carbonate platforms in the St. Cassian Basin.

Key words: Stunting, bivalves, gastropods, brachiopods, Early Carnian, Dolomites.

Introduction

The Cassian fauna is a well-known example of a dwarfed fauna in early literature. Recently, it was interpreted as stunted. However, dwarfism is defined as restricted to a genetically controlled small size of specimens, whereas stunting results from restricted ecological conditions (Hallam, 1965). In general, the bulk of the Cassian fauna is small-sized (Fürsich & Wendt, 1977), reinforced first of all by the abundance of juvenile specimens of bivalves, gastropods, ammonoids, and brachiopods. Furthermore, ecologically controlled extreme small size applies to some horizons (Fig. 1). These faunas are stunted because they contain small-sized adult specimens of elsewhere normal-sized species. However, a documentation of the stunting was not provided by the early authors cited in literature (summarized by Urlichs, 2004). To detect stunting, adult specimens from different beds were compared with each other. At the onset of maturity, the growth generally slows down rather than ceases. This leads to a crowding of the growth lines in bivalves and brachiopods respective septa in ammonoids (Vogel, 1959).

Stunting was studied in detail only in ammonoids (merely in *Lobites*) and ostracods (Urlichs, 1971, 2004). The ammonoids *Lobites nautilinus* (Münster) and *L. pisum* (Münster) are usually adult and completely preserved with their eccentric body chambers, hoods, contracted peristomes, and crowded sutures at the ends of the phragmocones. The septal spaces were measured on polished, exactly orientated sagittal sections and plotted against the number of septa (Urlichs, 2004, figs. 4, 6-11). Specimens from claystones and argillaceous marls have approximated sutures, beginning from the protoconch onwards, whereas specimens collected from marls have normal-spaced septa. Both have furthermore crowded sutures at the ends of the phragmocones and the same number of septa and whorls; thus they have the same individual age. The adult small-sized *Lo-*

bites specimens attain in average 69-72% of the diameter of normal-sized ones. Therefore, these small-sized specimens are genuinely stunted. The septal spaces were also measured on sagittal sections of several other ammonoids: *Joannites klipsteini* (Mojsisovics), *Lecanites glaucus* (Münster), *Megaphyllites jarbas* (Münster), *Proarcestes bicarinatus* (Münster), and *Trachyceras muensteri* (Wissmann). In contrast to *Lobites*, these species do not show differences of the septal spaces between the different horizons and have a septal spacing like in specimens from the coeval Hallstatt Limestone. Therefore, they are considered to be of normal size, and they are mostly represented by juvenile specimens with their body chambers and rarely by small nuclei. Adult specimens of the ostracods *Bairdia cassiana* (Reuss) and *Hungarella limbata* (Reuss) have equal sizes in the horizons with stunted and with normal-sized molluscs (Urlichs, 1971).

The material for this study was collected bed by bed in the type area of the Cassian Formation (GSSP Ladinian/Carnian: Broglio Loriga et al., 1999; Gaetani, 2009) southwest and south of St. Cassian (localities see Urlichs 2004, Fig. 1). The bulk of the faunas was found weathered out of the argillaceous or marl rocks. Collecting was very time-intensive because one had to rely on weathered out fossils, as only in this way large samples could be obtained.

Fauna assemblages

Two different types of faunal assemblages are present in the type area of the Cassian Formation. Allochthonous faunas occur in few beds (Fig. 1: faunas 1a, 7, 11, 13a, 16b, 20 and 23). These faunas yield calcareous sponges and corals without attachment areas. Bivalves are univalved and often fragmented. Echinoids are more frequently represented by isolated spines than by ossicles. Crinoids are rare and only represented by isolated columnalia or at best by short stem fragments. The skeletal material of these assemblages was mainly transported by turbitites from the adjacent buildups and patch reefs from shallow areas into deeper water settings. The reef-dwelling bivalves, gastropods, and brachiopods are represented by quite other taxa than in the autochthonous faunas. Therefore, the allochthonous assemblages were discarded from investigating stunting.

The bulk of the Cassian faunas in the type area comes from autochthonous horizons from which two faunal associations, the *Rhaphistomella radians/Palaeonucula strigilata* association and the *Koninckina leonhardi* association, were already described by Fürsich & Wendt (1977). The first one is represented in the faunas 5, 6, 8, 9, 12, 13b, 14, 16a, 17, and 22, the second one in the faunas 10 and 15 (Fig. 1). A further association has a trophic nucleus composed of *Polygyrina lommeli* (Münster) and *Rhaphistomella radians* (Münster). It is represented in the faunas 1b-4. Another association, fauna 19, shows a predominance of *Koninckina leonhardi* (Wissmann), *Halobia fluxa* (Mojsisovics) and *Lobites nautilinus* (Münster).

Stunting

The aim of this study is to investigate the most common infaunal bivalves of the autochthonous deposits of the Cassian Formation, *Palaeonucula strigilata* (Goldfuss) and *Prosoleptus lineatus* (Goldfuss), the gastropod *Rhaphistomella radians* (Münster), and the brachiopods *Koninckina leonhardi* (Münster) and *Camerothyris subangusta* (Münster) whether stunting is present in these taxa or not (Figs. 2A-Q). Specimens of *Palaeonucula* which come from marls are obviously normal-sized when compared with Recent nuculids. The specimens from claystones and argillaceous marls are small-sized, but of the same shape. Comparing the lengths of adult specimens of *Palaeonucula strigilata* with crowded growth rings, the small-sized specimens attain only 45-55% of the normal-sized ones (Figs. 2A-C); hence, they are genuinely stunted. The growth rings in *Prosoleptus lineatus* are quite oblique. Therefore, the tiny concentric ribs were counted and the length at each tenth was measured. Adult small-sized specimens with approximated ribs have about the same number of ribs and thus have the same individual ages. They attain only 60-70% of the normal-sized ones. Therefore, these specimens are also stunted (Figs. 2D-F).

In *Rhaphistomella radians* (Figs. 2G-K), differences in size are striking, but these are smaller than in bivalves. Comparing the sizes of specimens from different beds, the diameter at the end of the fourth postembryonal whorl was measured. Stunted specimens have a mean diameter which is 20-23% smaller than in normal-sized ones, and an about 10 degrees smaller apical angle.

The end-size of adult brachiopods *Koninckina leonhardi* and *Camerothyris subangusta* was investigated (Figs. 2L-Q). Comparing the widths of adult specimens, the small-sized specimens attain 71-79% of the normal-sized ones; hence they are also stunted.

Stunting was observed in the faunas 1b, 4, 8, 12, 22 and partly 19 (Fig. 1). The faunas 5, 6, 9, 10, 13b, 14, 15, 16a, 17, 18b, and partly 19 are normal-sized, whereas the faunas 2, 3, 18a are intermediate. The fauna 19 was obtained from an about 15 m thick sequence of marly and argillaceous beds alternating with limestones. All *Lobites* specimens from these beds are stunted. In contrast, two size classes of adult *Koninckina* specimens without transitions were found. The bigger specimens are normal-sized and the small-sized ones stunted when comparing them with the sizes of material from other horizons. The *Camerothyris* specimens are normal-sized in this fauna. Probably the stunted brachiopods and ammonoids come from different beds as the normal-sized brachiopods. Obviously, different faunas were mixed up during sampling.

Conclusions

The stunted faunas have a reduced diversity, but they are still fully marine since stenohaline organisms like ammonoids and brittlestars are present. Therefore, low salinity cannot be the reason for the stunting in the Cassian Formation. The low diversity is an indicator of restricted live conditions. Furthermore, if one species is stunted, the whole population is concerned too. The normal-sized faunas occur in marls, whereas the stunted ones come from dark claystones and argillaceous marls which are rich in framboidal and finely dispersed pyrite (faunas 1, 4, 8, 12, 16a, 22 and partly 19). Possibly, the presence or abundance of certain cations such as Cu, Pb, Sn, and Ag may retard or stop the growth as in Recent invertebrates (Tasch, 1953: 428). However, special geochemical investigations do not exist for the Cassian Formation. The high pyrite content of some beds indicates a plausible reason for the stunting. Growth and development are retarded in Recent marine invertebrates by sulfoxide, an incompletely oxidized derivate of sulfhydryl occurring in the natural circuit (Tasch, 1953). Probably, during poorly oxygenated intervals in the Cassian Formation, the sulfhydryl was incompletely oxidized to the toxic sulfoxide which was later precipitated as pyrite. These restricted live conditions characterized by stunted molluscs occurred at the end of transgressive cycles, when the St. Cassian Basin was narrowed and stagnation took place therein. This can be demonstrated in the Forcella di Settsass section. The surface of the Richthofen Reef is eroded and karstified (Cros, 1977, p. 341; De Zanche et al., 1993, p. 15). After the sea level high stand of the Cassian Dolomite 1 of the Richthofen Reef, this karstification indicates a low stand. During this time, the margins of the buildups were eroded. Sediments from the buildups like oncolites and fossils from the patch reefs were transported by turbidites into the St. Cassian Basin. Therefore, the karstified surface of the Richthofen Reef corresponds with an allochthonous fauna (here fauna 20) in the St. Cassian Basin. The slope of the Richthofen Reef is diachronously onlapped by deep water claystones lacking fossils (Bosellini, 1984, Fig. 17; Doglioni et al. 1990, Fig. 15). These beds are at first overlain by marly greenish-gray limestones with *Halobia fluxa* and rare ammonoids (fauna 21 on Fig. 1), then by argillaceous grey marls and dark clays. The frequent occurrence of *Halobia* indicates a deep neritic environment. The uppermost part of these beds bears a stunted fauna (fauna 22) with the predominance of the nuculids *Palaeonucula strigilata* and *P. expansa*. The sediment with framboidal and finely dispersed pyrite indicates a reduced environment and stagnation. These beds are then overlain by marls bearing a very diverse allochthonous faunal assemblage of shallow-water skeletal material (fauna 23). It indicates the next sea level low stand with erosion and karstification on the carbonate platforms.

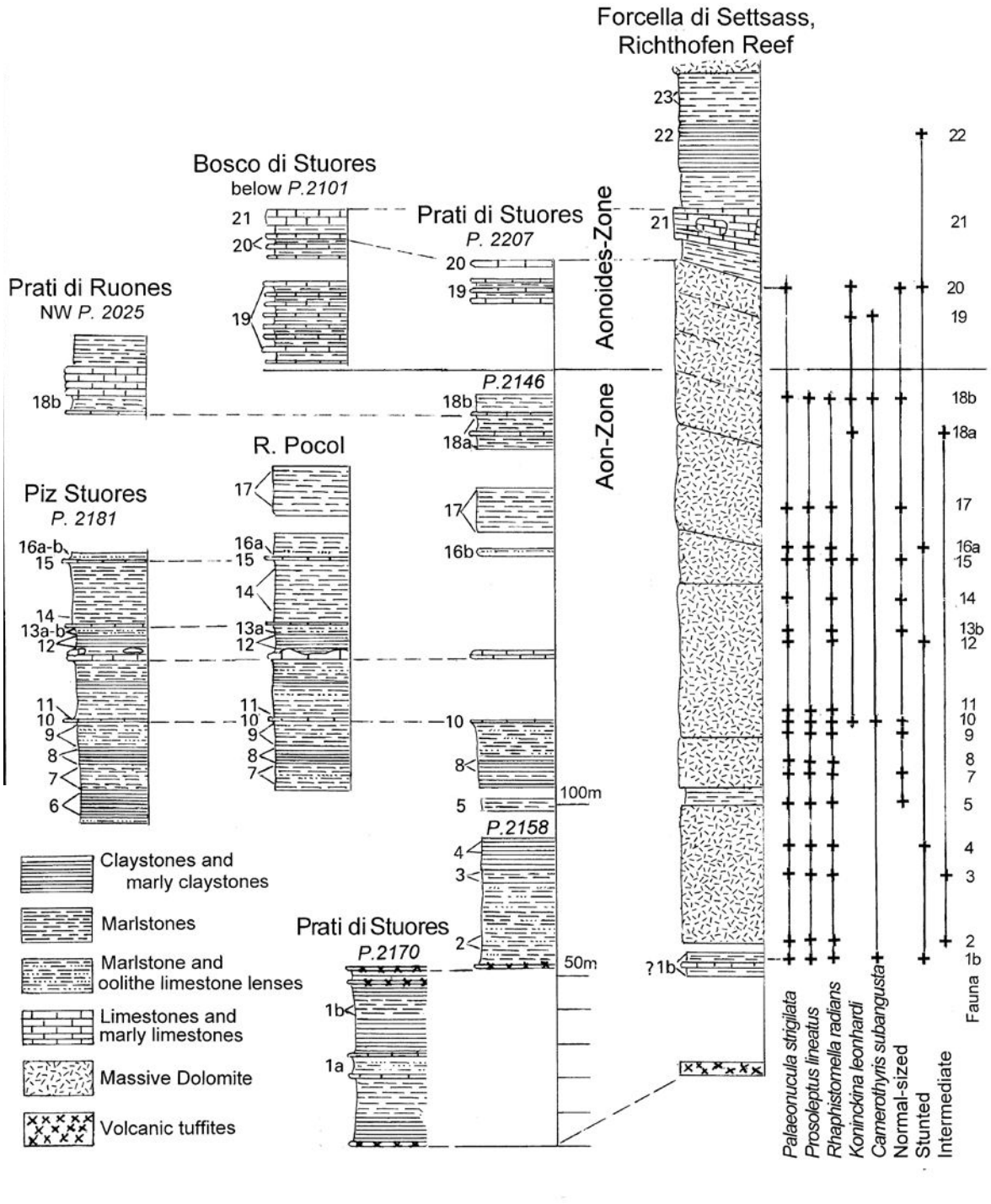

Fig. 1: Sections of the Cassian Formation in its type area south of St. Cassian (Dolomites, Italy), with the stratigraphical ranges of investigated species and occurrences of stunting (sections after Urlichs, 2004; for localities see Urlichs, 2004, Fig. 1).

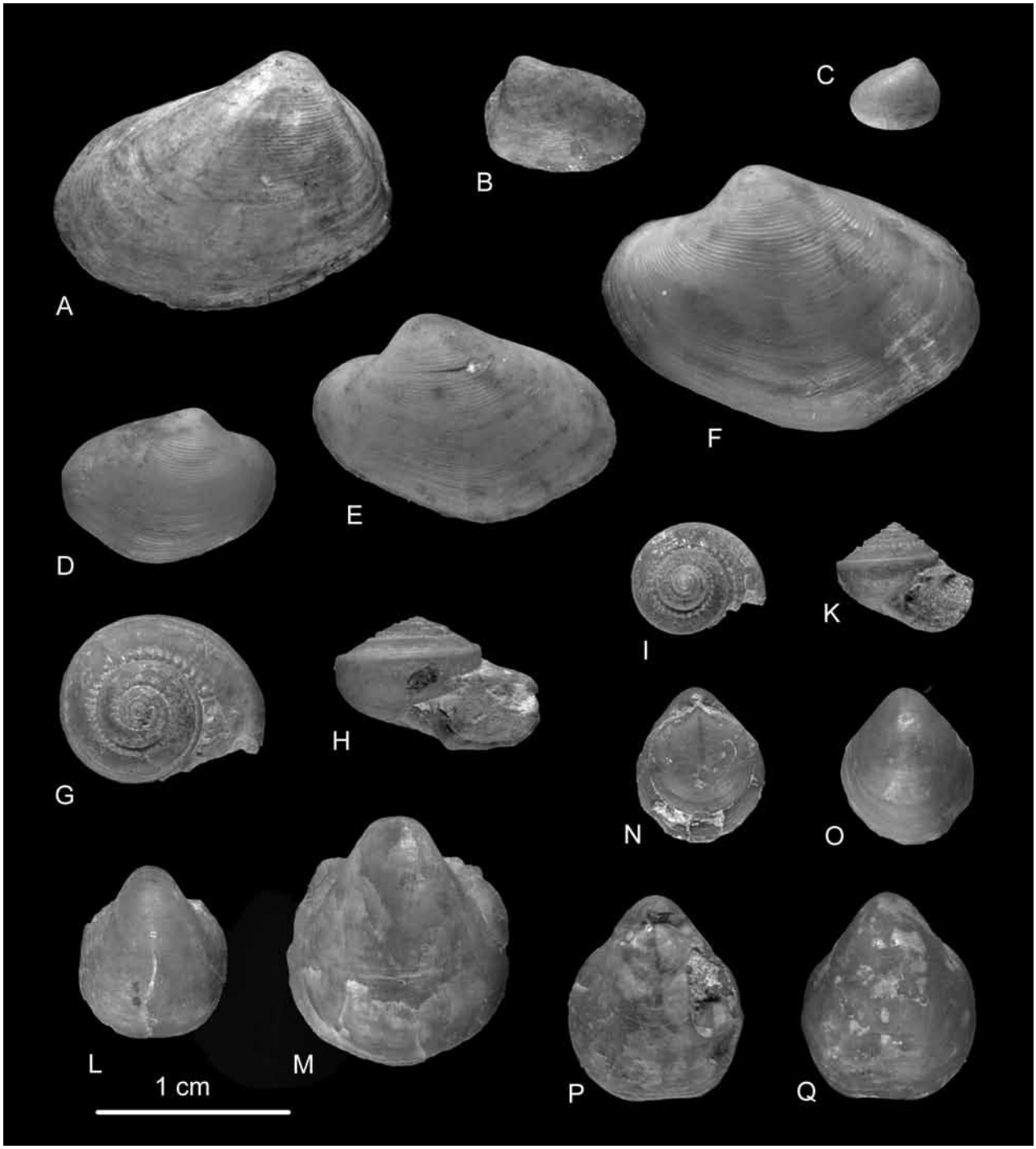

Fig. 2: Stunted and normal-sized adult specimens of the investigated species from the Cassian Formation.
Figs. A-C: *Palaeonucula strigilata* (Goldfuss), A: normal-sized, fauna 10, Piz Stuores, B: stunted, fauna 1b, Prati di Stuores, C: stunted, Fauna 22, Forcella di Settsass, Figs. D-F: *Prosoleptus lineatus* (Goldfuss), D: stunted, fauna 8, Rio Poccol, E: intermediate, fauna 9, Rio Poccol, F: normal-sized, fauna 17, Rio Poccol; Figs. G-K: *Rhaphistomella radians* (Münster), G-H: normal-sized, fauna 10, Piz Stuores, I-K: stunted, fauna 12, Piz Stuores; L-M: *Koninckina leonhardi* (Wissmann), L: stunted, fauna 19, Bosco di Stuores, M: normal-sized, fauna 19, Prati di Stuores; Figs. N-Q: *Camerothyris subangusta* (Münster), N-O: stunted, fauna 1b, below Richthofen Reef, P-Q: normal-sized, fauna 19, Rio Stuores.

References

Bosellini, A. (1984): Progradation geometries of carbonate platforms: examples from the Triassic of the Dolomites, northern Italy. – Sedimentology, 31: 1-24.

Broglio Loriga, C., Cirilli, S., De Zanche, V., Di Bari, D., Gianolla, P., Laghi, G. F., Lowrie, W., Manfrin, S., Mastandrea, A., Mietto, P., Muttoni, G., Neri, C., Posenato, R., Rechichi, M.C., Rettori, R. & Roghi, G. (1999): The Prati di Stuores/Stuores Wiesen section (Dolomites, Italy): as GSSP candidate for the Ladinian-Carnian boundary. – Riv. Ital. Paleont. Stratigr., 105: 37-78.

Cros, P. (1977): Données nouvelles sur la dolomitisation des carbonates triasiques des Dolomites Italiennes. – Sciences de la Terre, 21: 307-355.

De Zanche, V., Gianolla, P., Mietto, P., Siorpaes, C. & Vail, P. R. (1993): Triassic sequence stratigraphy in the Dolomites (Italy). – Mem. Sci. Geol., 45: 1-27.

Doglioni, C., Bosellini, A. & Vail, P. R. (1990): Stratal patterns: a proposal of classification and examples from the Dolomites. – Basin Research, 2: 83-95.

Fürsich, F. T. & Wendt, J. (1977): Biostratinomy and palaeoecology of the Cassian Formation (Triassic) of the Southern Alps. – Palaeogeogr., Palaeoclimatol., Palaeoecol., 22: 257-323.

Gaetani, M. (2009): GSSP of the Carnian Stage defined. – Albertiana, 37: 36-37.

Hallam, A. (1965): Environmental causes of stunting in living and fossil marine benthonic invertebrates. – Palaeontology, 8: 132-155.

Tasch, P. (1953): Causes and paleontological significance of dwarfed fossil marine invertebrates. – J. Paleont., 27: 356-444.

Urlichs, M. (1971): Variability of some ostracods from the Cassian Beds (alpine Triassic) depending on the ecology. – Bull. Centre Rech. Pau - SNPA, 5 supplement: 695-715.

Urlichs, M. (2004): Kümmerwuchs bei *Lobites* Mojsisovics, 1902 (Cephalopoda, Ammonoidea) aus dem Unter-Karnium der Dolomiten (Ober-Trias, Italien) mit Revision der unterkarnischen Arten. – Stuttg. Beitr. Naturk., Serie B, 344: 1-37.

Vogel, K. (1959): Wachstumsunterbrechungen bei Lamellibranchiaten und Brachiopoden. Ein Beitrag zur Beurteilung fossiler Kleinfaunen und zu Frage „Bio- oder Thanatocoenose. – N. Jb Geol. Paläont. Abh,, 169: 109-129.

Gredleriana

11

2011

NATURMUSEUM SÜDTIROL
MUSEO SCIENZE NATURALI ALTO ADIGE
MUSEUM NATÖRA SÜDTIROL

Die Veröffentlichungsreihe „Gredleriana" des Naturmuseums Südtirol (Bozen) ist ein Forum für naturwissenschaftliche Forschung in und über Südtirol. Sie stellt eine Kommunikationsplattform dar für alle jene, die in Südtirol forschen oder in der Ferne Südtirol und den alpinen Raum als Ziel ihrer naturwissenschaftlichen Forschung haben.

Band 11/2011: 25 Euro (Abonnement: 20 Euro), ca. 350 Seiten, ISSN 1593-5205

GEO.ALP

Veröffentlichung des Instituts für Geologie und Paläontologie der Universität Innsbruck
und des Naturmuseums Südtirol/Museo Scienze Naturali Alto Adige, Bozen/Bolzano

ISSN 1824-774

Inhalt